EFFECTS OF HYDRAZINE AND OTHER TOXICANTS ON EARLY LIFE STAGES OF CALIFORNIA BROWN ALGAE

Thesis by

David E. James

In Partial Fulfillment of the Requirements

for the Degree of

Doctor of Philosophy

California Institute of Technology

Pasadena, California

1989

(Submitted December 2, 1988)

ACKNOWLEDGEMENTS

Scholastic work, though solitary in nature, is made much easier because of the support and encouragement received from a community of mentors, colleagues, family and friends as we surmount obstacles encountered on previously untravelled roads of inquiry.

Expert guidance provided by the three core members of my Ph.D. committee, Wheeler J. North (Chairman), James J. Morgan and Norman H. Brooks, was extremely helpful in refining experimental plans and data analysis. Thanks to George Jackson and the staff at Scripps Institution of Oceanography for their hospitality during a stimulating year as an exchange student. Tim Horiuchi (BSEE, Caltech,'89) wrote superb computer programs used to operate the digitizing equipment. The cooperation of the Pacific Gas & Electric Company and Southern California Edison in sharing hydrazine emission data is very much appreciated.

I am grateful for financial support from an Earl C. Anthony Fellowship, the ARCS Foundation, the Gas Research Institute, the William and Flora Hewlett Foundation, a Virginia Steele Scott Fellowship, the Josephine de Karman Fellowship Trust and the Pacific Gas and Electric Company.

Through good times and bad, many extended friendship and moral support. Thanks also go to Sue Larson, Bob Arnold, Tom DiCristina, Bruce and Nancy Vogelaar, Brian Wong, Ranajit Sahu, Tina Morris, members of the Caltech Glee Clubs, Rhonda and Ken Gebhart, Bruce Daube, Bonnie & Jack James, St. Michael and All Angel's Episcopal Church and numerous others for being there when I needed them.

ABSTRACT

Toxicity of hydrazine to early life stages of several species of California brown algae was demonstrated to occur at environmentally relevant concentrations. Effects of hydrazine on benthic organisms had not been previously studied.

Preliminary studies evaluated toxicity of boric acid, chlorine (as hypochlorite), lithium ion, tributyltin chloride and Zn(II).

A reliable bioassay technique was developed using digital image analysis to measure vegetative growth inhibition of brown algal gametophytes. Hydrazine toxicity threshold of Macrocystis pyrifera gametophytes was almost constant in 10 96-hour experiments, ranging from 3 - 5 ppb (96-160 nM).

Differences in resistance to short-term hydrazine exposures were observed among three algal families of the order Laminariales. Two of three tested members of the family Alariaceae, Pterygophora californica and Eisenia arborea were among the most resistant species tested. The three tested species in the family Lessoniaceae, Macrocystis pyrifera, Nereocystis luetkeana and Pelagophycus porra, all fast-growing canopy-formers, were among the most sensitive tested species. Tested representatives of the family Laminariaceae varied in resistance. Laminaria farlowii was resistant. Laminaria dentigera and Laminaria ephemera were fairly sensitive.

Hydrazine autoxidation rates varied by an order of magnitude in seawater sampled from different locations. Rates showed strong temperature dependence. Autoxidation at 10°C and below was much

slower and indicated a higher activation energy than autoxidation at 20°C and above.

Undiluted trace hydrazine powerplant emissions from a time period when algal community composition changed in the vicinity of an outfall were compared to growth inhibition results from multivariate hydrazine toxicity experiments on Macrocystis gametophytes. Results indicated that several trace hydrazine discharges were of sufficient duration and concentration to have inhibited algal microscopic stages.

TABLE OF CONTENTS

	Page
ACKNOWLEDGEMENTS	iii
ABSTRACT	iv
TABLE OF CONTENTS	vi
LIST OF FIGURES	ix
LIST OF TABLES	xvi
LIST OF ABBREVIATIONS	xx
CHAPTER 1: INTRODUCTION	
I. History of Toxicity Research using Kelp	1
II. Research Overview	11
III. Organization of Contents	12
References	13
CHAPTER 2: MATERIALS AND METHODS	
I. Collection of Materials	19
II. Culturing	21
III. Measurement of Toxicant Effects	25
IV. Statistical Methodologies	28
References	35
CHAPTER 3: USE OF DIGITAL IMAGE ANALYSIS IN KELP BIOASSAYS	
I. Background	37
II. Materials and Methods	41
III. Calibration and Error Analysis	
A. Digitizer Calibration	48
B. Hardware Errors	48
C. Operational Errors	52

D. Propagation of Digitizer Error into Size Distribution Error 66

IV. Comparison between Digitizing and Eyepiece Micrometer Methods 70

V. Conclusions 76

VI. Operational Conditions for Digitization 76

References 77

VII. Appendix: Propagation of Error in kelp measurements 81

CHAPTER 4: COMPARISON OF TOXICANTS AND ALGAL LIFE STAGES

I. Introduction 85

II. Screening Trials: Macrocystis pyrifera Series G & H 89

III. Life Stage Trials using Hydrazine: Macrocystis pyrifera Series I & J 104

IV. Continuous Hydrazine Assays of Macrocystis Gametophytes Measured with Digital Image Analysis 131

V. Comparison Among Different Species in Pulsed Hydrazine Trials 143

VI. Toxicity of Other Compounds to Macrocystis Gametophytes 164

References 178

VI. Appendix: Macrocystis pyrifera continuous growth inhibition data in hydrazine 185

CHAPTER 5: HYDRAZINE EMISSIONS AND CHEMISTRY IN SEAWATER

I. Introduction and Background 191

II. Use of Hydrazine in Electric Generating Stations 192

III. Powerplant Emissions

A. Data Collection and Reporting Methodology 196

B. Diablo Canyon Powerplant Emissions 198

C. San Onofre Nuclear Generating Station Emissions 207

IV. Hydrazine Chemistry in Seawater

A. Hydrazine Speciation in Seawater 213

B. Autoxidation in Seawater 217

V. Conclusions 237

VI. Appendix: Prediction of toxicity event risk from historical data 239

References 243

CHAPTER 6: PREDICTING INHIBITION UNDER VARYING ENVIRONMENTAL CONDITIONS

I. Introduction 249

II. Materials and Methods 250

III. Multivariate Experiments

A. Series AB; Intermittent Hydrazine Exposures 252

B. Series AD; Effects of Age and Temperature 272

IV. Modeling Cyclic Exposure to Hydrazine

A. Series AG; Single worst-case event 280

B. Series M; Cycled Chemical Exposure 282

C. Series O; Combined Thermal & Chemical Cycling 288

V. Conclusions 291

VI. APPENDIX: Additional Statistical Tables 293

References 297

CHAPTER 7: SUMMARY AND CONCLUSIONS

I. Summary of Results In Separate Chapters 301

II. Main Conclusions of Thesis 306

LIST OF FIGURES

Figure		Page
1.1	Schematic kelp forest diagram.	2
1.2	Life cycle of Laminarian brown algae using Macrocystis pyrifera as an example.	4
1.3	Historical changes in extent of surface canopy area in kelp beds in vicinity of San Onofre.	6
2.1	Collection sites for California brown algae.	20
2.2	Scheme for initiation of gametophyte cultures from Macrocystis sporophylls.	22
2.3	Example of broadening of gametophyte size distribution with time. Data shown for Pterygophora californica control culture.	29
3.1	Representative sizes and shapes of fertile and vegetative gametophytes. Magnification approximately 800X.	38
3.2	Measurement of gametophytes with eyepiece micrometer.	39
3.3	Simple example of conversion of brightness in digitizer grid to numerical pixel intensity.	42
3.4	Schematic diagram of components of image analysis system.	43
3.5	Photo of video screen showing software-generated square cursor surrounding target organism.	45
3.6	Comparison of resolution limits for different components of image analysis system.	51
3.7	Influence of proportion of object area on edge pixel brightness.	54
3.8	Example of effect of edge threshold setting on perceived object size.	55
3.9	Experimental precision of 10 repeated digitizations of single spheres.	57
3.10	Effect illumination intensity on contrast difference between object and background.	60

Figure		Page
3.11	Effect spatially varying object optical density on transmitted light intensity.	61
3.12	Effect of extinction coefficient on intensity difference variability for simple model shown in Figure 3.11.	62
3.13	Interaction of optical density and threshold setting on measured object size for model in Figure 3.11.	63
3.14	Interaction of optical density and threshold setting on measured object size for two different gametophytes.	65
3.15	Partitioning of observed standard deviations into components for organisms and digitizer.	68
3.16	Comparison of error bars for Macrocystis pyrifera gametophyte sizes with and without machine error.	69
3.17	Comparison of gametophyte areas determined by eyepiece micrometer and digital image analysis.	71
3.18	Comparison of coefficients of variation determined from area measurements using both methods.	73
3.19	Comparison of determination of inhibition of growth compared to controls in 6-hour 250 ppb daily hydrazine exposures.	74
3.20	Coefficients of variation for control cultures of Figure 3.19.	75
4.1	Map of Diablo Cove showing area impacted by April 1984 event.	86
4.2	Simplified Schematic of Hydrazine Injection and Discharge in Pressurized Light-Water Reactor Circuits.	88
4.3	Diablo Canyon Power Plant Hydrazine Effluent Concentrations, April-May 1984.	93
4.4	Series G screening trial. Effect lithium ion on gametophyte vegetative growth at 10X and 100X over seawater background concentrations.	95

Figure		Page
4.5	Series G screening trial. Effect boric acid on gametophyte vegetative growth.	96
4.6	Series G screening trial. Effect hydrazine on gametophyte vegetative growth	97
4.7	Macrocystis pyrifera Series H gametophyte growth.	98
4.8	Cumulative frequency distributions for discharges of lithium, hydrazine and boric acid during April-May, 1984.	105
4.9	Concentration vs. duration relationships for Diablo Canyon hydrazine emissions, April-May 1984	107
4.10A	Series I: Effect pulsed hydrazine exposures on growth of three-day old M.pyrifera gametophytes.	111
4.10B	Series I: Effect pulsed hydrazine exposures on growth of eight-day old M.pyrifera gametophytes.	112
4.11	Series I: Mean counts per field of view at 160X motile sperm produced by M.pyrifera gametophytes after early and late exposures to 1-day 250 ppb hydrazine pulses.	113
4.12	Series I: Total counts in 20 scans per day at 160X of embryonic sporophytes recruited from M.pyrifera Series I gametophyte cultures after early and late exposures to 1 day/250 ppb pulses.	117
4.13	Series J: Inhibition of M.pyrifera zoospore motility in Type I trial in 2500 ppb hydrazine.	118
4.14	Series J: Inhibition of M.pyrifera zoospore motility in a Type II (open beaker) trial in 250 ppb hydrazine.	119
4.15	Series J: Effect pulsed hydrazine exposures applied during germination (Day -1) on growth.	124
4.16	Comparison lowest observed hydrazine doses significantly inhibiting Macrocystis pyrifera microscopic life stages.	128
4.17	Series M: Comparison of least-squares fits to daily area data; Macrocystis pyrifera.	132
4.18	Series Z: Example of Growth vs. hydrazine concentration curve for 96-hour continuous exposure test. Measured Day 8	136

Figure		Page
4.19A	Series AF & AG: Hydrazine sensitivity comparison. Central (AG) vs. Southern (AF) gametophytes in simultaneous culture.	137
4.19B	Comparison of effects of hydrazine on M.pyrifera growth rates; central vs. southern California gametophytes.	138
4.20	Comparison of daily-growth and germination of simultaneously-cultured central and southern California gametophytes.	142
4.21	Example of temporary vegetative growth inhibition in Eisenia arborea gametophytes after application of a 250 ppb/1 day pulse.	144
4.22	Effect hydrazine on vegetative growth of Pelagophycus porra gametophytes showing signif-icant inhibition at 2 ppb.	153
4.23A	Effect of one-day hydrazine pulses on Pterygophora californica gametophyte vegetative growth; December 1985, Diablo Cove and Laguna Beach.	155
4.23B	Effect of one-day hydrazine pulses on Pterygophora californica gametophyte vegetative growth; April 1987, Diablo Cove.	156
4.24A	Nereocystis luetkeana; Series A. Effect pulsed hydrazine exposure on vegetative growth measured by eyepiece micrometer, May 1986, Diablo Cove.	158
4.24B	Nereocystis luetkeana; Series B. Effect continuous hydrazine exposure on vegetative growth; digital image analysis, Sept. 1987, Diablo Cove.	159
4.25	Macrocystis pyrifera; Series V. Range-finding test for tributyl-tin chloride toxicity.	169
4.26	Macrocystis pyrifera; Series V. Range-finding test for sodium hypochlorite toxicity.	170
4.27	Macrocystis pyrifera; Series AE. Effect total added Zn(II) on germ-tube length.	171
4.28	Macrocystis pyrifera; Series AE. Effect total added Zn(II) on vegetative growth.	172

Figure		Page
4.A.1	Macrocystis pyrifera; Series X and Y Continuous growth inhibition in hydrazine.	186
4.A.2	Macrocystis pyrifera; Series Z and AA Continuous growth inhibition in hydrazine.	187
4.A.3	Macrocystis pyrifera; Series AB and AC Continuous growth inhibition in hydrazine.	188
4.A.4	Macrocystis pyrifera; Series AD and AE Continuous growth inhibition in hydrazine.	189
4.A.5	Macrocystis pyrifera; Series AF and AG Continuous growth inhibition in hydrazine.	190
5.1	Hydrazine injection and discharge in pressurized light-water reactor circuits.	193
5.2	Monthly peak emissions from Diablo Canyon Nuclear Power Plant.	201
5.3A	Frequency distribution of peak undiluted monthly emissions for Diablo Canyon Power Plant.	202
5.3B	Cumulative frequency distribution of peak monthly emission data, Diablo Canyon.	204
5.4	Example of annual emissions pattern: Diablo Canyon, 1986.	205
5.5	Peak monthly undiluted emissions from San Onofre Nuclear Generating Station Units 1,2,3.	209
5.6A	Frequency distribution for peak monthly data shown in Figure 5.5.	211
5.6B	Cumulative frequency distribution of peak monthly emission data, San Onofre.	212
5.7	Dependence of hydrazine speciation on pH and temperature.	216
5.8	Association of several divalent cations with hydrazine.	218
5.9	Autoxidation of hydrazine in different seawaters.	224
5.10	Comparison of half-order and first-order fits to hydrazine autoxidation data in Newport Harbor seawater.	227

Figure		Page
5.11	Comparison of half-order and zero-order fits to hydrazine autoxidation data in Newport Harbor seawater.	228
5.12A	Comparison of experimental data for offshore seawater to time course of reactions for several types of ideal kinetics.	229
5.12B	Fit of three kinetic models to hydrazine autoxidation, offshore seawater.	230
5.13	Effect of temperature on hydrazine autoxidation rate.	232
5.14	Arrhenius plot for hydrazine autoxidation in Diablo Cove seawater using pseudo-first order rate constants.	235
5.15	Historical power-plant hydrazine discharge risk.	241
6.1	Schematic time sequence of events in transient-exposure vegetative growth toxicity assays using Macrocystis pyrifera gametophytes.	251
6.2	Series AB: Relationship between combined concentration variable and level means for M.pyrifera.	258
6.3	Series AB: Mean inhibitions (error bars removed) vs. $\log_{10}$hydrazine concentration.	260
6.4A	Series AB: Mean inhibition against combined hydrazine concentration exposure time variable.	261
6.4B	Series AB: Least-squares fit to data means.	263
6.5	Series AB: Least-squares fit to entire data set.	264
6.6	Series AB: Contours of constant inhibition derived from regression on M.pyrifera data set.	265
6.7	Relationship of toxicity data range to undiluted powerplant emissions data for 1986 and April-May 1984.	267
6.8	Superposition of undiluted powerplant concentrations on M.pyrifera Series AB inhibition contours showing several possible inhibitory events.	268

Figure		Page
6.9	Contours near 100% of control growth demonstrating applicability for powerplant emissions regulation	269
6.10	Series AD: Age-dependence of 96-hour continuous growth inhibition.	273
6.11	Series AD: Temperature-dependence of 96-hour continuous growth inhibition.	274
6.12	Series AD: Comparison of data distributions about predictions.	277
6.13	Series AD: Predicted response surface from regression developed for M.pyrifera gametophytic growth vs. hydrazine concentration and temperature.	278
6.14	Series AD: Contour map for prediction of vegetative growth as function of hydrazine concentration and temperature.	279
6.15	Series AG: Interaction of concentration and temperature vegetative growth inhibition of M.pyrifera.	281
6.16	Series AG: 96-hour growth of M.pyrifera gametophytes continuously exposed to different temperatures.	283
6.17	Series M: M.pyrifera gametophyte growth inhibition in daily 6-hour hydrazine exposures.	286
6.18	Series O: M.pyrifera gametophyte growth in 18-hour daily exposures.	289
6.19	Example temperature record from station near Diablo Canyon Power Plant discharge.	292

LIST OF TABLES

Table		Page
1.1	Taxonomic classification of algae used in this study.	3
1.2	Summary of prior toxicity research using microscopic life stages of Laminarian and Fucalean brown algae.	10
3.1	Calibration of image analysis system to objects of known size.	49
3.2	Minimum resolvable separation (microns) for each component of image analysis system.	49
4.1	DCPP April-May 1984 Emissions at Point of Discharge to the Sea.	92
4.2	Effect Removal Anomalous Data from Analysis of Covariance.	99
4.3	Effect effluent constituents on embryonic sporophyte recruitment; M.pyrifera Series G	100
4.4	Series H embryonic sporophyte recruitment. Comparison mixed effluents to hydrazine alone.	102
4.5	Series I: Effect of 250 ppb/1 day hydrazine pulses on sperm production in Macrocystis gametophytes.	110
4.6	Series I: Effect hydrazine pulses on embryonic sporophyte recruitment.	110
4.7	Series I: Embryonic sporophyte mortality after hydrazine pulse application.	115
4.8	Series J: Spore motility trials; tests of significance using within-group variation.	116
4.9	Series J: Spore germination trials. Tests of significance of effect of hydrazine treatment on degree of spore germination.	116
4.10	Summary of observed pulsed hydrazine inhibition M.pyrifera gametophyte vegetative growth; Series I,J,M,N.	122

Table		Page
4.11	Series J: gametophyte survival in hydrazine pulses. Number surviving gametophytes on Day 12.	123
4.12	Comparison hydrazine sensitivity in several Macrocystis life microscopic life stages.	126
4.13	Summary of M.pyrifera gametophyte growth rates measured by digital image analysis system.	134
4.14	Summary of inhibition of M.pyrifera gametophyte growth in hydrazine as measured by digital image analysis.	135
4.15A	Laminarian brown algae comparison; measured pulsed hydrazine inhibition of gametophytic growth.	150
4.15B	Laminarian brown algae comparison; embryonic sporophyte recruitment in pulsed hydrazine; reported as percent recruitment compared to control.	151
4.16	Laminarian brown algae comparison; logarithmic gametophytic growth rates at 10°C, 24 hr light.	152
4.17	Laminarian brown algae comparison; one-day pulse sensitivity of brown algal species ranked in order of increasing duration of significant inhibition.	152
4.18	Compound toxicity comparison; 96-hour vegetative growth inhibition of Macrocystis pyrifera gametophytes.	168
4.19	Comparison Zn(II) toxicity to M.pyrifera spore germination and gametophytic growth.	173
5.1	DCPP monthly hydrazine emissions; 1982-84. DCPP monthly hydrazine emissions; 1985-87.	199 200
5.2	Emitted hydrazine concentrations exceeding 5 ppb at Diablo Canyon.	203
5.3	Major calendar year 1986 hydrazine releases from Diablo Canyon Power Plant.	206

Table		Page
5.4	Peak monthly hydrazine emissions from San Onofre Nuclear Generating Station, 1984-87.	208
5.5	Emitted hydrazine concentrations exceeding 5 ppb at San Onofre.	210
5.6	Fraction $N_2H_5^+$ in seawater vs. pH & temperature.	215
5.7	Speciation of 8 nM Copper(II) in Seawater with N_2H_4.	217
5.8	Observed hydrazine autoxidation rates in seawater.	225
5.8A	Summary of kinetic parameters for hydrazine autoxidation.	226
5.9	Total copper contents in studied seawaters.	231
5.10	Effect of temperature on initial decay rate and predicted half-life of 10^{-4} M hydrazine in Diablo Cove seawater.	231
5.11	Effect of 0.22 um filtration on hydrazine degradation rate in Diablo Cove seawater.	234
6.1	Analysis of Variance for Series AB area on pulse duration (hours) and concentration (ppb).	257
6.2	Series AB: Vegetative growth inhibition of M.pyrifera gametophytes in pulsed dose assay.	259
6.3	Series AB: Ratio of data to control; M.pyrifera pulsed dose assay.	259
6.3A	Series AF: Mean sizes and fraction inhibitions of M.pyrifera gametophytes after constant doses of pulsed hydrazine.	271
6.4	Series AD: (1) Analysis of variance using Log_e(area) as dependent variable. (2) Analysis of Covariance of Log_e(area).	276
6.5	Series M: One-way analysis of variance of effect of hydrazine concentration in 6-hour daily pulses.	284

Table		Page
6.6A	Series M: Results of Chi-square tests on distribution of embryonic gametophytes among health and size classes.	285
6.6B	Series M: Mean size of embryonic sporophytes in pulsed culture.	287
6.7	Series O: Effect of hydrazine & thermal pulses on sporophyte recruitment.	288
6.A.1	Series AD: Table of means for Log_e(area) with time trend removed.	294
6.A.2	Series AG: Analysis of variance for Log_e(area)	295
6.A.3	Series M: Relative abundance data, sporophyte recruitment. Total counts in 20 random scans at 100X.	296

LIST OF ABBREVIATIONS

ABBREVIATION	DEFINITION
ANCOVA	Analysis of Covariance
ANOVA	Analysis of Variance
ASCII	American Standard Code for Information Interchange
C	Celsius
ca.	circa (Latin: in the neighborhood of)
CG_{50}	concentration required to inhibit vegetative growth by 50%
cm^2	square centimeters
cm	centimeter
DCPP	Diablo Canyon Power Plant
gpm	gallons per minute
hr	hour
LC_{50}	toxicant concentration causing death in 50% of a test population
LRW	liquid radioactive waste treatment system
m^2	square meters
m^3	cubic meters
mg	milligrams
MGD	million gallons per day
ml	milliliter
mm	millimeters
n	sample size

ABBREVIATION	DEFINITION
N_2H_4	hydrazine
nM	nanomolar
NPDES	National Pollutant Discharge Elimination System
p	probability
PCB	polychlorinated biphenyl
%	percent
pixel	picture element
ppb	parts per billion
ppm	parts per million
ppt	parts per trillion
r	regression coefficient
r^2	correlation coefficient
SCUBA	self-contained underwater breathing apparatus
sec	second
SONGS	San Onofre Nuclear Generating Station
TBT	tributyltin
uE	microEinstein
ug	microgram
ul	microliter
um	microns (micrometers)
um^2	square microns
uM	micromolar
X	magnification

CHAPTER 1: INTRODUCTION

I. HISTORY OF TOXICITY RESEARCH USING KELP

Brown algae of the central and southern California coasts are economically and ecologically important parts of nearshore subtidal communities. Different brown algal species typically occupy various ecological niches in subtidal communities (Figure 1.1). One of the fast-growing surface canopy-formers in this group, Macrocystis pyrifera (giant kelp), is commercially harvested for its alginate content (Neushul, 1987). Canopies formed by Macrocystis and Nereocystis luetkeana (bull kelp), form important larval settlement substrates and serve as refuges for juvenile and adult life stages of many invertebrates and fish (North, 1971). Pelagophycus porra (elkhorn kelp) forms subsurface canopy structures in deep water. Other species, Egregia mensziesii, Eisenia arborea, Pterygophora californica, Laminaria dentigera, Laminaria ephemera, and Laminaria farlowii are often important understory components of subtidal ecological communities (Dayton et al. 1984). Wynne & Kraft (1981) described taxonomic relationships among the brown algae (Table 1.1).

Brown algae in the order Laminariales have a dioecious life cycle featuring alternation of generations between a diploid macroscopic sporophyte phase and a free-living haploid microscopic gametophyte phase. Macrocystis' life history is similar to other algae in the order Laminariales (Figure 1.2). The large sporophytes reproduce asexually by releasing motile biflagellated haploid zoospores from

Figure 1.1: Schematic kelp forest diagram showing relative shapes and sizes of brown algal species used in this study.

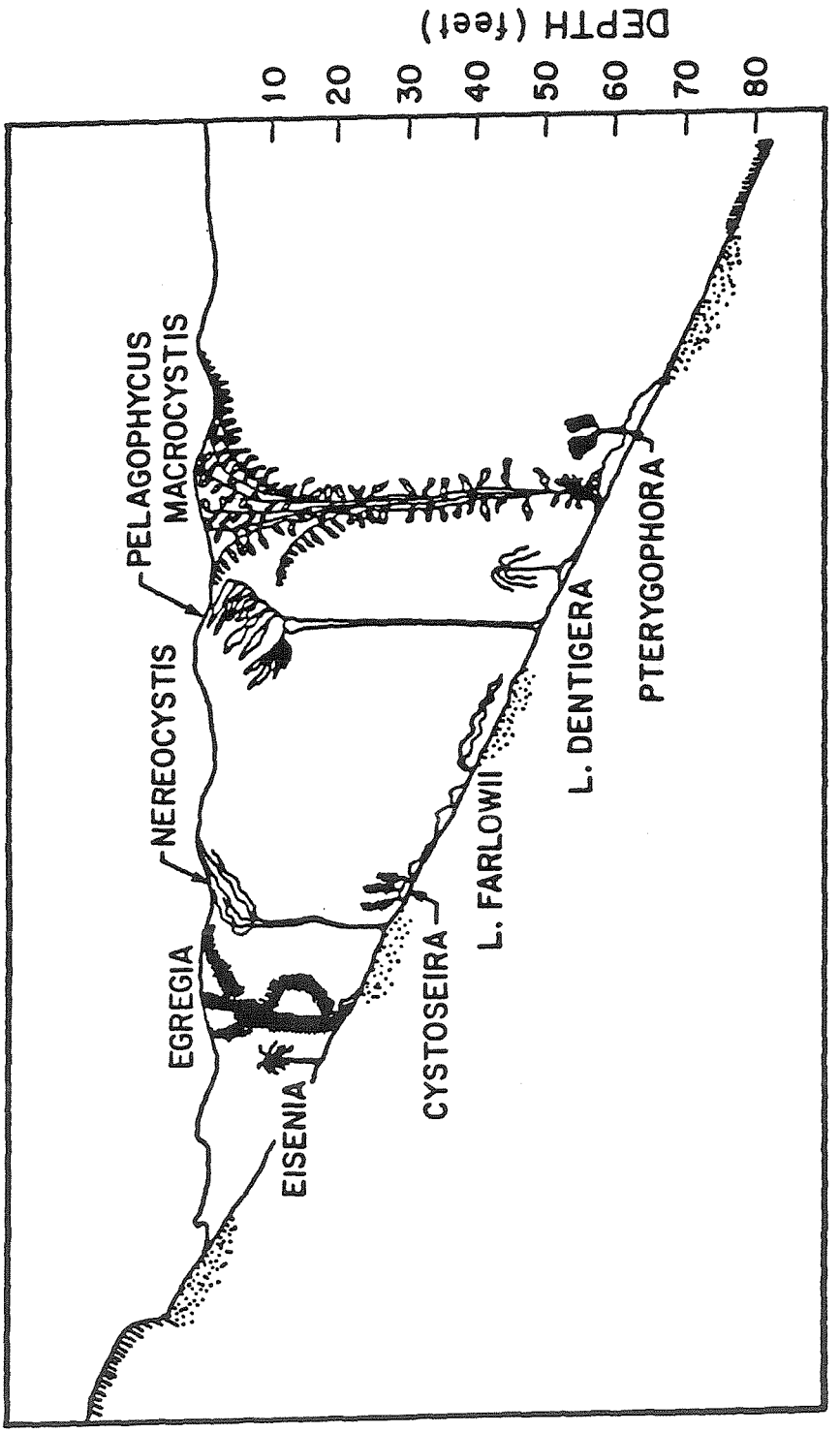

Table 1.1 Taxonomic classification of algae used in this study
After Wynne & Kraft (1981)

Division Phaeophyta

Class Phaeophyceae

Order Laminariales

Family Alariaceae

Genus	Species
Eisenia	arborea
Egregia	mensziesii
Pterygophora	californica

Family Laminariaceae

Genus	Species
Laminaria	dentigera
"	ephemera
"	farlowii

Family Lessoniaceae

Genus	Species
Nereocystis	luetkeana
Macrocystis	pyrifera
Pelagophycus	porra

Figure 1.2: Life cycle of Laminarian brown algae using Macrocystis pyrifera as an example. Dotted region encloses microscopic (10 um – 1000 um) stages used in this study

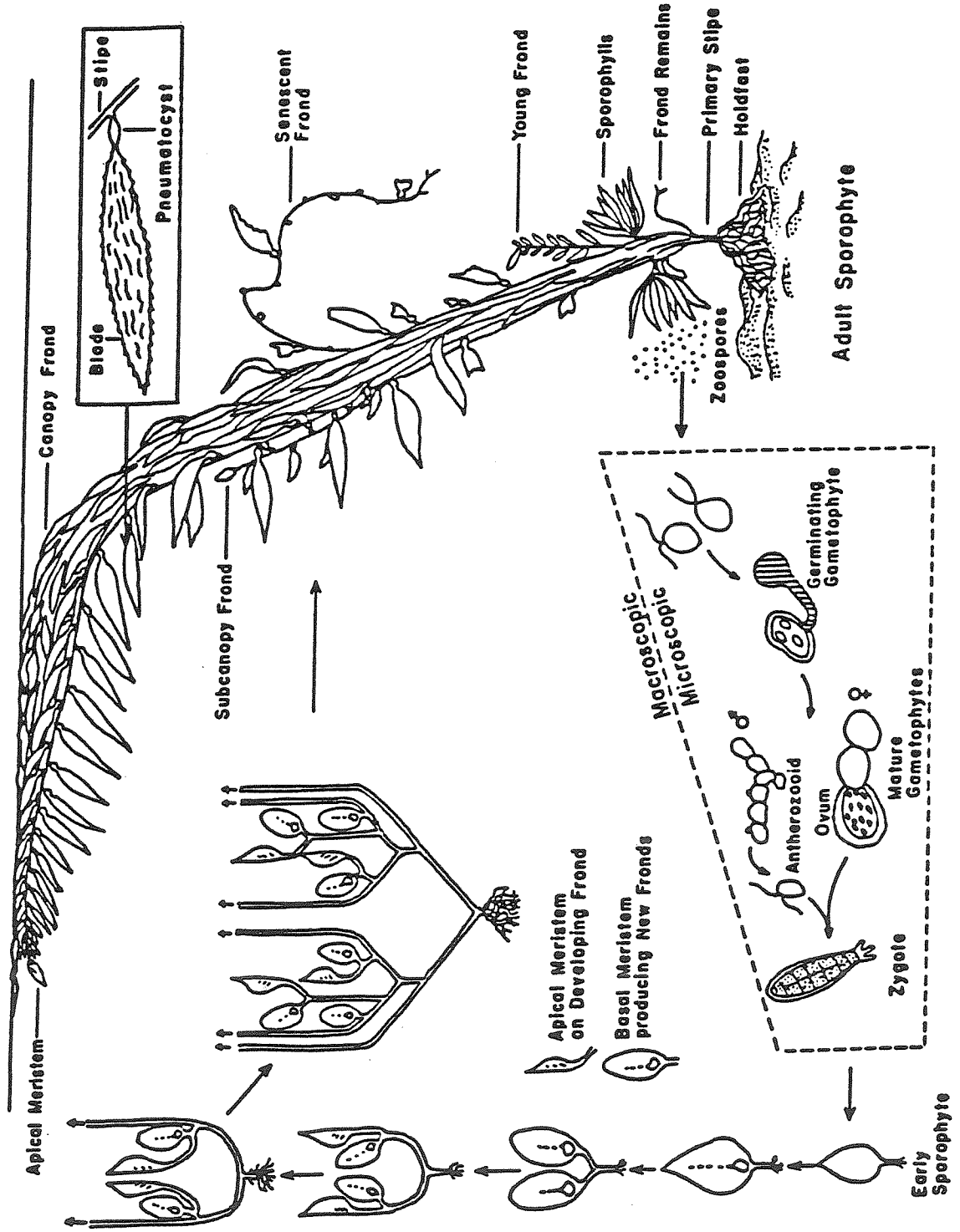

specialized structures on their laminae called sori. The spores eventually settle to the bottom, lose their flagella and germinate to form microscopic male and female gametophytes with characteristic dimensions of 10 to 100 um (Figure 1.2). Gametophytes grow, differentiate in size and become reproductively fertile in two weeks to several months. Males generate specialized reproductive structures called antheridia, which release motile sperm into surrounding waters. Fertile females form an oogonium, which attracts swimming sperm by releasing soluble sex attractants (Muller et al., 1985). Sperm and oogonium unite to form a diploid embryonic sporophyte 100 to 1000 um in size, which then grows to adult dimensions.

Duration and timing of reproductive periods differ among the Laminariales. Macrocystis pyrifera is a perennial, fertile year-round. Egregia menziesii, Eisenia arborea, Laminaria farlowii, Laminaria dentigera, and Pterygophora californica are seasonally fertile perennials typically fruiting in late spring or summer. Nereocystis luetkeana, Pelagophycus porra, and Laminaria ephemera are usually annuals with seasonal fertility.

Human impacts on coastal kelp beds have been studied intensively for about 40 years. The impetus for this research arose from extensive areal decline (example: Figure 1.3) of southern California kelp beds (State Water Pollution Control Board, 1964). These declines seemed to be associated with increasing urbanization. Extensive additional losses of kelp canopy occurred during the 1957-1959 warm-water period now known as an El Nino. By the early 1960's, southern California kelp beds occupied a small fraction of the area observed

Figure 1.3: Historical changes in extent of surface canopy area in kelp beds in the vicinity of San Onofre, northern San Diego County, California.

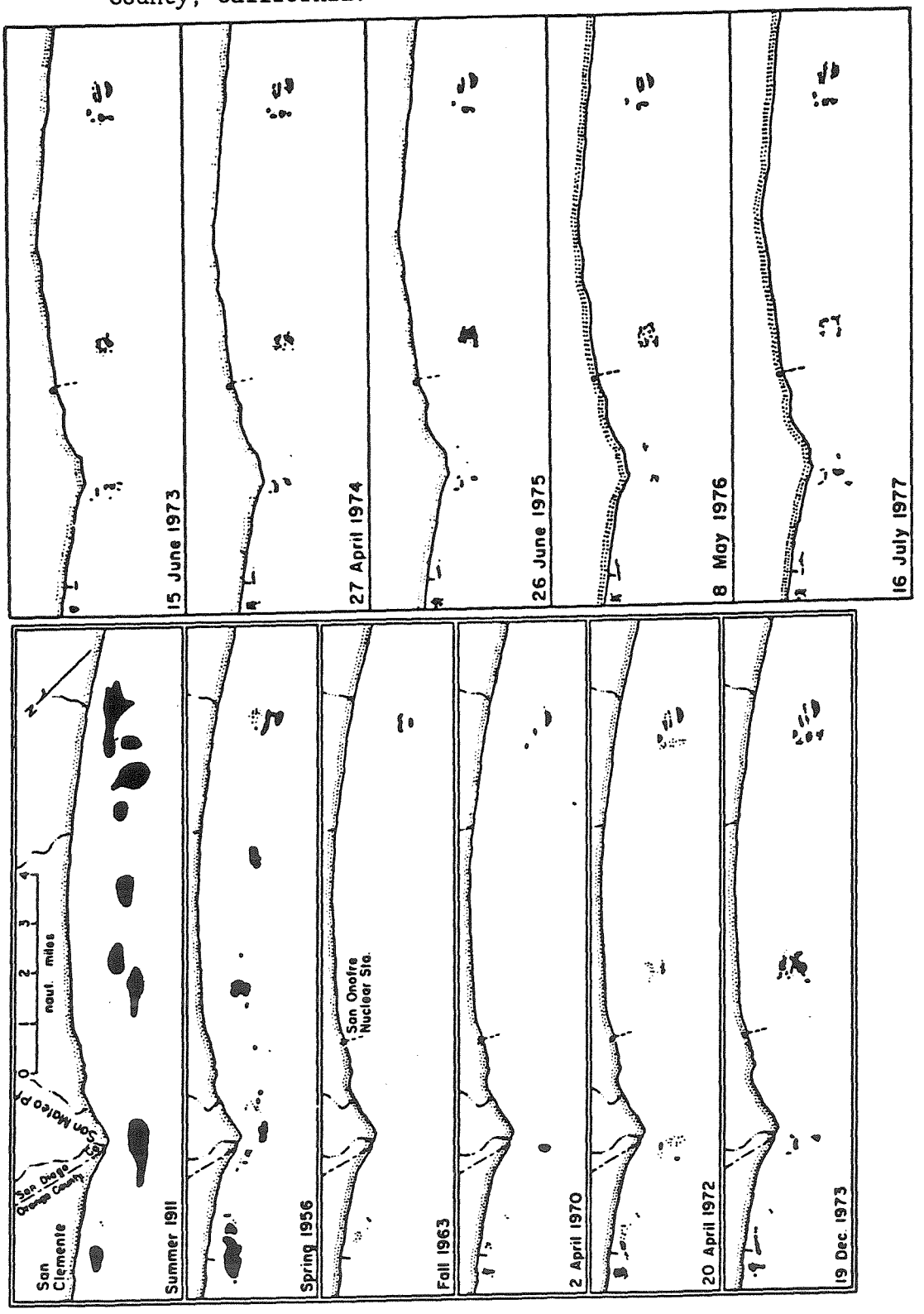

during a survey early in the 20th century (compare top three left-hand side panels, Figure 1.3).

Research on impacts of discharged wastes on kelp began in the mid-1950's. Clendenning (1958, 1959, 1960, State Water Pollution Control Board, 1964) studied the effects of trace metals, detergents, diluted sewage and industrial wastewater effluents on photosynthetic rates of adult Macrocystis pyrifera laminae. Leighton et al. (1966) studied effects of removal of sea urchin predators on kelp bed growth. Reforestation efforts occurred throughout the 1960's and 1970's by transplanting healthy adult plants into areas where kelp beds had formerly existed (Wilson et al. 1977). Coincident with reforestation efforts, concentrations of particles, organic compounds (especially DDT and PCBs) and transition metals in sewage effluents were reduced by several orders of magnitude between 1960 and 1983 because of application of industrial source controls and addition of advanced primary and secondary treatment (Schafer, 1984).

It has been generally accepted that a combination of light attenuation caused by emitted sewage particles, increased urchin predation, and El Nino climatic perturbations were principally responsible for disappearance of kelp beds. Reforestation efforts and improved wastewater quality contributed to a partial recovery of kelp beds since the nadir of the late 1950's and early 1960's. Mechanisms contributing to the original decline, however, were never completely understood. Some kelp beds have yet to recover their former areal extents. Information was missing about potential impacts from anthropogenic activities on reproduction in California brown algae.

Microscopic, embryonic life stages might be expected to be more sensitive than adults to pollutants. Their small sizes reduce the characteristic time for a toxicant to equilibrate with exterior concentrations compared to that of adults. Gametophytes and embryonic sporophytes have thinner cell walls and a smaller portion of their internal volume dedicated to structural purposes, so their capacity to sequester harmful compounds in nonessential tissue might be less than that for adults.

Toxicity assays using brown algal microscopic stages were needed to establish inhibiting concentrations for specific chemicals at or below levels known to have been discharged from wastewater outfalls. Such information might partially explain historic disappearances of kelp beds during the initial period of intensive urbanization and poorly restricted sewage discharges in southern California in the 1940's and 1950's.

Unanswered questions were:

1) Could past or present discharges of compounds from sewage outfalls have contributed to kelp bed decline by inhibiting growth and/or reproduction of microscopic life stages through chemical action?

2) Do the several stages in the microscopic part of the life cycle have dissimilar resistances to a given pollutant discharge?

Light, temperature and nutrient conditions required for optimum growth and reproduction of southern California Macrocystis pyrifera gametophytes are well known (cf. Deysher and Dean, 1984; Kuwabara, 1980, 1981, 1982; Luning and Neushul, 1978), but extant literature

shows scarce information for their toxicity resistance. Smith and Harrison (1978) reported inhibition of Macrocystis pyrifera gametophyte growth by Cu(II) in batch culture. Devinney and Volse (1978) showed that sedimentation could inhibit growth and reproduction of Macrocystis gametophytes. Additional toxic limits could be inferred from work on related topics. Kuwabara (1980, 1981, 1982), and Kuwabara and North (1980) identified micronutrient requirements for Macrocystis gametophytes. Anderson (1982) conducted similar work on blade-stage Macrocystis sporophytes. Some of the trace-metal concentrations used in these studies inhibited vegetative growth and development and could be interpreted as toxicity results.

Working with Atlantic species, Steele and Hanisak (1977) determined toxic levels of crude oil fractions to Laminaria saccharina gametophytes and juvenile sporophytes (Table 1.2). British workers identified toxic levels of several transition metals (Kain & Hopkins, 1971, Thompson & Burrows, 1984) and oil-dispersing detergents (Pybus, 1973) to gametophytes of Laminaria hyperborea. Recent work by State of California personnel determined toxic levels of sodium pentachlorophenate, Zn(II) and domestic sewage to gametophyte germination and reproduction (Martin et al., 1986; Hunt et al., 1987; Anderson et al., 1988).

Available toxicity data indicate that brown algal gametophytes could be sensitive indicators of toxicity in marine waters. They are generally inhibited at concentrations on the order of parts per billion by mass or 10-1000 nM.

Table 1.2: Summary of prior toxicity research using microscopic life stages of Laminarian and Fucalean brown algae. Stage numbers in ( ):

(0): Spore germination (0A): Germ-tube length
(1): Gametophytic growth after treatment during spore release
(2): Gametophytic growth after treatment of older gametophytes
(3): Sperm motility (4): Male gametophyte formation
(5): Embryonic sporophyte recruitment
(6): Embryonic sporophyte growth

Author	Species	(stage)	Compound	Signif. toxicity Concentration
Anderson, et al. 1988	M. pyrifera	(0)	Zn(II)	1700-5500 ppb
	"	(5)	Zn(II)	1100 ppb
Hunt, et al. 1987	M. pyrifera	(0A)	Zn(II)	<560 ppb
	"	(0)	Na-pentachlorophenol	<32 ppb
Kain & Hopkins, 1971	L. hyperborea	(2)	Hg(II)	10 ppb
	"	(2)	Cu(II)	50 ppb
	"	(2)	Zn(II)	250 ppb
	"	(2)	herbicides	10-100 ppb
Martin et al. 1986	M. pyrifera	(5)	Na-pentachlorophenol	<32 ppb
Pybus, 1973	L. hyperborea	(2)	anionic detergent	100 ppm
Scanlan and Wilkinson, 1986	F. serratus	(3)	Dodigen 181-1[1]	0.1 ml/l
	"	(6)	"	0.25ml/l
Smith & Harrison, 1978	M. pyrifera	(2)	Cu(II)	50-100 ppb
Steele & Hanisak, 1977	L. saccharina	(1)	#2 fuel oil	2 ppb[2]
	"	(2)	#2 fuel oil	1-3 ppm[3]
	"	(4)	#2 fuel oil	1-3 ppm[3]
	"	(4)	JP-4	1-3 ppm[3]
	"	(4)	JP-5	1-3 ppm[3]
	"	(4)	Willamar crude	18-28 ppm[3]
	"	(5)	#2 fuel	2 ppb[2]
Thompson and Burrows, 1984	L. saccharina	(2)	Cu(II)	10 ppb
	"	(2)	Zn(II)	100 ppb
	"	(2)	Hg(II)	5 ppb
	"	(2)	Hg(II)-CH_3	0.5 ppb

Footnotes for compounds used:

[1]Hoecsht trade name: marine antifouling compound

[2]Total added oil

[3]Extracted from water after addition at 20 ppm

II. RESEARCH OVERVIEW

Experimental methodology was developed in 1984 using polychlorinated biphenyl compounds both in aqueous solution and sorbed to sediment particles. Funding availability in June 1985 allowed expansion of the scope of the research to include chemical components of cooling water effluents discharged from nuclear power plants sited on coastlines. The intermittent nature of powerplant chemical discharges required a shift of experimental emphasis to designs simulating episodic toxicant releases. Some experiments specifically simulated emissions from the Diablo Canyon Power Plant (Pacific Gas & Electric Company, San Ramon, Calif.), which is a coastally sited nuclear-electric generating station with an across-the-beach cooling water outfall discharging into a 40-acre cove.

Several additional questions were added to the original list:

1) Which chemical constituents of power-plant effluent were most likely to be toxic?

2) Does gametophyte resistance vary seasonally or with locale?

3) Can degree of inhibition be predicted for an accidental power-plant discharge of any duration or concentration?

4) Might sensitivity to a given toxicant differ among the several brown algal species found near Diablo Cove?

5) Could past discharges of compounds from power plants have caused harm to biota in the vicinity of the outfall?

Research activities occurred in two phases over a four-year period.

I) Phase one required 22 months to develop culturing techniques, equipment and software for digital image analysis system, and run 17 screening experiments evaluating initial compound toxicity. The screening experiments, described in Chapter 4, showed that hydrazine was the most toxic compound likely to be discharged in effluent from the nuclear powerplant we were studying.

II) Twenty-seven phase-two experiments covering 25 months narrowly defined toxic ranges for hydrazine, explored impacts of pulsed hydrazine exposures on growth, and developed predictions of vegetative growth inhibition resulting from pulsed exposures.

III. ORGANIZATION OF CONTENTS

Materials and methods are discussed in detail in Chapter 2. Development of digital image analysis methods is separately described in Chapter 3. Screening of several compounds, evaluation of sensitivity of several Macrocystis life stages, and comparison of toxicant resistance among species in the Laminariales are discussed in Chapter 4. Emissions and seawater chemistry of hydrazine are discussed in Chapter 5. Response surface designs using image analysis and estimates of discharge risk are discussed in Chapter 6. Chapter 7 contains the summary and conclusions.

REFERENCES

Anderson, B.S., J.W. Hunt, M. Martin, S.L. Turpen, F.H. Palmer 1988. Marine Bioassay Project; Third Report Protocol Development: Reference Toxicant and Initial Complex Effluent Testing, State Water Resources Control Board, Division of Water Quality Report No.88-7: April 1988.

Anderson, L.M. 1982. Iron Reduction and Micronutrient Nutrition of Juvenile Macrocystis pyrifera (L.) C.A. Agardh (Giant Kelp) Determined by a Chemically Defined Medium, Aquil. Doctoral dissertation, California Institute of Technology, Pasadena, Calif.

Clendenning, K.A. 1958. "Laboratory Investigations", in Annual Progress Report; 1 July 1957 - 30 June 1958; The Effects of Waste Discharges on Kelp. University of California Institute of Marine Resources. Publication 58-11: 4,26-36.

Clendenning, K.A. 1959. "Laboratory Investigations", in Annual Progress Report; 1 July 1958 - 30 June 1959; The Effects of Waste Discharges on Kelp. University of California Institute of Marine Resources. Publication 59-11: 9-13.

Clendenning, K.A. 1960. "Laboratory Investigations", in Annual Progress Report; 1 July 1959 - 30 June 1960; The Effects of Waste Discharges on Kelp. University of California Institute of Marine Resources. Appendix I,II,III.

Dayton, P.K., V. Currie, T. Gerrodette, B.D. Keller, R.Rosenthal, and D. Ven Tresca 1984. Patch dynamics and stability of some California kelp communities. Ecological Monographs. 54(3):253-289.

Devinney, J.S. and L.A. Volse 1978. Effects of sediments on the development of Macrocystis pyrifera gametophytes. Marine Biology. 48: 343-348.

Deysher, L.E. and T.A. Dean 1984. Critical irradiance levels and the interactive effects of quantum irradiance and dose on gametogenesis in the giant kelp Macrocystis pyrifera. Journal of Phycology. 20: 520-524.

Hunt, J., B. Anderson, M. Martin 1987. Interim Summary Report on the Results of Reference Toxicant Testing; February 1, 1987. Granite Canyon Laboratory, California Department of Fish and Game. Prepared for California State Water Resources Control Board. 65pp.

Kain, J.M. and R. Hopkins 1971. Effects of pollutants on Laminaria hyperborea gametophytes and early sporophytes. Marine Pollution Bulletin. 2:78-80.

Kuwabara, J.S. 1980. Micronutrient Requirements for Macrocystis pyrifera (L.) C.A. Agardh (giant kelp) Gametophytes Determined by Means of a Chemically Defined Medium, Aquil. Doctoral dissertation, California Institute of Technology, Pasadena, Calif. 185pp.

Kuwabara, J.S. 1981. Gametophytic growth by Macrocystis pyrifera (Phaeophyta) in response to various iron and zinc concentrations. Journal of Phycology. 17:417-419.

Kuwabara, J.S. 1982. Micronutrients and kelp cultures: evidence for cobalt and manganese deficiencies in southern California deep seawater. Science. 216:1219-1221.

Kuwabara, J.S. and W.J. North 1980. Culturing microscopic stages of Macrocystis pyrifera (Phaeophyta) in Aquil, a chemically defined medium. Journal of Phycology. 16:546-549.

Leighton, D.L., L.G. Jones, and W.J. North 1966. Ecological relationships between giant kelp and sea urchins in southern California. Proceedings of the Fifth International Seaweed Symposium. 5:141-153.

Luning, K. and M. Neushul 1978. Light and temperature demands for growth and reproduction of Laminarian gametophytes in southern and central California. Marine Biology. 45: 297-309.

Martin, M., D. Schlafman, J. Hunt, B. Anderson, L. Espinoza 1986. Selection of an Inorganic Reference Toxicant. Interim Report, Marine Bioassay Project, California Department of Fish and Game May 1, 1986. 23pp.

Muller, D.G., I. Maier and G. Gassman 1985. Survey on sexual pheromone specificity in Laminariales (Phaeophyceae). Phycologia. 24(4): 475-484.

Neushul, P. 1987. "Energy from Marine Biomass: The Historical Record", in K.T. Bird and P.H. Benson (eds.), Seaweed Cultivation for Renewable Resources. Elsevier: New York, pp.69-93.

North, W.J. 1971. "Introduction and Background", in W.J. North (ed.), The Biology of Giant Kelp Beds (Macrocystis) in California. J. Cramer: Lehre, pp.1-97.

Pybus, C. 1973. Effects of anionic detergent on the Growth of Laminaria. Marine Pollution Bulletin. 4: 73-76.

Scanlan, C.M. and M. Wilkinson 1987. The use of seaweeds in biocide toxicity testing. Part 1. The sensitivity of different stages in the life-history of Fucus, and of other algae, to certain biocides. Marine Environmental Research. 21:11-29.

Schafer, H,A. 1984. "Characteristics of Municipal Wastewater Discharges, 1977", in W. Bascom, (ed.), Coastal Water Research Project: Biennial Report: 1983-84. Southern California Coastal Water Research Project: El Segundo, Calif. pp.16-17.

Smith, B.M. and F.L. Harrison 1978. Sensitivity of Macrocystis gametophytes to copper. U.S. Nuclear Regulatory Commission, NUREG/CR-0694; UCRL-52481.

State Water Pollution Control Board 1964. An Investigation of the Effects of Discharged Wastes on Kelp, Publication No. 26, State Water Pollution Control Board: Sacramento, Calif. 124 pp.

Steele, R.L. and D. Hanisak 1977. Sensitivity of some brown algal reproductive stages to oil pollution. Proceedings of the Ninth International Seaweed Symposium. 9:181-190.

Thompson, R.S. and E.M. Burrows 1984. "The toxicity of copper, zinc and mercury to the brown macroalga Laminaria saccharina", in G.Persoone, E.Jaspers, C.Claus, (eds.) Ecological Testing for the Marine Environment, Volume 2, State University of Ghent, Belgium: Ghent, pp. 259-270.

Wilson, K.C., P.L. Haaker, and D.A. Hanan 1977. "Kelp restoration in southern California". in R.W. Krauss (ed.), The Marine Plant Biomass of the Pacific Northwest Coast. Oregon State University Press: Corvallis, pp. 183-202.

Wynne, M.J. and G.T. Kraft 1981. "Appendix: Classification Summary", in Lobban, C.S. and M.J. Wynne (eds.), The Biology of Seaweeds. University of California Press: Berkeley, Calif. 786pp.

CHAPTER 2: MATERIALS AND METHODS

I. COLLECTION OF MATERIALS

Several California coastal locations were sampled for reproductive adult tissue needed to initiate cultures of embryonic life stages (Figure 2.1). Collection frequency and location for all species except Macrocystis pyrifera were determined by seasonal availability (usually late fall through early spring) of reproductive material. Fertile tissues from Macrocystis pyrifera, Nereocystis luetkeana, Laminaria ephemera, Laminaria dentigera, and Pterygophora californica were obtained from Diablo Cove and the immediate vicinity to assure results relevant to the Diablo Canyon Power Plant site. Sporophylls from Eisenia arborea, Egregia menziesii, Laminaria farlowii, Macrocystis pyrifera, and Pterygophora californica were collected from the vicinity of Laguna Beach. Pelagophycus porra was collected from the outer edge of the Pt. Loma kelp bed offshore from the City of San Diego. Macrocystis pyrifera sporophylls were also collected from the vicinity of Big Fisherman's Cove, Catalina Island. Macrocystis' distribution encompassed the entire studied region, and fertile material was available year-round. The majority of my data represent this species because of its broad geographic and temporal availability.

Reproductive tissue was collected by divers using SCUBA techniques. Macrocystis was sampled by plucking sporophylls from plants selected on a random swim path through a kelp bed. Other

Figure 2.1: Collection sites for California Brown Algae

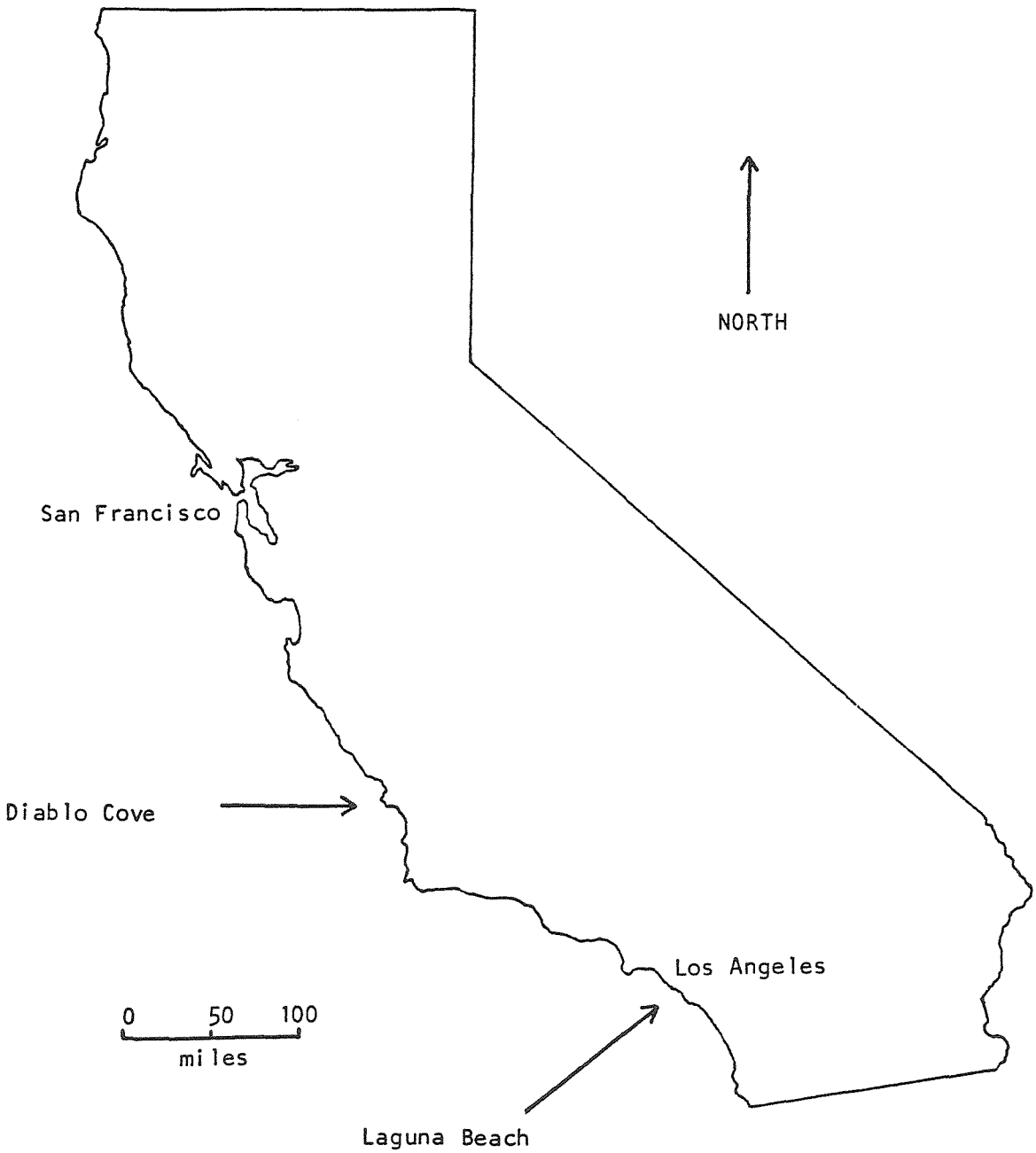

species were sampled by removing entire plants from the bottom. For Egregia, Pelagophycus, and Laminaria ephemera, comparative scarcity and seasonal fertility combined to restrict sampling to single plants selected after diligent searches. Eisenia arborea, Laminaria dentigera, Laminaria farlowii, Nereocystis luetkeana, and Pterygophora californica were haphazardly collected two or three times when fertile material was found.

Macrocystis sporophylls or whole plants of other species were packed in moist paper towels and ice at the collection sites and transported to the laboratory in styrofoam ice chests.

II. CULTURING

Macrocystis pyrifera sporophylls were used whole. For other species, sori were excised from surrounding tissue with a scalpel from collected plants. Intact sporophylls or excised sori were wiped with paper towels to remove encrusting organisms and placed in 0°C chilled, unfiltered offshore seawater to release spores (Figure 2.2). Spore suspensions were transferred after one hour to 37 cm tall, plastic, one litre graduated cylinders for gravitational settling of non-motile contaminants. Spore density was estimated after 90 minutes to 2 hours' storage at 10°C by withdrawing a 50 microliter (ul) sample from 1-2 cm under the liquid meniscus. The sample was placed under a 50 um thick 22 mm x 22 mm cover slip. Spores rapidly become nonmotile in the thin film of water supporting the cover slip, permitting accurate spore counts. Spores were counted by sampling

SCHEME FOR INITIATION OF GAMETOPHYTE CULTURES FROM MACROCYSTIS SPOROPHYLLS

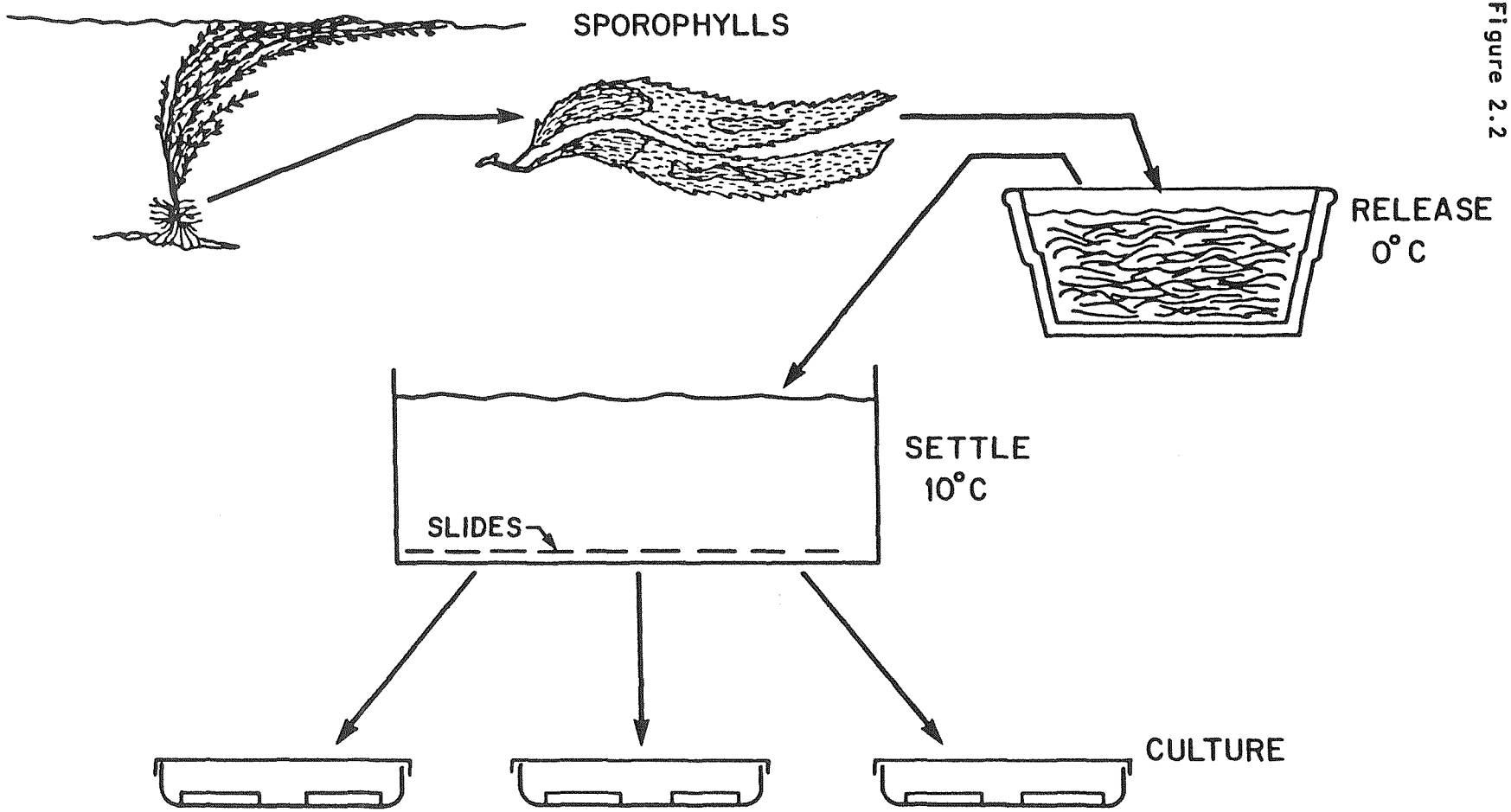

Figure 2.2

10-20 randomly-selected areas with a 16X microscope objective and a 10X eyepiece fitted with a rectangular, crosshatched grid and computing average densities. Data from several aliquots were combined to estimate spore suspension density.

Dilutions required to achieve a target-settled density were calculated from the spore-suspension density as follows:

$$D = E \times p \times d, \qquad (2.1)$$

where D = settled density, E = settlement efficiency (typically 50%), p = spore solution density, d = depth of suspension over slides. A designated volume of spore suspension was diluted to target density with 0.45 micron-filtered unfertilized offshore seawater containing 10 ppm added germanium dioxide (GeO_2) to inhibit growth of contaminating diatoms. The mixture was poured into two-liter, plastic culture containers containing 12-18 glass 75 mm x 25 mm slides, one end frosted. Spores were allowed to settle under continuous 200 microEinsteins per square meter per second (uE/m^2-sec) illumination for 16-36 hours. The settled suspension was then decanted and replaced with our standard culturing medium, 0.45 um-filtered, offshore seawater containing 100 uM added NO_3^- (as $NaNO_3$) and 6 uM added $HPO_4^=$ (as $KHPO_4$). Desired settlement densities were between 5,000 and 15,000 organisms per square centimeter for vegetative growth cultures. Settlement efficiency was typically 50% of the total spore count in suspension. Remaining spores presumably went to container walls or the water-air meniscus.

Gametophytes were grown in a 10 $\pm$ 2 °C walk-in culture chamber originally fabricated for high-volume production of embryonic kelp

plants and described in Anderson and North (1972). Illumination was continuous at 200 uE/m^2-sec irradiance from Westinghouse Cool-White 96" 80 watt fluorescent lamps. Culture temperatures in the 10-12°C range could be achieved by changing position of culture plates within the culture room. Temperatures of 14-16°C were attained in a Vering Scientific refrigerator (Vering Inc. Los Angeles, Calif.). Temperatures exceeding 16°C were achieved by placing culture dishes in proximity to a twin 24 inch-lamp, fluorescent light fixture and controlling ventilation with curtains in an air-conditioned room held at 14 $\pm$ 1°C.

Culture slides were transferred to acid-cleaned 150mm x 25mm polystyrene Petri dishes for toxicant testing. Each culture dish accommodated two slides. No replicate dishes were employed; replication was achieved instead by repeating entire assay sequences at the same concentrations. Positioning of dishes in culture chambers was randomly varied each day to compensate for possible differences in light intensity and temperature in the culture chamber.

Master solutions of toxicant at 100 to 1000 times the target test concentration were prepared in advance and stored under refrigeration alongside the cultures. Volumes ranging from 50 to 2000 ul were withdrawn with adjustable-volume Eppendorf pipettes from toxicant solutions and mixed to desired concentration with 100 ml of filtered, fertilized offshore seawater by vigorous swirling in a 125 ml Erlenmeyer flask. Stirred solutions were then carefully poured into Petri dishes to minimize detachment of gametophytes from slide surfaces.

For exposures lasting longer than 24 hours, toxicant and control solutions were changed daily to minimize micronutrient limitations known to occur in southern California offshore seawater (Kuwabara, 1982). For exposures lasting less than 24 hours, toxicant solutions were replaced with 0.45-um filtered 100 ml macronutrient-enhanced offshore seawater at the end of the exposure period, which was thereafter renewed on a daily basis. Cultures exposed to high concentrations of toxicant were rinsed with 100 ml offshore seawater to dilute residual solution adhering to slide surfaces and container walls before returning organisms to standard culture medium.

III. MEASUREMENT OF TOXICANT EFFECTS

Spore motility was assessed by mixing concentrated spore suspension with 0.45 um-filtered seawater containing specific concentrations of toxicant. Spore suspensions were transferred to 1 ml Sedgewick-Rafter counting chambers, which consist of a 5 cm long x 2 cm wide x 0.1 cm deep pool and 0.5 mm thick coverslip. Two types of tests were conducted. In a Type I test, spores were maintained in the counting chambers on ice packs and alternately counted under the microscope. Control spore cultures tended to deactivate over time in the chambers as they contacted chamber walls, so an alternative test strategy was developed in which spores were maintained in control and toxicant solutions in chilled 400 ml Pyrex beakers. Beakers were alternately sampled by gentle agitation, then withdrawal of one milliliter aliquots for counting in the Sedgewick-Rafter cells. One

toxicant-spiked chamber and a control chamber cell were repeatedly measured over a 1 hour period, alternating between chambers, regardless of the type of exposure method. Motile spores in randomly selected fields of view were tallied in each chamber and results statistically compared.

Spore germination and vegetative growth were measured by placing the slides in a wet-well holder constructed to retain a 75mm x 25mm culture slide and a 1.5-2 ml overlying layer of seawater, giving a water film thickness of 0.8-1.1 millimeters. Slides were transported in their Petri dishes from culture room to the microscopy area in a shaded box and held in the same dishes on ice packs during measurement. Slides were returned to culture dishes if measurements required more than five minutes to minimize heating effects on live cultures. Cultures were repeatedly viewed over periods lasting from one to four weeks.

Slides were randomly scanned with a 16X objective and 10X ocular containing a calibrated crosshatched grid to estimate settled spore density and degree of germination. Spores that remained round were counted as nongerminated. Spores producing germ tubes were counted as germinated.

Vegetative growth of germinated gametophytes was assessed by periodic measurements of either the longest dimension with an eyepiece micrometer, or cross-sectional area using digital image analysis.

a) Micrometer methods: Microslides were randomly scanned with 10X, 16X or 20X microscope objectives. The organism nearest the center

of the field of view was selected for length measurement. Sample sizes, typically 20-40 individuals per treatment, were kept constant throughout a two-week experimental run.

b) Digital image analysis: Organism sizes were measured within randomly chosen fields depicted by the computer as a square on the video screen. Images were digitized and contiguous areas of all nonoverlapping organisms within the square field were automatically calculated. Digital methods employed a fixed number of scans per treatment. Sample sizes from digital measurements were not constant because organism counts varied among scans. Numbers of scanned organisms generally declined as cultures aged because of losses from slide surfaces and increasing occurrences of overlap of adjacent organisms as they grew larger. Development of digital methods is discussed in detail in Chapter 3.

Toxicant effects were assessed by comparing vegetative growth of test cultures to controls using two-tailed Student's t-tests (Alder and Roessler, 1972) and analyses of variance and covariance (Sokal and Rohlf, 1981; STSC Inc., 1987). The criterion for significance of an effect was set as $p < 0.05$ for all tests. Lower probabilities were reported when they were obtained.

Sporophyte recruitment was estimated by random positioning of microscope slides under 10X or 16X objectives with a 10X eyepiece fitted with the calibrated crosshatched disk. Sporophytes falling within the hatched area were counted and abnormalities noted. Toxicant effects were estimated by comparing treated cultures to

controls using nonparametric statistical methods (Alder and Roessler, 1972; Bray, 1988; Sokal and Rohlf, 1981).

IV. STATISTICAL METHODOLOGIES

Parametric statistics were used to compare data sets for gametophyte lengths and areas. Random size samplings from brown algal gametophyte cultures often yielded size data that were not normally distributed. One tail of the size distribution was often skewed to larger sizes in cultures aged one week and older (Figure 2.3). Variances usually increased proportionally with the means as cultures aged. If this was detected, raw data were transformed to their natural logarithms to stabilize variances. Transformations permitted comparisons of control and treated cultures by rendering variances homogeneous. Means computed from log-transformed data ("geometric" means) were usually smaller than means calculated from the original data. Geometric means were back-transformed prior to graphic display. Influences from log-transformations on means, standard deviations and 95% confidence limits usually did not alter determinations of significance as computed from untransformed data. Occasionally transformations did not render variances homogeneous. Significance tests relying on pooled data were avoided if this was found to be the case.

Significance of results was initially assessed by computing 95 percent confidence limits from the sample size (n) and standard deviation:

$$95\%\ \text{conf.} = \text{std.dev.} \cdot t_{95} / (n-1)\ , \qquad (2.2)$$

Figure 2.3: Example of broadening of gametophyte size distribution with time. Data shown for Pterygophora californica Series C control culture.

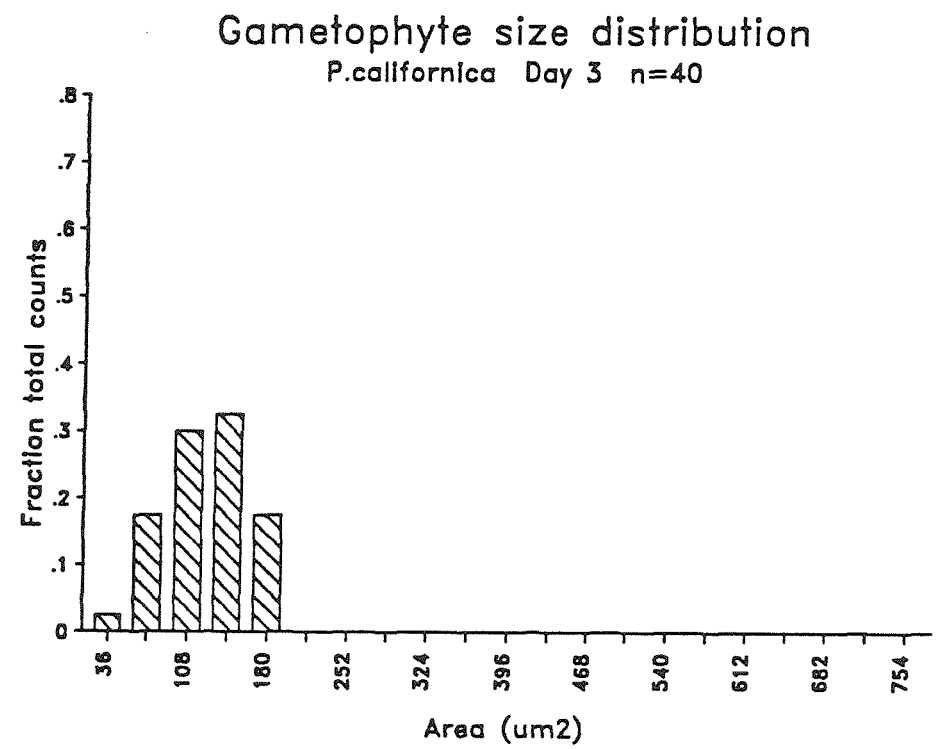

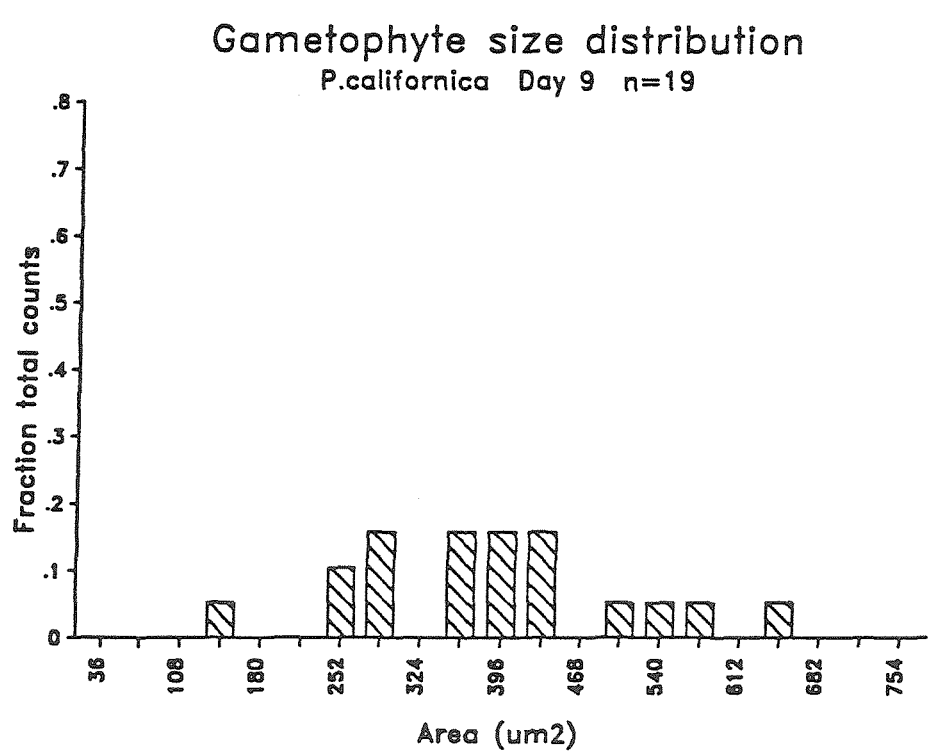

where t_{95} is the two-tailed tabulated Student's t-value for n-1 degrees of freedom as found in standard statistical tables (Rohlf and Sokal, 1981). The assumed null hypothesis when comparing means from two samples is that the samples were drawn from populations with identical means. The null hypothesis was rejected at the 5 percent confidence level if the confidence limits from the two samples did not overlap.

An alternative method of computing t-statistics for comparison of data from two samples employs a pooled standard deviation, which is computed using data from both samples (Alder and Roessler, 1972). A t-value is computed directly from the data and compared to tabulated values of t for $n_1 + n_2 - 2$ degrees freedom, where n_1 and n_2 are sizes of the two samples. This method assumes that samples are drawn from populations with identical standard deviations even if the means are found to be different. The pooled standard deviation method was avoided because this assumption was not valid for our experimental systems. Measured standard deviations increased proportionately with means as cultures grew with time and occasionally did not stabilize when transformations were applied. Standard deviations in control cultures became large with time because of a distribution of growth rates in tested cultures. Fertile gametophytes usually grew more slowly than non-fertile organisms causing the size distribution of randomly sampled organisms to spread with time. Cultures which been inhibited by toxicants and did not grow had much smaller standard deviations than control cultures.

Student's t-statistics proved to be conservative estimates of significance. Student's t-tests occasionally indicated no significant difference between means that proved significantly different when tested by a combination of ANOVA and a priori multiple range tests (Sokal and Rohlf, 1981). ANOVA and multiple-range tests were used to make the final determination of significance if data satisfied conditions of independence and homogeneity.

Two types of nonparametric statistics were employed for analyzing counts of viable organisms obtained from random scans of slide surfaces with a cross-hatched reticule (spores, sperm, sporophytes):

1) Wilcoxon rank-sum tests. (Alder and Roessler, 1972; Sokal and Rohlf, 1981),

2) Complete and sampled randomization tests (Bray, 1988; Sokal and Rohlf, 1981).

Nonparametric statistical tests were used because experimental organism counts were seldom normally distributed. Normal, or near-normal distributions are required for valid outcomes of parametric tests such as Student's t-test or ANOVA (Alder and Roessler, 1972).

Randomization tests employ the following strategy (Sokal and Rohlf, 1981):

> "(1) Consider an observed sample of variates or frequencies as one of many possible but equally likely different outcomes that could have arisen by chance.
> (2) Enumerate the possible outcomes that could be obtained by randomly rearranging the variates or frequencies.
> (3) On the basis of the resulting distribution of outcomes, decide whether the single outcome observed is deviant (=improbable) enough to warrant rejection of the null hypothesis. In other words, is the probability of obtaining an observation as deviant as or more deviant than the single outcome less than the desired significance level?"

Exact randomization tests can be performed when sample sizes are small enough to keep the total number of combinations of random rearrangements of the data small. Total combinations rise rapidly with increasing sample size.

For comparison of two samples of unequal size,

$$\#\ \text{combinations} = (n_1 + n_2)!/\ (n_1! \cdot n_2!). \qquad (2.3)$$

For comparison of two samples of equal size,

$$\#\ \text{combinations} = (2n)!/\ (n!)^2. \qquad (2.4)$$

The "!" indicates a factorial. A sample table illustrates growth in number of combinations for equal sample sizes:

n in each sample	# of combinations
5	252
10	184,756
15	155,117,520
20	13,784,652,880

Computer time and memory limitations make complete randomization trials for large samples infeasible, so sampled randomization trials are performed using only a fraction of the possible combinations. The difference between means (or other test statistics) are computed from 500 or 1000 randomly selected recombinations of the pooled original data and compared to the values that were actually obtained in the experiment. If only a small percentage of the random recombinations exceeds the value obtained in the original experiment, then it is concluded that the observed experimental outcome had a small probability of occurring by chance. Confidence limits must be applied to percentages calculated from sampled randomizations (Sokal and Rohlf, 1981; Rohlf & Sokal, 1981). Computer routines (Bray, 1988) were made available to the author to facilitate analysis of data sets

by complete and sampled randomizations. These methods were used extensively to test of significance of toxicant effects on sporophyte recruitment (Chapter 4).

Errors arising from computation of powers, products or quotients of two uncertain quantities were treated by propagation-of-error methods described in Bevington (1969). Propagation-of-error theory was employed in estimation of magnitude of machine error in the digitization process and when computing ratios of treated means to control means. The essence of the theory is that for a quantity x which is a function of several variables:

$$x = f(u,v, \ldots) \tag{2.5}$$

each of which has a known mean and variance, the uncertainty of x is given by:

$$\sigma_x^2 \simeq \sigma_u^2 \left(\frac{\delta x}{\delta u}\right)^2 + \sigma_v^2 \left(\frac{\delta x}{\delta v}\right)^2 + 2\sigma_{uv}^2 \left(\frac{\delta x}{\delta u}\right)\left(\frac{\delta x}{\delta v}\right) + \cdots \tag{2.6}$$

Assuming that the fluctuations of u and v are uncorrelated, the expression simplifies to:

$$\sigma_x^2 \simeq \sigma_u^2 \left(\frac{\delta x}{\delta u}\right)^2 + \sigma_v^2 \left(\frac{\delta x}{\delta v}\right)^2 + \cdots \tag{2.7}$$

An example would be the computation of a quotient:

$$x = \pm \frac{au}{v} \tag{2.8}$$

Substitution of this expression for x into (2.6) gives

$$\frac{\sigma_x^2}{x^2} \simeq \frac{\sigma_u^2}{u^2} + \frac{\sigma_v^2}{v^2} - 2\frac{\sigma_{uv}^2}{uv} \tag{2.9}$$

For computations of ratios of treated means to control means, 95% confidence limits were substituted for sample variances in (2.9). This was done to facilitate comparison of 95% confidence limits of ratios computed from differently-sized samples. (Variations in sample size arose from variable gametophyte counts obtained in a fixed number of scans with the digital image analysis system.)

Treatment of data by this method resulted in typical 95% confidence limits on ratios of $\pm$ 20%; e.g., the ratio of a toxicant mean area to control mean area would be 0.60 ± 0.20. This data treatment tended to obscure significant differences in the original dimensional data and was only employed when comparison of data of unequal magnitudes from different experiments was necessary (i.e., the mean control size in one experiment was twice the size of the control mean in another experiment and comparisons of degree of inhibition of a certain concentration of toxicant were desired).

REFERENCES

Alder, H.L. and E.B. Roessler 1972. Introduction to Probability and Statistics; 5th edition. W.H. Freeman, Inc.: San Francisco, Calif. 373pp.

Anderson, E.K. and W.J. North 1972. Chapter 8 in Kelp Habitat Improvement Project Annual Report; 1971-72. W.M. Keck Engineering Laboratories, California Institute of Technology: Pasadena, California, 84pp.

Bevington, P.R. 1969. Data Reduction and Error Analysis for the Physical Sciences. McGraw-Hill Book Company: New York, 336pp.

Bray, R. 1988. Random-T; Non-parametric sampled randomization program for comparison of means of two samples. California State University: Long Beach. Magnetic media.

Kuwabara, J. 1982. Evidence for cobalt and manganese deficiency in southern California offshore seawater. Science. 216:1221-1225.

Rohlf, F.J. and R. R. Sokal 1981. Statistical Tables, 2nd edition. W.H. Freeman Press: San Francisco, Calif. 219pp.

Sokal, R.R. and F.J. Rohlf 1981. Biometry, 2nd edition. W.H. Freeman Press: San Francisco, Calif. 859pp.

STSC, Inc. 1987. Statgraphics; version 2.6 STSC Inc.: Rockville, Maryland. Magnetic media.

CHAPTER 3: USE OF DIGITAL IMAGE ANALYSIS IN KELP BIOASSAYS

I. BACKGROUND

Brown algal gametophytes differentiate during growth into a wide variety of sizes and shapes. Shapes depend on age, sex and fertility. (Levyns, 1933; Luning and Neushul, 1978). Sexual differences become apparent about a week after complete germination. Fertility is triggered by environmental conditions (Cosson, 1977; Deysher and Dean, 1984, 1986; Luning and Neushul, 1978). Females will either stay infertile and grow vegetatively to large size or become fertile, remaining small and protruding an ovum. Males show a similar pattern but exhibit different shapes, being typically narrower and less densely pigmented than females (Figure 3.1).

The wide distribution of gametophytic sizes and shapes introduces difficulties for accurately assessing mean size in a random sampling of organisms. Traditional measurement methods used an eyepiece micrometer. The gametophyte of interest was moved to the center of field of view, a ruled line (installed in the microscope eyepiece) superimposed on the longest dimension, and the data recorded (Figure 3.2). A random sampling of organism lengths determined by eyepiece micrometer may not be an accurate estimate of mean culture biomass, since gametophytes exhibit a variety of shapes at ages exceeding one week. It is possible to measure several dimensions of a

Figure 3.1: Representative sizes and shapes of fertile and vegetative gametophytes. Magnification approximately 800x

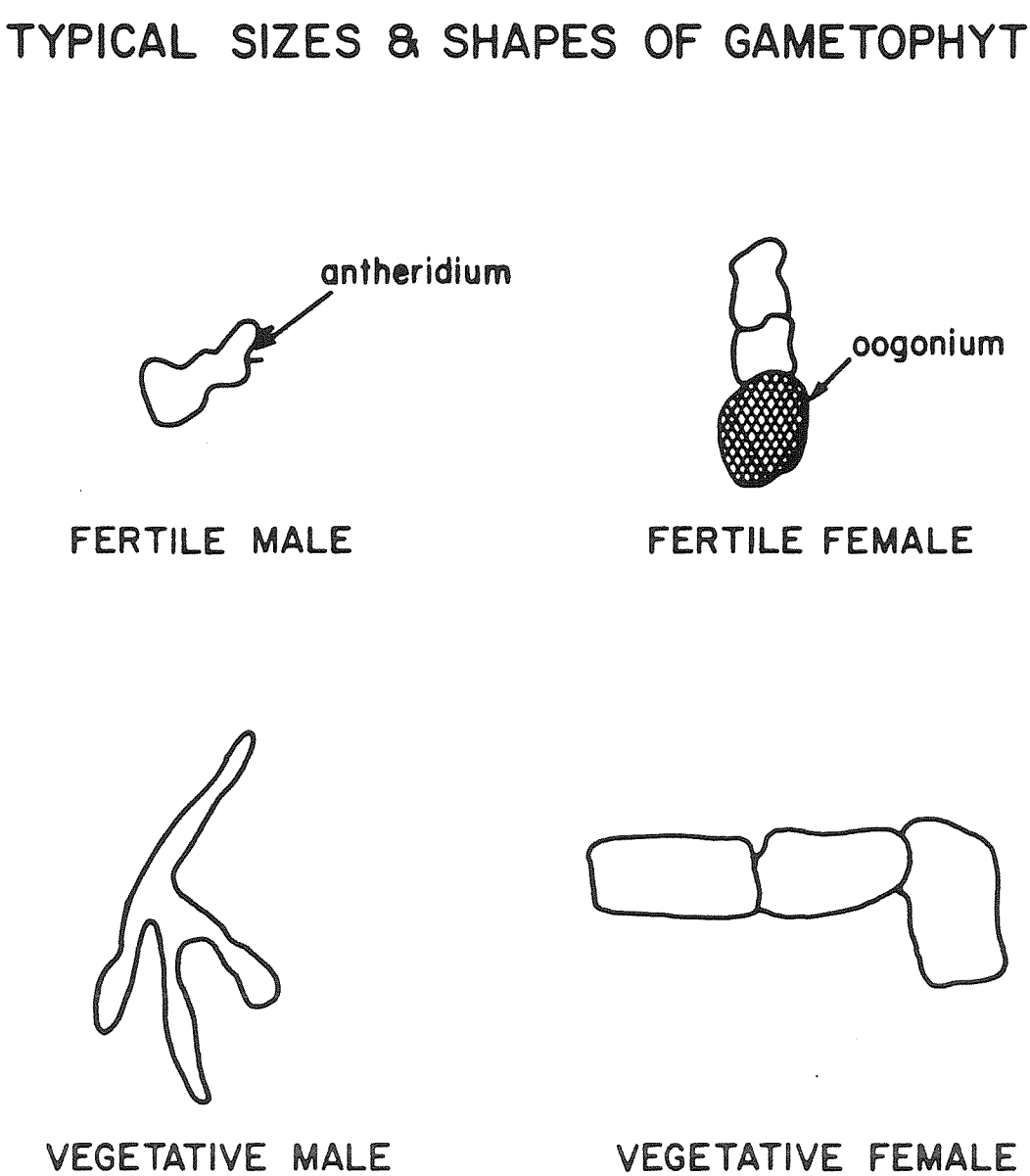

Figure 3.2: Measurement of gametophytes with eyepiece micrometer. Ruled line is positioned over longest dimension and the number of divisions counted. Last significant digit (e.g. the 6 in 2.6 divisions) estimated by visually interpolating between divisions.

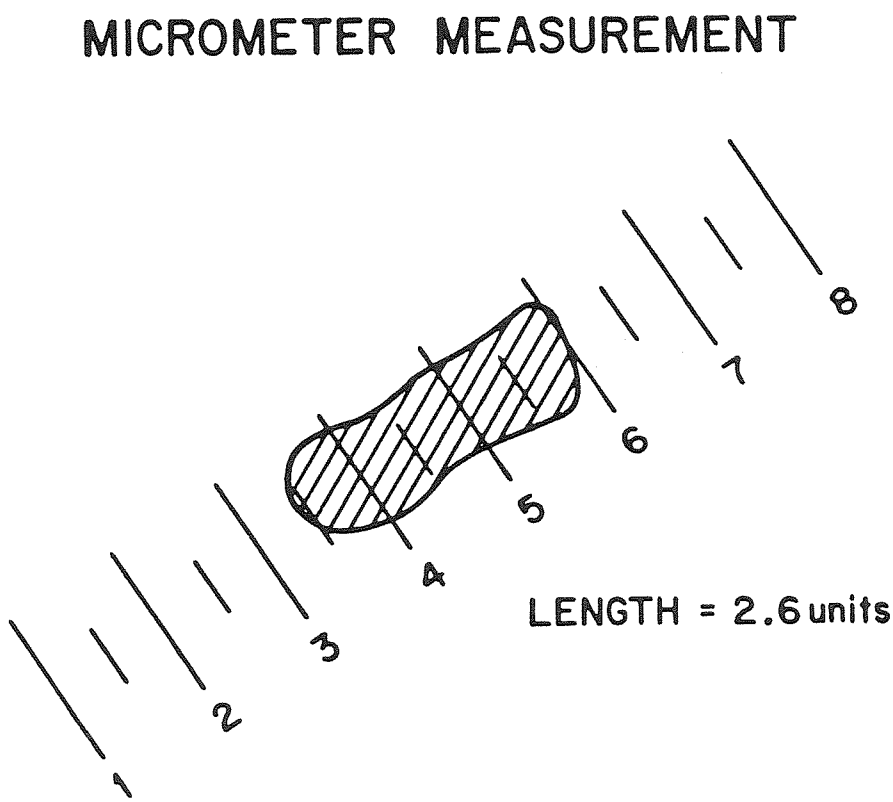

given gametophyte with a micrometer, but this alternative has several disadvantages:

1) Longer exposure times in an environment of high-intensity illumination and warm ambient temperature occur for each culture slide, increasing risk of damage to live gametophytes.

2) Measurement and data logging time increase, raising operator fatigue and impairing objective judgement.

Multiple measurements with an eyepiece micrometer in experimental designs of modest size would thus require many hours' tedious viewing and data entry. Digitization of video microscopic images offered optimal possibilities for increasing both accuracy and rates of data acquisition as well as rapid, accurate measurements of true gametophyte size.

Inexpensive microcomputer-based image analysis equipment became available in 1985. Image analysis has been recently applied to the measurement of phytoplankton (Furuya, 1982), bacterioplankton and nanoplankton (Bjornsen, 1986; Sieracki et al., 1985; Estep et al., 1986), analysis of sewage particle shapes (Wang, 1988); and measurement of mycelial filaments (Adams and Thomas, 1988).

Techniques of image analysis have been described by Castleman (1979); Green (1981); and Pratt (1978). A video signal or photograph is first scanned and converted into a two-dimensional spatial array of binary numbers. The process is somewhat akin to laying a fine square-mesh screen over an image, measuring the light intensity in each picture element (pixel), then recording position and intensity of the pixel as a set of three numbers in the form (x,y,intensity);

(Figure 3.3). Pixel data stored in computer memory can then be manipulated to analyze image features. An irregularly shaped gametophyte can be easily separated from the background on the basis of intensity difference and the area calculated, by adding up all the pixels within its boundary.

II. MATERIALS AND METHODS

The SSP(r) Image Analysis System, developed by Carl Zeiss, Inc. (Thornwood, N.Y.), was selected as the least expensive off-the-shelf system which would meet requirements for automated image analysis. The system consists of a Zeiss Axioplan(r) microscope, black and white video camera, and a microcomputer containing a "frame-grabber" digitizing board, monitor controller card and other display and recording devices (Figure 3.4).

Gametophytes were imaged by Koehler brightfield illumination (Inouye, 1986) using 546 nanometer (nm) green light to obtain the highest possible contrast between background and organism. Images from Zeiss Neofluar(r) microscope objectives magnified through a 10X trinocular tube were converted to EIA standard video signals by a Hitachi KP-120U CCD-type video camera (Hitachi Denshi Ltd, Woodbury, N.Y.). Video and computer signals were simultaneously displayed on a Sony PVM-1271Q video monitor controlled by a Zeiss SMC-1 monitor controller card (Max Erb Instrument Company, Burbank, Ca.). Images were digitized by a Tecmar Video Van-Gogh(r) frame-grabbing board (Tecmar Inc., Cleveland, Ohio) with full-frame resolution of

Figure 3.3: Simple example of conversion of brightness in each square of the grid to a numerical pixel intensity. Object and background each assumed to have uniform brightness. Edge pixel brightness a function of proportion of area occupied by object (Figure 3.7)

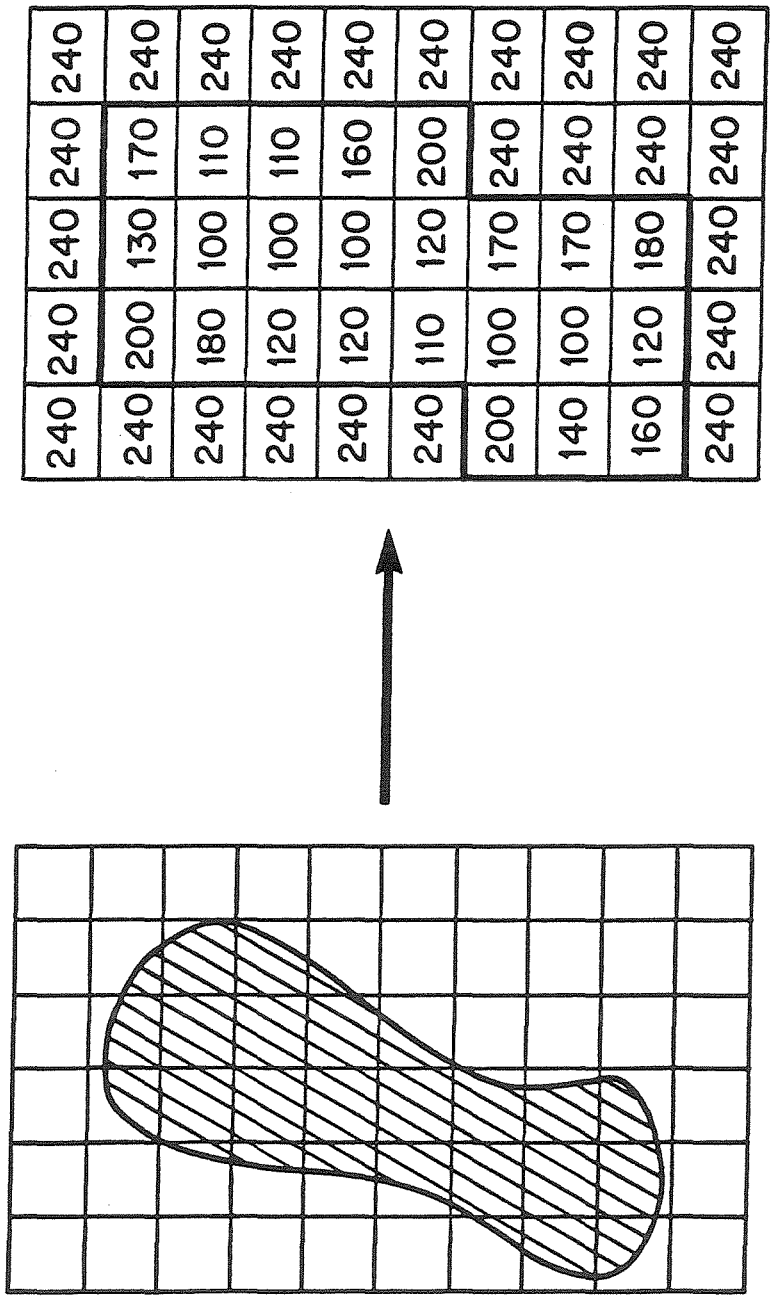

Figure 3.4: Schematic diagram of components of image analysis system.

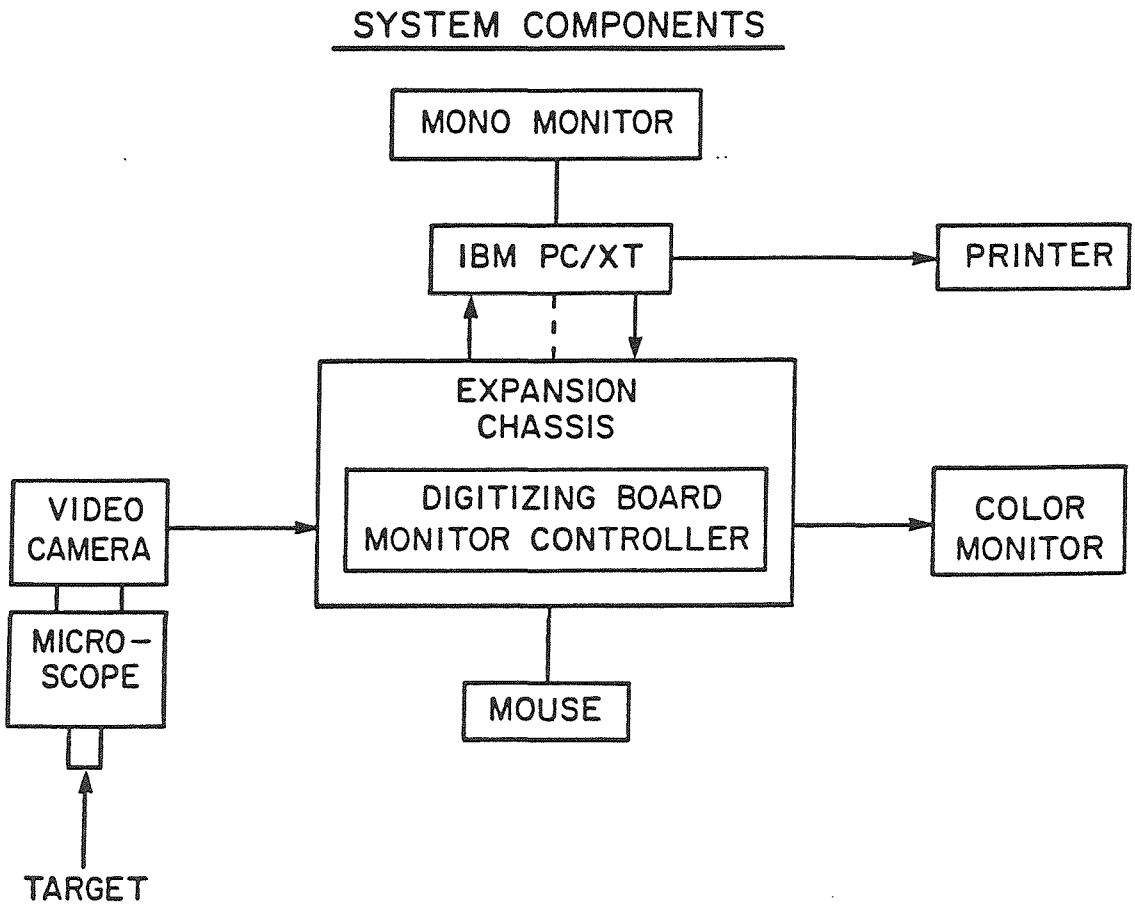

256 x 256 pixels x 8 bits per pixel. With optimum illumination and a stable camera signal, each pixel in the array was assigned a numerical intensity (grey level) on a scale of 0 to 255 (8 bits, 2^8=256 possible values), with 0 equivalent to black and 255 to white. Grey level data were stored in random access memory of an IBM PC-XT-5160 microcomputer (International Business Machines, Boca Raton, Florida) using the IBM PC-DOS 3.10 operating system.

Software for analyzing the digitized images was written in the Turbo Pascal(r) 2.0 and 3.0 programming languages (Borland International, Inc., Scotts Valley, CA.) during the summer of 1986. The programs, named Eyeball 2.1 (Horiuchi, 1986a) and Imageplot 3.1 (Horiuchi 1986b) analyze video images using the following scheme.

Video images were superimposed on the monitor with a software-generated square cursor outlining the area to be digitized (Figure 3.5). The square corresponded to a 100x100 pixel array in the center of the image. The frame-grabbing board digitized the array on software command and placed the information in the random access memory of the computer.

Acquired images were analyzed to separate gametophytes from the background using a process called global thresholding (Castleman, 1979). Intensity thresholds were set to include pixels corresponding to biological specimens but exclude background pixels. Gametophytes were darker than the background when imaged with brightfield microscopy. Thresholds were typically set to include the lower three-fourths of the intensity range but exclude the intensity maximum corresponding to the background. The grey-level value of each pixel

Figure 3.5: Sketch of software-generated screen prompts and square frame surrounding two irregularly shaped target organisms. Frame delineates a 100 pixel x 100 pixel x 256 grey-level box. Arrow shows left-to right direction of motion of vertical cursor which indicates progress of frame digitization. Memory and disk storage requirements per frame: 10,240 bytes.

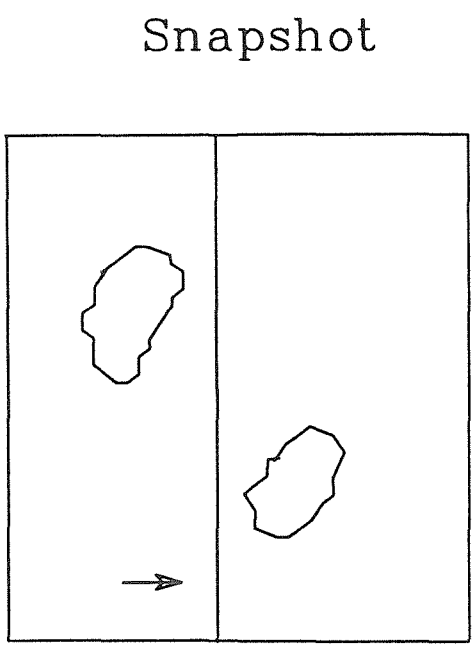

in the image was then compared to the preset lower and upper brightness thresholds. If it was between threshold settings, a spatially corresponding pixel in a new memory array was assigned the value 1. Pixels with intensities outside the thresholds were assigned the value 0. This procedure simplified the image representation from eight bits per pixel to one bit per pixel, reducing the total amount of manipulated information by a factor of eight and enhancing computational speed.

Sizes were calculated for all objects formed from contiguous areas of retained pixels by applying a scale factor appropriate for the microscope magnification. Size distribution was then computed for the objects. A minimum size threshold was set to remove most visual "contaminants" smaller than gametophytes (bacteria, phytoplankton, small sediment particles and optical flaws) from the analyzed image. A maximum size threshold was occasionally set to remove very large objects formed by overlapping gametophytes. Once set, the size thresholds automatically eliminated objects too large or too small from computations of gametophyte size.

The step after elimination of optical contaminants involved filling "holes" formed in the retained images by nonuniform intensity distributions in the area within the organism boundary. Holes occurred because light absorption was not spatially uniform within the organism. Cell walls typically absorb more light than cytoplasm. Organism edges may thus appear darker than the interior when viewed from above with transmitted light. Holes reduce calculated object size below its true value because missing pixels

are not added into the total representing the object area. Computer routines were developed (Horiuchi, 1986a) to fill multiple holes within an object boundary. Areas of retained objects were then recalculated to correct for the hole-filling operation.

Data from the completely analyzed image were stored as ASCII files on the Seagate ST-225 hard disk of the IBM microcomputer. Information was stored in the following format:

FILE LISTING	TYPICAL VALUE
N (number of organisms in field of view)	6
Mean size of organisms in pixels	67.233
Multiplication factor for magnification used	1.795
Data point #1 (in pixels)	70
Data point #2 "	65
Data point #3 "	58
. . . . . "	..
. . . . . "	..
Data point #6 "	68

One to ten organisms were typically contained in a single scanned image. A typical measuring run consisted of ten scans per slide and two slides per treatment for a total of 20 scans per treatment. Files from individual scans were combined into larger files containing data for a given treatment and measurement day. Usual sample sizes in these combined files ranged from 25 to 70. Data files acquired from different treatments could be analyzed graphically or compared using standard statistical tests.

III. CALIBRATION AND ERROR ANALYSIS

The process of converting a continuous image signal into a digital representation of an object introduced errors of both accuracy and precision into determination of gametophyte areas.

A) DIGITIZER CALIBRATION

Video images of a 50 um x 50 um ruled grid from an American Optical No. 1492 hemacytometer (American Optical Instrument Company, Buffalo, N.Y.) were used to calibrate the size accuracy of the image analysis system. A least-squares linear regression was performed on log-transformed data to develop a relationship describing change in pixel area with magnification (Table 3.1). The regression yielded the best results for objective magnifications between 10X and 100X, giving estimates within 3 percent of the true value. Sizes were poorly estimated at 2.5X, where error was 14 percent. The size calibration regression was incorporated into custom software written specifically for gametophyte analysis (Horiuchi, 1986a).

B) HARDWARE ERRORS

1) Resolution: High resolution is defined as the ability to distinguish two objects that are very close together as separate (Inouye, 1986). Ultimate resolution in optical microscopy is limited by a relationship among the numerical apertures of the microscope condenser and objective and the wavelength of the illuminating light (Inouye, 1986):

$$D = \frac{1.22 \times \text{lambda}}{NA_{obj} + NA_{cond}} , \qquad (3.1)$$

where D = separation distance lambda = light wavelength

NA = effective numerical aperture of light-focussing device.

Table 3.1: Calibration of image analysis system to objects of known size. Regression equation: Area = $718 \cdot (\text{objective magnification})^{-2}$

Objective Magnification	Actual area pixels	Calculated area pixels	Error
2.5 X	100.0	114.9	+14.9 %
10.0	6.97	7.18	+ 3.01
20.0	1.782	1.795	+ 0.73
40.0	0.436	0.449	+ 2.92
100.0	0.070	0.072	+ 3.02

Table 3.2: Minimum resolvable separation (microns) for each component of image analysis system (see text) and for eyepiece micrometer. Data plotted in Figure 3.6

Objective Magnification	Microscope Optics	Video Camera line separation	Digitizer grid size	Eyepiece micrometer
2.5 X	2.42 um	2.78 um	20.0 um	19.5 um
10.0	1.33	0.69	5.78	5.0
20.0	0.95	0.35	2.66	2.5
40.0	0.70	0.17	1.32	1.2
100.0	0.44	0.07	0.52	0.5

We assumed illumination by green light (lambda = 546 nm) when calculating resolutions of the objectives and condensers used in this study (Figure 3.6).

2) Conversion of the optical signal into a video signal.

The fixed number of scan lines in a video camera might reduce resolution below that of the microscope objective. Resolution limitations in video cameras were determined from expressions given by Hansen (1986):

a) Relationship between size of image area in camera and video scan rate:

$$f_t = N_j / (1.2 \cdot D), \qquad (3.2)$$

where f_t = target spatial frequency ("target" is the image-forming device in the video camera),

N_j = scan lines per picture height, with

j = v, vertical or h, horizontal

and D = diameter of image-forming device in camera.

b) Relationship between target frequency at camera and spatial frequency at the specimen plane:

$$f_t = fsp / (Mobj \cdot Mrel), \qquad (3.3)$$

where fsp = spatial frequency at specimen plane,

Mobj = objective magnification,

Mrel = relay optics magnification.

Equating (2) and (3), one obtains

$$fsp = Nj \cdot Mobj \cdot Mrelay/ 1.2D, \qquad (3.4)$$

which gives the spatial frequency at the specimen plane that can be detected by the camera. From the Nyquist theorem (Pratt 1978), no

Figure 3.6: Comparison of resolution limits for different components of image analysis system.

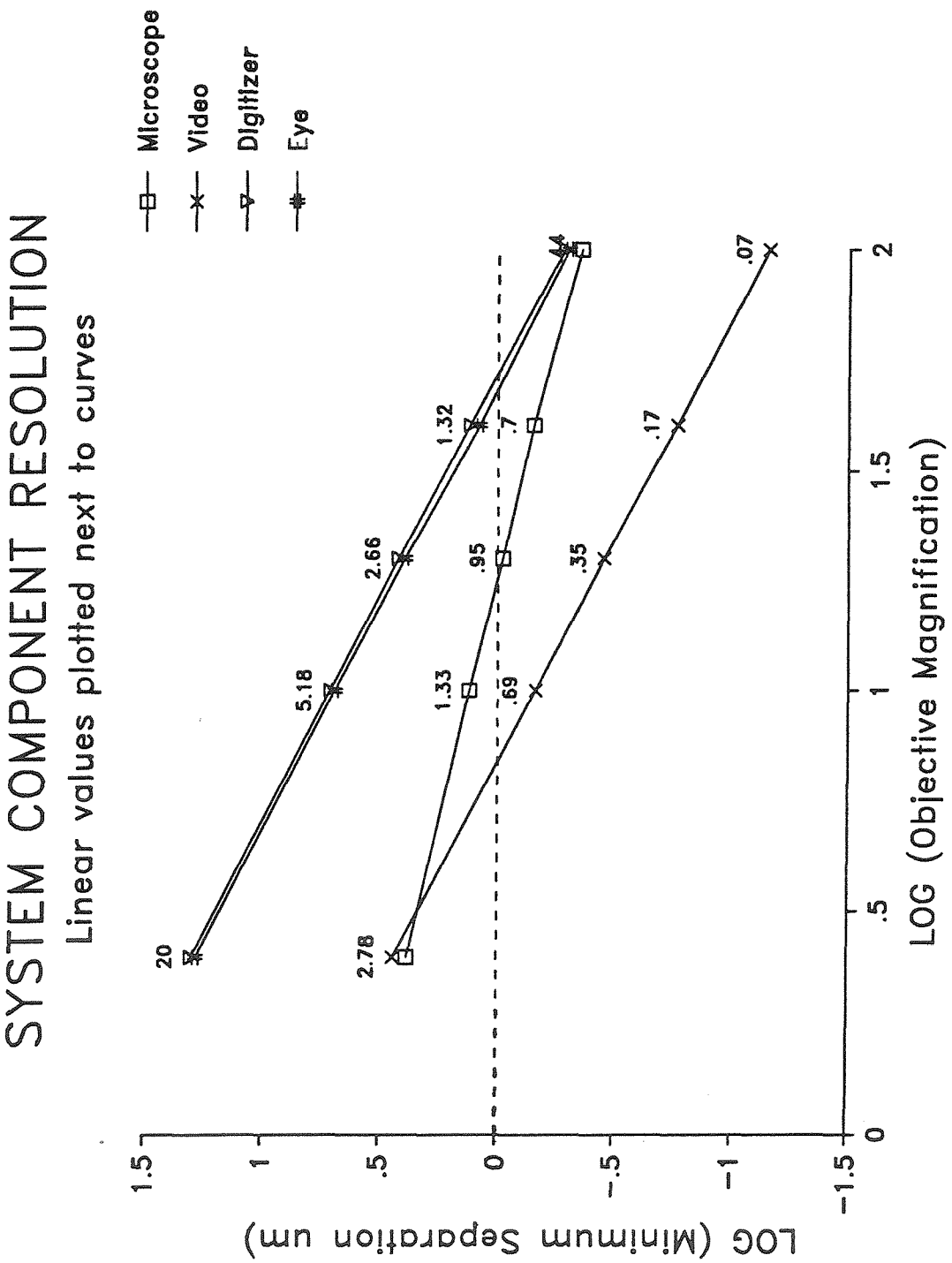

loss of resolution would occur if the video camera scanned the image with lines separated by less than half the minimum separation resolvable by a given objective (Hansen, 1986). Data for camera line scan rates (for the Hitachi CCD camera, Nj is 240 lines horizontal and 190 lines vertical) and microscope objective optics and relay magnifications were substituted into Equation (4). For all magnifications except 2.5x, video resolution exceeded theoretical objective resolution and met the Nyquist sampling requirement (Table 3.2, Figure 3.6).

3) Digitization of the video signal. The fixed grid size of a frame-grabbing board may also limit resolution if pixel dimensions are larger than half the line separation in the video signal. Data from the calibration of pixel size against the hemacytometer grid were converted from areal to linear dimension and compared to resolution obtained from the video camera (Figure 3.6). The digitizing board limited total system resolution to values similar to those obtainable with the eyepiece micrometer.

Gametophyte linear dimensions typically ranged from 5 to 50 micrometers. The 20X microscope objective was most often used for measuring size, providing adequate resolution (Figure 3.6) for organisms in this size range.

C) OPERATIONAL ERRORS

Erroneous size determinations could occur if incorrect settings of thresholds or illumination intensity were used. Size errors are principally caused by uncertainties in locating an object's true

edge. Pixels on the image boundary will have brightnesses which depend on:

a) relative proportions of object and background occupying the pixel, and

b) relative intensity difference between background and object (Figure 3.7).

An idealized mathematical representation of these relationships is:

$$I_p = I_{back} \text{ (gamma)} + I_{obj} \text{ (1 - gamma)}, \qquad (3.5)$$

where I_p = edge pixel intensity I_{back} = background intensity

I_{obj} = object intensity

gamma = proportion of pixel area occupied by background.

Edge pixels will have intensities intermediate between values for object and background. Inclusion of edge pixels in a measurement of object area depended on the numerical value of the set threshold relative to distribution of edge pixel intensities. The effect of changing the threshold setting on measured object area is shown for a simple high-contrast (Iback = 1, Iobj = 0) case in Figure 3.8. If the upper threshold for inclusion of edge pixels in an object is set to a value close to background intensity, then pixels containing only a small portion of edge will be included in measurements of the object's area and the computed area will be high. If the threshold is set to a value close to object intensity, then only pixels containing large portions of edge will be included in the object and calculated area will be low. As discussed below, the size of the error also depends on the relative size of pixels in relation to object size and the degree of contrast between object and background pixels.

Figure 3.7: Influence of proportion of object area on edge pixel brightness

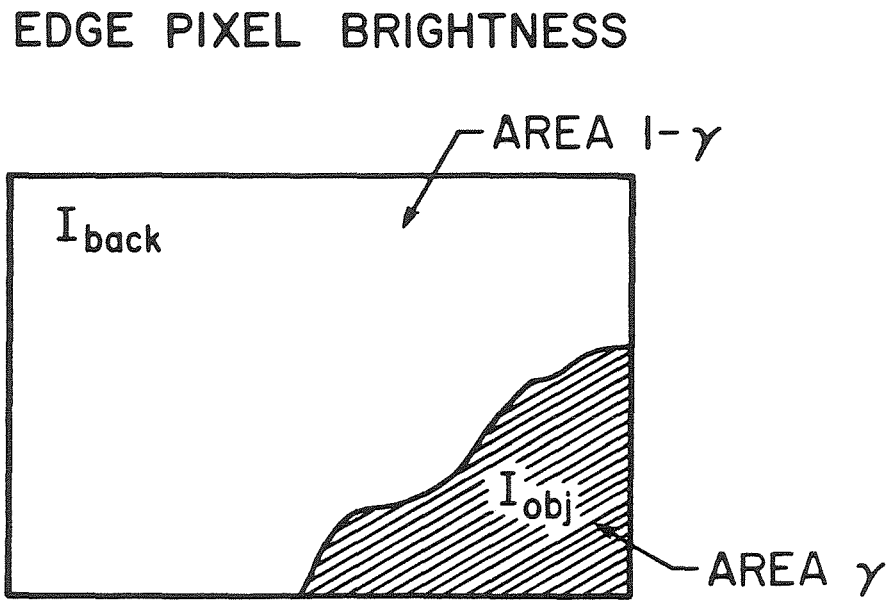

$$I_{obj} < I_{back}$$

$$I_{edge} = \gamma I_{obj} + (1-\gamma) I_{back}$$

Figure 3.8: Example of effect of edge threshold setting on perceived object size. Percentages shown are for fraction of edge pixel occupied by object included in digital representation. Numbers below objects are number of pixels included in object.

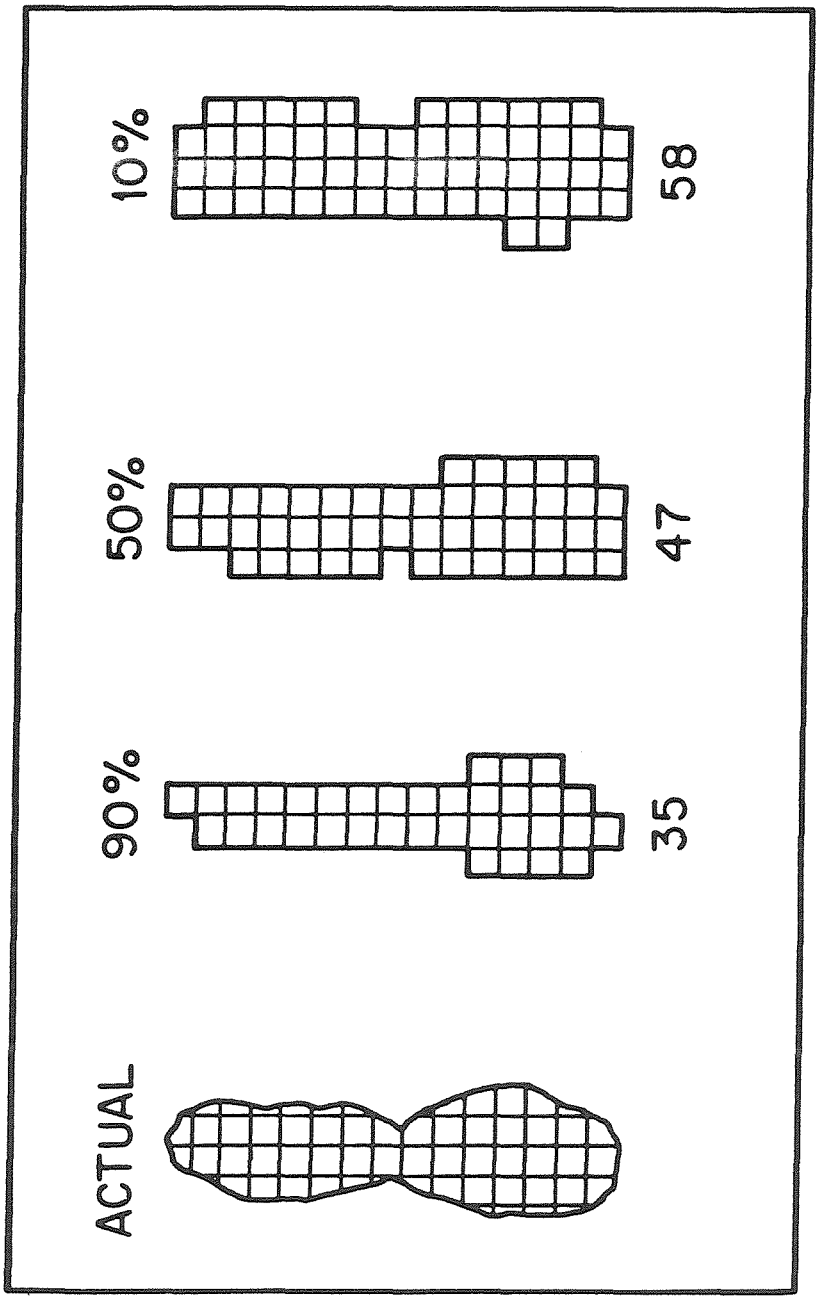

Several physical phenomena influenced edge pixel brightness:

1) Fluctuating illumination intensity: Line voltage variations on the order of ± 2 percent produced intensity fluctuations in the tungsten lamp illuminating the objects. Varying lamp intensity altered background pixel brightness relative to object pixel brightness (discussed in Section 3a below). Edge pixels containing both object and background would have fluctuating grey-level values that varied with changes in background brightness and might oscillate above and below the preset threshold value at the moment the image is digitized. If edge pixels were below the threshold value, they were included in the object. They were excluded from the object if above the threshold value. The magnitude of the error introduced by this process depended on the number of perimeter pixels relative to total pixels in the object. The perimeter-area ratio declines as 4/D for circular and square objects, where D is the characteristic diameter of the object. The relative magnitude of errors arising from edge effects might be expected to decline with increasing object size. When single polystyrene latex spheres of known size (Dow Chemical Company, Indianapolis, IN.) were repeatedly digitized in fluctuating light using constant threshold values, relative errors of 0.2-3.0 percent were obtained (Figure 3.9). Error initially declined with increasing object size, then became constant. Experimental error was much lower than the worst-case estimate of a shift in area caused by loss or gain of a one pixel-wide "ring" along the entire

Figure 3.9: Experimental precision of 10 repeated digitizations of single spheres.
Top: Standard deviation in pixels vs. mean sphere area.
Bottom: Coefficient of variation vs. mean sphere area. Line is error for change in edge position by ± 1 pixel around entire object.

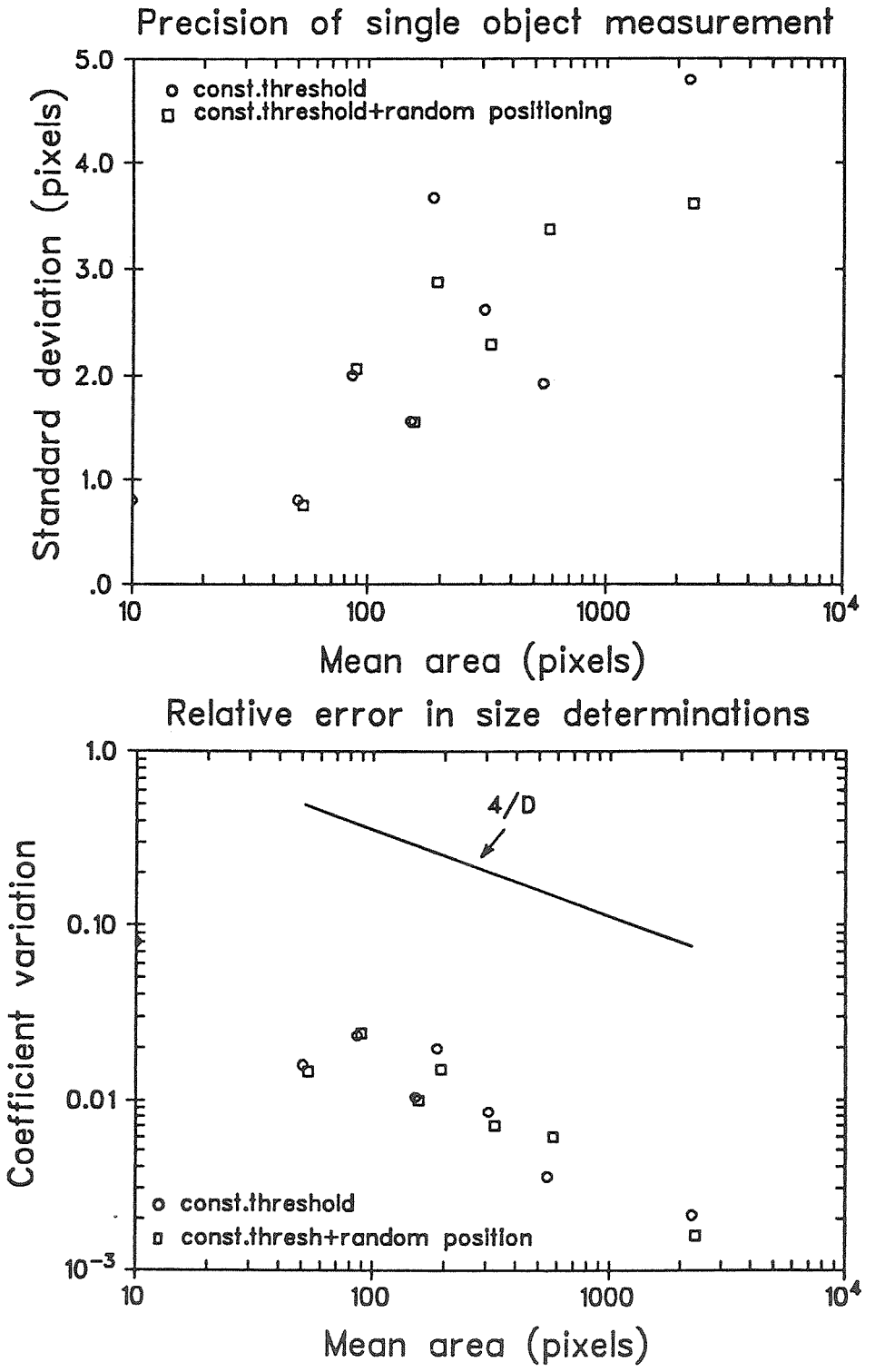

object boundary. It is possible to conclude that at least for high contrast objects, a small proportion of available edge pixels were fluctuating in and out of the analysis.

2) Fluctuation in apparent size of object that is due to random positioning in field of view. The net gain or loss of edge pixels around an object as it is moved over the digitizing grid may not sum to zero for irregular objects that are small relative to pixel size. Error resulting from repeated measurements of randomly positioned objects was roughly twice the error caused by illumination fluctuations alone (Figure 3.9). Relative error generally declined with increasing object size, and was never more than 3 percent of "true" object size.

3) Interaction between image contrast and threshold levels set by the experimenter:

a) Influence of illumination intensity: Assume Lambert-Beer extinction of light within an object:

$$I_o = I_b \exp(-kz), \tag{3.6}$$

where I_b = background light intensity

I_o = light intensity transmitted through object

k = extinction coefficient z = thickness of object.

The intensity difference between object and background will be:

$$I_{diff} = I_b - I_o. \tag{3.7}$$

Substituting from 6),

$$I_{diff} = I_b (1 - \exp(-kz)). \tag{3.8}$$

From Equation (8), intensity differences between object and background should increase proportionately with incident

illumination intensity (Figure 3.10). In practice, contrast differences between object and background increased to a maximum value as illumination intensity increased, then declined as the video imager became light-saturated (detector output voltages reached maximum values) and contrast was lost.

b) Influence of spatially varying light extinction on object intensity: If the extinction coefficient or thickness in Equation (8) varies with (x,y) position within an object, then intensity differences between background and object will vary with location inside the object. Extinction coefficient and thickness act similarly to determine the light extinction at any point within the object. Optical density is defined as the logarithm of the ratio of incident to transmitted light, which for Lambert-Beer extinction is the product of extinction coefficient and thickness, kz (McGraw-Hill, 1977). High contrast occurs when an object has high optical density (the product, kz, is large). Background illumination intensity and varying optical density interact to determine variability in light intensity transmitted through the object (Figure 3.11). Coefficients of variation (standard deviations divided by respective means) computed for this one dimensional case declined with increasing optical density (Fig. 3.12).

c) Interaction between contrast difference and threshold setting: The impact of threshold selection on measured object size is shown in Figure 3.13 for the simple models described above. Thresholds set to include only a portion of object intensities resulted in inaccurate size determinations. Error in object area

Figure 3.10: Effect illumination intensity on contrast difference. between object and background.

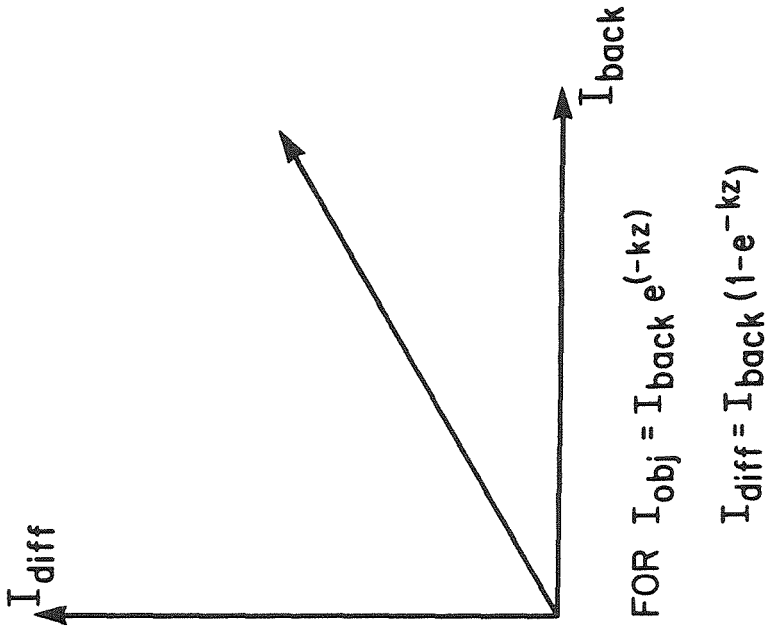

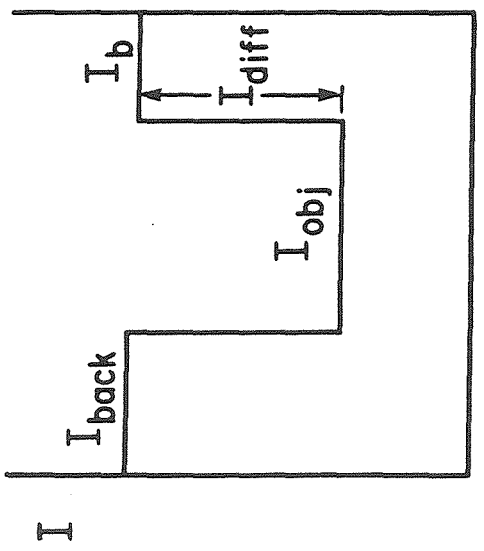

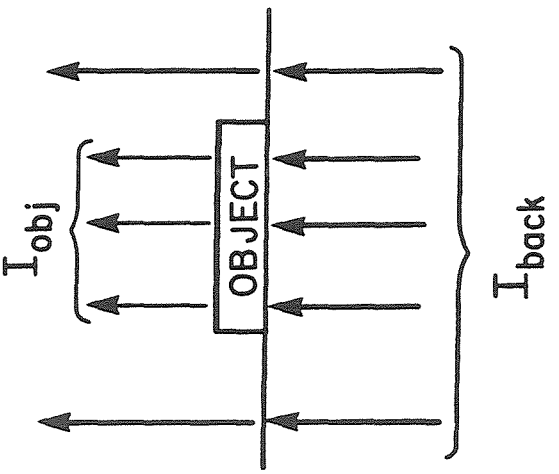

Figure 3.11: Effect spatially varying object optical density on transmitted light intensity. Hatched regions in lower figure simulate cell walls with higher extinction coefficient (k=0.25) than surroundings. Upper figure is resulting transmitted intensity for light with background intensity = 1

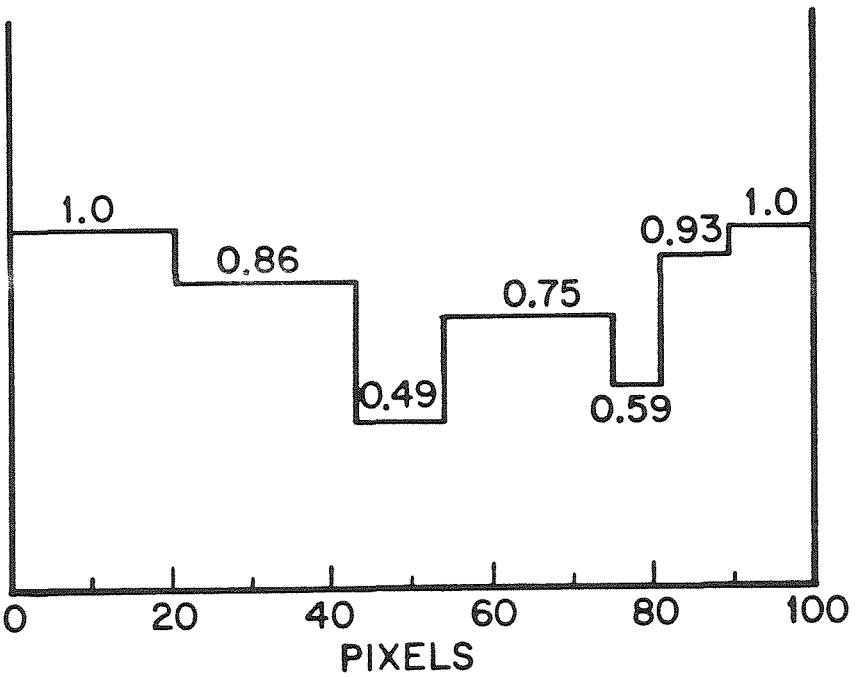

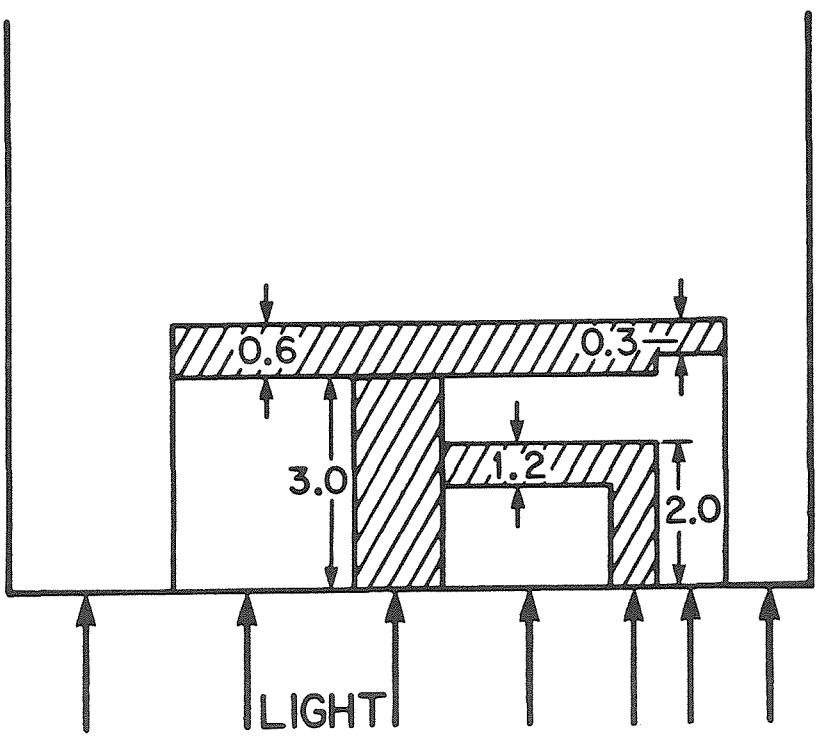

Figure 3.12: Effect of extinction coefficient on intensity difference variability within object for simple model shown in Figure 3.11. Intensity difference computed as Idiff = Iback(1-e^{-kz}) with Iback = 1 for each shaded thickness (z) in Figure 3.11. Extinction coefficient corresponds to shaded regions in Figure 3.11. Summary statistics computed for resulting set of intensity differences. Coefficient of variation = standard deviation / mean.

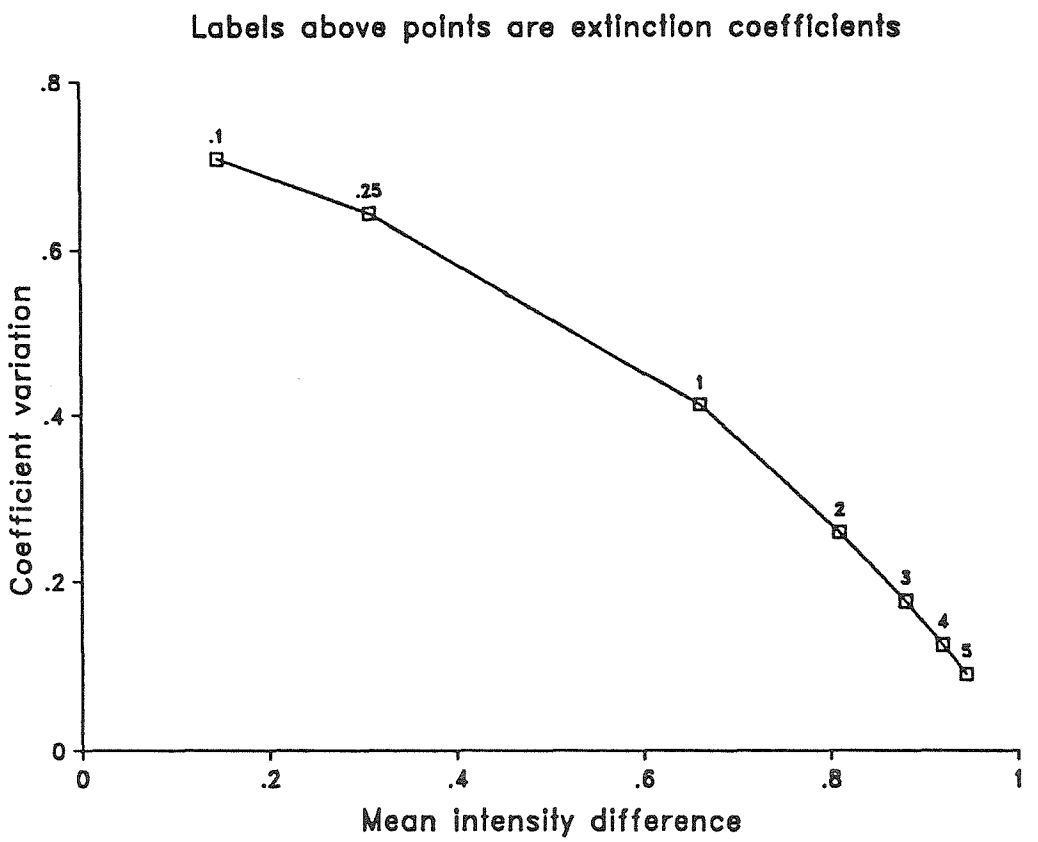

Figure 3.13: Interaction of optical density and threshold setting on measured object size. Data using simple model in Figure 3.11 with three different extinction coefficients.

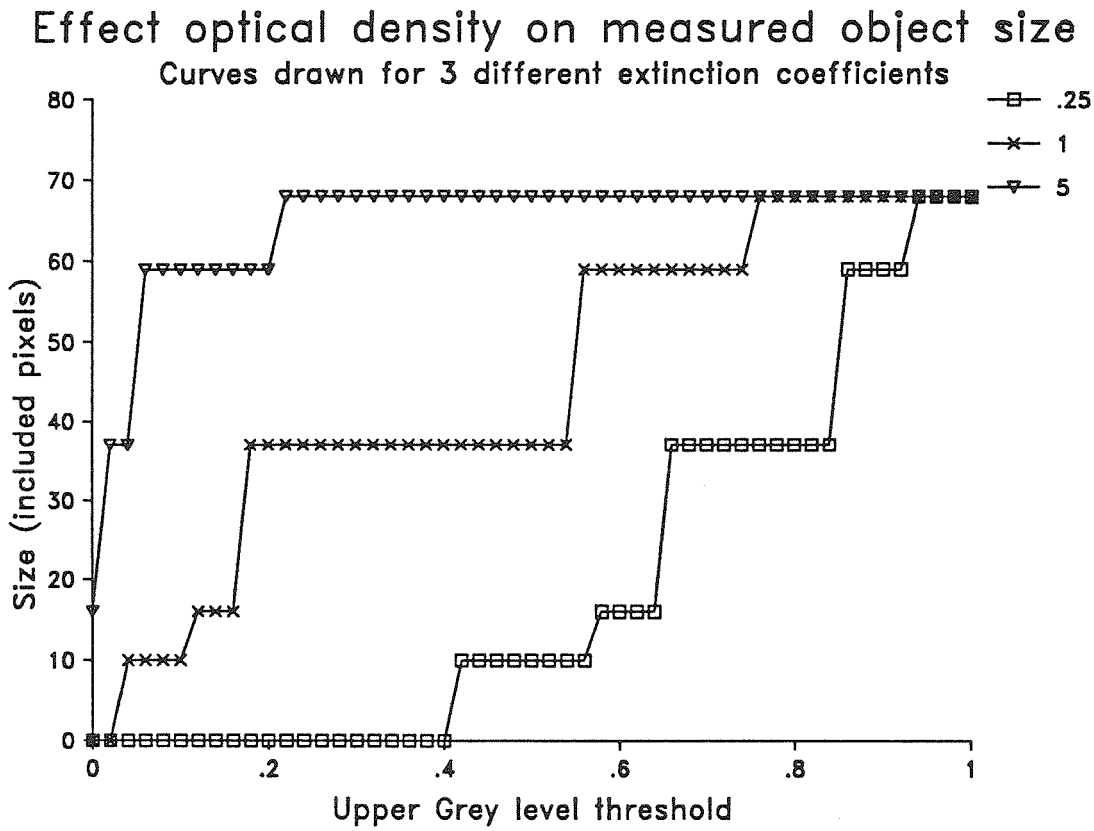

determinations declined when contrast between image and background was high. Experimental impacts of setting different intensity thresholds on object area are shown for two similarly sized gametophytes of different optical density distributions in Figure 3.14. Very small changes in computed size occurred over a broad range of threshold settings for a female gametophyte of high uniform optical density. Larger changes were observed for a male gametophyte that had low, variable optical density.

Intensity thresholds during experimental runs were set by comparing single-bit images generated from all pixels included between the high and low grey-level thresholds to actual video images and three or four grey-level false-color images. Regions of low sensitivity in edge growth to change in grey level (exemplified by flat curves in the grey-level range from 115 to 120 in Figure 3.14) were sought by manually changing upper grey-level thresholds until regions of low-sensitivity were found. Thresholds were seldom changed once set for a particular culture.

Optical density differences within gametophytes increased as the organisms aged. When optical density occasionally became low near the true object edge in older gametophytes, grey-level values in this region of the organism would thus be close to values for the background, and gaps in the edge could result. The relative magnitude of the introduced error depended on the variable size of the low-optical density region. Gametophytes were excluded from analysis if they contained large gaps that could not be closed by changing illumination intensity or resetting intensity thresholds.

Figure 3.14: Interaction of optical density and threshold setting on measured object size for two different gametophytes.

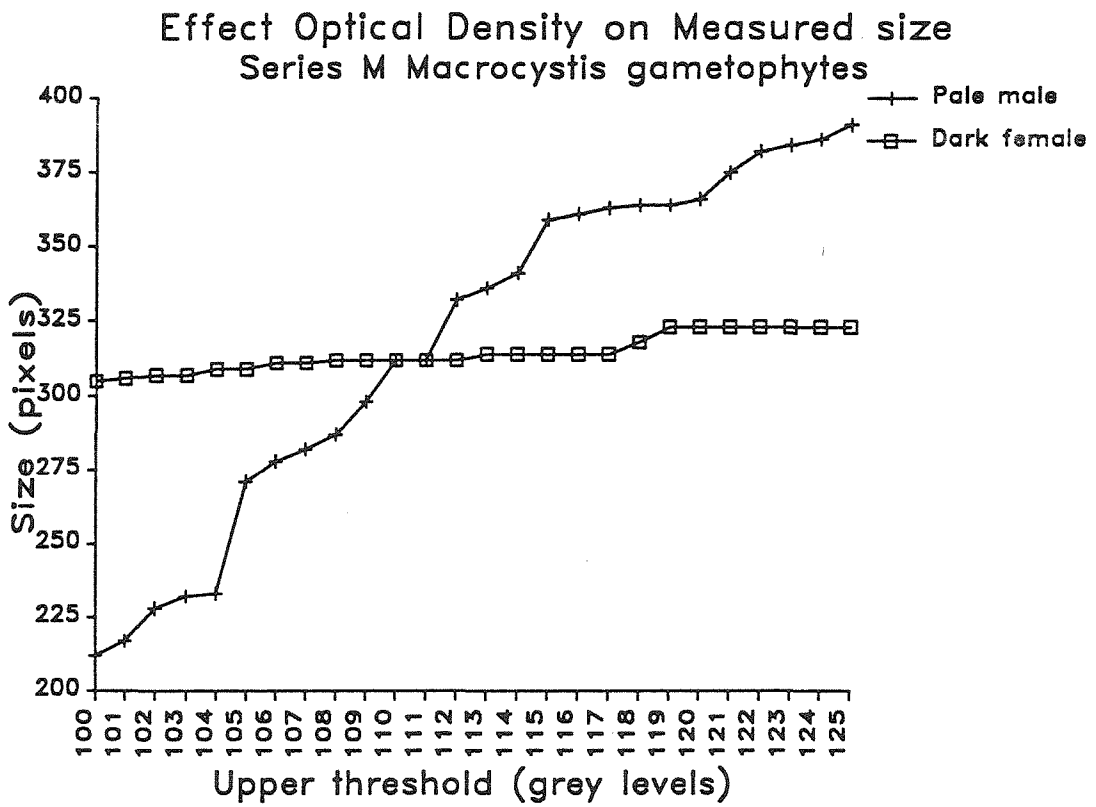

D) PROPAGATION OF DIGITIZER ERROR INTO SIZE DISTRIBUTION ERROR

Uncertainties in size determinations of individual objects complicate computation of descriptive statistics when organisms display a wide distribution of sizes. Measurement uncertainty might increase dispersion of variates around a sample mean if the equipment error is sufficiently large, obscuring determinations of significance when pairs of samples are compared. Measurement uncertainty is usually ignored in statistical computations commonly used in biology. We examined the effects of measurement uncertainty on observed dispersion and determinations of significance because gametophyte size distributions varied widely from very narrow (10 percent of the mean or less) to very broad (40 percent of the mean) during an experimental run.

The equipment error contribution to observed variances in mean sizes of sampled populations was determined by extending the propagation-of-error theory described by Bevington (1969) to computation of variances in a population of organisms with a distribution of sizes. Work with repeated digitization of single objects showed that single-object error was 1.5-3% of its size (Figure 3.9) so uncertainty, ξ_i, was assumed to be a constant proportion of object size:

$$\xi_i = kx_i. \tag{3.9}$$

where k is the proportionality constant between error and size and x_i is the size of each object.

A detailed derivation of the effect of this error on measured

standard deviation is shown in the Appendix to Chapter 3. The conclusions are, with:

$\sigma_{x_m}^2$ measured variance,

$\sigma_{x_i}^2$ true variance,

and n sample size,

$$\sigma_{x_m}^2 = \sigma_{x_i}^2 + \left((k^2 + 2k)(\frac{1}{n}\sum_{i=1}^{n} x_i^2) - 2k(\frac{1}{n}\sum_{i=1}^{n} x_i)^2\right). \quad (3.10)$$

Since $\sigma_{x_m}^2$ is the original measurement, n is known, and k is available from experimental measurements, we can solve for $\sigma_{x_i}^2$. For the case where $k \ll 1$,

$$\sigma_{x_m}^2 \simeq (1 + 2k)\,\sigma_{x_i}^2. \quad (3.11)$$

The theory was applied to a set of gametophytes measured over a 10-day period using the experimentally determined individual object uncertainty k = 0.015. It was found that with one exception[1], propagated measurement error ranged from 0.25 percent to 4 percent of the total experimental variance, roughly twice the magnitude of size determination errors observed for single organisms (Figure 3.15).

Significance levels for growth inhibition experiments were not affected by removal of propagated individual error from the calculations (Figure 3.16). Uncorrected variances therefore appeared to be accurate estimates of variance in the sampled populations. The

---

[1]Machine error was 30 percent on the first measurement day when organism areas were only 20-30 pixels. A 3-pixel error at 20 pixels (15 percent) doubles to 30 percent. At 100 pixels, a 3-pixel error doubles to 6 percent.

Figure 3.15: Partitioning of observed standard deviations into components for organisms and digitizer. Digitizer error range 5-30% of total, usually 10% or less.

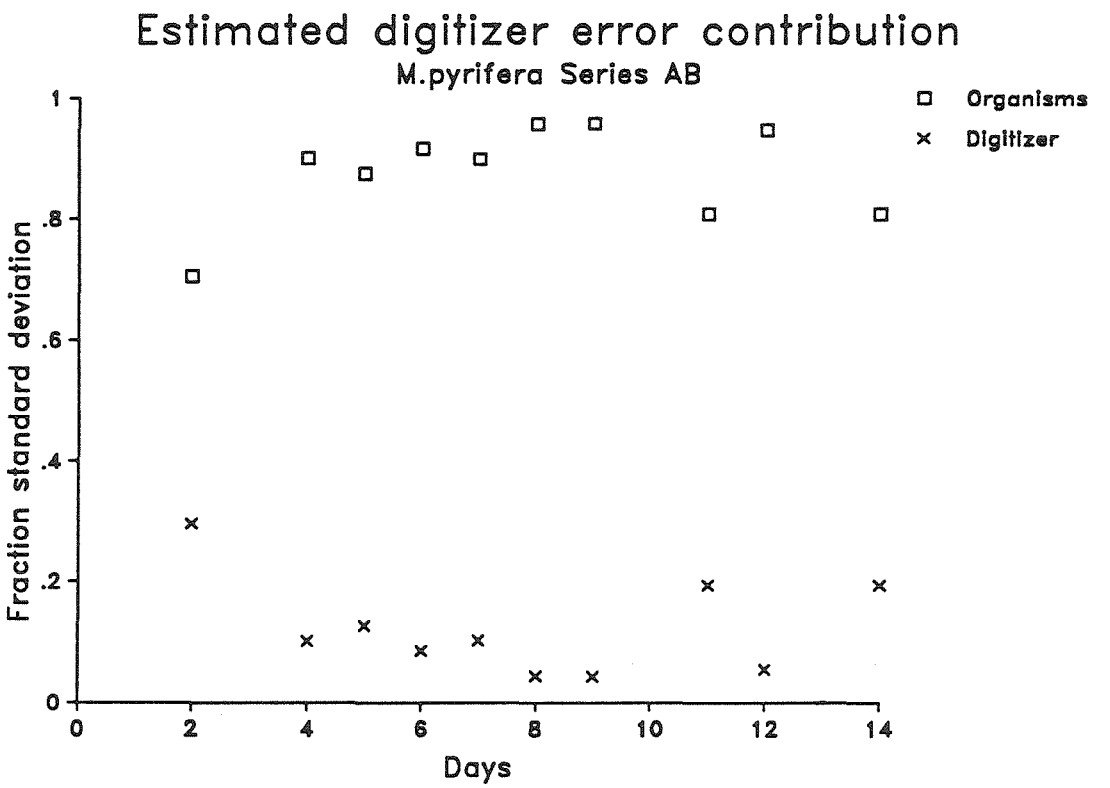

Figure 3.16: Comparison of error bars for Macrocystis pyrifera gametophyte sizes with and without machine error removal

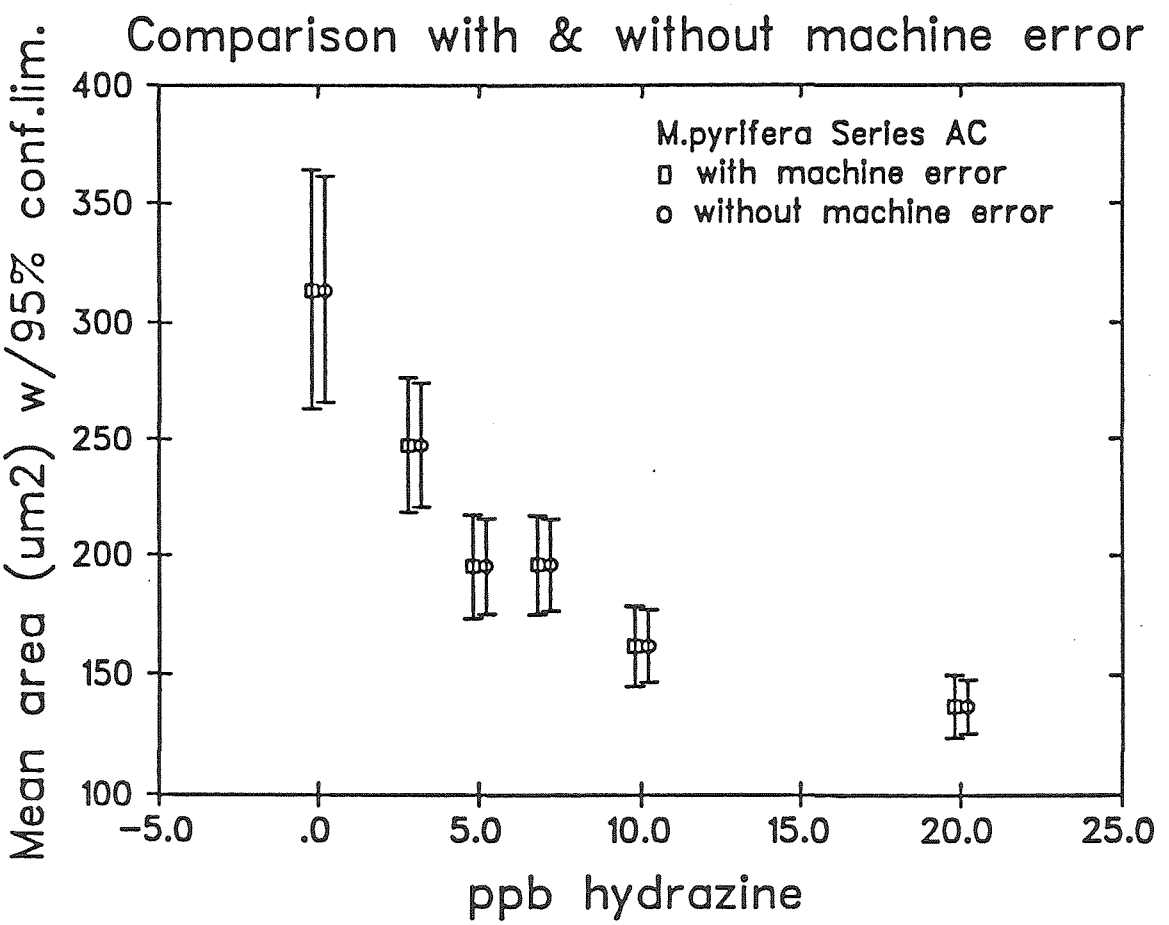

likelihood of committing a Type II error (incorrectly confirming a null hypothesis as true when, in fact, the alternative hypothesis is true (Sokal and Rolf, 1981)) was not appreciably increased by individual measurement errors originating from digitization process. Errors associated with the data thus appeared to be reasonably well defined.

IV. COMPARISON BETWEEN DIGITIZING AND EYEPIECE MICROMETER METHODS

The image-analysis system and eyepiece micrometer were compared by measuring identical gametophytes with each instrument, and by performing parallel random samplings of identical control and hydrazine-treated cultures.

1) Identical measurements of given organisms with both instruments:

Series AB Macrocystis gametophyte lengths and widths were measured on the same microscope with an eyepiece micrometer and with digital image-analysis equipment. Areas from micrometer measurements were approximated by assuming rectangular shapes and calculating the product of length and width. Digitizer areas were plotted against micrometer-derived areas and compared to a line of slope 1 through the origin (Figure 3.17). Excellent correlation was achieved up to areas of 400 square microns, but micrometer areas lagged behind digitizer measurements. Cause of this divergence was inaccuracy of the rectangular approximation used to compute areas of large gametophytes because shapes became very irregular.

Coefficients of variation were computed for the daily sample size distributions directly from digitizer areas and estimated from length and width measurements using propagation-of-error theory for the

Figure 3.17: Comparison of gametophyte areas determined by eyepiece micrometer and digital image analysis.

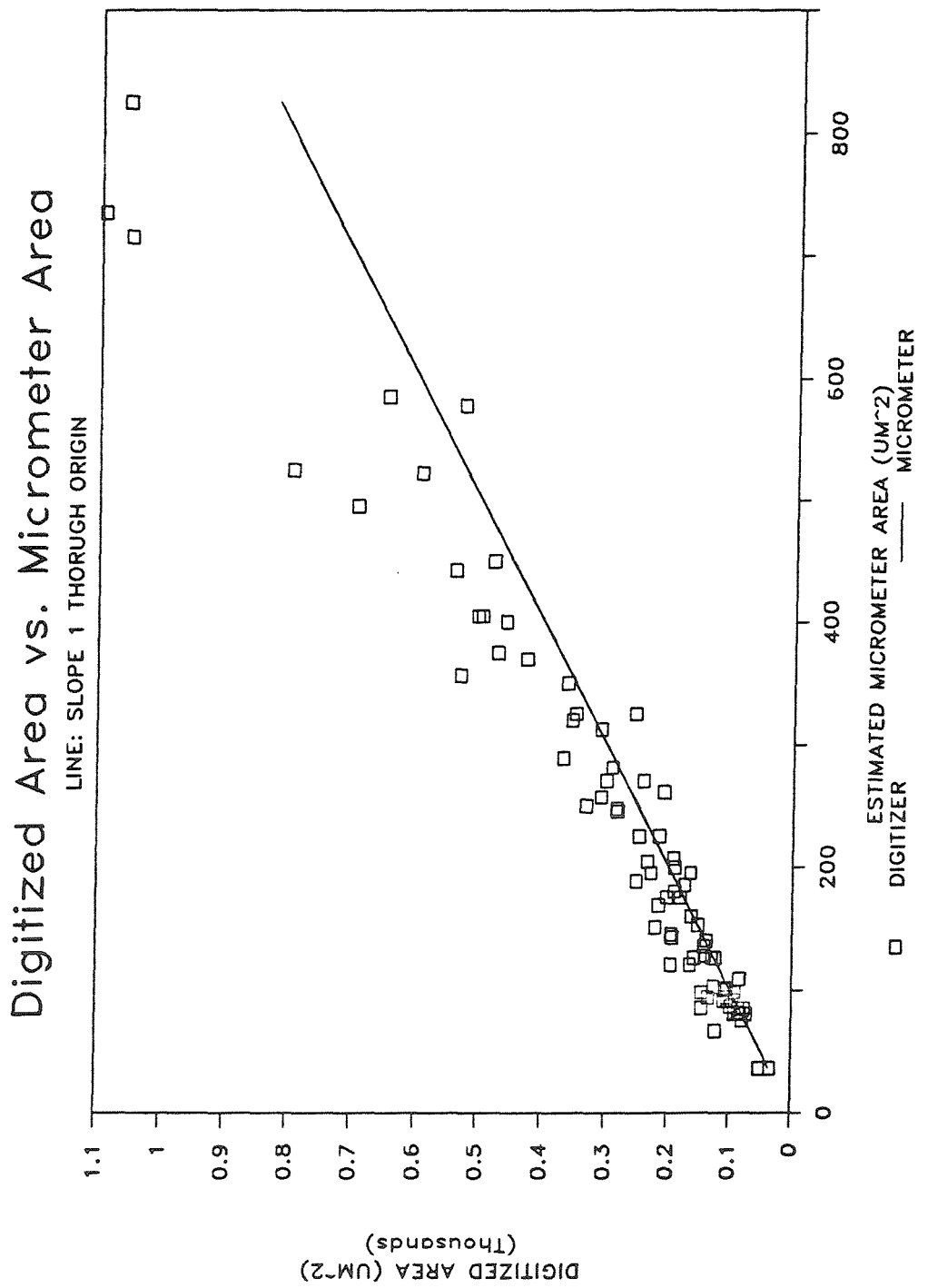

eyepiece micrometer[2]. On eight of nine measurement days, digitizer-determined variation was smaller than micrometer-determined variation for samples composed of identical organisms (Figure 3.18).

2) Random sampling of cultures during a growth-inhibition experiment.

Series M Macrocystis pyrifera control and hydrazine-inhibited cultures were measured by both eyepiece micrometer and image-analysis methods. Nonidentical organisms were randomly sampled on the slides in separate runs with the two instruments. Significant vegetative growth inhibition was detected with the digitizer three days after application of toxicant (Figure 3.19). Micrometer methods required seven days to detect inhibition with the toxicant. Directly determined coefficients of variation were similar in magnitude (Figure 3.20). The digitizer's coefficients of variation were related to area measurements, however, while hand methods were for length. When propagation-of-error theory (described above, Bevington, 1969) was applied to calculation of area measurements from the lengths, assuming similar coefficients of variation for both length and width micrometer measurements, relative error doubled for the micrometer-derived areas. Coefficients of variation for area as determined by the digitizer were smaller than those estimated from micrometer methods. Combined operator and instrumental error were apparently higher for micrometer methods than for the digitizer.

---

[2]See formula 2.9 for the formula for relative uncertainty in area, x, computed from length, u, and width, v, but the sign on the last term changes to a "+".

Figure 3.18: Comparison of coefficients of variation determined from area measurements using both methods on the same sample of 10 randomly-selected organisms each day.

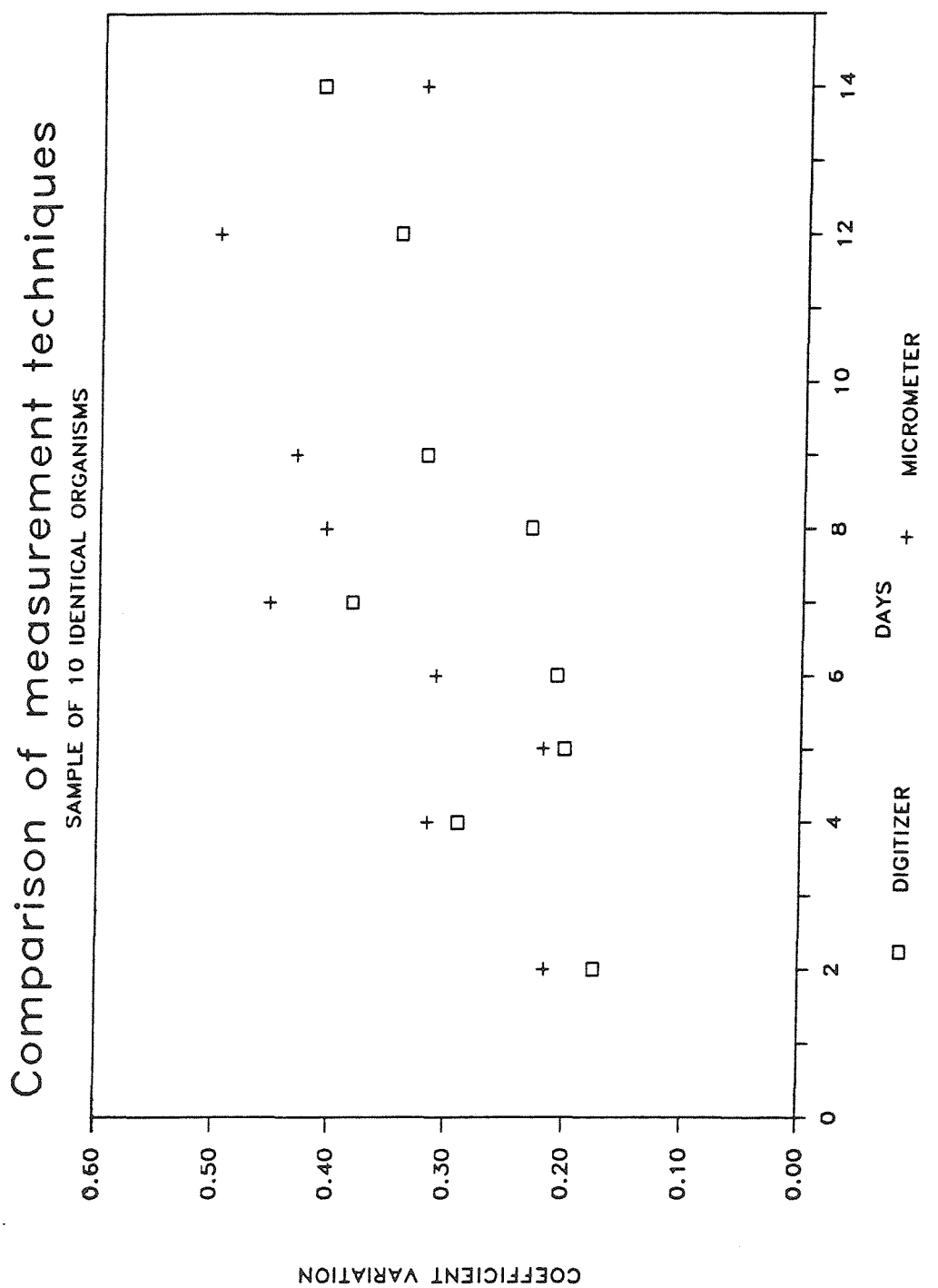

Figure 3.19: Macrocystis pyrifera Series M.
Comparison of methods of measurement of growth inhibition relative to controls in 6 hour, 250 ppb daily hydrazine exposures. Data normalized to control object size on Day 3.
IMAGE ANALYSIS AREAS: Top set of curves, shifted by +2 units.
EYEPIECE MICROMETER LENGTHS: Lower set of curves.

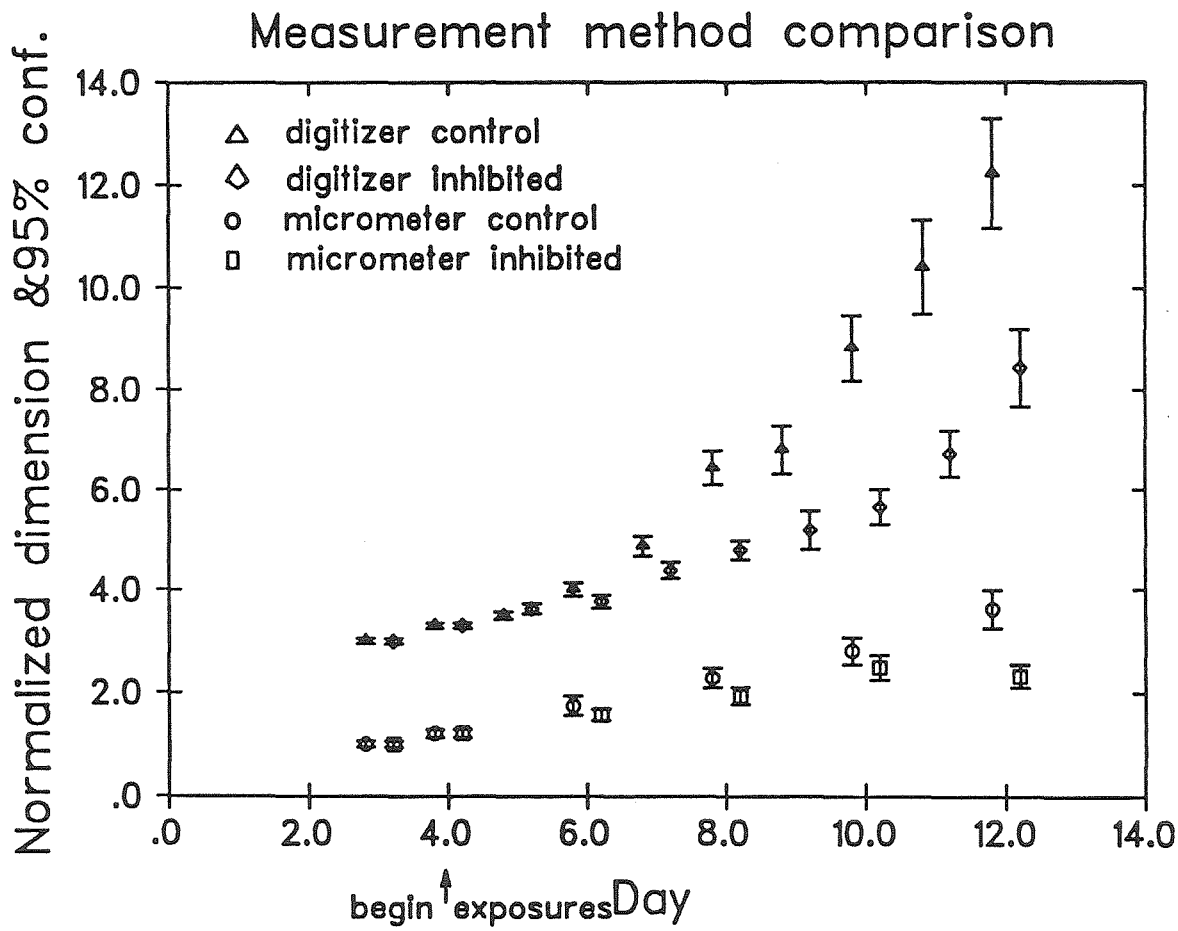

Figure 3.20: Coefficients of variation (standard deviation divided by mean) for control cultures of Figure 3.19. Top set of points estimated for area using propagation of error theory (see text).

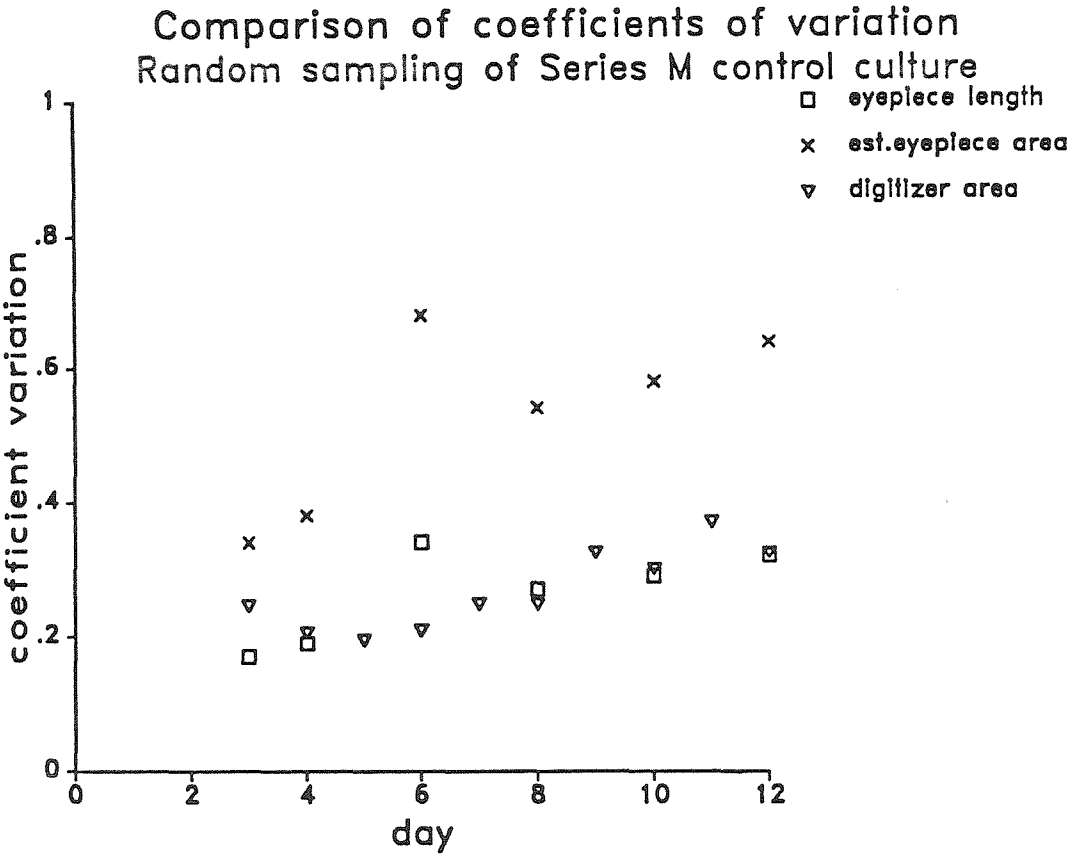

V. CONCLUSIONS

1) Accuracy of the digitizer in practice was within three percent of true object size. Instrument precision was a function of object size, but was typically less than five percent of object area.

2) Propagation of equipment-derived errors into determination of mean areas for organisms of a range of sizes typically contributed 5 to 20 percent of computed sample variances and had negligible impacts on determinations of significance for differences in mean population sizes.

3) Coefficients of variation in identical populations of organisms were lower when measured with digital image analysis than with an eyepiece micrometer, indicating larger contribution of measurement error to observed variance with micrometer methods.

4) Significant growth inhibition in randomly-sampled cultures was detected earlier when measuring with image analysis than with eyepiece micrometer methods.

VI. OPERATIONAL CONDITIONS FOR DIGITAL IMAGE ANALYSIS

Illumination intensities were fixed at 4.5V, condenser numerical aperture = 0.2 using brightfield illumination and green (546 $\pm$ 20 nm) light for most measurements. Thresholds were typically set at 0 and 180, with the median background intensities at 225. Fixed illumination and intensity thresholds permitted comparisons among different experimental runs. Upper intensity thresholds had to be set to higher values to retain a contiguous object edge for increasingly transparent live gametophytes at ages exceeding 10-12 days.

REFERENCES

Adams, H.L. and C.R. Thomas 1988. The use of image analysis for morphological measurements on filamentous microorganisms. Biotechnology and Bioengineering. 32: 707-712.

Bevington, P.R. 1969. Data Reduction and Error Analysis for the Physical Sciences. McGraw-Hill: New York, pp.56-65.

Bjornsen, P.K. 1986. Automatic determination of bacterioplankton biomass by image analysis. Applied and Environmental Microbiology. 51(6): 1199-1204.

Castleman, K.R. 1979. Digital Image Processing. Prentice Hall: New York, 429pp.

Cosson, J.M. 1977. Action de la durée d'éclairment sur la morphogenèse des gametophytes de Laminaria digitata (L.) Lamoureux (Phaeophyceae, Laminariales) Bulletin, Society Phycologique de France. 22:19-26.

Deysher, L.E. and T.A. Dean 1984. Critical irradiance levels and the interactive effects of quantum irradiance and dose on gametogenesis in the giant kelp Macrocystis pyrifera. Journal of Phycology. 20: 520-524.

Deysher, L.E. and T.A. Dean 1986. Interactive effects of light and temperature on sporophyte production in the giant kelp Macrocystis pyrifera. Marine Biology. 93: 17-20.

Estep, K.W., F.MacIntyre, E.Hjorleifsson, and J.M. Seiburth 1986.. MacImage: a user-friendly image-analysis system for the accurate mensuration of marine organisms. Marine Ecology - Progress Series. 33:243-253.

Furuya, K. 1982. Measurement of phytoplankton standing stock using an image analyzer system. Bulletin Plankton Society of Japan. 29: 133-135.

Green, W. B. 1981. Digital Image Processing. Van Nostrand Reinhold: New York, 192pp.

Hansen, E. 1986. "Modulation Transfer Function Analysis in Video Microscopy." Appendix II in S. Inouye, (ed.) Video Microscopy. Plenum Press: New York. pp. 459-475.

Horiuchi, T.K. 1986a. Eyeball 2.3. Image-processing software written for Summer Undergraduate Research Project, 1986. California Institute of Technology: Pasadena, CA. 91125.

Horiuchi, T.K. 1986b. Image Plot 3.1. Image-processing software written for Summer Undergraduate Research Project, 1986. California Institute of Technology: Pasadena, CA. 91125.

Inouye, S. 1986. Video Microscopy. Plenum Press: New York, 565pp.

Levyns, M.R. 1933. Sexual Reproduction in Macrocystis pyrifera, L.C. Agardh. Annals of Botany. 27(186):349-353.

Luning, K. and M. Neushul 1978. Light and temperature demands for growth and reproduction of Laminarian gametophytes in southern and central California. Marine Biology. 45: 297-309.

Pratt, W. K. 1978. Digital Image Processing. Wiley-Interscience: New York, 750pp.

Sieracki, M.E., P.W. Johnson, J. M. Seiburth 1985. Detection, enumeration and sizing of planktonic bacteria by image-analyzed epifluorescence microscopy. Applied and Environmental Microbiology. 49(4): 799-810.

Sokal, R.R. and F.J. Rolf 1981. Biometry, 2nd edition. W.H. Freeman Press: San Francisco, 859pp.

Walter, R.J. and M.W. Berns 1986. "Digital Image Processing and Analysis". Chapter 10 in S. Inouye, (ed.) Video Microscopy. Plenum Press, N.Y. 565pp.

Wang, R.F. 1988. Laboratory analysis of settling velocities of wastewater particles in seawater using holography. Doctoral dissertation. California Institute of Technology, Pasadena, CA. 311pp.

APPENDIX: CHAPTER 3

EFFECT OF MEASUREMENT ERROR PROPORTIONAL TO OBJECT SIZE ON OBSERVED SAMPLE VARIANCE

Let $x_m = x_i + \xi_i$, where: (3.A.1)

x_m is the measured object size,

x_i is the true object size, and

ξ_i is the error for any single digitization of an object,

Assume that $\overline{\xi} = 0$, where $\overline{\xi}$ is the mean of the individual errors ξ_i.

Assume that the errors ξ_i are uncorrelated, that is $(\sum_{i=1}^{n} \xi_i)(\sum_{i=1}^{n} \xi_i) \neq (\sum_{i=1}^{n} \xi_i^2)$.

Assume that individual errors are a constant small fraction, k, of object size,

$\xi_i = kx_i$.

Let $\sigma_{x_i\xi_i}^2 = \frac{1}{n} \sum_{i=1}^{n} (\overline{x} - x_i)(\overline{\xi} - \xi_i)$, covariance of actual value and error. (3.A.2)

With $\overline{\xi} = 0$ and $\xi_i = kx_i$, then, substituting into (3.A.2),

$$\sigma_{x_i\xi_i}^2 = \frac{1}{n} \sum_{i=1}^{n} (\overline{x} - x_i)(0 - kx_i) \tag{3.A.3}$$

$$= -\frac{k}{n} \sum_{i=1}^{n} (\overline{x} - x_i)(x_i) \tag{3.A.4}$$

$$= -\frac{k}{n} \sum_{i=1}^{n} (\overline{x}x_i - x_i^2) \tag{3.A.5}$$

$$= -\frac{k\overline{x}}{n} \sum_{i=1}^{n} (x_i) + \frac{k}{n} \sum_{i=1}^{n} (x_i^2). \tag{3.A.6}$$

Since $\overline{x} \equiv \frac{1}{n} \sum_{i=1}^{n} x_i$, then

$$\sigma_{x_i\xi_i}^2 = -k\overline{x}^2 + \frac{k}{n} \sum_{i=1}^{n} (x_i^2). \tag{3.A.7}$$

From propagation of error theory (Bevington, 1969), we have that for a case where a quantity x is a function of several variables, $x = f(u,v)$, then the

variance of x is approximated by:

$$\sigma_x^2 \simeq \sigma_u^2\left(\frac{\delta x}{\delta u}\right)^2 + \sigma_v^2\left(\frac{\delta x}{\delta v}\right)^2 + 2\sigma_{uv}^2\left(\frac{\delta x}{\delta u}\right)\left(\frac{\delta x}{\delta v}\right) \text{ (Bevington's eq. 4.8).} \quad (3.A.8)$$

For a measured quantity, x_m, which is an additive function of the true value, x_i and the error, ξ_i (Equation (3.A.1)), then the partial derivatives in (3.A.8) become, substituting x_m for x, x_i for u and ξ_i for v,

$$\left(\frac{\delta x_m}{\delta x_i}\right) = 1 \quad \text{and} \quad \left(\frac{\delta x_m}{\delta \xi_i}\right) = 1. \quad (3.A.9)$$

Substituting these partial derivatives into (3.A.8), one obtains

$$\sigma_{x_m}^2 = \sigma_{x_i}^2 + \sigma_{\xi_i}^2 + 2\sigma_{x_i\xi_i}^2, \quad (3.A.10)$$

where $\sigma_{x_m}^2$ is the measured variance, $\sigma_{x_i}^2$ is the variance of the organisms without measurement error, and $\sigma_{\xi_i}^2$ is the variance of the measurement error.

Expanding the first term in (3.A.10),

$$\begin{aligned}\sigma_{x_i}^2 &= \frac{1}{n}\sum_{i=1}^{n}(\bar{x} - x_i)^2 = \frac{1}{n}\sum_{i=1}^{n}(\bar{x}^2 - 2x_i\bar{x} + x_i^2) \\ &= \frac{1}{n}\sum_{i=1}^{n}\bar{x}^2 - 2\bar{x}\frac{1}{n}\sum_{i=1}^{n}x_i + \frac{1}{n}\sum_{i=1}^{n}(x_i^2). \end{aligned} \quad (3.A.11)$$

The first term is $\bar{x}^2$. Since $\frac{1}{n}\sum_{i=1}^{n}x_i \equiv \bar{x}$, the second term becomes $2\bar{x}^2$.

Equation (3.A.11) reduces to:

$$\sigma_{x_i}^2 = \frac{1}{n}\sum_{i=1}^{n}(x_i^2) - \bar{x}^2. \quad (3.A.12)$$

Expanding the second term in (3.A.10),

$$\sigma_{\xi_i}^2 = \frac{1}{n}\sum_{i=1}^{n}(\bar{\xi} - \xi_i)^2 \simeq \frac{1}{n}\sum_{i=1}^{n}(0 - kx_i)^2 = \frac{k^2}{n}\sum_{i=1}^{n}(x_i^2). \quad (3.A.13)$$

The $\sigma_{x_i\xi_i}^2$ in the third term in (3.A.10) is known from equation (3.A.7).

Substituting equations (3.A.7) and (3.A.13) into (3.A.10), one obtains,

$$\sigma_{x_m}{}^2 = \sigma_{x_i}{}^2 + \frac{k^2}{n}\sum_{i=1}^{n}(x_i{}^2) + \frac{2k}{n}\sum_{i=1}^{n}(x_i{}^2) - 2k\bar{x}^2. \qquad (3.A.14)$$

Factoring out $k^2 + 2k$ and with $\bar{x} = \frac{1}{n}\sum_{i=1}^{n} x_i$, then,

$$\sigma_{x_m}{}^2 = \sigma_{x_i}{}^2 + \left((k^2 + 2k)(\frac{1}{n}\sum_{i=1}^{n} x_i{}^2) - 2k(\frac{1}{n}\sum_{i=1}^{n} x_i)^2\right). \qquad (3.A.15)$$

Then, substituting from (3.A.12) into (3.A.15),

$$\sigma_{x_m}{}^2 = \frac{1}{n}\sum_{i=1}^{n} x_i{}^2 - \bar{x}^2 + \left((k^2 + 2k)\sum_{i=1}^{n} x_i{}^2 - 2k(\frac{1}{n}\sum_{i=1}^{n} x_i)^2\right). \qquad (3.A.16)$$

Rearranging and using the definition $\bar{x} = \frac{1}{n}\sum_{i=1}^{n} x_i$,

$$\sigma_{x_m}{}^2 = (k^2 + 2k + 1)(\frac{1}{n}\sum_{i=1}^{n} x_i{}^2) - (2k + 1)(\frac{1}{n}\sum_{i=1}^{n} x_i)^2. \qquad (3.A.17)$$

The k terms come from the uncertainty attributed to digitization of individual objects. If k is 0, then the expression for the variance collapses to the expression for no measuremenent uncertainty. An alternative way to visualize this is to rearrange (3.A.17) as a sum of terms for variance of objects without uncertainty and for the uncertainty alone:

$$\sigma_{x_m}{}^2 = \left\{\frac{1}{n}\sum_{i=1}^{n} x_i{}^2 - (\frac{1}{n}\sum_{i=1}^{n} x_i)^2\right\} + \left\{(k^2+2k)(\frac{1}{n}\sum_{i=1}^{n} x_i{}^2) - 2k(\frac{1}{n}\sum_{i=1}^{n} x_i)^2\right\}. \qquad (3.A.18)$$

The term in the first set of brackets is the variance without measurement error. The term in the second set of brackets is the contribution of measurement error. For small values of k, ($k < 0.1$), k^2 is much less than $2k$ (at $k = 0.1$, the error introduced by this assumption is $k^2/2k = 0.01/0.2 = 0.05$) , and hence,

$$\sigma_{x_m}{}^2 \simeq \left\{\frac{1}{n}\sum_{i=1}^{n} x_i{}^2 - (\frac{1}{n}\sum_{i=1}^{n} x_i)^2\right\} + \left\{(2k)(\frac{1}{n}\sum_{i=1}^{n} x_i{}^2) - 2k(\frac{1}{n}\sum_{i=1}^{n} x_i)^2\right\}. \qquad (3.A.19)$$

Rearranging (3.A.19),

$$\sigma_{x_m}{}^2 \simeq (1 + 2k)\left\{\frac{1}{n}\sum_{i=1}^{n} x_i{}^2 - \left(\frac{1}{n}\sum_{i=1}^{n} x_i\right)^2\right\}. \qquad (3.A.20)$$

Using the definition of sample variance without measurement error, this becomes

$$\sigma_{x_m}{}^2 \simeq (1 + 2k)\, \sigma_{x_i}{}^2. \qquad (3.A.21)$$

The impact of measurement uncertainty was determined by calculating numerical values of k from repeated measurements of individual gametophtyes. Calculated k values ranged from less than 0.01 to 0.03. When these estimates of k were incorporated in (3.A.21), it was found that individual measurement error caused a 2% to 6% increase in the total observed experimental variance over the condition where no measurement uncertainty existed. Measurement uncertainty thus did not significantly increase observed variance. It was therefore unlikely that digital measurement error obscured significant differences among sampled gametophyte populations.

REFERENCE

Bevington, P.R. 1969. Data Reduction and Error Analysis for the Physical Sciences. McGraw-Hill: New York, 336pp.

CHAPTER 4: COMPARISON OF TOXICANTS AND ALGAL LIFE STAGES

INTRODUCTION

Several algal species displayed abnormal tissue development and unusually high coverage by diatoms during NPDES[1] surveys in Diablo Cove on May 16, 1984. Bleaching, tissue loss and abnormal development were observed at depths of less than 20 feet in the red alga Botryoglossum and the brown alga Cystoseira osmundaceae in a zone extending from south Diablo Cove northerly to the structure for discharging effluent from the Diablo Canyon Power Plant (Pacific Gas and Electric Company, 1985; Figure 4.1). No abnormalities had been observed during the April 5, 1984 survey. North (1985) observed morphological abnormalities and decreases in abundance of the red alga Calliarthron cheliosporioides along the shoreward 40 meters of a survey transect located directly in front of the discharge in late August, 1984. Increases in the proportion of the Pterygophora californica and Laminaria dentigera populations which had shed their blades were observed in the same area in August 1984 but were not outside historically observed (1976-1984) variations in this parameter. The green alga Ulva lactuca and juvenile Pterygophora were observed in unusually high abundance in the affected region between May and September 1984, a pattern suggesting early phases of colonization of new territory (TERA, 1985). Ulva abundances declined and tissue health of Botryoglossum gradually returned to normal between October and December 1984.

---

[1]NPDES: National Pollutant Discharge Elimination System

Figure 4.1: Map of Diablo Cove showing area impacted by April 1984 event.

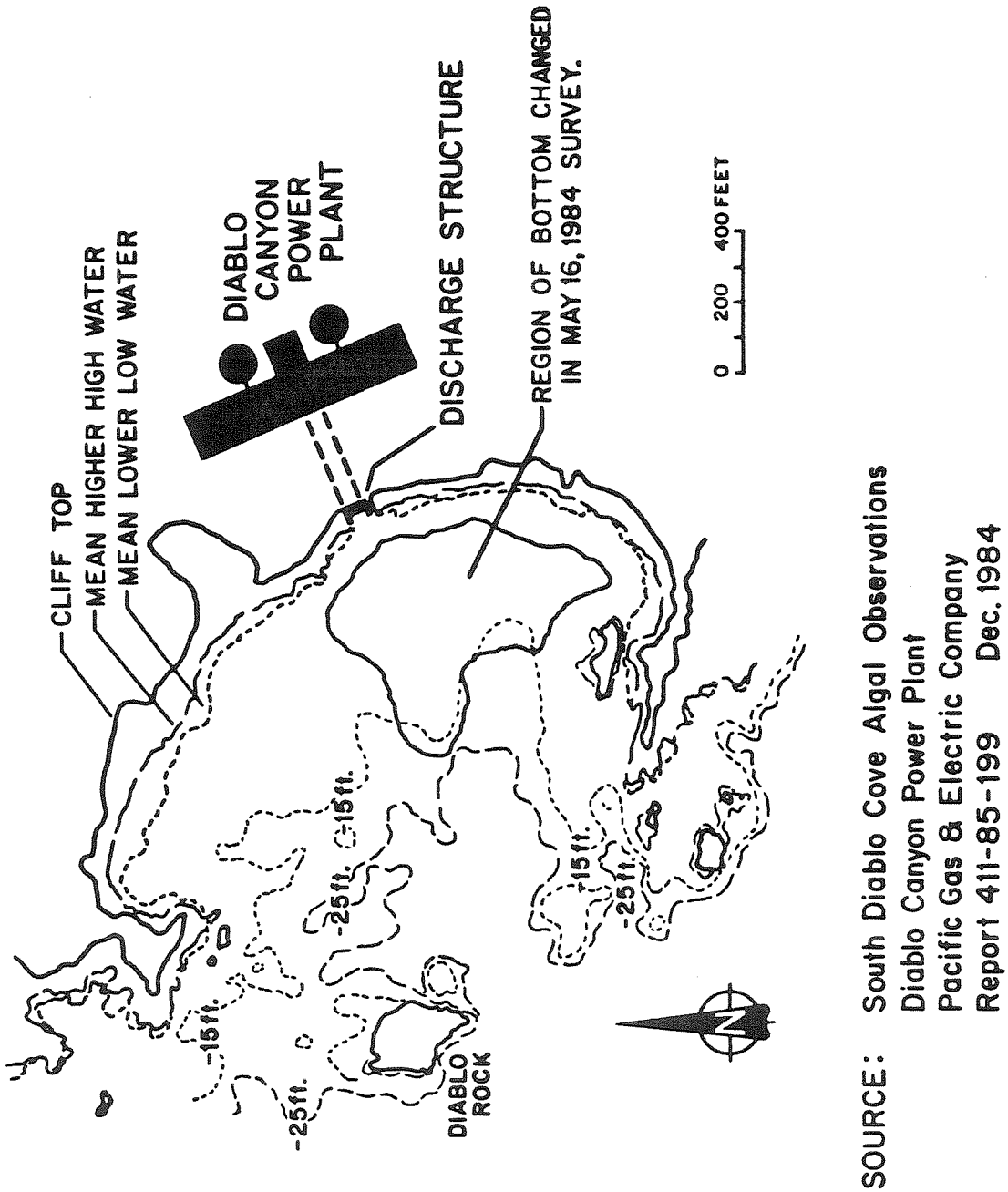

Power plant effluent remained at background temperatures as of the occurrence dates for this event[2]. Pacific Gas and Electric Company was concerned that release of waste from some process in the power plant might have contributed to observed algal stress symptoms. One possibility involved routine discharge of potential toxicants in treated effluent from the liquid radioactive waste-treatment system (LRW) during a low-flow period when the powerplant's main cooling-water discharge pumps were not operating[3]. Coolant in the circulating loop that passes through the reactor core is continuously replaced during power operations to maintain chemical properties within acceptable limits (cf. Chapter 5). Removed primary coolant (called blowdown) is sent through a liquid radioactive waste-treatment system consisting of settling tanks, filters and ion exchange columns designed to remove dissolved and suspended radioactive materials from water bled from the pressurized primary coolant circuit (Glasstone & Sesonske, 1981). Removed radioactive materials are sent to a safe disposal site (California Regional Water Quality Control Board, 1985). Wastes from other processes inside the power plant are also collected and treated by this system prior to discharge.

Combined treated wastes are released from the LRW into the main cooling water discharge before release to the ocean (Figure 4.2). Released volumes are small, typically 10,000-50,000 gallons per day

---

[2]DCPP Unit 1 went critical on April 29, 1984, commenced low-power testing October 18, 1984 and began commercial generation in May 1985..

[3]At least one of the powerplant's four main circulating pumps was usually operating continuously during 1984, discharging 612 MGD of unheated effluent into Diablo Cove.

Simplified Schematic Of Hydrazine Injection
And Discharge In Pressurized Light-Water Reactor Circuits.

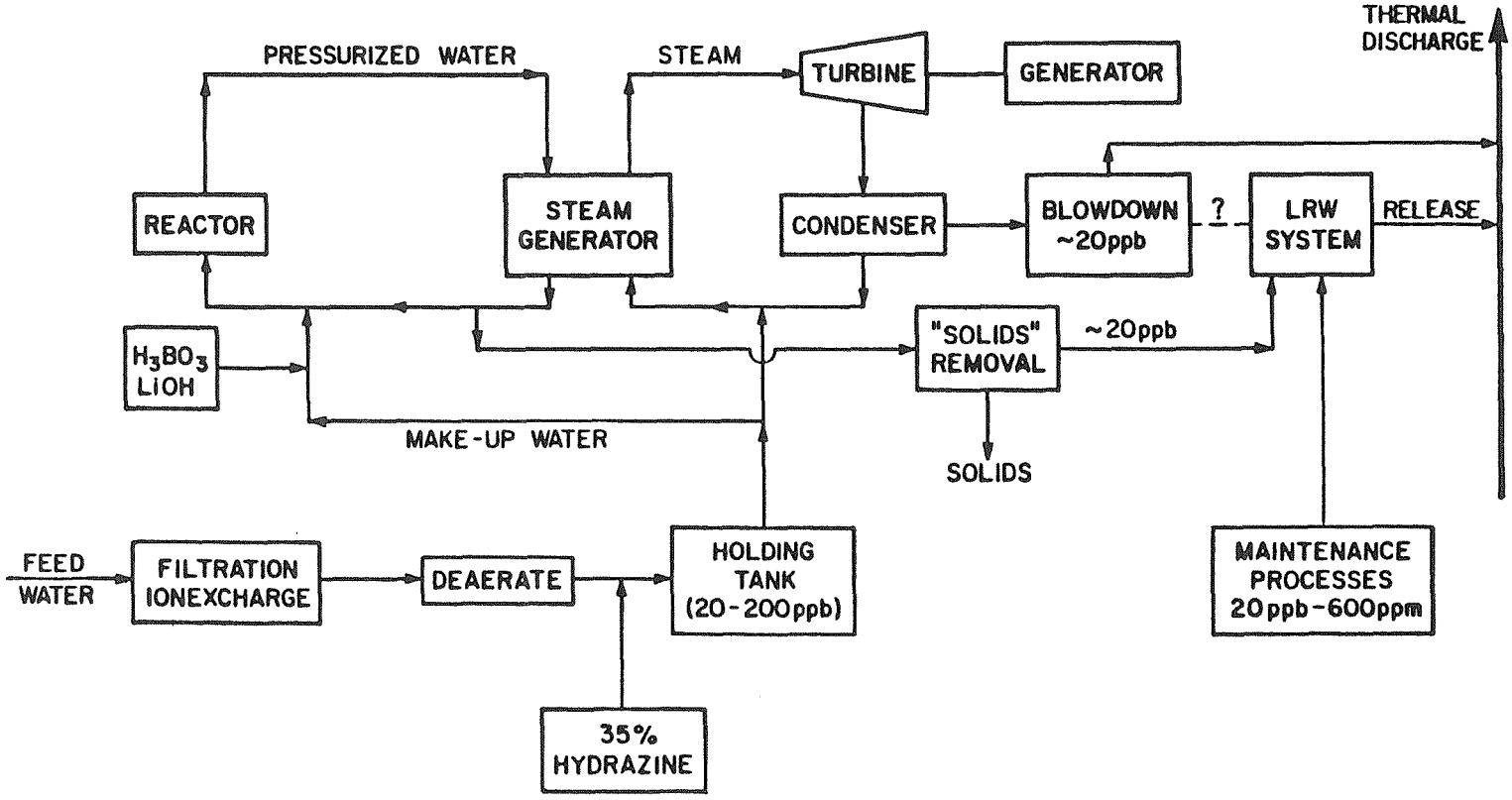

Figure 4.2

(California Regional Water Quality Control Board, 1985; Southern California Edison Company; 1986). Dilution factors are usually high. Discharge from the LRW system at DCPP is metered into the mains at 25 gallons per minute. Overall within-plant dilutions of LRW waste in the final effluent ranged from 1:440 when only auxiliary pumps were operating (16 MGD) to 1:70,560 with all four main circulating pumps operating at full capacity (2540 MGD).

Compounds discharged from the LRW system included lithium ion, boron (as boric acid, H_3BO_3) and hydrazine. Lithium hydroxide is used for pH control in reactor coolant. Boric acid is used as a chemical shim in reactor coolant to moderate the rate of nuclear fission. Hydrazine is used to remove dissolved oxygen from make-up water utilized for replacing both pressurized reactor coolant and blown-down steam from the power-generation circuit. A stoichiometric excess of 20-200 ppb hydrazine is commonly employed to ensure removal of all dissolved O_2 from make-up water before introduction to pressurized coolant and steam-generating circuits (cf. Chapter 5 for a more complete discussion). Average background concentrations of Li^+ and boric acid in seawater are 25 uM and 420 uM, respectively (Bruland, 1983). Hydrazine does not occur in natural waters.

I. SCREENING TRIALS: MACROCYSTIS PYRIFERA SERIES G AND H

Materials and Methods

Concentrations of lithium, borate and hydrazine reported on NPDES-mandated Q2 forms in the DCPP LRW system were surveyed for a two-month period immediately preceding the algal "event" for discharged

maxima to determine the order-of-magnitude concentration ranges for initial toxicity tests. Concentrations at the point of discharge were calculated by assuming complete mixing of the LRW discharge with the cooling water flow and multiplying reported LRW concentrations for each compound by the ratio of the flow rate of the LRW discharge to that of the cooling water stream. Release durations were estimated from reported LRW holding tank volumes (typically 10,000 to 20,000 gallons; Pacific Gas and Electric Company, 1985) and flow rates (25 gallons per minute, D.Behrens, personal communication).

Macrocystis pyrifera gametophytes were selected for initial testing because culture techniques were well developed; fertile adult tissue was available year-round, and some toxicity information was available. Preliminary screening trials followed protocols described in Chapter 2. Toxicant solutions were prepared from reagent grade compounds in either 18 mega-ohm deionized water or double-distilled water. Lithium was added as lithium chloride. Borate was added as sodium tetraborate. Hydrazine was added as hydrazine sulfate ($N_2H_4 \cdot H_2SO_4$).

Initial toxicant concentrations were representative of levels present in effluents released from the liquid radioactive waste (LRW) treatment system before inside-the-powerplant mixing with the main discharge during the April-May 1984 period (Table 4.1). Macrocystis Series G gametophytes aged 5-6 days were continuously exposed to two concentrations each of borate, lithium and hydrazine in screening trials to determine order-of-magnitude concentration ranges for inhibition of vegetative growth and reproduction.

A second set of experiments was performed, testing for effects of synergism or antagonism of Li^+, $B(OH)_4^-$ and N_2H_4. Macrocystis pyrifera Series H gametophytes were exposed to mixtures of 25/170/2400 ppb (Blend A) and 250/1700/24000 ppb (Blend B) added hydrazine/lithium/borate and compared to cultures exposed to 2.5, 25, 250 ppb hydrazine alone. Toxicant effects were measured by methods described in Section 2.III.

Initial screening experiments took place before development of the digital image-analysis system (Chapter 3). Macrocystis pyrifera gametophyte lengths were measured daily on a microscope fitted with an eyepiece micrometer. Sizes of treated cultures were compared to control cultures using one-way analysis of variance (Sokal and Rohlf, 1981) and Student's t-test (Alder and Roessler, 1972).

Sporophyte counts were made by scanning randomly selected fields of microslide surfaces with a microscope eyepiece fitted with a cross-hatched grid. Viable sporophytes appearing within grid boundaries were counted within each field of view. Data were analyzed by Student's t-test if individual field abundances were high. Non-parametric methods were used to test data when abundances were low.

Results: Analysis of Discharge Concentrations

There was a one-week period in mid-April 1984 when flow in the DCPP cooling water discharge was reduced from the usual 595-612 MGD to 16-32 MGD (Table 4.1). Calculated concentrations of all three chemical components in the discharge increased over normal levels by one to three orders of magnitude during the low-flow period (Table 4.1). An additional large hydrazine spike occurred in late May

Table 4.1: DCPP April-May 1984 Emissions at Point-of-Discharge to Sea

Days from April 1		001 flow MGD	Dilution factor*	Concentration ppb Li+	B(OH)4	N2H4	Duration minutes
1		610.6	16961	.03	18.10		25
2		610.6	16962	.01	5.72	.06	1032
3		610.6	16961	.01	8.08		478
4		610.6	16961				
5		610.6	16962	.01	8.14	.35	524
6		610.6	16961				
7		610.6	16960				
8		610.6	16961	.00	.83		466
9		189.3	5259	.01	138.81		483
10	low flow	18.2	506	.66	33.63	3.96	24
11	"	21.5	598	1.07	184.01		500
12	"	21.5	598	.31	870.29	6.69	478
13	"	28.2	783	.55	1385.60	38.31	494
14	"	37.4	1038				
15	"	28.8	801	.10	399.58	164.83	24
16	"	37.4	1039	.83	1405.72		494
17	low flow	45.3	1258	.40	872.37	8.75	932
18		527.4	14650	.08	103.75		492
19		627.0	17418	.05	107.42		
20		627.2	17422	.01	11.77	.34	422
21		627.0	17418	.06	115.98		467
22		675.5	18764	.00	6.40	2.34	503
23		643.7	17881				
24		643.7	17881	.04	37.69	.06	435
25		643.8	17883	.00	6.82	5.59	422
26		643.8	17882	.04	38.59		496
27		643.8	17882	.00	6.71	2.52	510
28		643.8	17882	.07	111.28	.22	530
29		643.7	17881				
30		643.8	17883	.01	4.25	.11	489
31		643.8	17883	.10	11.18	1.01	450
32		643.8	17883	.00	8.50	.34	488
33		643.8	17884	.04	101.77	.45	529
34		643.9	17885				
35		643.8	17883	.00	3.97	.22	422
36		643.8	17884	.04	55.92		505
37		643.7	17881				
38		643.8	17882	.03	68.06		1025
39		643.7	17881	.00		.06	494
40		643.8	17882	.02	53.41		529
41		643.7	17882			.03	
42		643.7	17881	.02	60.12		1046
43		643.7	17881	.00	5.20	.11	500
44		643.7	17881				
45		359.0	9972	.00	15.04	.30	505
46	low flow	31.7	881	.86	1216.26	1.13	511
47		133.7	3715	.08	131.91		477
48		643.7	17881	.02	26.17		501
49		643.8	17883	.07	79.40		438
50		645.7	17935	.04	70.20		500
51		643.7	17881	.02	35.57		944
52		643.7	17881	.05	67.11		477
53		649.4	18040	.00	1.05		488
54		646.2	17951	.03	57.38	.11	513
55		643.7	17882	.03	50.00		944
56		643.7	17880				
57		643.7	17880		55.93		511
58		175.8	4883		5.53	118.79	477
59		312.2	8673				
60		643.8	17882	.07	5.31	.17	505
61		643.8	17882				

*Dilution factor is within-plant value for mixing of LRW discharge with main outfall (001) assuming 25 gpm LRW flow rate.	MAX	1.07	1405.72	164.83
	MIN	.00	.83	.06
	N	46.00	47.00	25.00
	AVG	.13	171.63	14.27
	STD.DEV.	.25	352.62	38.90
	MEDIAN	.05	50	2

Figure 4.3: Diablo Canyon Hydrazine Emissions April-May 1984.
Upper curve: Hydrazine concentration.
Lower curve: Flow in cooling water discharge.

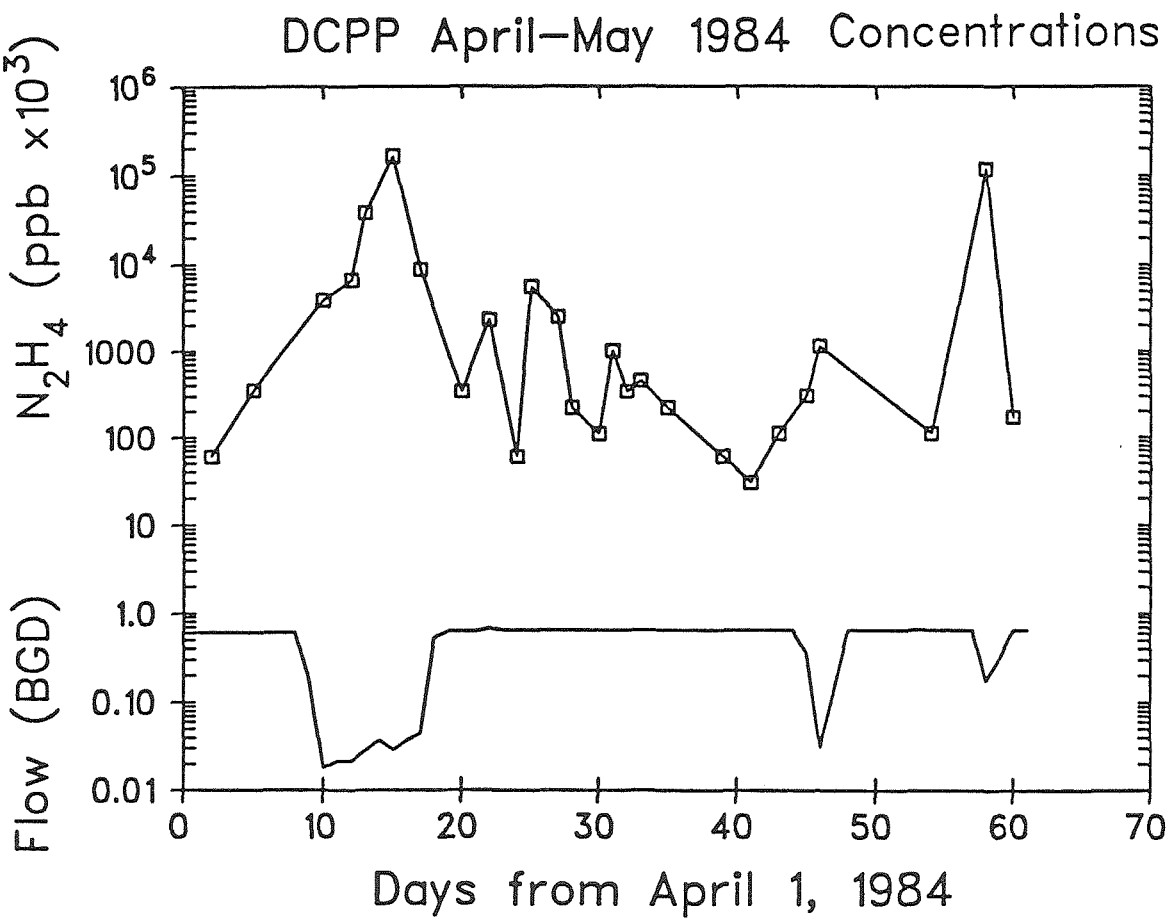

(Figure 4.3). Maximum estimated at-point-of-discharge lithium and boric acid concentrations resulting from LRW discharges, 0.15 uM (1 ppb) and 24 uM (1400 ppb), respectively, were 0.6 percent and 6 percent elevations over average seawater background concentrations of 25 uM (0.17 ppm) for Li+ and 420 uM (24ppm) for H_3BO_3 (Bruland,1983).

Results: Series G

Neither Li^+ nor H_3BO_3 inhibited gametophytic vegetative growth at tested levels (Figure 4.4, 4.5). Apparent Day 11 inhibition may have been caused by a set of anomalously high measurements for the control culture. Mean control size measured on Day 16 was smaller than on Day 11. Observed inhibition was not significant at the $p < 0.05$ level when tested by Analysis of Covariance after removal of Day 11 from the lithium and borate data sets (Sokal & Rohlf, 1981; Table 4.2). Hydrazine significantly inhibited vegetative growth 4 days after application at 250 ppb (8 uM) and 3 days after application at 2500 ppb (80 uM) (Figure 4.6).

Significant[4] inhibition of sporophyte recruitment was observed in 1.7 ppm (246 uM) added Li^+ but not at 17 ppm (2460 uM) on nine measurement days (Table 4.3). Significant inhibition was observed at 24 ppm (320 uM) added borate but not 240 ppm (3200 uM) on Day 12. Both borate concentrations apparently inhibited sporophyte recruitment on Day 18 (Table 4.3). When comparisons were made across all measurement days, both boric acid concentrations were inhibitory.

---

[4]Sampled randomization tests, $p < 0.05$ (Bray, 1988)

Figure 4.4: Series G screening trial. Effect lithium ion (Li+) on gametophyte vegetative growth at 10X and 100X over seawater background concentrations

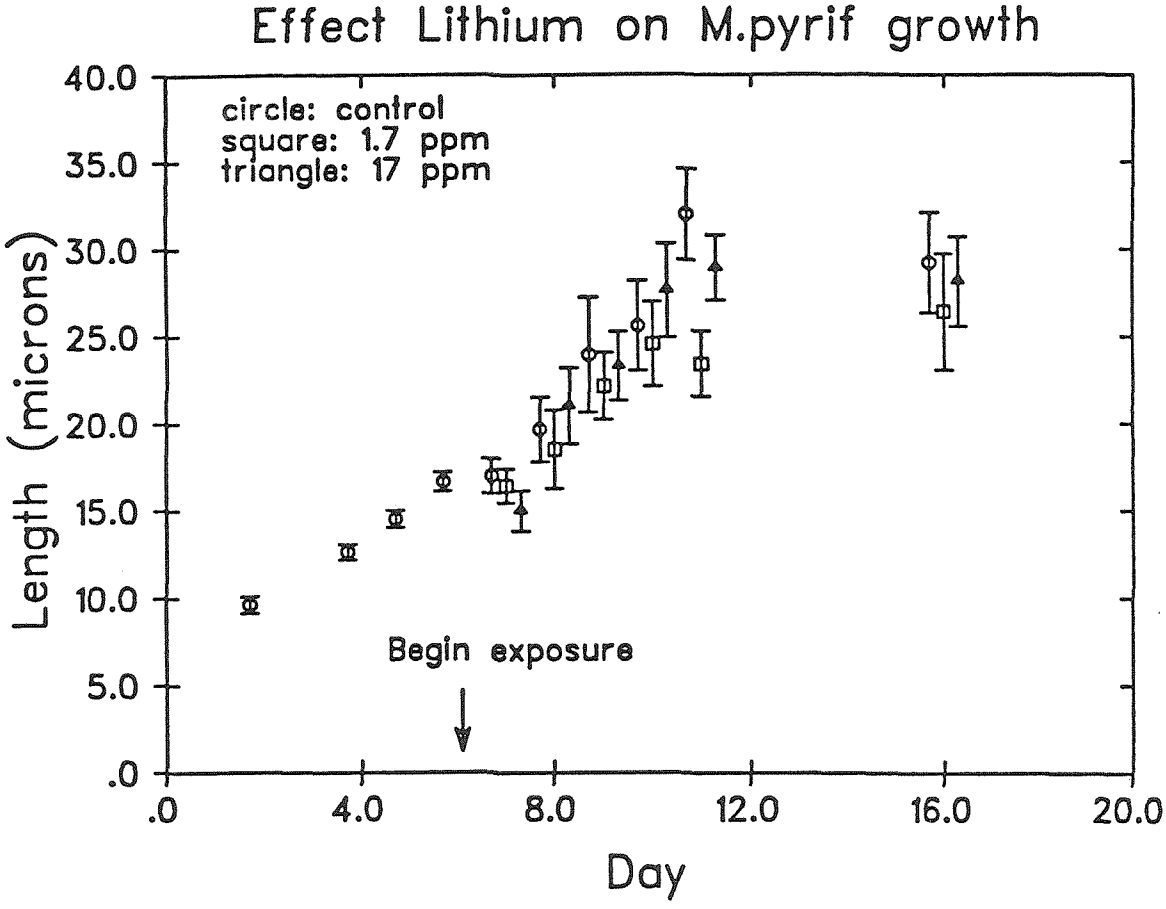

Figure 4.5: Series G screening trial. Effect added boric acid (H_3BO_3) on gametophyte vegetative growth at 2X and 10X over background seawater concentration

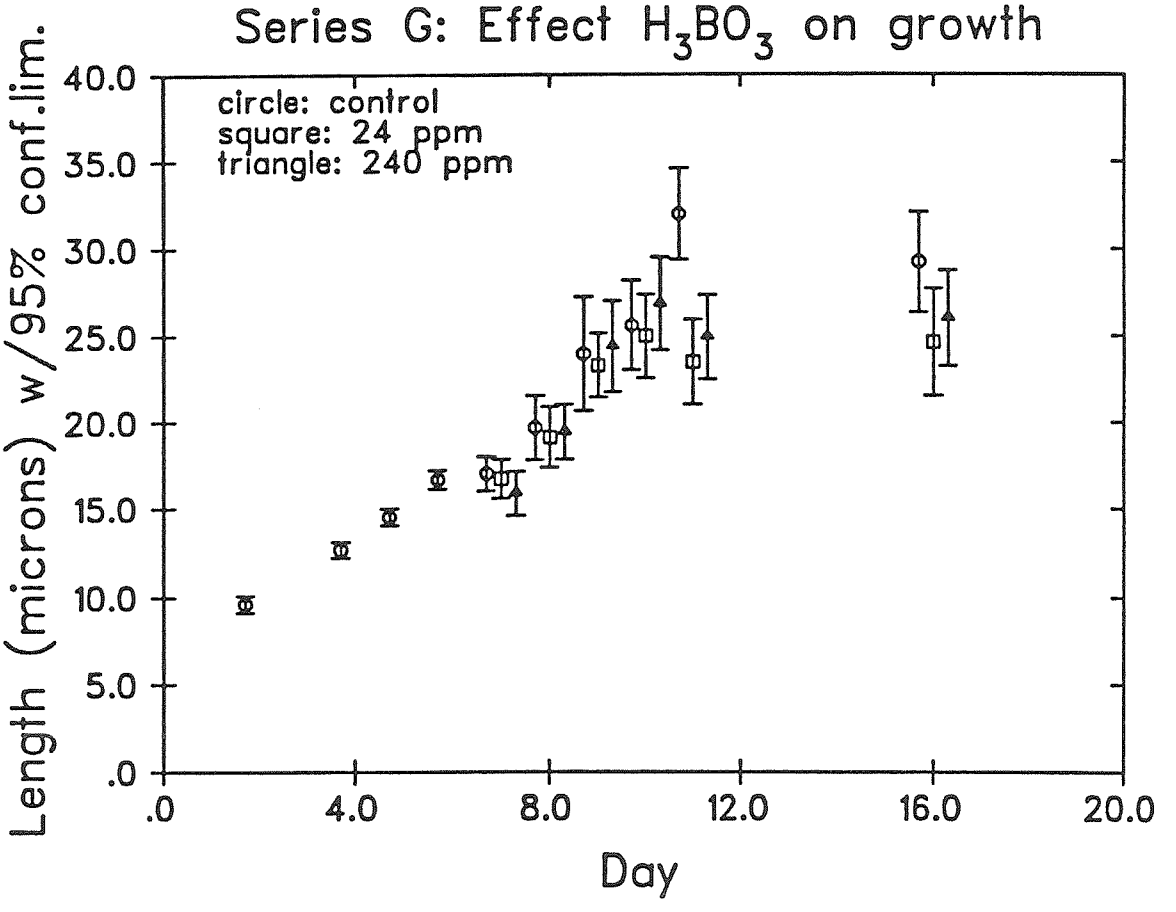

Figure 4.6: Series G screening trial. Effect added hydrazine, N_2H_4, on gametophyte vegetative growth

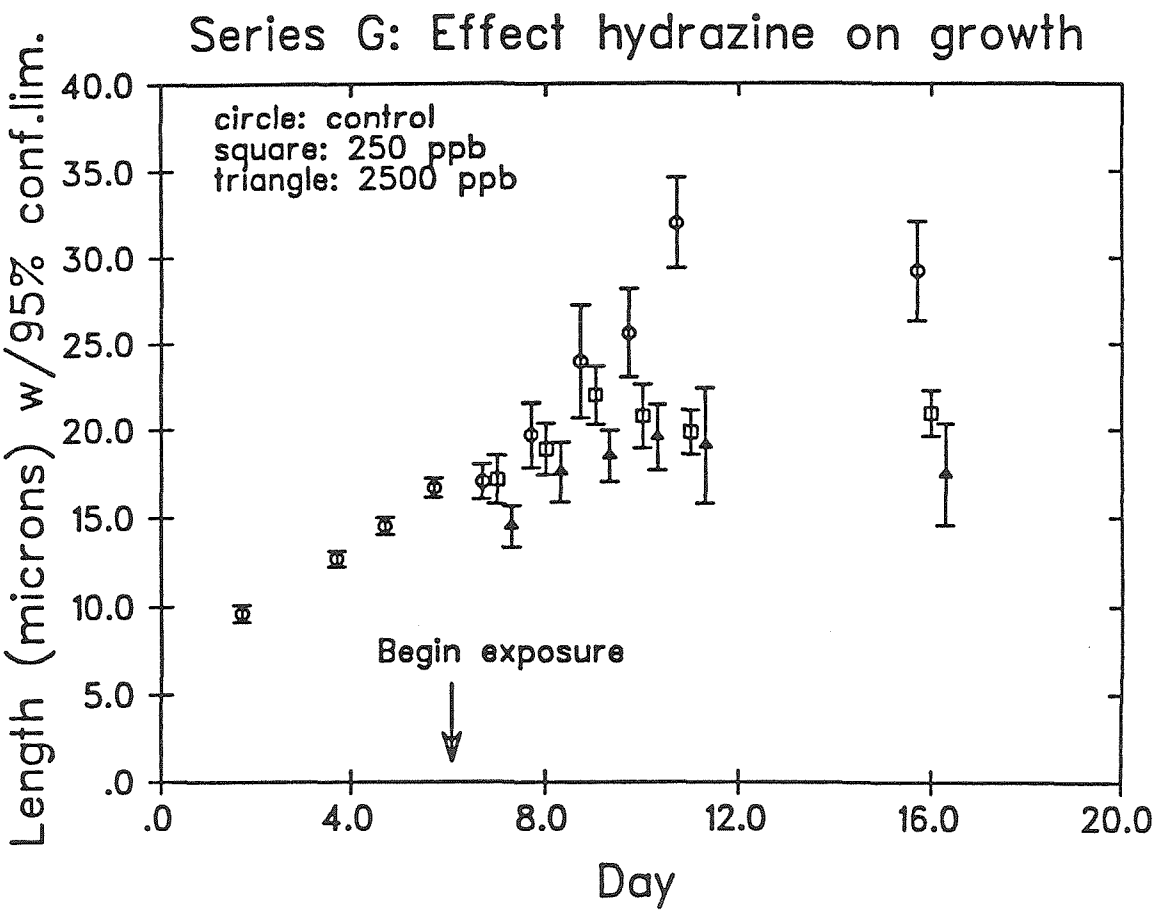

Figure 4.7: Macrocystis pyrifera Series H gametophyte growth.
Comparison of Li+/H3BO3/N2H4 blends with hydrazine alone.
Upper graph: 1700/24000/250 ppb blend vs. 250 ppb
Lower graph: 170/ 240/ 25 ppb blend vs. 25 ppb

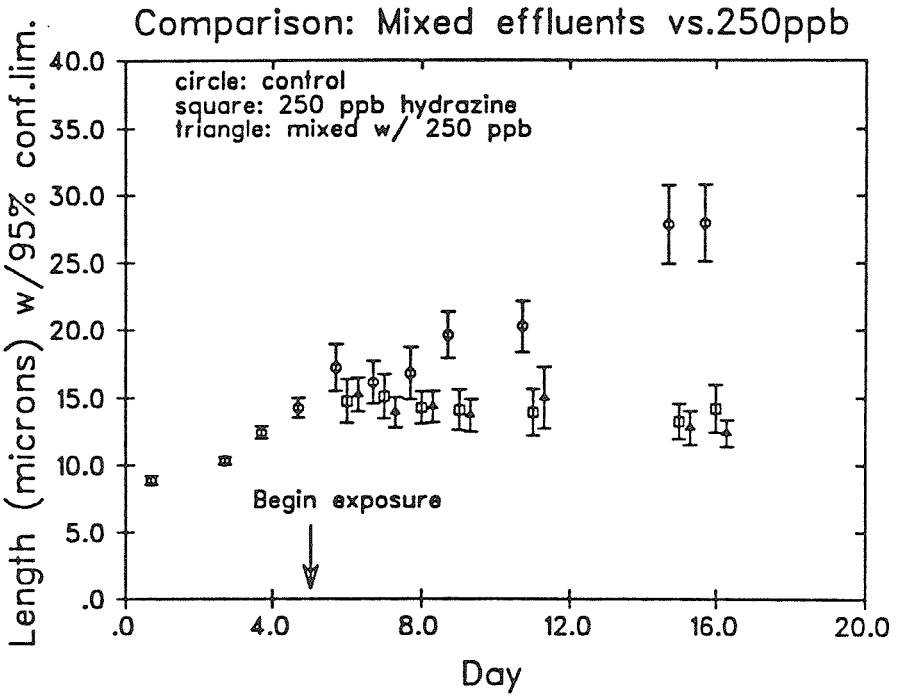

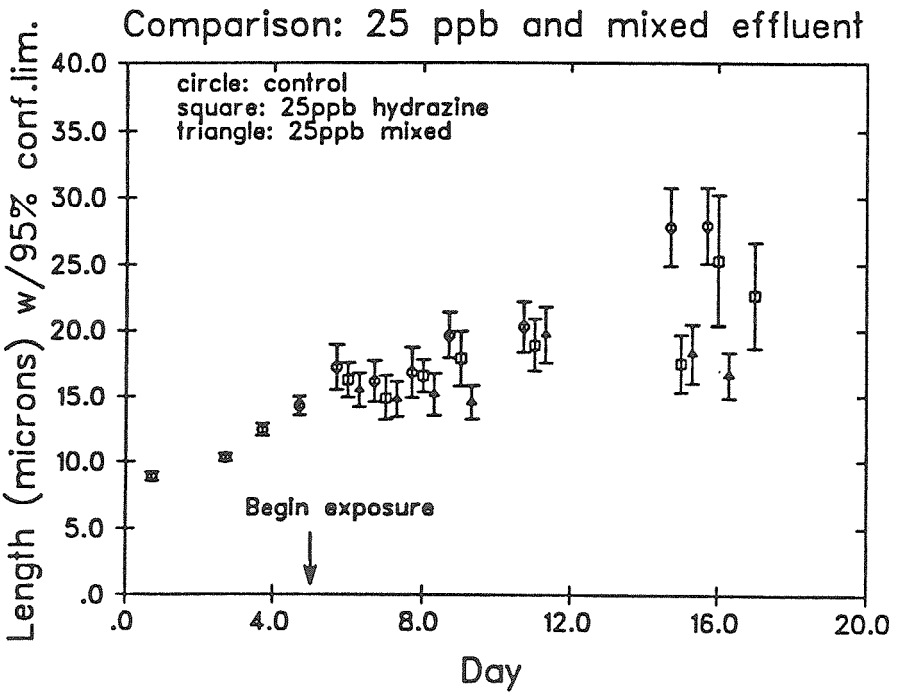

Table 4.2: Effect of Removal of Anomalous Data from Analysis of Covariance. Example data for Control vs. 24 ppm H_3BO_3

Independent variable:	Include Day 11		Exclude Day 11	
	PCT explained	Signif.	PCT explained	Signif.
Time:	18.6	$p < 0.0001$	21.6	$p < 0.0001$
Concentration:	3.3	$p < 0.0004$	1.1	$p < 0.0585$
Residuals	78.1		77.4	

Comparison of Mean lengths w/ 95 percent confidence limits (time trend removed)

	Include Day 11	Exclude Day 11
Control	4.13 ± 0.16	3.89 ± 0.17
24 ppm H3BO3	3.69 ± 0.17	3.65 ± 0.17
Difference between control and 24 ppm	Significant	Not significant
Covariate coefficient (slope of regression line) (used to de-trend data)	0.177	0.166

Table 4.3: M.pyrifera Series G
Effect of effluent constituents on embryonic sporophyte recruitment
Total counts in 26 scans at 160X with cross-hatched reticule

TREATMENT	CONTROL	HYDRAZINE		BORIC ACID		LITHIUM	
		250 ppb	2500	24 ppm	240	1.7 ppm	17
DAYS AFTER START OF TREATMENT							
8	0	0	0	1	0	1	2
9	1	0	0	0	2	3	2
10	5	0	0	4	2	3	12
11							
12	15	0	0	2	12	6	17
13	15	0	0	4	13	6	23
14	22	0	0	6	11	6	25
15	30	0	0	0	3	5	41
16	18	0	0	0	6	10	34
17							
18	28	0	0	1	1	5	29
SIGNIFICANCE ($p <$)		0.000	0.000	0.004	0.033	0.020	0.346

(Probability that null hypothesis was valid; i.e. no significant difference between control column and treatment column)

Test: Sampled randomization of 5% of possible combinations (Bray, 1988)

Hydrazine completely inhibited sporophyte recruitment at 250 ppb (8 uM) and 2500 ppb (80 uM) on all sampling days.

Results: Series H

Vegetative growth inhibition in the cultures exposed to blends of toxicants was similar to that observed in cultures exposed to hydrazine alone (Figures 4.7a, 4.7b). Hydrazine toxicity was slightly enhanced in the mixed toxicants compared to hydrazine alone at 25 ppb. Sporophyte recruitment indicated patterns that were similar in the mixed effluents and plain hydrazine. Stimulated (compared to controls) recruitment occurred in Blend A (25/170/2400 ppb hydrazine/lithium/borate) and in 2.5 and 25 ppb hydrazine. Control cultures did not recruit in adequate density in this experiment. Complete inhibition occurred in Blend B (10X Blend A) and in 250 ppb hydrazine (Table 4.4).

Discussion

Borate concentrations of 50 and 100 ppm (representing elevations of 2X and 4X over background) were previously shown to inhibit growth of 26 percent and 63 percent, respectively, of tested species of marine phytoplankton (Antia and Cheng, 1975). Concentrations of five to 10 ppm did not inhibit growth. Macrocystis pyrifera gametophyte growth was not inhibited at borate concentrations (24 and 240 ppm) bracketing maximum toxicity levels observed for phytoplankton. Sporophyte recruitment was completely inhibited by these levels, indicating that this final stage of Macrocystis reproduction was at least as sensitive an indicator of borate toxicity as phytoplankton growth.

Table 4.4: M.pyrifera Series H Embryonic Sporophyte Recruitment
Comparison of mixed effluents to hydrazine alone
Totals in 20 scans at 160X

TREATMENT:	CONTROL	HYDRAZINE			MIXED EFFLUENTS	
		2.5 ppb	25 ppb	250 ppb	BLEND A	BLEND B
DAYS AFTER START OF TREATMENT						
17	1	2	21	0	5	0
18	1	17	16	0	9	0
19						
20	1	14	34	0	22	0

BLEND A: 25 ppb N_2H_4| 0.17 ppm Li^+| 2.4 ppm H_3BO_3

BLEND B: 250 ppb N_2H_4| 1.7 ppm Li^+| 24 ppm H_3BO_3

Microalgae are sensitive indicators of hydrazine pollution. Harrah (1978) reported six-day EC_{50}[5] values of 0.4, 10 and 16 ppb and six-day safe limits of 0.1, 1, and 5 ppb for growth of the marine phytoplankton species Chlorella stigmatophera, Selenastrum capricornutum and Dunaliella tertiolecta, respectively, in hydrazine-contaminated seawater. Forty-eight hour LC_{50}[6] freshwater toxicity of hydrazine to salamander larvae (Slonim, 1986), was five (soft water) to eight ppm (hard water). Acute 96-hour LC_{50} toxicity to bluegill sunfish was observed at 1 ppm with a no-effect level of 0.43 ppm (Fisher et al., 1980). Macrocystis pyrifera gametophyte growth was significantly inhibited in ten-day 2.5-25 ppb exposures, values close to those observed by Harrah (1978) for phytoplankton inhibition.

Borate and lithium inconsistently inhibited life processes at concentrations one and two orders of magnitude respectively above their estimated seawater background values. The patterns of non-significant growth inhibition and inconsistent sporophyte inhibition by lithium and borate suggested that the lowest tested concentrations (1.7 ppm Li^+, 10X over background; 24 ppm H_3BO_3, 2X over background) were near toxicity thresholds for these compounds. Further research is needed at these low concentrations to establish toxicity thresholds.

Hydrazine was the only tested compound that significantly inhibited growth at concentrations near values estimated to have

---

[5] EC_{50} is the concentration giving a response in 50 percent of a sample population.

[6] LC_{50} is concentration producing death in 50 percent of a sample population.

occurred in the discharge during the April 1984 low-flow period. Hydrazine also exhibited the highest molar toxicity of the three compounds, inhibiting growth at 1/30 the molar concentrations observed for Li^+ and H_3BO_3. Stimulated reproduction may have been caused by decreased coverage of microslide surfaces by vegetative tissue, providing more space for embryonic sporophyte attachment.

Cumulative frequency-distribution data for DCPP emissions during the two-month period preceding the event indicate that a worst-case effluent from the power plant might contain 164 ppb (5 uM) hydrazine, 1 ppb (0.15 uM) lithium and 1400 ppb (23 uM) boric acid elevations over background levels (Figure 4.8). These lithium and boric acid levels represent small incremental increases over seawater background concentrations. Series H test results with Blend B showed that hydrazine toxicity will probably dominate in a worst-case effluent.

High molar toxicity, growth inhibition at concentrations close to environmentally relevant levels and dominant toxicity in mixed effluent tests combined to indicate that hydrazine was the most likely chemical cause of the April-May 1984 events in Diablo Cove possibly associated with stressed algae.

II. LIFE STAGE TRIALS USING HYDRAZINE; M.PYRIFERA SERIES I & J

Introduction

Our initial continuous-exposure bioassays indicated relative toxicity of discharged compounds but did not accurately model the characteristics of discharges from DCPP. Discrete episodes of varying concentration lasting from 20 to 900 minutes occurred during the

Figure 4.8: Cumulative frequency distributions for discharges of lithium, hydrazine and boric acid during April-May 1984, assuming complete mixing within discharge & before dilution in receiving waters.

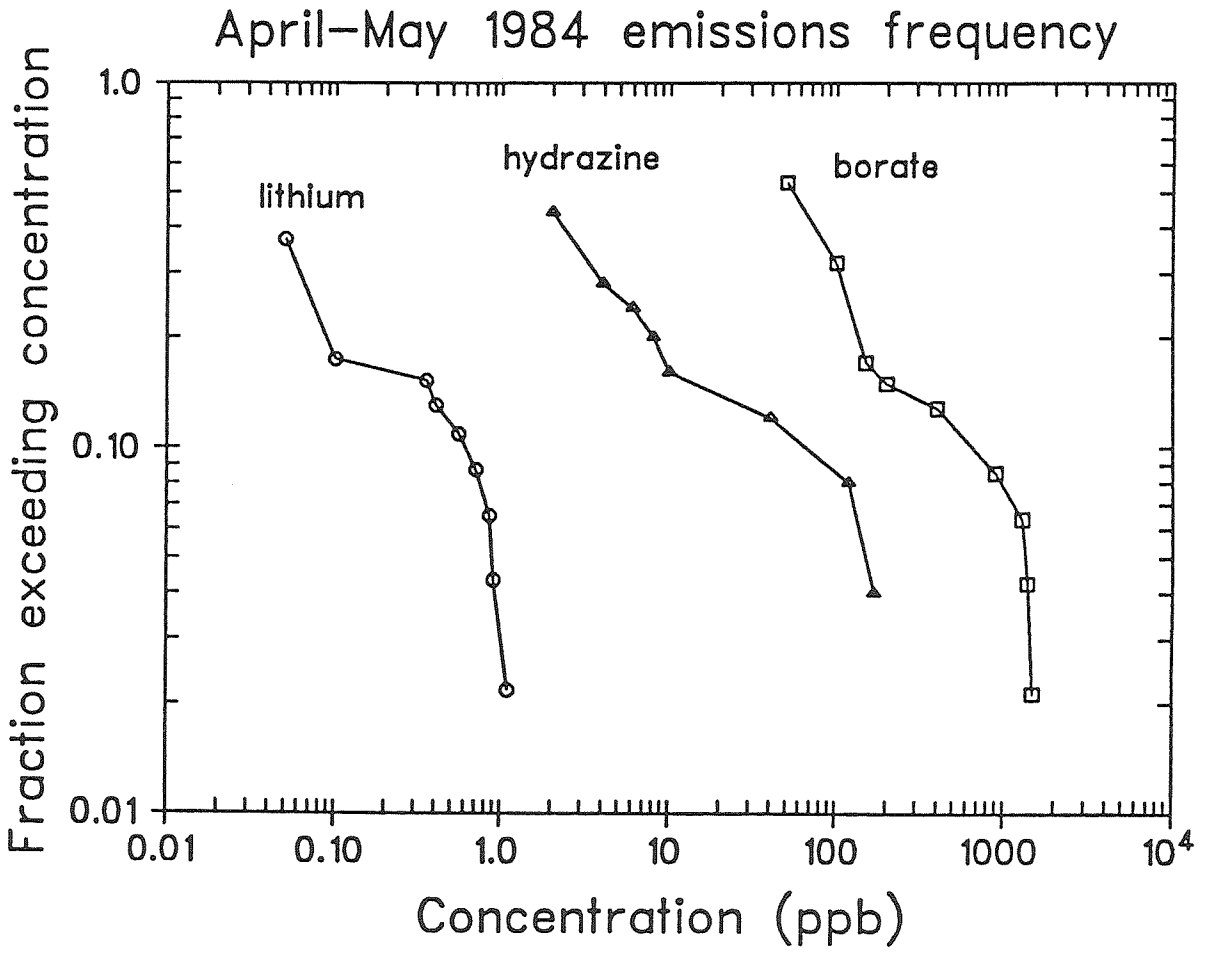

April-May 1984 period (Figure 4.9). The three most likely toxic events appeared to be a 24 minute-165 ppb exposure on 15 April, a 494 minute-38 ppb event on 13 April and a 477 minute-119 ppb discharge on 28 May. (This last event occurred after algal degradation was first observed in the Cove).

High molar toxicity exhibited by hydrazine in early trials led to the question: How does exposure to a discrete episode or pulse of hydrazine affect the several stages in the microscopic part of Macrocystis' life cycle? Motile spores, germinating spores, gametophytes at different ages and embryonic sporophytes might exhibit different sensitivities to the same toxicant exposures.

It was decided to model toxic-pulse episodes with transient exposures whose combinations of duration and concentration bracketed highest known discharges from DCPP. Durations of one hour and one day and concentrations of 25 and 250 ppb were selected for pulsed-exposure trials. These combinations form the four corners of the box shown in Figure 4.9.

Materials and Methods

Culture protocols for Series I vegetative growth and sporophyte recruitment were similar to those described in Chapters 2 and 4.I. Macrocystis pyrifera Series I gametophytes aged three and eight days were exposed to 25 and 250 ppb, 1-hour and 1-day pulses of hydrazine, simulating episodic releases from a power plant. Vegetative growth, sperm production by male gametophytes, sporophyte recruitment, and sporophyte survival were followed for two weeks after application of the toxicant. Gametophyte sizes were measured by

Figure 4.9: Concentration vs. duration relationships for Diablo Canyon hydrazine emissions, April-May 1984. Corners of square indicate pulsed-dose test conditions used for comparisons of algal sensitivity to episodic hydrazine emissions.

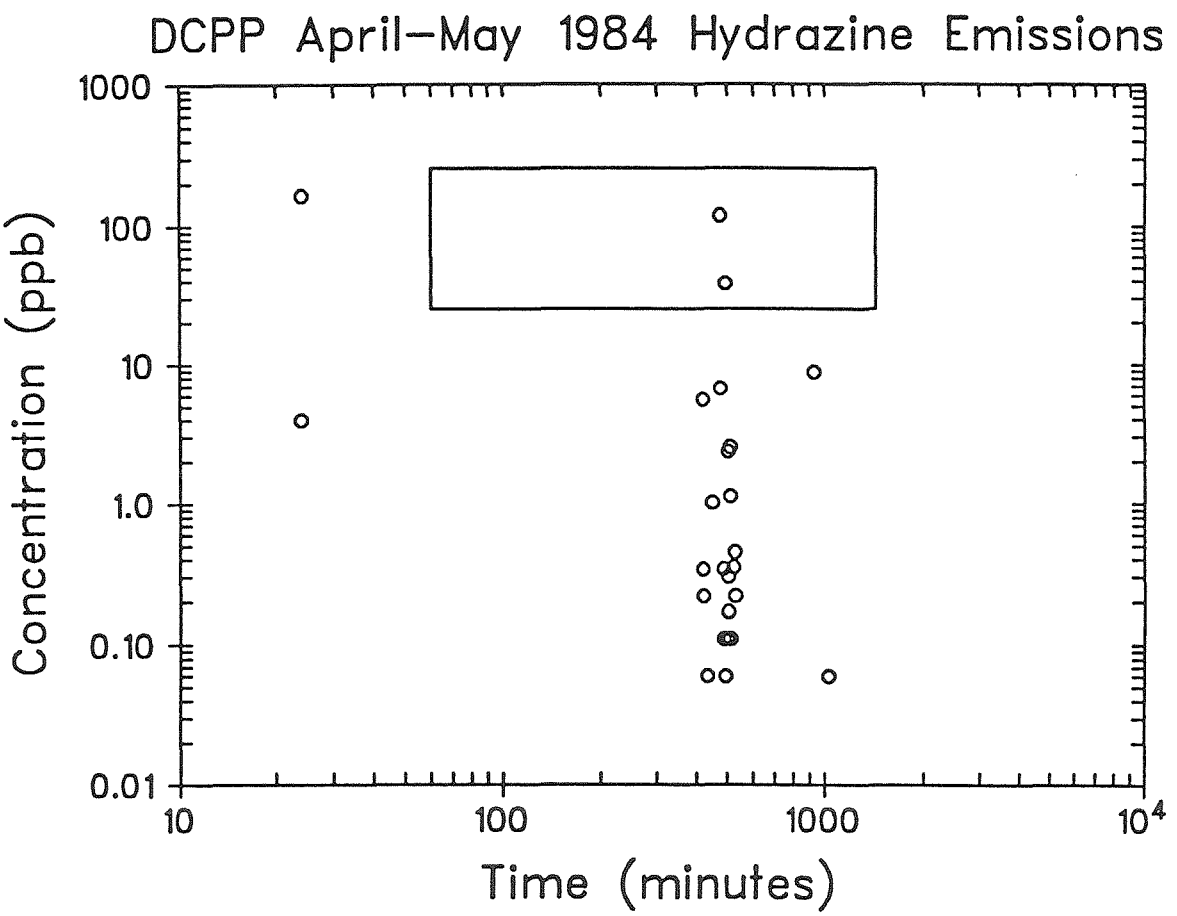

randomly sampling organisms with the eyepiece micrometer at 160X. Sperm and sporophyte densities were estimated by random sampling with the cross-hatched grid at 160X.

Additional techniques were developed to evaluate sensitivity of motile and germinating spores to hydrazine. Recently released Series J spores were blended with seawater containing 2500 and 250 ppb of hydrazine. Two types of trials were used. Type I trials measured change in motility over time in 1 mm deep Sedgewick-Rafter counting chambers. Motile spores in a control and treated cell were maintained on ice and alternately counted under a microscope by random scanning with a cross-hatched grid at 160X. Motility in treated cultures was statistically compared to control motility through analysis of variance and randomization trials. Procedures in the Type II trial were similar, except that spores were maintained in 400 ml beakers at 0°C in control and dilute hydrazine solutions. Aliquots were removed from the beakers at specified time intervals and counted in Sedgewick-Rafter cells. This technique eliminated observed deactivation with time of spores kept too long in the shallow counting chambers, where they were in close proximity to settling surfaces.

Effects on spore germination were evaluated by exposing recently settled spores to a battery of single hydrazine pulses comprised of 25 and 250 ppb concentrations and 1 hour and 1 day durations. The microslide surface was randomly scanned at 160X with a cross-hatched grid in the microscope eyepiece. The total number of spores and number of germinated spores were counted. Germination frequency of

treated spores was statistically compared to controls by an analysis of covariance, which removed effects of local variation in settled spore density.

Inhibition of Series J gametophytes was evaluated by following growth and sperm production of organisms that had been exposed to the standard battery of hydrazine pulses in the germination stage (called Day 0), measuring and evaluating data with methods identical to those used for Series I. Gametophyte survival was estimated by measuring frequencies of completely discolored organisms found in random scans of slide surfaces and by comparing frequency of discolored organisms in treated cultures to that of the controls. Embryonic sporophytes that recruited successfully in Series J cultures were exposed to a set of hydrazine pulses, and their sensitivity was estimated by comparing the relative occurrence frequency of embryos with discolored or disorganized cellular structures in treated cultures to that of controls.

Results: Series I

Significant[7] reduction of vegetative growth occurred only for the Day 3/250 ppb/1 day culture (Figure 4.10). Inhibition was first detected 48 hours after treatments began and persisted throughout the remainder of the experiment. Growth was completely inhibited for four days after application of the hydrazine pulse, then recommenced at a slow rate but remained significantly below controls.

---

[7]One-tailed Student's t-test; $p < 0.05$

Table 4.5: Effect of 250 ppb/1 day hydrazine pulses on sperm production in Macrocystis gametophytes

Mean counts per scan w/ 95% confidence limits
Average of 20 scans at 160X

	Treatment	Pulse Applied on	
Day #	Control	Day 3	Day 8
11	12 ± 4	5 ± 1	9 ± 4*
13	25 ± 6	11 ± 1	8 ± 2
15	67 ± 13	14 ± 2	9 ± 2
18	260 ± 87	14 ± 5	21 ± 8

All Day 3 & Day 8 measurements significantly less than controls (Student's t-test, two-tailed, $p < 0.05$) except for measurement marked with *

Table 4.6 Effect of hydrazine pulses on embryonic sporophyte recruitment
Pulse characteristics described by x1x2x3
x1= Treatment Day x2= Pulse duration (hours) x3= concentration (ppb)
Total counts in 20 scans at 160X

		Treatment							
		x1 Day	3	3	3	3	8	8	8	8
Day	Control	x2 Hours	1	1	24	24	1	1	24	24
		x3 ppb	25	250	25	250	25	250	25	250
17	36		33	51	10	14	58	69	67	$ 4
19	128		148	117	58	37	97	143	83	$22
21	176		110	132	111	59	112	167	112	$15
23	136		125		136	52				49
25	161					62				$35
27	108					64				$41
29	121					63				$39
31	146					49				35
33	131					69				$43
35	101					48				51
37	102					45				37
Significant*			No	No	No	Yes	No	No	No	Yes

*p <0.05 by Wilcoxon rank-sum distribution of counts within each field compared to counts in control fields

$ Day 8 density significantly lower than Day 3 density ($p < 0.05$) by sample randomization and Wilcoxon rank-sum tests.

Figure 4.10A: Effect of pulsed hydrazine exposures on growth of three-day old M. pyrifera gametophytes.

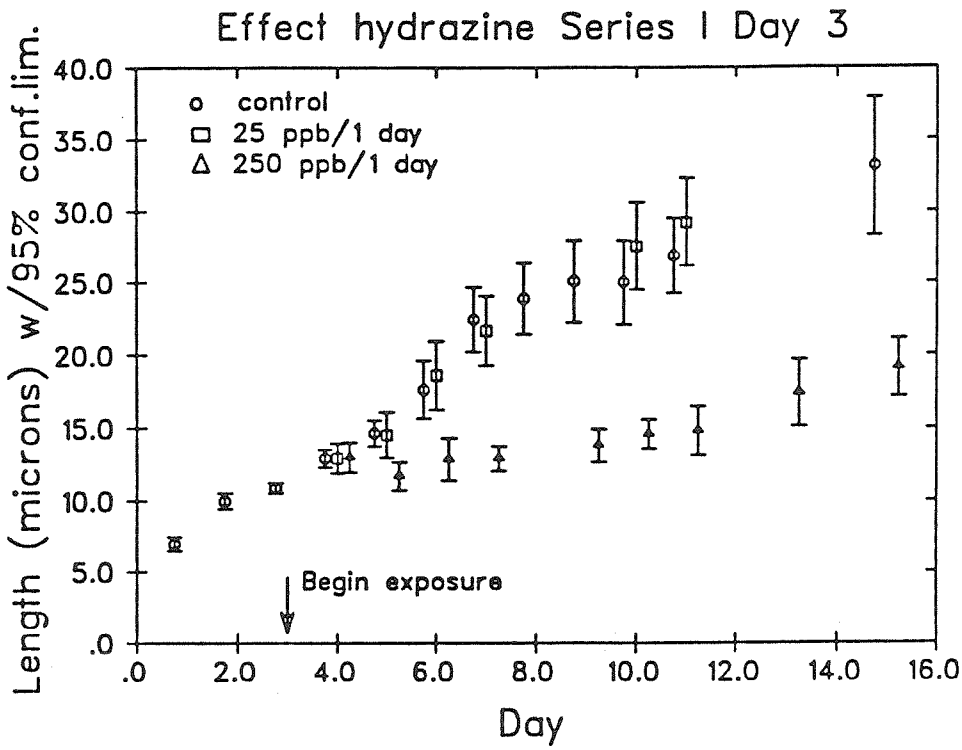

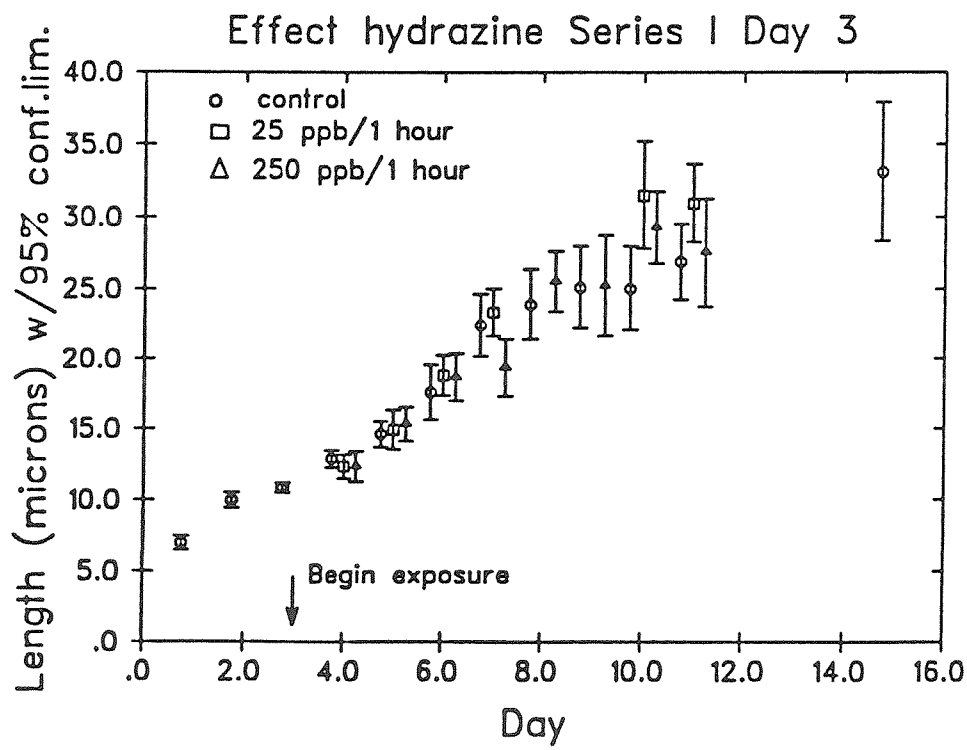

Figure 4.10B: Effect of pulsed hydrazine exposures on growth of eight-day old M. pyrifera gametophytes.

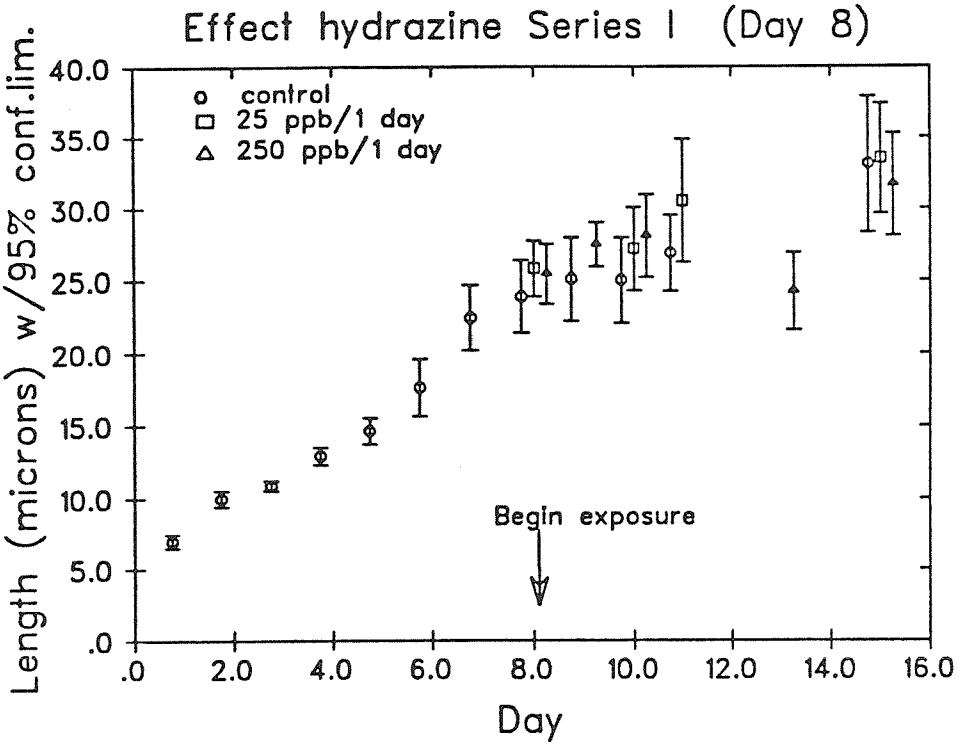

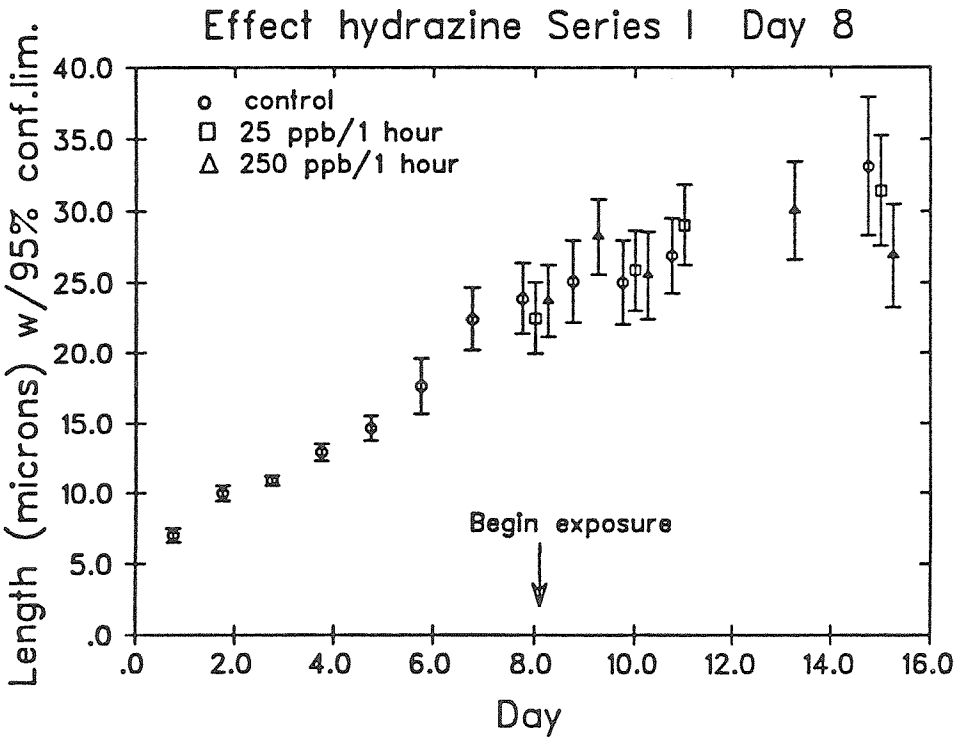

Figure 4.11: Mean counts per field of view of motile sperm at 160X produced by M. pyrifera gametophytes at 160X after early and late exposures to 1-day 250 ppb hydrazine pulses

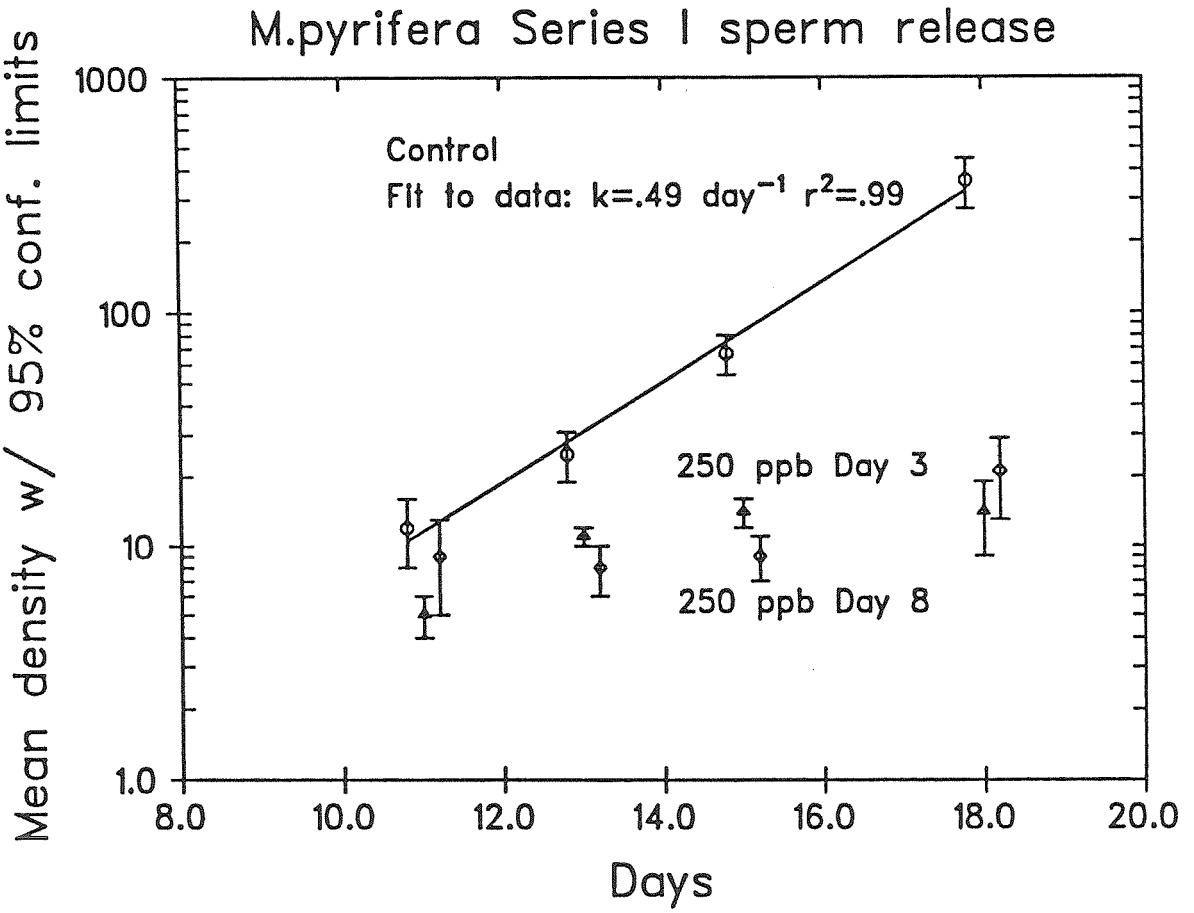

Significant[7] reduction of sperm counts compared to controls occurred in 250 ppb/1 day cultures exposed on Day 3 and Day 8 (Table 4.5; Figure 4.11). No significant reductions were observed in other combinations of concentration and duration.

Significant[8] reduction of recruited sporophytes occurred at the same dose as for sperm inhibition (Table 4.6; Figure 4.12). Sporophyte densities on Days 17,19 and 21 were significantly[9] lower following a Day 8 treatment than after a Day 3 treatment. Recruited density increased until Day 20, then levelled off in each treatment.

Significant[10] increases in embryonic sporophyte mortality were observed after exposure to the 250 ppb/1 day hydrazine dose (Table 4.7). Twenty-five ppb/1 hour and 250 ppb/1 hour doses did not significantly change sporophyte mortality up to seven days after exposure. Time lag between application of dose and detection of increase in mortality decreased when doses more severe than 250 ppb/1 day were applied (Table 4.7).

Results: Series J

Significant[11] inhibition of spore motility took place within 18 minutes at 2500 ppb hydrazine in a Type 1 spore motility trial (Figure 4.13). Erratic inhibition was observed in a Type 2 trial when

---

[8]Sequential Wilcoxon rank-sum tests on each measurement day; $p < 0.05$; (Alder & Roessler, 1972)

[9]Wilcoxon rank-sum and complete randomization tests; $p < 0.05$

[10]Distributions of data within treated samples compared to those of controls by Wilcoxon rank-sum method on each measurement day.

[11]Wilcoxon rank sum test; $p < 0.05$.

Table 4.7: *Macrocystis pyrifera* Series I
Embryonic sporophyte mortality after hydrazine pulse application
Per-cent mortality observed in 20 scans at 160X

Day	Control	Treatment: x1 Day	22	29	29	29
		x2 Hours	24	120	1	24
		x3 ppb	250	250	2500	2500
31	n.m.#		27%	2%	0%	0%
33	n.m.#		1%	1%	9%	<u>99%</u>
35	6%		5%	<u>25%</u>	<u>15%</u>	<u>95%</u>
37	1%		<u>36%</u>	<u>80%</u>	<u>17%</u>	<u>100%</u>
	Days required to develop significant mortality*		15	8	6	4

Underlined values significant compared to controls by Wilcoxon rank-sum method ($p < 0.05$)

*Mortality defined as loss of chlorophyll and/or cellular disruption
#n.m. means not measured

Table 4.8: Macrocystis pyrifera Series J Spore motility trials. Tests of significance using within-group variation. Data: mean number of motile spores ± 1 standard deviation.

			Statistical Test method#		
Minutes	Control	250 ppb	Student's t	Randomization	ANOVA*
10	11.9 ± 2.5	7.8 ± 2.2	$p < 0.005$	0.00249	$p < 0.05$
25	11.4 ± 2.0	10.8 ± 2.1	$p > 0.1$	0.36193	$p > 0.05$
38	13.8 ± 4.2	11.4 ± 1.6	$p > 0.05$	0.08959	$p > 0.05$
55	9.6 ± 1.3	7.6 ± 1.4	$p < 0.01$	0.00886	$p > 0.05$
85	11.4 ± 1.9	9.2 ± 2.4	$p < 0.05$	0.04623	$p > 0.05$

#Probability that the populations from which the samples are drawn have identical means.

*If all sample times were lumped together and compared between control and 250 ppb, then probability by ANOVA was 0.0003. (Analysis of Covariance showed time to be insignificant variable).

Tests of significance comparing control and 250 ppb treatments using only total number motile spores observed in each treatment.

STATISTICAL TEST	PROBABILITY#
Wilcoxon rank-sum	0.047
Randomization	0.03175

Table 4.9: Series J Spore germination trials. Tests of significance of effect of hydrazine treatment on degree of spore germination. Data shown: Means of 16 scans each treatment at 160X.

Method I. Multiple range analysis by computing percentages in each field using Analysis of variance: Significance of treatments: $p < 0.0023$.

LEVEL	SAMPLE SIZE	AVERAGE	95% CONF.	HOMOGENEOUS GROUPS	
250ppb/1 hour	13	0.788	0.036	*	A group is a column
250ppb/1 day	16	0.807	0.032	*	of asterisks. All
25ppb/1 hour	16	0.840	0.032	**	treatments in a group
Control	16	0.850	0.032	**	are not significantly
25ppb/1 day	16	0.880	0.032	*	different.

Method II. Multiple range analysis by removing density effect through Analysis of Covariance: Significance of treatments: $p < 0.0027$.

LEVEL	SAMPLE SIZE	AVERAGE	95% CONF.	HOMOGENEOUS GROUPS
250ppb/1 day	16	28.3	1.2	*
25ppb/1 hour	16	29.6	1.2	**
250ppb/1 hour	13	29.6	1.3	**
25ppb/1 day	16	31.4	1.2	*
Control	16	35.0	1.1	*

Germinated density on average was 86.5 percent of total spore density
Fluctuating density accounted for 90 percent of variance in data.
Treatments accounted for 2% of variance; Residuals were 8% of variance.

Figure 4.12: Total counts in 20 scans per day at 160X of embryonic sporophytes recruited from M. pyrifera Series I gametophyte cultures after early and late exposures to 1 day 250 ppb hydrazine pulses.

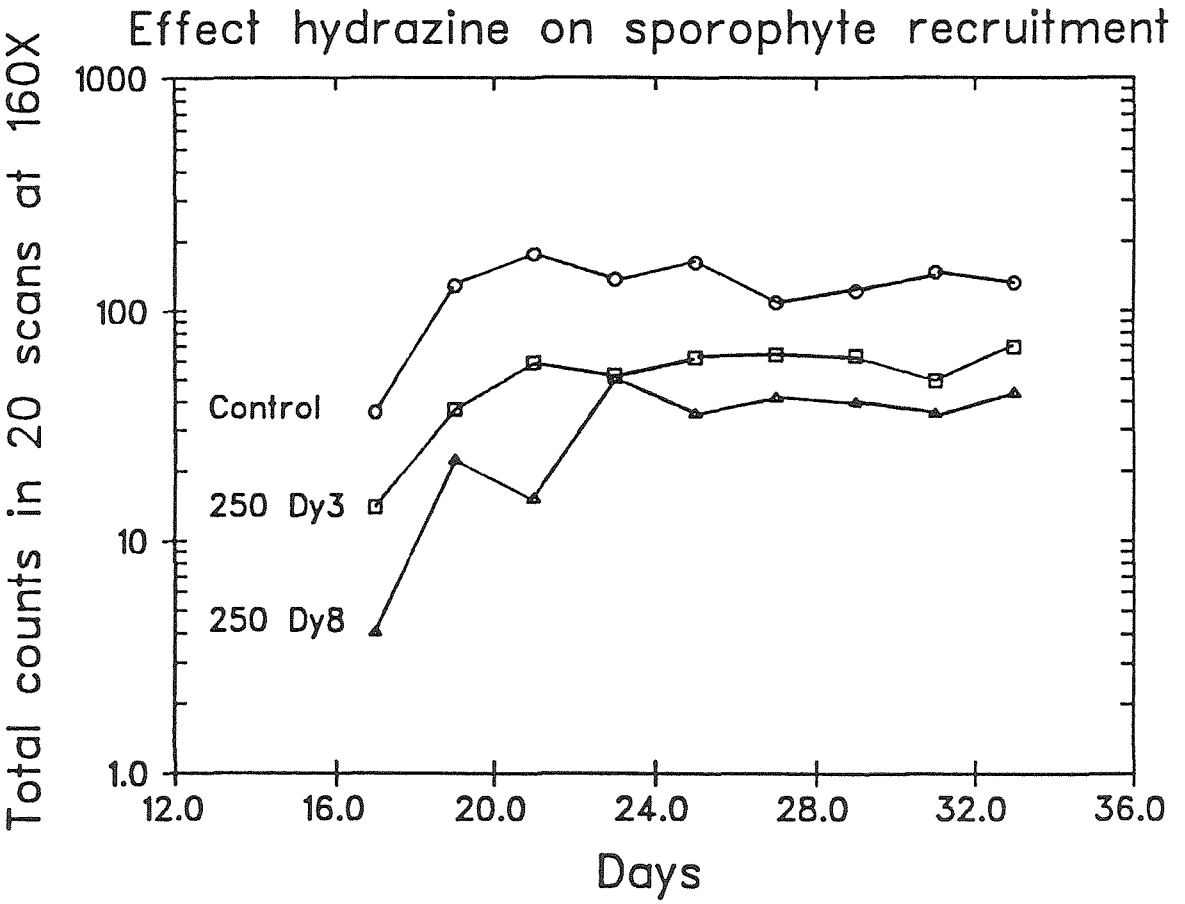

Figure 4.13: Inhibition of M. pyrifera zoospore motility in a Type I (Sedgewick-Rafter cell) trial in 2500 ppb hydrazine.

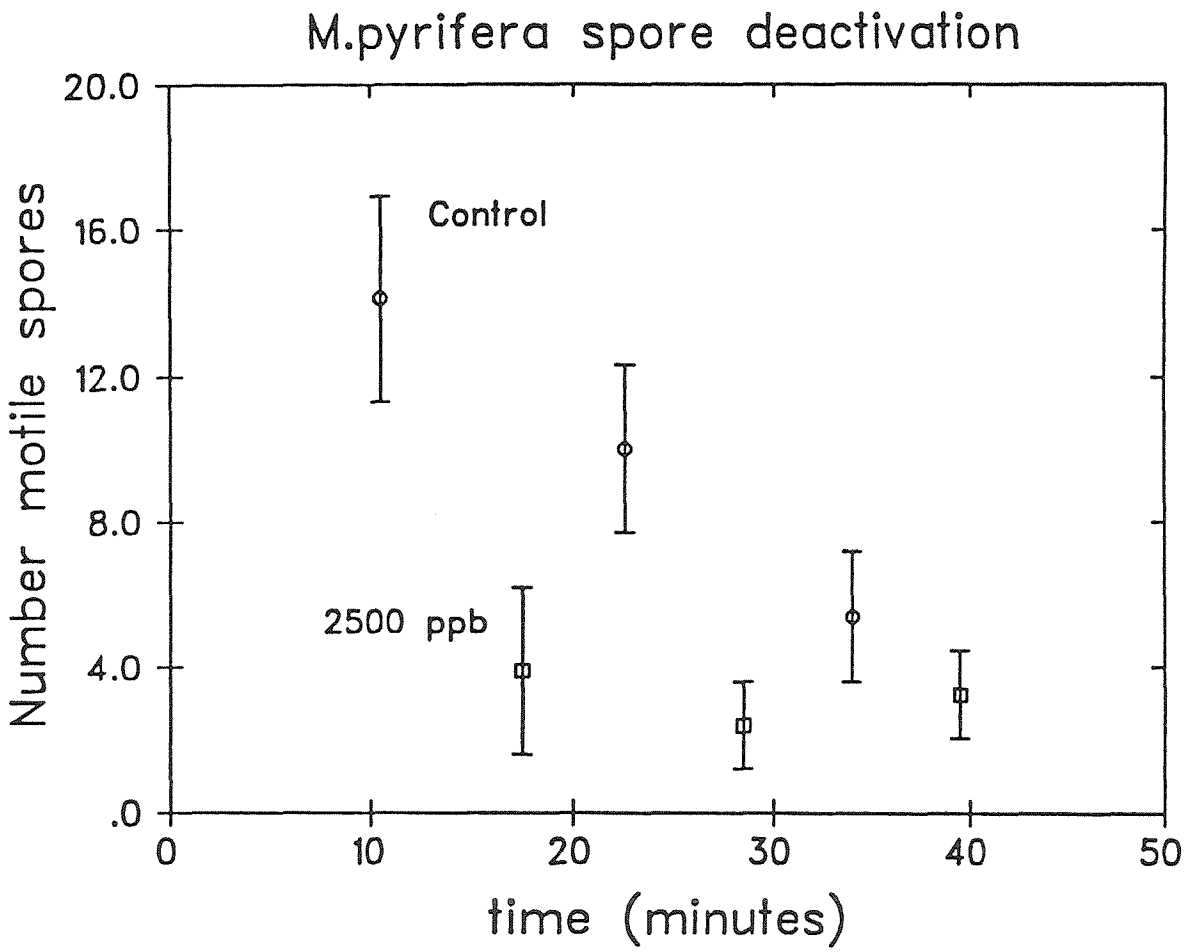

Figure 4.14: Inhibition of M. pyrifera zoospore motility in a Type II (open beaker) trial in 250 ppb hydrazine.

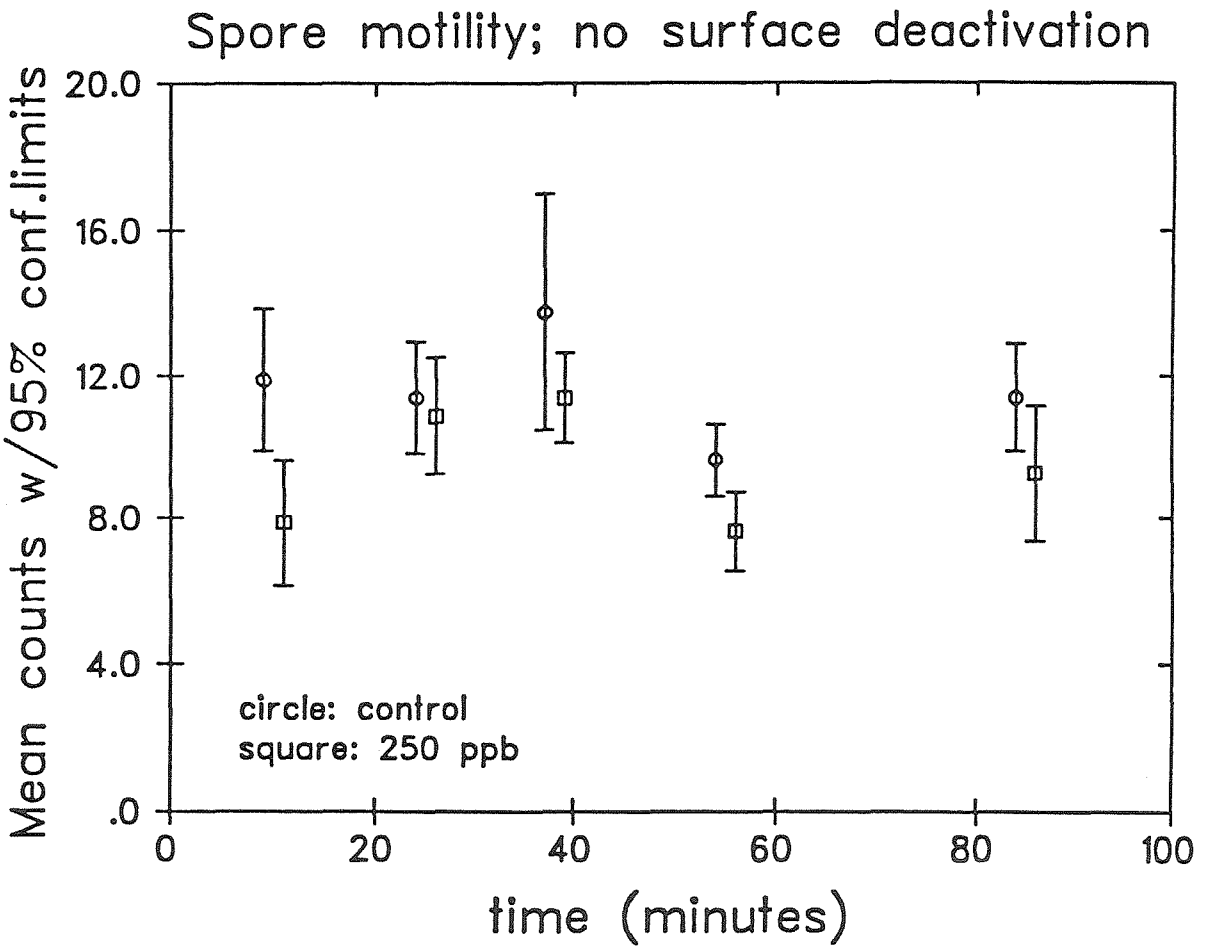

control and 250 ppb treatments were applied without surface deactivation (Figure 4.14). Within-sample variation was large. Randomization tests (Bray, 1988) and analysis of covariance (Sokal and Rohlf, 1981) comparing distributions of data within pairs of control and 250 ppb samples at each measurement period indicated varying probability that the lower activity of treated spores was a random event (Table 4.8). Randomization trials were emphasized because the test does not assume any type of distribution for the population from which the samples were drawn.

Tests of between-group variation, comparing total counts of active spores in all samples of the control and 250 ppb treatments by randomization trials, showed that there was a 3.18 percent (one-tailed) probability that the mean for treated spores was lower purely by chance (Table 4.8). Analysis of covariance, which showed that there was no significant trend in density with time, indicated that 250 ppb-treated spores were significantly inhibited compared to controls ($p < 0.0003$; Table 4.8).

Pulsed hydrazine doses reduced spore germination frequency compared to controls, but effects were small (Table 4.9). Significance of the outcome depended on how data were manipulated. No significant difference was detected when mean germinated spore density was compared among treatments by analysis of variance. This result occurred because settled spore density varied locally on the slide surfaces. Significance was detected when settled density was removed from the raw data by analysis of covariance (Table 4.9, Method II). Spore germination was significantly reduced in all

treatments compared to controls after removal of local density. The outcome was different when germination frequencies (ratio of number of germinated spores to total number of spores) were computed for each field. Only the 250 ppb treatments were significantly reduced compared to controls (Table 4.9, Method I).

The outcomes differ because analysis of covariance corrects germinated spore density using a regression equation calculated using all the data. Direct calculation of germination frequency corrects for observed density in each field of view. The covariance technique gives results closer to expectation of greatest inhibition in harshest treatments, but results are still somewhat ambiguous as three treatments (25 ppb/1 hour and 1 day and 250 ppb/1 hour) showed no significant differences. Compared to vegetative growth inhibition and sporophyte recruitment, spore germination does not seem to be a sensitive indicator of toxicity. Resolution might be improved in a repeat experiment with replication and increased sample sizes.

Vegetative growth of gametophytes developing from the exposed germinating spores[12] was significantly inhibited at lower concentrations than was observed when gametophytes were exposed at later stages (Table 4.10; Figure 4.15). Cultures treated at 25 ppb/1 day and 250 ppb/1 hour were inhibited for only one day. Inhibition was permanent at 250 ppb/1 day.

---

[12] 24-48 hours are necessary for germination, extension of the germ-tube and migration of cytoplasm from spore case into the germ-tube before vegetative growth begins. The date of completed germination is arbitrarily called Day 0.

TABLE 4.10: Summary of observed pulsed hydrazine inhibition
M.pyrifera gametophyte vegetative growth
Reported as days significant inhibition/maximum percent inhibition

Series	Method	Day Pulse applied	Pulse concentration & duration 25ppb 1 hour	250ppb 1 hour	25ppb 1 day	250ppb 1 day
J	micrometer	0	0/ 0	1/ 34%	1/ 14%	14/ 92%
I	micrometer	3	0/ 0	0/ 0	0/ 0	9/ 70%
M	micrometer	5	no data	no data	0/ 0	1/ 56%
M	digit	5	no data	no data	0/ 0	7/ 46%
I	micrometer	8	0/ 0	0/ 0	0/ 0	0/ 0

Uncertainty in degree of inhibition calculations is $\pm$ 15 percent.

Table 4.11: Series J gametophyte survival in hydrazine pulses
Number of surviving gametophytes found on Day 12

Application Day Duration Concentration	Control	-1 24 hours 250 ppb	6 24 hours 50 ppb	6 24 hours 125 ppb	6 120 hours 125 ppb
Raw Counts	30	11	35	10	27
per field	48	6	35	10	13
at 160X	26	5	33	11	23
	32	5	35	23	23
	54	18	29	23	38
	20	12	24	36	24
	31	8	27	25	22
	24	12	23	29	22
Mean	29	7	18	21	19
standard dev.	16	5	14	10	12
Fraction control		0.24	0.60	0.71	0.64
absolute uncertainty		± 0.22	0.60	0.52	0.48
Significance*		0.0008	0.277	0.025	0.045

Survival judged as gametophytes retaining pigmentation and cell-wall integrity

*Probability that null hypothesis (treated culture not less than control culture) is valid.

Significance computed by complete randomization trials on raw data.

Figure 4.15: Effect of pulsed hydrazine exposures applied during germination (Day -1) on growth of M. pyrifera gametophytes

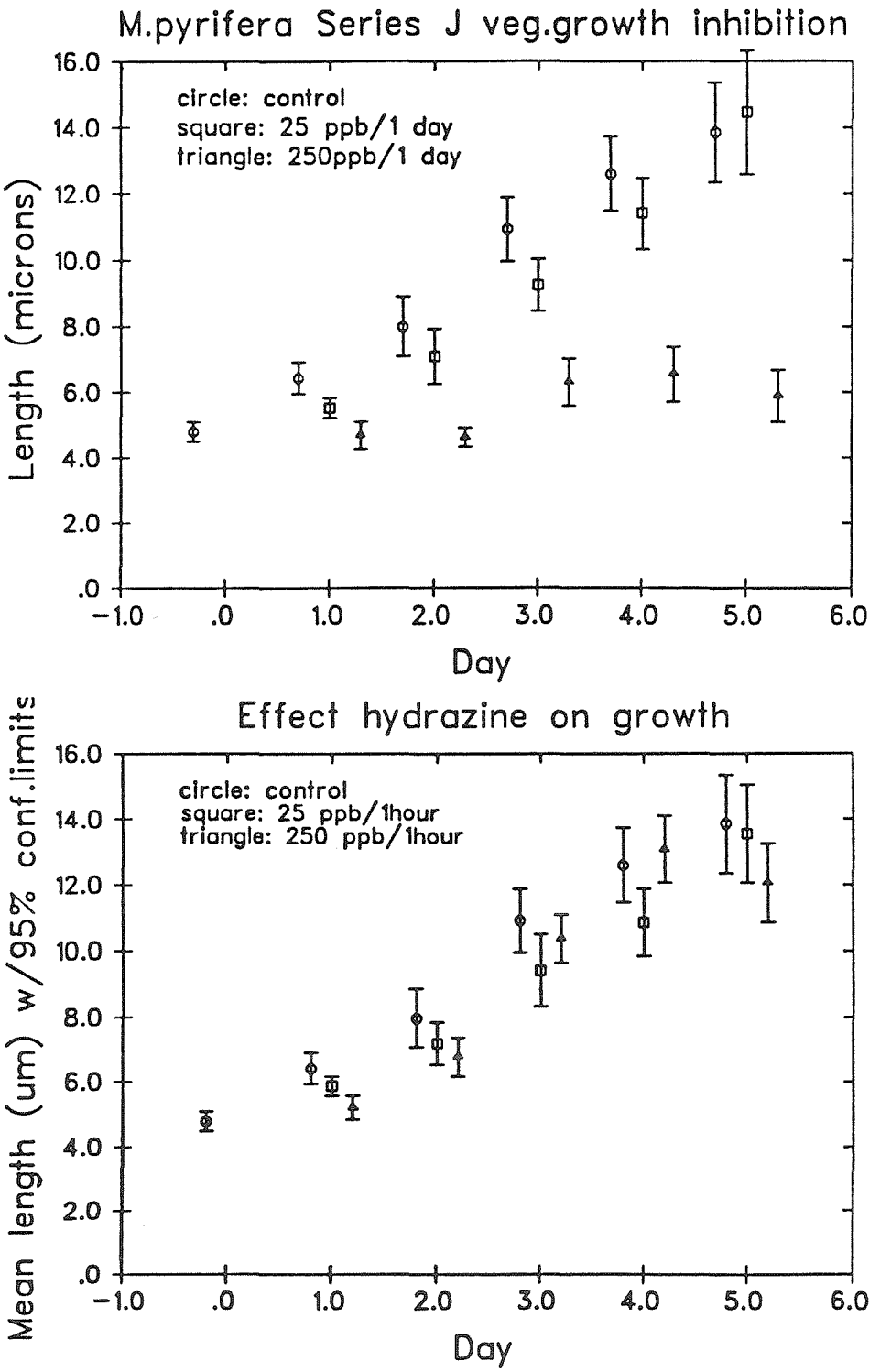

Gametophyte survival was significantly[13] reduced compared to controls twelve days after the 250 ppb/1 day treatment was applied at the germination stage (Table 4.11). Lower concentration pulses applied to vegetatively growing gametophytes (Day 6) inhibited survival, but the reduction was not as strong as for a germination-stage exposure.

Discussion

Significant inhibition of spore motility was detected in less time than for any other test at 250 ppb hydrazine, indicating the potential of this technique as a short-term toxicity screening test. Screening tests have been developed using sea urchin sperm motility as an indicator of toxicity (Nacci, et al., 1986).

Significance in spore germination results depended on methods used to treat the data. No clear trend could be discerned with increasing exposure time or concentration, indicating that germination may not be a sensitive indicator of toxicity.

The several microscopic life stages of Macrocystis pyrifera exhibited different sensitivities to episodic hydrazine exposures (Table 4.12). Each life stage has not yet been exhaustively tested, but available data suggest several trends:

1) Time lag for detection of inhibition tended to increase with increasing size and complexity of each microscopic life stage. Spore motility inhibition could be detected in one hour at 250 ppb. Gametophyte growth inhibition detection in a 250 ppb/1 day pulse took

---

[13]Student's t-test, one-tailed, $p < 0.05$

Table 4.12: Comparison of hydrazine sensitivity in several Macrocystis microscopic life stages.
Minimum tested pulsed N_2H_4 dose giving significant effect.

Process	ppb hydrazine causing effect	Exposure Time
Spore motility	250	1 hour
Gametophyte survival	5000	1 hour
	250	1 day
Gametophyte growth rate	1000	1 hour
	50	1 day
Antherozoid production	250	1 day
Sporophyte production	250	1 day
	25	15 days

one day after application on Day 0 and three days after a Day 3 application. Detection of inhibited sporophyte recruitment took five to eight days after a 250 ppb/1 day dose. Detection of embryonic sporophyte mortality required 15 days after a 250 ppb/1 day pulse. Scanlan and Wilkinson (1986) observed that spermatozoa motility and egg fertilization were more sensitive to several marine biocides than growth of three week old germlings or photosynthesis of adult segments of the brown alga Fucus serratus.

2) Timing of a discharge event could influence the degree of observed inhibition in microscopic life stages. Macrocystis vegetative growth was inhibited at lowest doses in youngest gametophytes. Cultures exposed on Day 0 showed significant vegetative growth inhibition to 25 ppb/1 day and 250 ppb/ 1 hour pulses (Table 4.10). Older cultures did not exhibit observable inhibition at 25 ppb/1 day. Degree of inhibition at 250 ppb/1 day declined with increasing age. Hydrazine exposures on Day 8 produced greater inhibition of sporophyte recruitment than on Day 3.

3) Short-term duration tests of physiological responses required higher applied concentrations to observe a significant effect than long-term assays (Figure 4.16). Data appeared to lie in a diagonal band, suggesting that concentration-time thresholds could be drawn above and below the band to estimate concentration-time limits for complete inhibition and no effects, respectively. Combinations in the upper right region of the plot would inhibit all life phases. Hydrazine doses in the lower left region of the plot would be harmless. Mattice and Zittel (1976) applied a similar technique to

Figure 4.16: Comparison of lowest observed hydrazine doses significantly inhibiting Macrocystis pyrifera microscopic life stages. Lines connect data points of similar stages and may not accurately represent intermediate inhibitions.

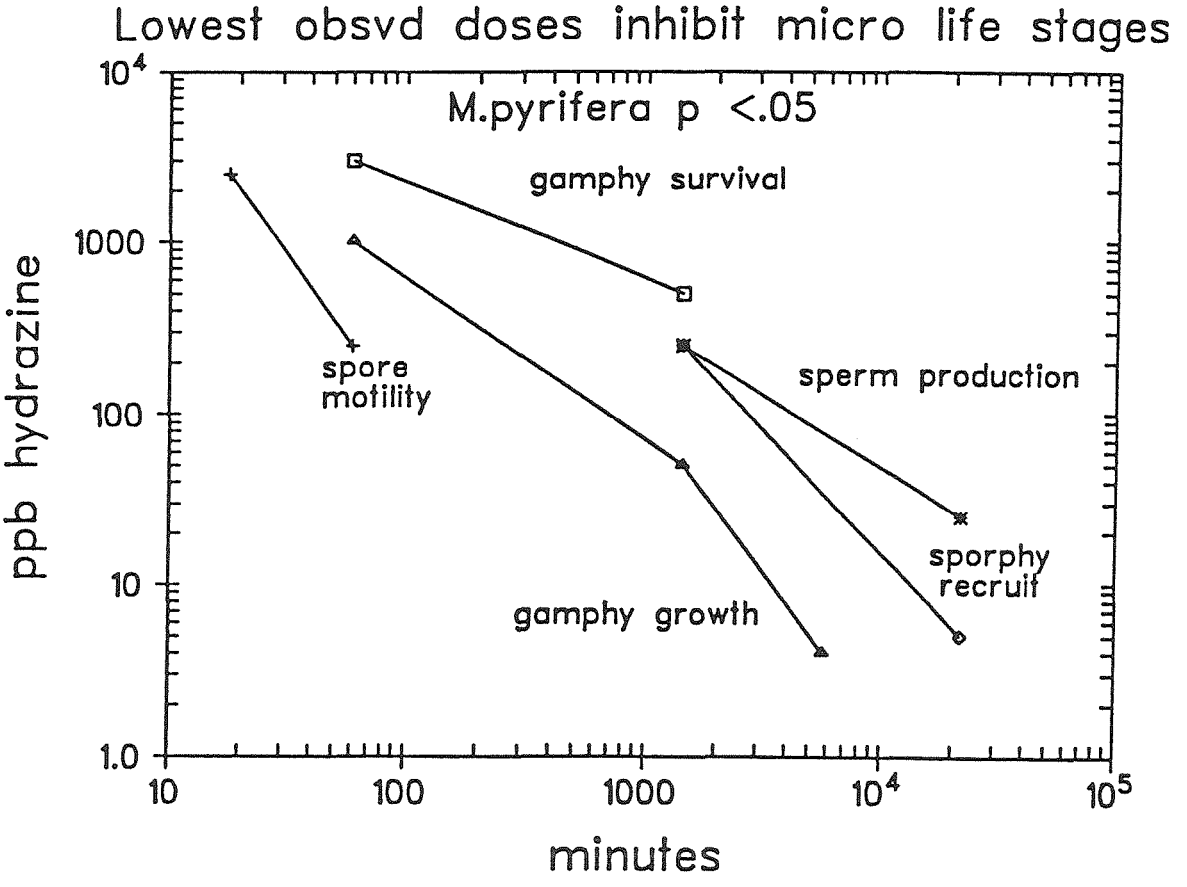

chlorination of power plant effluents, evaluating concentration-time data for many different species to develop no-effect level relationships for chlorination of power plant effluents in both marine and fresh waters. They applied overall scale factors to reported concentrations for the most sensitive species to estimate chlorine residual concentrations causing no effects at each exposure duration. Their result was a log-linear concentration-time relationship for acute chlorine toxicity and a constant, long-term chronic threshold of 0.02 ppm in marine waters.

No inhibition was observed for any Macrocystis life stage at 25 ppb/1 hour, suggesting that this dose may lie in the no-effect region of Figure 4.16. Only spore motility and germination were inhibited at 250 ppb/1 hour. Growth of recently germinated gametophytes was inhibited at 25 ppb/1 day and 250 ppb/1 hour. Doses in this region may affect the most sensitive phases of the Macrocystis life cycle. All life stages were inhibited by a 250 ppb/1 day exposure. Concentrations of 2500 ppb were fatal in short- and long-term exposures. Continuous exposure experiments (Section 4.III) showed inhibition of vegetative growth at concentrations exceeding 2 ppb in 96-hour experiments. Application of Mattice and Zittel's (1976) technique to Macrocystis data might establish a long-term toxicity hydrazine threshold at 1 ppb (32 nM).

Most observed effects occurred at the 250 ppb/1 day exposure, a concentration-time combination in excess of known DCPP discharges (Figure 4.9). One of the three worst-case undiluted field exposures estimated from discharge data (May 28, 1984 (Day 58), 119 ppb, 477

minutes, Table 4.1) exhibited concentration-time characteristics possible inhibition of gametophyte growth. This dose was released 12 days after first observations of observed changes in algal morphology. Data were not sufficiently complete at this stage of my investigation to predict outcomes for each life stage for all combinations of discharge events. Systematic study of the effects of hydrazine concentration vs. exposure time on Macrocystis gametophyte growth is described in Chapter 6.

Mixing conditions in Diablo Cove could modify the concentration-time profile of episodic discharges by means of any or all of the following phenomena:

1) Dilution of effluent between the point-of-discharge and target algal populations, reducing the discharged concentration and risk of toxic effects.

2) Possible deflection of an effluent plume away from the target populations by currents or winds in the cove, reducing toxic effects.

3) Recirculation of a portion of a previously mixed plume and receiving water back into the vicinity of the algae, increasing contact time at a lower concentration.

Because mixing usually reduces discharged concentrations, links between sensitivity of algae to specific concentration-duration profiles and similar profiles at the point of discharge should be regarded as worst-case events.

III. CONTINUOUS HYDRAZINE ASSAYS OF MACROCYSTIS GAMETOPHYTES MEASURED WITH DIGITAL IMAGE ANALYSIS

Introduction

Macrocystis pyrifera gametophytes were used in experiments designed to test sensitivity to other toxicants (Chapter 4.V) and to evaluate sensitivity to other types of episodic releases (Chapter 6). A continuous exposure toxicity test involving a range of hydrazine concentrations was developed as a "standard experiment." The standard experiment was included as a part of most of the later experiments to calibrate results against a standard outcome and to determine if geographic location or seasonal variations influenced sensitivity of gametophytes to hydrazine.

Materials and Methods

Gametophytes derived from spores extracted from adult Macrocystis populations off Laguna Beach (southern California) and Diablo Canyon (central California) were cultured using methods described in Chapter 2. All cultures were grown under identical conditions of temperature and illumination. Daily changes of filtered macronutrient-supplemented offshore seawater were used to minimize nutrient limitations. Gametophytes were measured by digital image analysis on the third day after complete germination. They were then exposed for 96 or 120 hours to a series of hydrazine concentrations usually ranging from 1 to 20 ppb. Growth of control cultures was

Figure 4.17: Comparison of least-squares fits to daily area data of M. pyrifera gametophytes. Correlation coefficients shown are for fits to entire (n = 606) data set. Data points are means and 95% confidence limits.

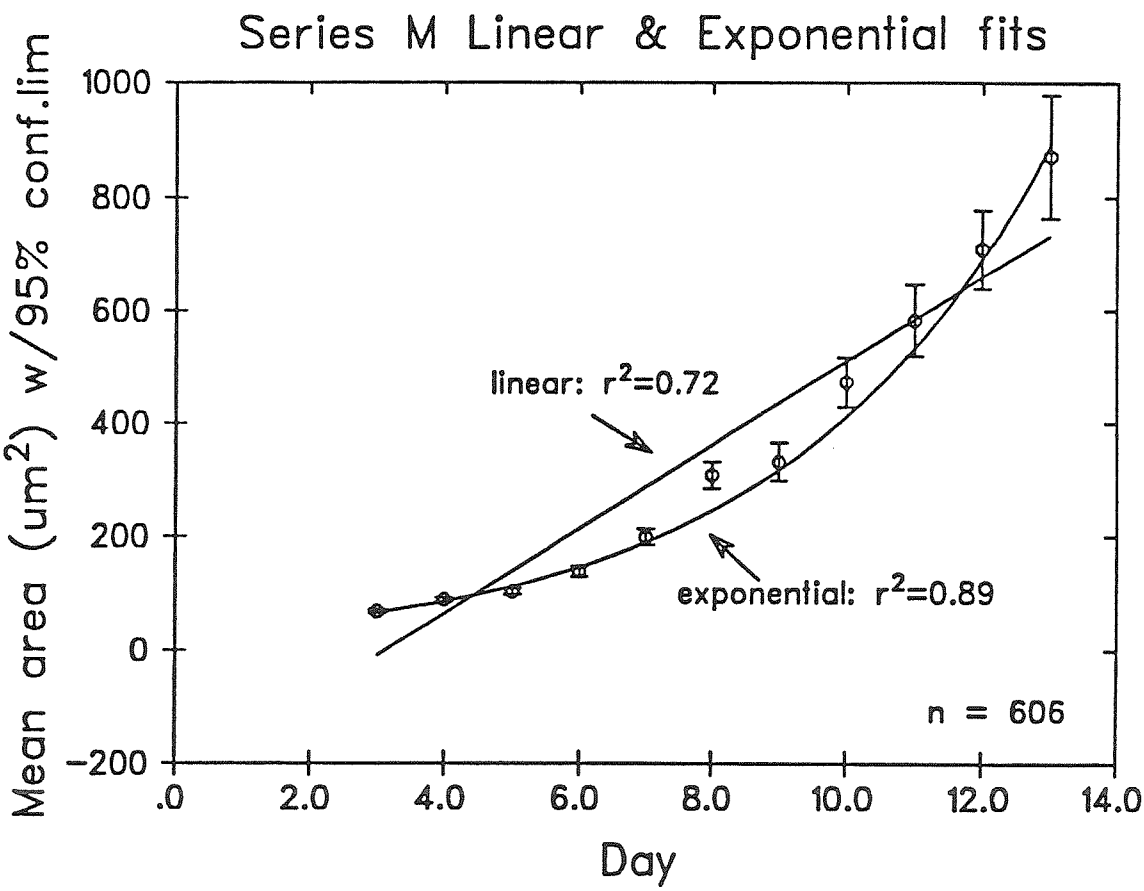

measured daily by digital image-analysis. Control growth rates were determined by a linear least-squares minimization of a model assuming exponential growth in gametophyte area over time (Figure 4.17).

Gametophyte sizes in all test concentrations were measured at the end of the exposure period and the resulting size data statistically compared to control sizes. Minimum concentration observed for vegetative growth inhibition was determined from Student's t-tests (Alder and Roessler, 1972) and one-way analysis of variance (Sokal and Rohlf, 1981; STSC, 1987). Concentration required to inhibit vegetative growth by 50 percent (CG_{50}) was determined from a linear least-squares fit to log-transformed size data after the method of Walsh et al., 1987.

Results

Control growth rates varied from 0.14 to 0.32 day^{-1} (Table 4.13). Randomization tests (Sokal and Rohlf, 1981, Bray, 1988) comparing regression-derived growth rates showed that there was no significant difference between growth rates of Diablo Canyon and Laguna Beach-derived gametophytes or between winter (November-April) and summer (May-October) rates.

A distinct decline in vegetative growth occurred between 2 and 5 ppb (64 and 160 nM) total hydrazine in most of the experimental runs (Figure 4.18; cf. Chapter 4 Appendix for plots of each experimental run). Concentration ranges for significant (Student's t, $p < 0.05$) inhibition by hydrazine varied little during the study period (Table 4.14). However, CG_{50} concentrations varied from 4 to 20 ppb.

Table 4.13: Summary of M. pyrifera gametophyte growth rates measured by the digital image-analysis system.

Date	Series	Sampling location	Duration days	rate day^{-1}	confidence limits	r^2	Sample size
Sep 86	M	Laguna	10	0.26	0.004	0.89	606
Oct 86	O	Laguna	11	0.27	0.005	0.85	433
Jan 87	Q	Laguna	14	0.14	0.005	0.66	333
Aug 87	U	Laguna	10	0.20	0.011	0.56	213
Oct 87	X	Diablo	12	0.24	0.007	0.79	268
Nov 87	Y	Diablo	12	0.31	0.007	0.90	258
Dec 87	Z	Laguna	8	0.32	0.012	0.78	194
Feb 88	AB	Laguna	14	0.21	0.007	0.81	259
Mar 88	AC	Laguna	8	0.28	0.009	0.81	237
Apr 88	AD	Laguna	13	0.25	0.005	0.85	488
May 88	AE	Laguna	8	0.19	0.010	0.70	82
Jul 88	AF	Dana Pt	6	0.27	0.020	0.48	295
Jul 88	AG	Diablo	6	0.30	0.014	0.62	284
		Grand avg.		0.249	0.009	0.746	3950
		Grand std.		0.050	0.004	0.050	
		95 percent conf.lim.		0.032	0.003	0.032	

Rates computed by unweighted least-squares linear regression on on $\log_e$-transformed data points in control cultures.

Conditions: 10°C, 24-hour illumination in macronutrient-enhanced offshore seawater in static cultures, renewed daily.

Table 4.14: Summary of inhibition of M. pyrifera gametophyte growth in hydrazine measured by digital image-analysis.

MONTH	SERIES	SITE	TEST DURATION	SIGNIFICANCE RANGE LOWER LIMIT	SIGNIFICANCE RANGE UPPER LIMIT	ESTIMATED GC_{50}
Oct 87	X	Diablo	120 hr	0 ppb	4.5 ppb	8 ppb
Nov	Y	Diablo	120	3	4.5	4
Dec	Z	Laguna	120	3	4.5	6
Jan 88	AA	Diablo	100	3	4.5	20
Feb	AB	Laguna	96	2	5	10
Mar	AC	Laguna	100	3	5	11
Apr	AD	Laguna	96	2	5	20
May	AE	Laguna	96	2	5	5
July	AF	Dana Pt	120	2	3	4
July	AG	Diablo	120	3	4	4

GC_{50} is concentration giving a size 50 percent of control at the end of the stated test period.

Significance determined by Student's t-test (one-tailed, $p < 0.05$)

UPPER LIMIT: Lowest concentration at which significant measured inhibition occurred.

LOWER LIMIT: Highest concentration that did not give significant growth inhibition.

Figure 4.18: Example of Growth vs. hydrazine concentration curve for 96-hour continuous exposure test. Measured on Day 8

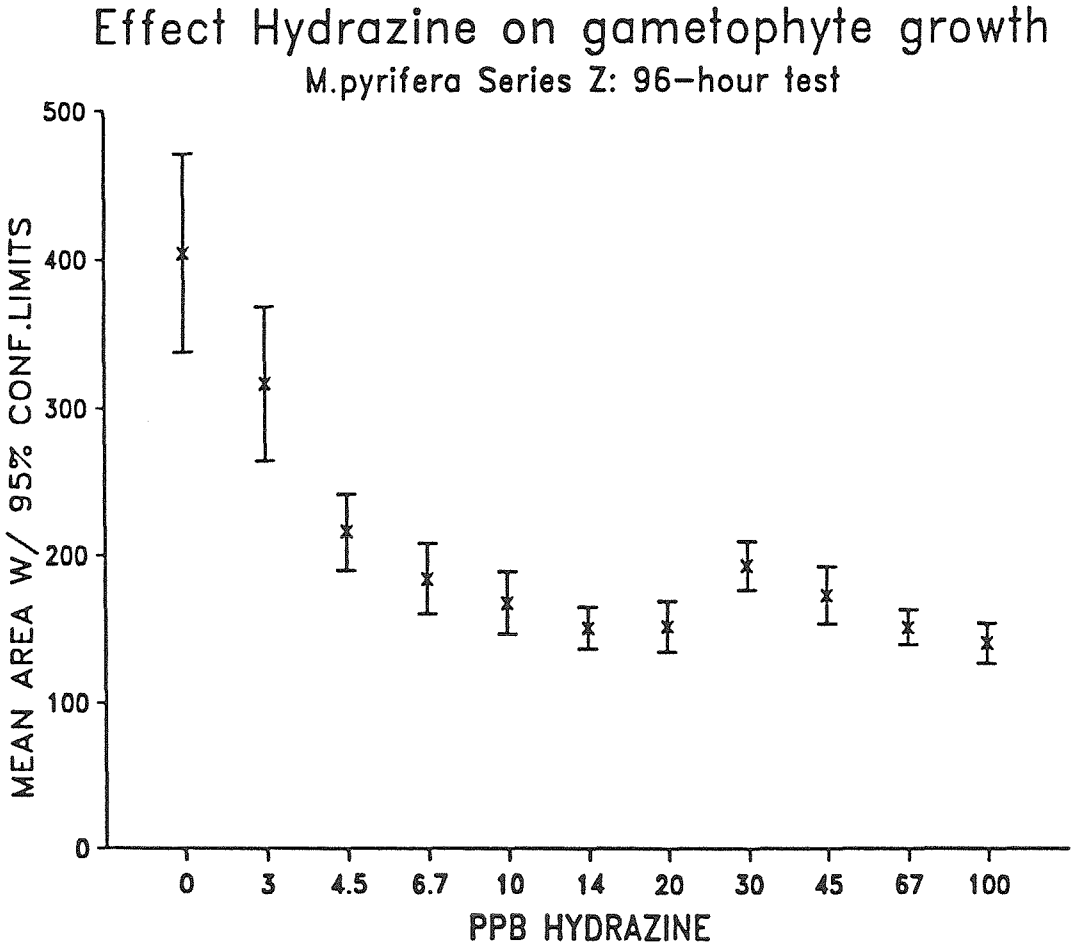

Figure 4.19A: Hydrazine sensitivity comparison of central (Series AG) and southern (Series AF) gametophytes in simultaneous culture.

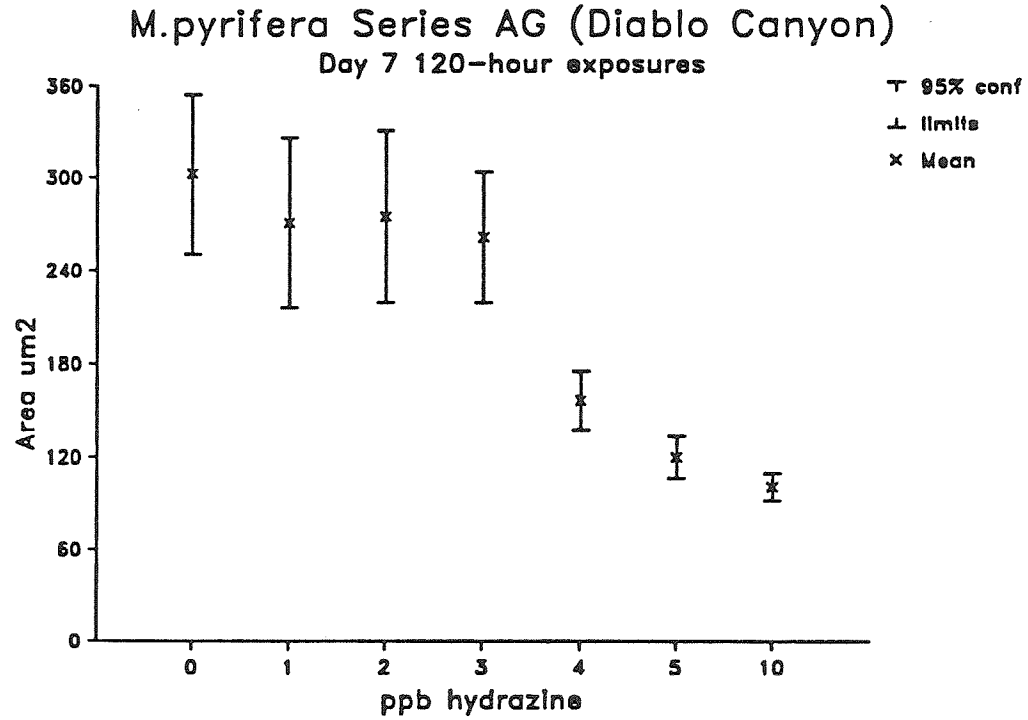

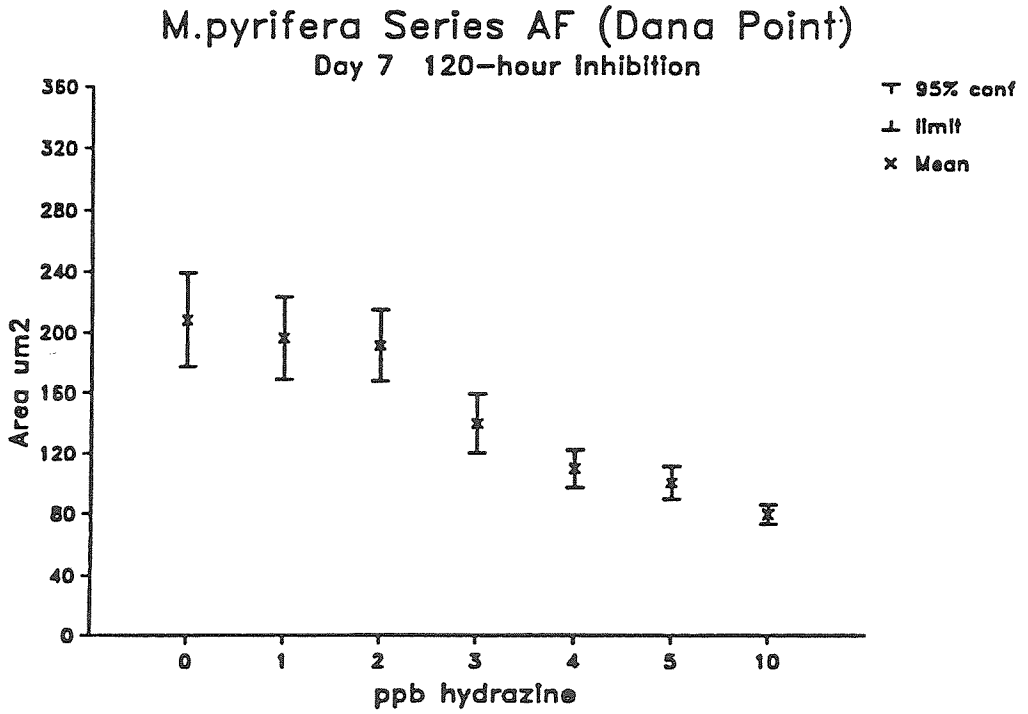

Figure 4.19B: Top: Comparison of effects of hydrazine on growth rates of central and southern California gametophytes.
Bottom: Sigmoid fit to southern Calif. growth rate data
Lambda is interaction coefficient (n, in text)

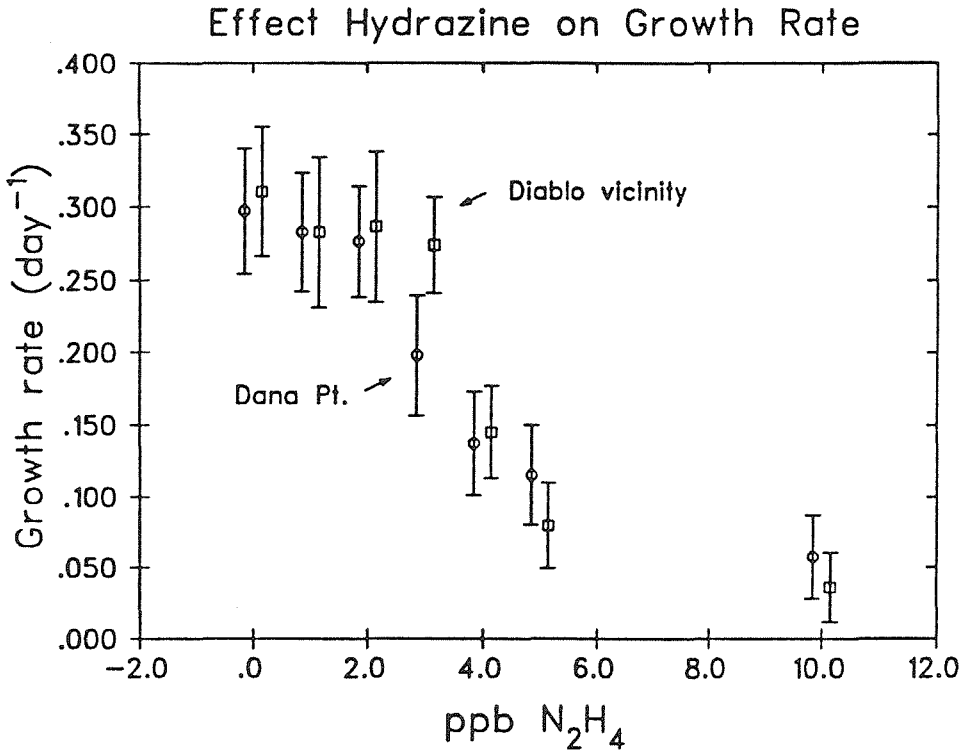

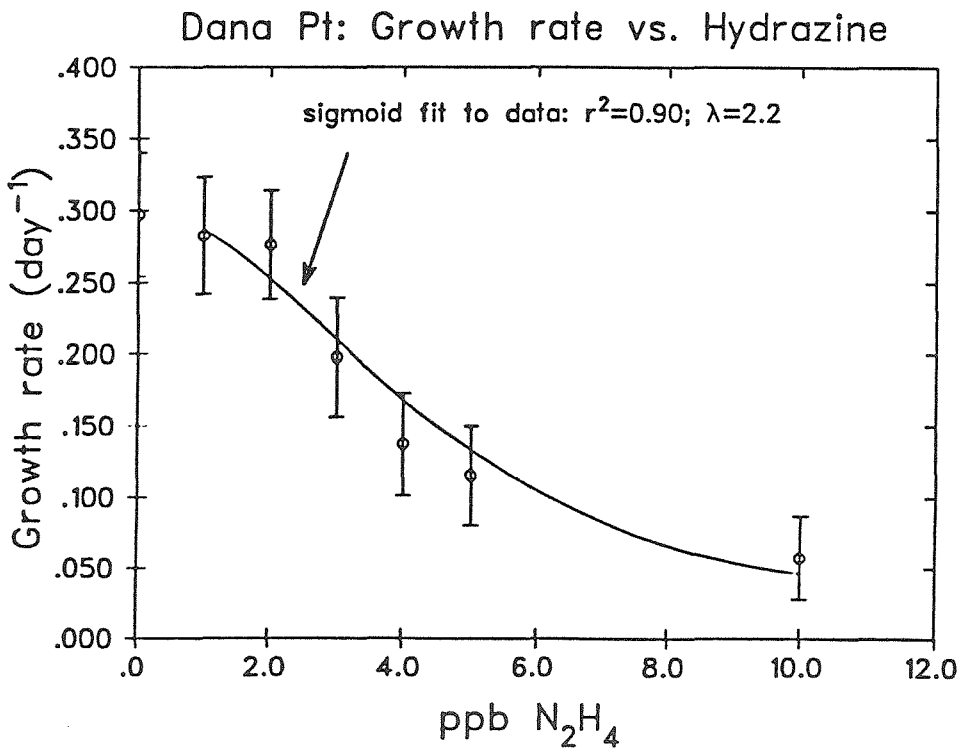

Randomization tests of the distribution of CG_{50} values showed that there was no significant difference between means for cultures from Laguna Beach and Diablo Cove, but there was a significant difference ($p = 0.04286$) between summer-collected and winter-collected cultures.

Gametophytes from central and southern California sites cultured simultaneously in hydrazine showed slightly different sensitivities. Diablo Canyon gametophyte sizes were inhibited between 3 and 4 ppb. Dana Point gametophytes were inhibited between 2 and 3 ppb (Figure 4.19a). Growth rates were estimated by assuming log-linear growth with time and computing rates in all hydrazine concentrations from the difference between the treated size on Day 7 and the initial size on Day 3. Comparison of mean growth rates at each hydrazine concentration showed that the growth rate of Series AF (southern California) gametophytes was significantly[14] lower at 3 ppb hydrazine than the rate for Series AG (central California) gametophytes that had been cultured simultaneously in identical media (Figure 4.19b), suggesting slightly greater resistance in gametophytes derived from central California spores.

Growth rate vs. hydrazine data were least-squares fit to a model of sigmoidal inhibition kinetics of the form (Segel, 1968):

$$\frac{R}{Ro} = \frac{K}{K + [N_2H_4]^n} \qquad (4.1)$$

Ro = control growth rate

R = observed growth rate

$K = [N_2H_4\text{-}50]^n$, where N_2H_4-50 is concentration to inhibit growth rate by 50 percent

n = interaction coefficient.

---

[14] Student's t-test, two-tailed $t = 2.37$, giving $0.02 < p < 0.05$ for 62 degrees of freedom.

Significant proportions of variance were explained by fits to this model (Figure 4.19b). Computed K and n values were nearly identical for the two cultures, despite faster apparent growth in the Diablo culture.

Table 4.14A: Comparison of M. pyrifera growth inhibition kinetics from two different sites.

Curve parameter	Dana Point	Diablo-vicinity
K	25.1	24.7
CG50	4.6 ppb	4.3 ppb
n	2.1	2.2
r^2	0.93	0.81
Significance	$p < 0.01$	$p < 0.02$

Simple empirical fits (i.e., rate vs. inverse concentration; rate vs. log concentration) also explained significant proportions of the variance, but the model assuming sigmoidal inhibition kinetics best explained the small initial response, sharp mid-range drop and asymptotic response at high concentrations observed in the data.

Discussion

Ten continuous-exposure experiments yielded low variability in the observed concentrations causing significant growth inhibition. Concentration ranges for 96-hour inhibition of Macrocystis pyrifera gametophytic growth determined by digital image analysis were similar to values previously obtained using eyepiece micrometer methods. Inhibition was detected at about 2.5 ppb by both methods, but 10 days were required for detection by eyepiece micrometer as compared to four days at 3-5 ppb for image analysis. The digitizer was a more sensitive technique for assessing inhibition in continuous assays.

Harrah (1978) reported six-day EC_{50} values of 0.4, 10 and 16 ppb and six-day safe-limits of 0.1, 1, and 5 ppb for growth of the marine microalgae Chlorella stigmatophera, Selenastrum capricornutum and Dunaliella tertiolecta, respectively, in hydrazine-contaminated seawater. Four-day CG_{50} values for Macrocystis gametophytes determined by the digitizer, ranging from 4-20 ppb, were similar in magnitude to values reported by Harrah for Selenastrum and Dunaliella.

Increased sensitivity of southern California (Series AF) compared to central California (Series AG) gametophytes may have been an artifact of their slower germination rates (Figure 4.20). Although gametophytes from the two sites grew at nearly identical rates in control cultures, Series AF organisms were smaller (48 ± 3 um^2) at the start of hydrazine exposures than Series AG (61 ± 3 um^2), as they were two days behind because of slower germination.

Spore condition may have been a function of health of the parent plant. Diablo Canyon sporophylls were collected from healthy plants, at a water depth of 14 meters, temperature 11°C. Sori covered the entire surface of the sporophylls. Dana Point spores were collected from plants that had been growing in 18-19°C sustained temperatures at a water depth of 15 meters. Sori covered 30-40 percent of the sporophyll. Nitrogen and chlorophyll contents in parent tissue from the two sites would have been helpful in correlating parent plant health with spore germination success and gametophytic growth, but these parameters were not measured. Lee and Brinkhuis (1986) observed distinct seasonality in growth rates, fecundity and reproductive

Figure 4.20: Top: Comparison of daily growth of simultaneously-cultured central and southern California gametophytes. Bottom: Comparison of germination rates of central and southern California gametophytes. Curves are empirical exponential fits to the data. Maximum fraction germinated and water temperature at time of collection noted next to each curve.

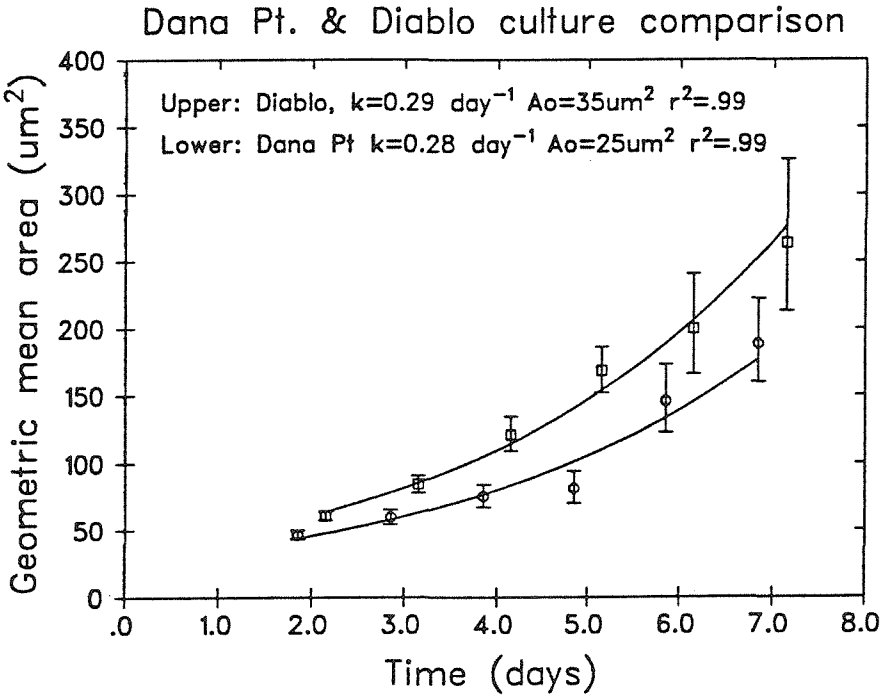

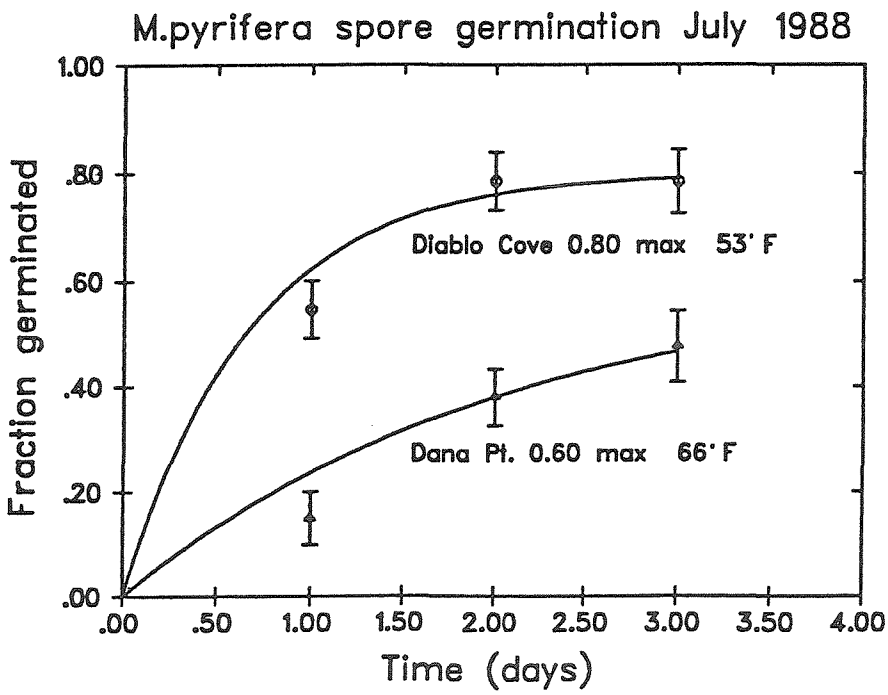

success in gametophytes of the Atlantic coast brown alga Laminaria saccharina. Although seawater temperature variation is less extreme in the Pacific Ocean than observed at their site, similar seasonal factors may be influencing Macrocystis gametophyte development.

Significant seasonality in CG_{50} values may have been an artifact of either the scheme used to classify CG_{50} values or of the greater prevalence (6 vs.4) of winter samples in the data set (Table 4.14). Continued testing through another calendar year could refute or verify existence of seasonally varying resistance to hydrazine among Macrocystis gametophytes.

IV. COMPARISON AMONG DIFFERENT SPECIES IN PULSED HYDRAZINE TRIALS

Introduction

Indication of hydrazine toxicity to Macrocystis pyrifera gametophytes encouraged the question: Which species in the central California brown algal communities would be most likely inhibited by episodic exposures? Several other brown algal species, Egregia menzsiesii, Laminaria dentigera, Nereocystis luetkeana and Pterygophora californica are common in the vicinity of Diablo Cove. Comparative information derived from toxicity experiments might partially predict or explain shifts in community composition in the vicinity of a power plant discharge which might occasionally release hydrazine doses sufficient to inhibit gametophytic life stages.

Figure 4.21: Example of temporary vegetative growth inhibition in Eisenia arborea gametophytes after application of a 250 ppb/1 day hydrazine pulse. Arrows indicated duration and extent of significant ($p < 0.05$) growth inhibition. CIRCLES: control culture. SQUARES: treated culture.

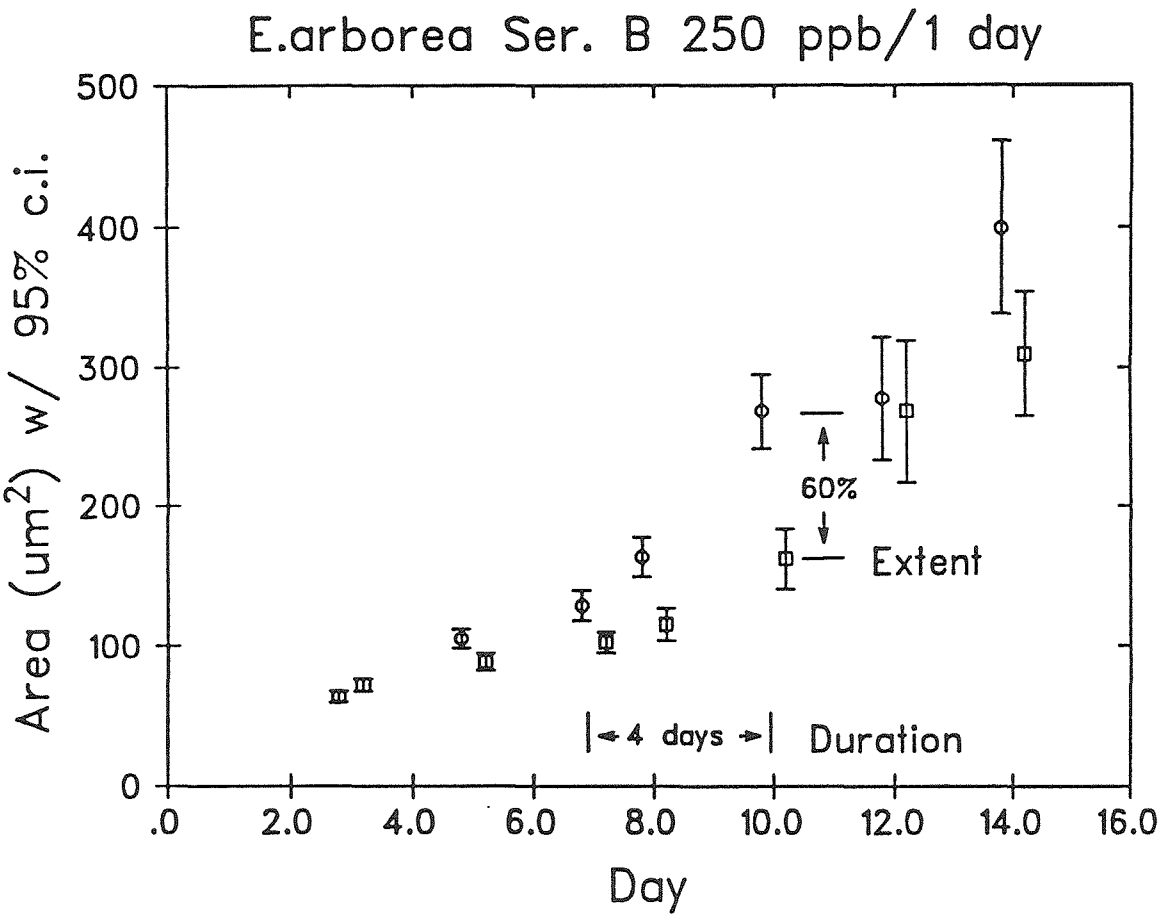

Methods

Eight additional species of algae were collected at sites in both southern and central California (Table 4.15A). Most California brown algae (with the exception of Macrocystis) exhibit seasonal fertility. Collection frequency varied with availability of algae with developed sori. Laminaria ephemera and Pelagophycus porra were relatively rare or difficult to obtain and are represented in the data by only one sampling. Egregia mensziesii was collected on five different occasions but proved fertile only once. Pterygophora californica was collected three times. Other species were collected twice.

Gametophytes of all species were cultured in lighting, nutrient and temperature conditions identical to those used for Macrocystis pyrifera. Vegetative growth inhibition was measured in the standard battery of 25 and 250 ppb/ 1 hour and 1 day pulsed hydrazine concentrations. Pulses were applied to cultures aged three to four days and growth followed for a week or more following application of the pulse. Cultures grown in each of the four standard treatments were compared to a hydrazine-free control for duration and degree of inhibition. Two canopy-forming species, Nereocystis luetkeana and Pelagophycus porra were also measured by the continuous 96-hour assay used to calibrate Macrocystis gametophyte experiments.

Most species exhibited temporary inhibition of growth that was due to application of the toxicant pulse (Figure 4.21). Ordinary statistical techniques were not well suited to this situation for the following reasons:

1) Analysis of covariance (ANCOVA) could not be used since slopes of control and treated growth curves were not parallel (parallelism is a requirement in ANCOVA since the technique removes a common slope from both data sets and then allocates the variance among remaining independent variables).

2) Regression techniques using simple linear or exponential models fit an average slope for the entire time course of the experiment through regions of both normal and inhibited growth. Such fits may explain significant portions of the experimental variance but do not accurately model observed events.

Two methods were adopted for comparing mean sizes on identical measurement days.

1) When distribution of data was approximately normal, pairwise comparison of the means from control and treated cultures using Student's t-test was used as the method of determining the duration and extent of significant ($p < 0.05$, two-tailed) inhibition. Control and treated data were not combined to compute a pooled standard deviation[15], as this requires an assumption that the samples come from populations with identical standard deviations. Ninety-five percent confidence limits were computed for each data set on the basis of its sample size and standard deviation. Control and treated data sets were then compared for overlap of the confidence limits. Tests with actual data showed this technique to be a more

---

[15]This is the usual technique for comparing two samples (Alder and Roessler, 1972), where a t-value is computed directly from the data using a pooled standard deviation. The underlying assumption is that populations have similar distributions about their means even if the means are different.

conservative estimator of significance than the technique of computing t directly from the data with a pooled standard deviation. 2) For cases where sample sizes were small (less than 15 measurements per sample) or data distributions skewed, sampled randomization trials were used to compare means (Sokal and Rohlf, 1981; Bray, 1988).

Duration of the period of significant inhibition was determined either by counting the number of days that 95 percent confidence limit error bars for control and treated cultures did not overlap (cf. Figure 4.21 for an example), or by counting the number of contiguous days that randomization tests indicated a small probability ($p < 0.05$) that the means were drawn from an identical population. The degree of growth inhibition was calculated for each day of significant inhibition by computing the value:

$$\text{Degree} = 100 \times \left[1 - \frac{\text{treated size}}{\text{control size}} \right]. \qquad (4.2)$$

Digitizer data and micrometer data were ranked by species according to the duration and the maximum degree of inhibition observed in the 25 ppb/1 day and 250 ppb/1 day exposures.

Digital image analysis became available while studies of the different algal species were in progress. Digitization was used to evaluate growth inhibition of gametophytes collected after September 1986. Digitized measurements, if available, were used to compute inhibition in the pulsed assays. Data for some species were available only as measured by eyepiece micrometer because they were obtained before development of digital techniques was completed. Micrometer

measurements were adjusted to permit comparisons to digitizer data by computing areas from the lengths using a regression model developed for predicting area from length in Macrocystis gametophytes. The model was of the form:

$$A_p = 35 + 0.29\ L^2, \qquad (4.3)$$

where A_p = predicted area and L = measured length.

Model data were obtained from the Series M Macrocystis gametophyte cultures, where simultaneous random samplings of length and area were available for the same measurement days. A fit of mean daily lengths to mean daily areas using this model explained 99 percent of the experimental variance, a significant result. Area ratios were then computed from the model predictions. Adjusted data were used only to determine fraction control area during the period of observed significant growth depression. Propagation-of-error theory shows that squaring mean lengths approximately doubles coefficients of variation (Bevington, 1969). Micrometer lengths were determined to about the same relative uncertainty as digitizer areas, so areas computed from micrometer measurements had twice the relative uncertainty of digitizer-determined areas. This error prevented use of adjusted data in determining duration of significant inhibition. Durations of inhibition were determined from un-adjusted length data. Pulsed assay data for Laminaria dentigera, Laminaria ephemera and Nereocystis luetkeana were computed and ranked by this technique.

Experiments measured an by eyepiece micrometer should be repeated using digitization techniques to improve the quality of the comparisons. Measurements of Macrocystis cultures by both methods

indicated that image analysis detected inhibition earlier than did an eyepiece micrometer and the degree of observed inhibition was greater (Chapter 3; Figure 3.20). Degree and duration of inhibition as determined from micrometer measurements probably represent a lower bound on the duration of inhibition detectable with digital image-analysis. Data from separate micrometer and image-analyzed experiments were available for two species. Both data sets are reported in summary data tables.

Results

Mean growth rates for gametophytes of six algal species as determined by digital image-analysis were lower than the 0.24/day mean of rates determined for Macrocystis gametophytes (Table 4.16).

Sensitivity to episodic hydrazine discharges varied among tested species of brown algal gametophytes (Table 4.15A; graphs for each culture available in Chapter 4 Appendix). Pelagophycus porra was the most sensitive tested species. Pelagophycus gametophytic growth was significantly inhibited at all concentration-duration combinations in the pulsed assay and at 2 ppb hydrazine in the 96-hour exposure (Student's t-test, one-tailed, $p < 0.05$) (Figure 4.22). When the entire data set was subjected to one-way analysis of variance (STSC, Inc. 1987; Sokal and Rohlf, 1981), an a priori comparison of means using Dunnett's multiple range test showed that 1 ppb hydrazine significantly depressed vegetative growth. Concentration thresholds for toxicity to Pelagophycus were half the values routinely determined for Macrocystis gametophytes.

Table 4.15A: Measured pulsed hydrazine inhibition of gametophytic growth in Laminarian brown algae.
Reported as # days significant inhibition / maximum percent inhibition.
Significance determined by Student's t-test, two-tailed, $p < 0.05$.

Species Sampling location	Date & Series letter	Method	Start Day for Pulse	Pulse Concentration & Duration 25ppb 1 hour	250ppb 1 hour	25ppb 1 day	250ppb 1 day
Egregia mensziesii (Laguna Beach)	1/87	A digit	2	1/11%	5/41%	5/23%	5/52%
Eisenia arborea (Laguna Beach)	10/85	A microm	4	n.m.	n.m.	n.m.	1/21%
Eisenia arborea (Laguna Beach)	6/87	B digit	2	n.m.	n.m.	*2/28%	6/40%
Laminaria dentigera (Diablo Cove)	12/85	A microm	3	n.m.	n.m.	3+/45%	3+/58%
Laminaria dentigera (Diablo Cove)	4/86	B microm	2	4/42%	0/ 0	0/ 0	3/25%
Laminaria ephemera (Diablo Cove)	5/86	A microm	3	0/ 0	2/36%	3/47%	2/42%
Laminaria farlowii (Laguna Beach)	11/85	A microm	4	n.m.	n.m.	n.m.	0/ 0
Laminaria farlowii (Laguna Beach)	10/86	B digit	5	n.m.	n.m.	0/ 0	2/35%
Nereocystis luetk. (Diablo Cove)	5/86	A microm	3	0/ 0	6+/61%	6+/69%	7+/46%
Pelagophycus porra (Point Loma)	5/88	A digit	3	1/23%	4+/38%	6+/46%	6+/67%
Pterygophora calif. (Laguna Beach)	12/85	A microm	2	n.m.	n.m.	0/ 0	0/ 0
Pterygophora calif. (Diablo Cove)	12/85	B microm	2	n.m.	n.m.	0/ 0	0/ 0
Pterygophora calif. (Diablo Cove)	4/87	C digit	3	n.m.	0/ 0	0/ 0	9+/49%

Eisenia Series B: value reported with * is for 80ppb/1 day.

Absolute uncertainty in maximum percent inhibition is ca. ± 15 percent, (i.e., for Eisenia Series B 80ppb/1 day: 28 ± 15%).

Data obtained from paired comparisons of treated cultures to controls.

Length converted to area for computation of inhibition using regression developed for M.pyrifera gametophytes: $\text{Area} = 35 + 0.29(\text{length})^2$.

n.m. = not measured.

Table 4.15B: Embryonic sporophyte recruitment in pulsed hydrazine.
Reported as per-cent recruitment compared to control.
Percent recruitment = 100 x (treated density/control density).
Measured two weeks after pulse. n.t. not tested n.m. not measured

Species (Sampling location)	Date & Series		Pulse Day	Day Counted	Concentration & duration 25ppb 1 hour	250ppb 1 hour	25ppb 1 day	250ppb 1 day
Egregia mensziesii (Laguna Beach)	1/87	A	2	15	430%$	62%	320%$	23%*
Eisenia arborea (Laguna Beach)	10/85	A	4	17	n.t.	n.t.	n.t.	11%*
Eisenia arborea (Laguna Beach)	6/87	B	2		Did not recruit			
Laminaria dentigera (Diablo Cove)	12/85	A	3	27	n.t.	n.t.	76%	82%
Laminaria dentigera (Diablo Cove)	4/86	B	2	17	10%*	10%*	130%	76%
Laminaria ephemera (Diablo Cove)	5/86	A	3		Did not recruit			
Laminaria farlowii (Laguna Beach)	11/85	A	4	17	n.t.	n.t.	n.t.	51%*
Laminaria farlowii (Laguna Beach)	10/86	B	5	15	n.t.	n.t.	25%*	44%*
				19	n.t.	n.t.	n.m.	186%$*
Macrocystis pyrifera (Laguna Beach)	9/85	I	3	17	92%	142%	28%*	39%*
			8	17	161%$	192%$	186%$	11%*
Macrocystis pyrifera (Laguna Beach)	10/85	J	-1	17	n.t.	n.t.	n.t.	29%*
Nereocystis luetkeana (Diablo Cove)	5/86	B	3		Did not recruit			
Pelagophycus porra (Pt. Loma)	5/88	A	3		Did not recruit			
Pterygophora calif. (Laguna Beach)	12/85	A	2	16	n.t.	n.t.	88%	165%$
Pterygophora calif. (Diablo Cove)	12/85	B	2	26	n.t.	n.t.	72%	139%$
Pterygophora calif. (Diablo Cove)	4/87	C	3	16	n.t.	200%$	179%$	79%

Significance determined by either sampled randomization or Wilcoxon rank-sum tests; $p < 0.05$. Symbols:

- $ Significant stimulation of recruitment.
- * Significant inhibition of recruitment.
- *$ Significant increase in density with significant decrease in size.

Data: Totals of 16 or 20 scans at 160X divided by control total.
Absolute uncertainty on calculated percentages: ± 10-15 percent.

Table 4.16: Logarithmic growth rates measured in gametophytes of Laminarian brown algae at 10°C, 24-hr illumination

Species	Series & Date	Duration days	rate day^{-1}	conf. limits	r^2	Sample size
Eisenia arborea	B Jun 87	11	.16	.006	.77	238
Egregia mensziesii	A Jan 87	9	.18	.004	.70	765
Laminaria farlowii	B Oct 87	10	.19	.004	.82	491
Nereocystis luetkeana	B Sep 87	8	.14	.015	.56	65
Pterygophora californica	C Apr 87	14	.20	.006	.76	438
Pelagophycus porra	A May 88	13	.21	.006	.77	374

Table 4.17: One-day pulse sensitivity of brown algal species. Ranked in order of increasing duration of significant inhibition of vegetative growth of cultures aged 2-3 days. Rank-ordering of data from Table 4.15.

Pulse hydrazine concentration			25 ppb		250 ppb	
			Inhibition			
Family	genus/species		Duration days	Extent pct	Duration days	Extent pct
Laminariaceae	L. farlowii	*	0	0	2	35
Alariaceae	E. arborea	*	0$	0$	6	40
Alariaceae	P. californica	*	0	0	9+	49
Lessoniaceae	M. pyrifera		0	0	9	70
Laminariaceae	L. dentigera		3+	45	3+	58
Laminariaceae	L. ephemera		3	47	2	42
Alariaceae	E. menziesii	*	5	23	5	52
Lessoniaceae	P. porra	*	6+	46	6+	67
Lessoniaceae	N. luetkeana		6+	67	7+	46
			800 nM		8000 nM	

Asterisk (*) means analyzed via digital image analysis

Dollar sign ($): Estimate. no data available at this concentration

Extent is 100 x [1 - smallest fraction control size measured during period of signficant growth inhibition]

SUM OF RANKS: Alariaceae: 12
Laminariaceae: 12
Lessoniaceae: 21

Figure 4.22: Effect hydrazine on vegetative growth of Pelagophycus porra gametophytes showing significant inhibition at 2 ppb, the lowest concentration observed for any tested alga.

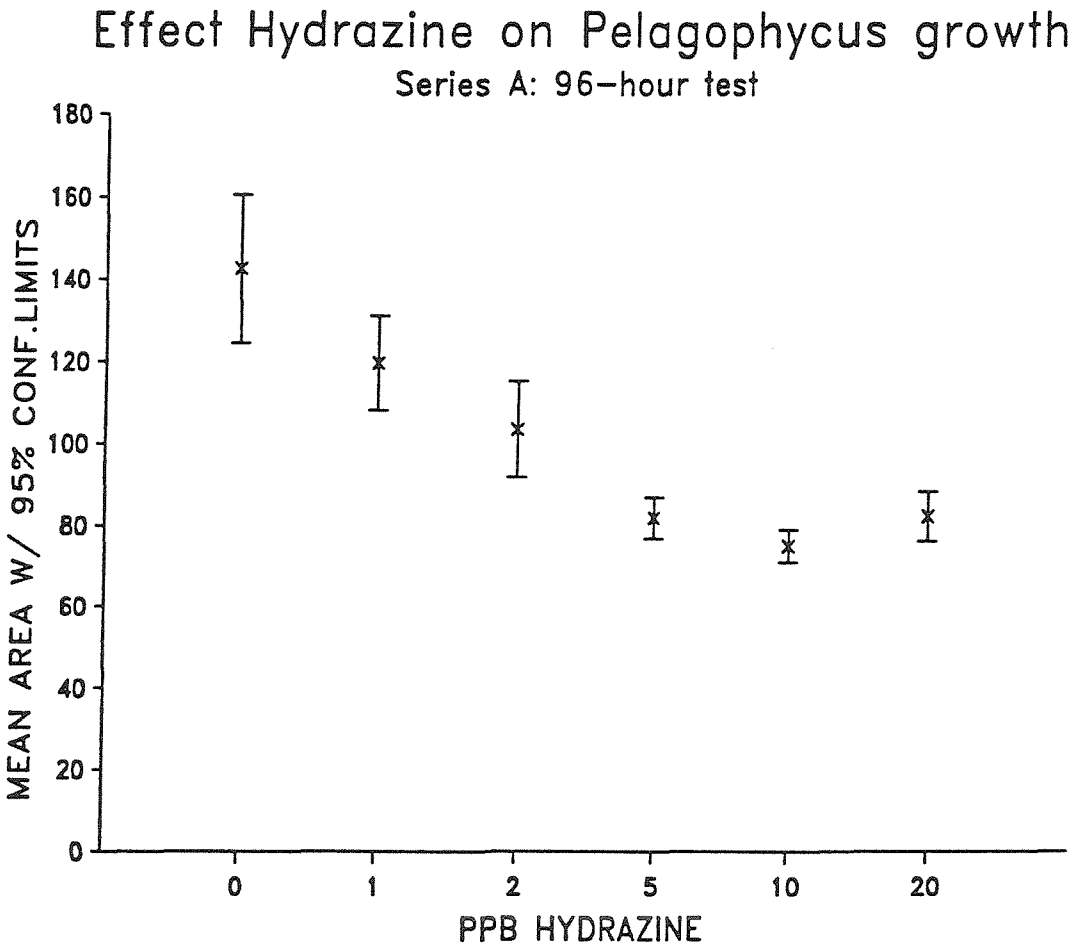

Pterygophora californica was the most resistant tested species. No inhibition was detected at any combination of concentration and duration in two trials measured with eyepiece micrometer (Figure 4.23A). Significant inhibition was observed for 250 ppb/1 day hydrazine when measured by digital image analysis (Figure 4.23B). Pterygophora thrice recruited significantly higher densities of sporophytes compared to controls after pulsed hydrazine exposures of 250 ppb/1 hour and 1 day (Table 4.15B).

Nereocystis luetkeana gametophytes were significantly inhibited (Student's t, one-tailed, $p < 0.05$) at 4.5 ppb in 96-hour and 9 ppb in 288-hour continuous exposure trials measured with digital image analysis (Figure 4.24B). CG_{50} levels were > 45 ppb at 96 hours and 10 ppb at 288 hours. Slow growth occurred in test concentrations exceeding 10 ppb.

Nereocystis gametophytes measured by eyepiece micrometer showed one of the highest tested sensitivities in the pulsed assay. Vegetative growth was inhibited for 6 days at 25 ppb/1 day and 250 ppb/1 hour and 7 days at 250 ppb/1 day (Table 4.15A, Figure 4.24A) Successful sporophyte recruitment was not observed in either Nereocystis culture.

The other two tested representatives of the Alariaceae exhibited varying sensitivity to hydrazine pulses. Eisenia arborea vegetative growth was moderately inhibited only at 250 ppb/1 day. No significant inhibition of Eisenia sporophyte recruitment was observed. Egregia mensziesii vegetative growth was inhibited at all four combinations of hydrazine concentration and duration (Table 4.15A, Figure 4A.1).

Figure 4.23A: Effect of one-day hydrazine pulses on Pterygophora californica gametophyte vegetative growth. Samples taken from indicated sites in December 1985.

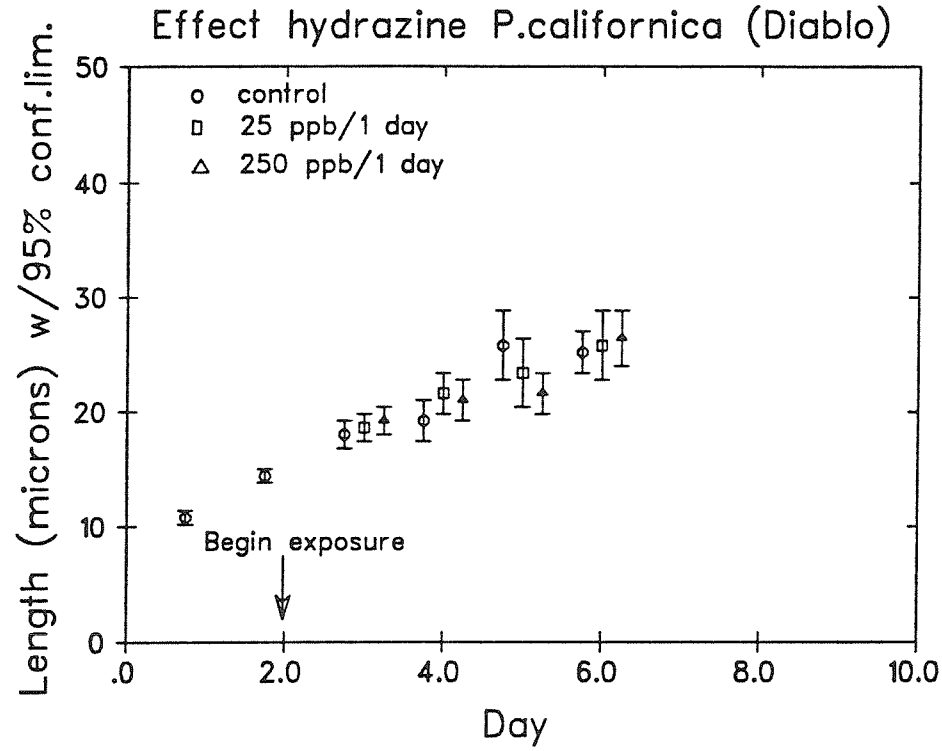

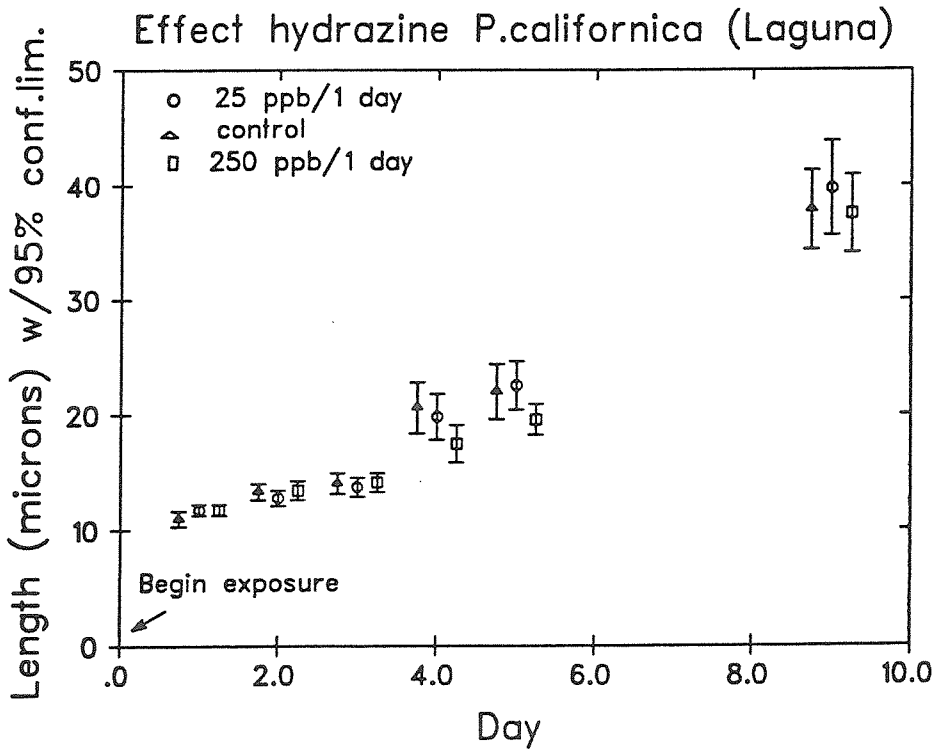

Figure 4.23B: Effect of one-day hydrazine pulses on Pterygophora californica gametophyte vegetative growth measured with digital image analysis. Sampled April 1987 from Diablo Cove.

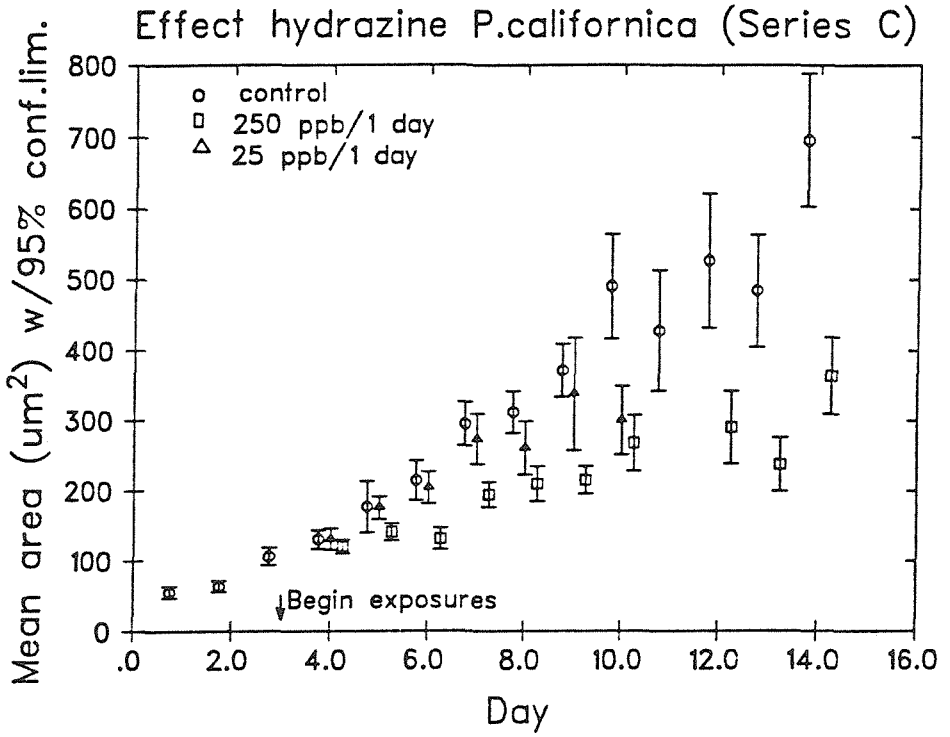

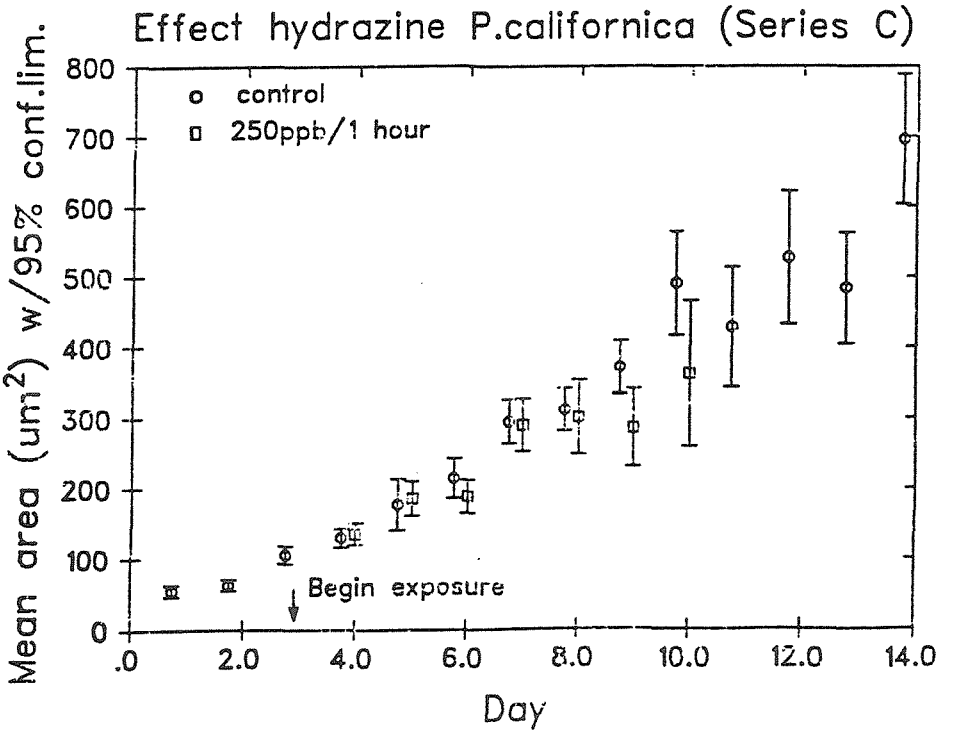

Sporophyte recruitment was significantly stimulated by the 25 ppb doses (despite vegetative growth inhibition) but inhibited by 250 ppb exposures.

Tested representatives of the family Laminariaceae (all in the genus Laminaria) showed varied results. Gametophytes of all three species showed modest 2-3 day inhibition at a 250 ppb/1 day dose. Laminaria ephemera gametophytes were more sensitive than L. farlowii, being inhibited for 3 days at 25 ppb/1 day, and 2 days at 250 ppb/1 hour and 250 ppb/1 day. L. dentigera sensitivity was close to that of L. ephemera, with inhibition at 25 ppb/1 day being one day shorter (probably within the margin of experimental error for this method). L. farlowii sporophyte recruitment was initially inhibited at 250 ppb/1 day but recovered five days later (Figure 4.A.2). L. ephemera gametophytes failed to reproduce in culture. L. dentigera sporophyte recruitment was either unaffected by hydrazine pulses (Series A) or stimulated at 1 day durations for concentrations of 25 and 250 ppb.

Discussion

Significant differences in resistance to hydrazine occurred among various species of the Laminariales. Gametophytes of the three tested fast-growing surface canopy formers Nereocystis, Macrocystis, Pelagophycus, all in the family Lessoniaceae, were the most sensitive to episodes of hydrazine exposure. Comparisons between and within the other families were not clear-cut. In the Alariaceae, Pterygophora was the most resistant of all tested algae, but Egregia mensziesii growth was very sensitive. Members of the family Laminariaceae also

Figure 4.24A: Effect pulsed-hydrazine doses on Nereocystis luetkeana vegetative growth measured by eyepiece micrometer. Sampled May 1986 from Diablo Cove

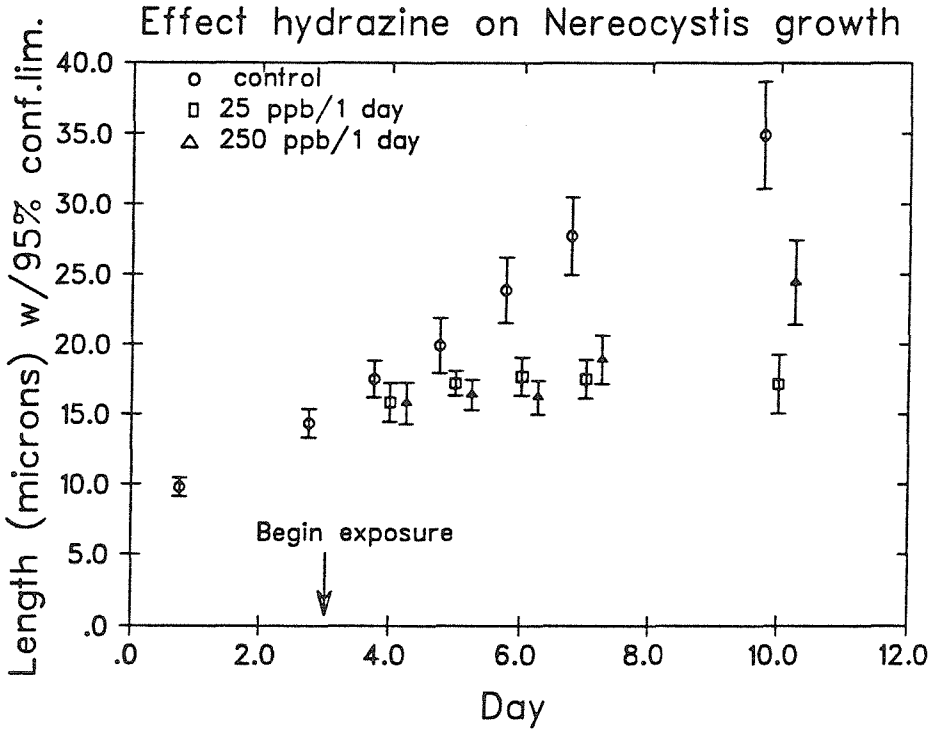

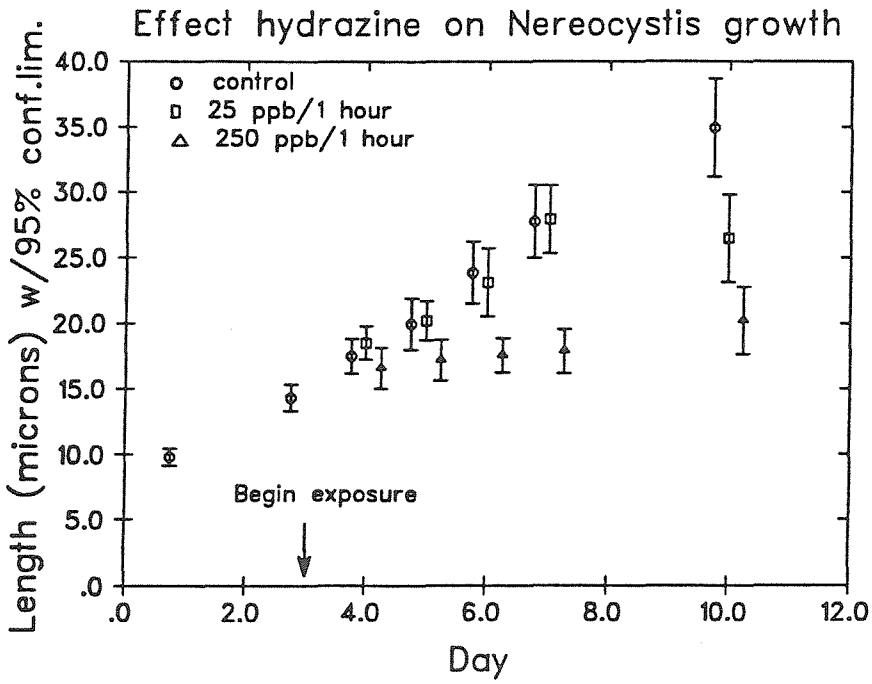

Figure 4.24B: Effect continuous hydrazine exposure on Nereocystis luetkeana vegetative growth measured with digital image analysis. Top: 4 day (96-hour) exposure. Bottom: 14 day (288 hour) exposure. Sampled Sept. 1987 Diablo Cove

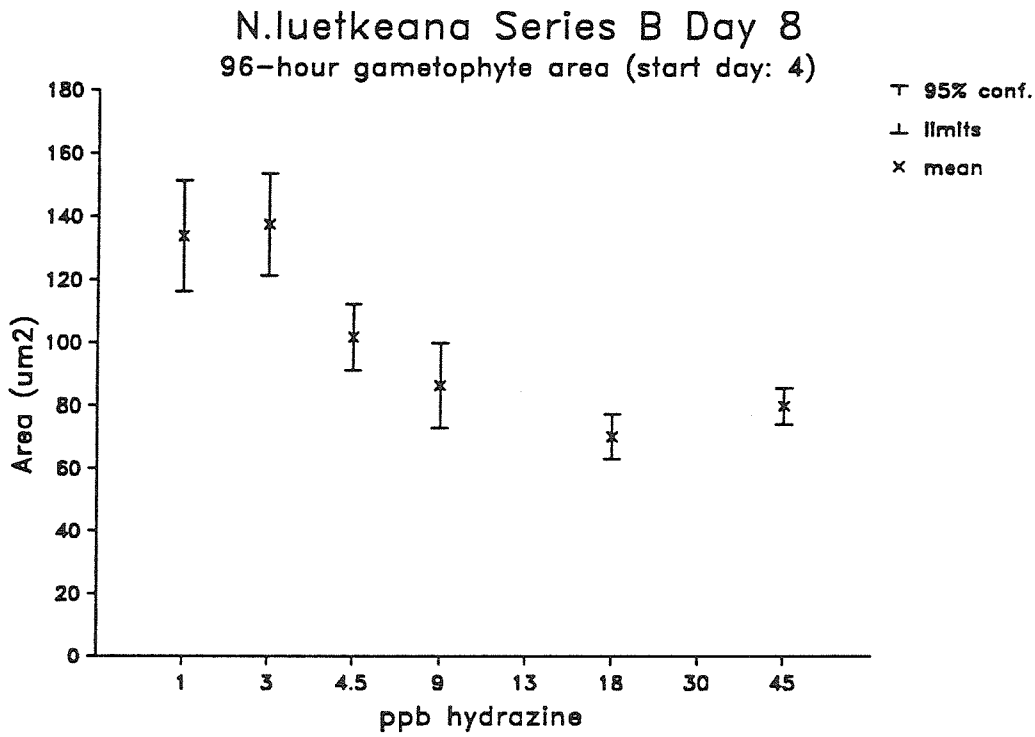

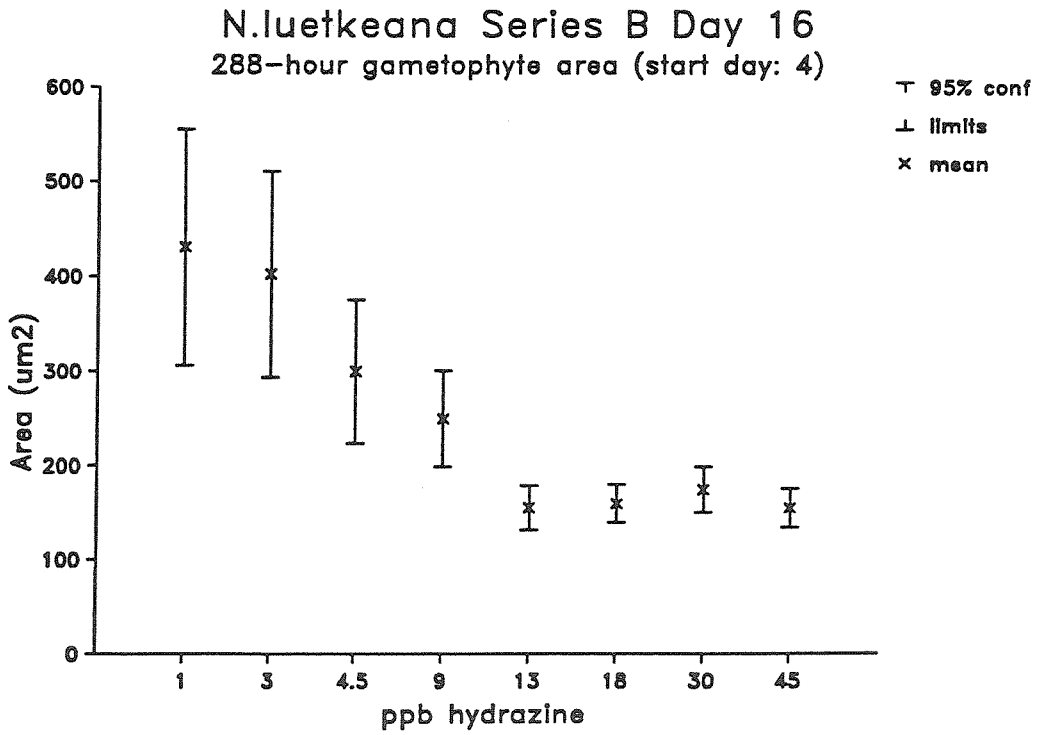

exhibited widely varying sensitivities. Laminaria farlowii was fairly resistant, but Laminaria dentigera and Laminaria ephemera were of intermediate-to-high sensitivity[16].

Reproductive patterns were more varied than trends observed for gametophytic growth. Inhibited vegetative growth did not always indicate inhibited reproduction. Three species, Pterygophora californica and Egregia mensziesii, both members of the Alariaceae, and Laminaria dentigera exhibited significant stimulation of sporophyte recruitment following significant inhibition of vegetative growth.

Possible mechanisms whereby hydrazine might have stimulated sporophyte production include:

1) increasing available resources for sporophyte recruitment through retarding either gametophytic vegetative growth or growth of competing organisms in the cultures (such as bacteria),
2) serving as a source of reduced nitrogen,
3) somehow enhancing gametogenesis.

Data showing stimulated or unaffected reproduction in all tested species of the Alariaceae suggest that this family could be more resistant to hydrazine pulses than other families of brown algae. From available data, overall ranking of tested algae by family in order of decreasing hydrazine resistance would be Alariaceae > Laminariaceae > Lessoniaceae.

---

[16]Laminaria species would need to be retested and measured with digital image-analysis for rankings to be definitive.

Variation in resistance to toxicants has been previously observed among phytoplankton. Harrah (1978) observed a one order-of-magnitude variation in sensitivity to hydrazine by three species from two different taxonomic orders. Blanck et al., (1984) observed up to three orders-of-magnitude variation in resistance among 13 species from eight orders to 19 different compounds and concluded that no one alga could serve as a sensitive predictor of toxicity for all compounds. Results of the present study show a one order-of-magnitude variation in sensitivity within gametophytes in the order Laminariales. Definitive comparison of gametophyte results to phytoplankton tests would require parallel experiments in identical media. Nereocystis or Macrocystis gametophytes might make good indicator species for tests restricted to hydrazine because of their high sensitivity to episodic exposures compared to that of gametophytes from the families Alariaceae and Laminariaceae.

Results suggest that species composition of the brown algal component of a subtidal algal community could shift if exposed to an undiluted 25-250 ppb/1 day hydrazine episode. Results would be most drastic if the episode affected a cohort of overwintering gametophytes of seasonally fertile species. Effects might not be immediately apparent. Absence of juvenile macroscopic plants might not become evident for several months. Decline in abundance of surface canopy formers and a relative increase in abundance of resistant types might first be observed after a toxic chemical event. North (1985) and TERA Corporation (1985) observed increased abundances of juvenile Pterygophora californica in southeast Diablo

Cove two to three months after deterioration of other species was first detected in May 1984. Increased field recruitment most likely occurred due to survival of gametophytes produced in the early spring. Released spores could have been transported into the area from elsewhere, but Pterygophora was not fertile during the period immediately after the May 1984 event. As Pterygophora gametophytes were the most resistant to hydrazine pulses, it is possible that gametophytes established prior to the algal "event" could have survived transient field exposures to hydrazine that inhibited other species. Whatever the causes, Pterygophora gametophytes were apparently able to exploit decreased competition for space and light and temporarily increase abundance of recruited sporophytes in the affected region.

Some environmental factors ameliorate impacts of an episodic toxicant discharge.

1) Plume dilution by mixing of ambient waters with the discharge would reduce toxicant concentrations during transit between discharge structure and contact with target organisms.
2) Macroscopic organisms may take up significant amounts of the compound, further reducing concentrations in waters contacting microscopic life stages.
3) Transient toxicant concentrations in the boundary layer (where microscopic-sized organisms reside) may be less than in overlying water.
4) An affected area could be reseeded with new microscopic life stages after a toxic event by drifting fertile adult tissue,

spores, or gametophytes and embryonic sporophytes dislodged from other locations.

Results from laboratory-scale toxicity tests indicate potential for harm but should be applied with great caution to field situations that modify exposure conditions as experienced at the end of the pipe. Field detection of an event impacting microscopic life stages might be difficult for two reasons.

1) Variability in sporophyte recruitment in the field. Available evidence indicates that recruitment of sporophytes from gametophytes even in the best environmental conditions is a highly variable event. Reed (1988) showed that recruitment of juvenile Pterygophora sporophyte on prepared substrates was highly variable, but somewhat dependent on initial gametophyte density. Lee and Brinkhuis (1986, 1988) showed that Laminaria sporophyte recruitment in the Atlantic ocean was a seasonal event. Deysher and Dean (1986) showed that "windows" of sufficiently high light intensity and sufficiently cold water, which encouraged recruitment of embryonic Macrocystis sporophytes, occurred only occasionally in southern California waters.

2) Power plant operations affect community interactions in ways besides chemical toxicity. Thermal effects of a heated discharge could mask chemical impacts. Accidental discharge of a toxic concentration might inhibit adult plant or grazing animal populations so drastically that detection of shifts in community composition resulting from inhibition of microscopic life stages would be difficult. Chemical toxicity to microscopic life stages might be

invoked as an explanation of observed changes in abundance, if adult species known to be tolerant of thermal effects decline in abundance or fail to recruit in expected densities in regions impacted by a discharge (North et al., 1989), and no other known consequence of the discharge (temperature, sedimentation, turbulence) can explain observed changes in abundance.

V. TOXICITY OF OTHER COMPOUNDS TO MACROCYSTIS GAMETOPHYTES

Introduction

Several additional compounds were tested against Macrocystis gametophytes during the course of the study. Preliminary order-of-magnitude trials were run in dilute seawater solutions of sodium hypochlorite, tributyltin chloride (TBT-Cl), and $ZnSO_4$.

Treated municipal sewage is often chlorinated to destroy coliform bacteria. Power plant effluent is chlorinated to control fouling on intake screens and heat-exchanger surfaces. Chlorine residuals measured inside power plants range from <10 to 700 ppb (Dykstra et al., 1988; Pacific Gas and Electric Company, 1987) with lower measured concentrations at the point of discharge.

Tributyltins are components of antifouling paints used on boats and other marine structures. Marine water concentrations vary with sampling locations. Concentrations up to 0.35 ug/litre have been observed in yacht marinas (Grovhoug, et al., 1986). Concentrations in more open harbor waters are typically one to two orders-of-magnitude lower than values found in restricted basins.

Zn(II) is the standard inorganic reference toxicant recommended by the State of California for use in marine toxicity bioassays to be performed by wastewater dischargers in compliance with requirements imposed by the 1990 California Ocean Plan (Martin et al., 1986a). Background Zn(II) concentrations in seawater range from 0.05 to 9 nM (0.003-0.6 ppb), and average 6nM (0.4 ppb) with predominant soluble species being $ZnOH^{+}$, Zn^{+2}, $ZnCO_3^{\circ}$, and $ZnCl^{+}$ (Bruland, 1983). Elevated Zn(II) levels were historically observed in wastewaters discharged into the ocean from municipal sewage outfalls but have been recently declining (Stull, et al., 1988). High Zn(II) concentrations persist (along with elevated concentrations of other metals and some organic compounds) in sediments partially composed of anthropogenic particles discharged from sewage outfalls.

Materials and Methods

Culture methods were similar to those used for continuous hydrazine assays (Chapter 4.III). Toxicant solutions were applied to three-to-four day-old gametophytes for 96 hours in static cultures with daily renewal. Cultures were measured with the digital image analysis system at the 96-hour endpoint and effects of concentration estimated by Student's t-tests and one-way analysis of variance. Measurements of germ-tube length were made in cultures exposed to Zn(II) using both eyepiece micrometer methods and digital image analysis to compare results to those obtained by the State of California Marine Bioassay Project (Hunt et al., 1987).

Zn(II) was added from a $ZnSO_4$ master solution made from double-distilled water and reagent-grade $ZnSO_4$. Speciation was not regulated through use of a defined medium or chelating agents, because an estimate of the inherent variability of results in uncontrolled media was a desired outcome for verification of State-developed bioassay protocols which used natural seawater. Results are reported as inhibition vs. total added Zn(II) with no experimental attempts to determine the fraction available Zn^{+2}.

Chlorine was added as 3.5 percent sodium hypochlorite solution. Our objective was simply an order-of-magnitude estimate of toxicity. Chlorine residuals were not determined. Clean seawater is estimated to have a 15-minute chlorine demand of 2-3 ppm (White, 1970) that is due to dissolved nitrogen and organic carbon compounds. Applied chlorine concentrations below the chlorine demand concentration would not persist, but reaction products (e.g., chloramines) might themselves have toxic effects.

Tributyltin chloride was diluted in a spectrophotometric-grade acetone vehicle, blended with an equal volume of double-distilled water and applied to cultures after intense agitation in a predetermined volume of seawater. Gametophytic growth was compared to cultures treated only with plain acetone and to acetone-free controls.

Results

Tributyltin chloride exhibited a molar toxicity range lower than observed for hydrazine (Table 4.18). The control acetone solutions exhibited some toxicity (Figure 4.25), contrasting with observations

from previous studies evaluating toxicity of PCBs (James et al., 1987), where no acetone toxicity was indicated.

Hypochlorite showed inhibition in the concentration range bracketing its expected 2 ppm demand in seawater (Table 4.18, Figure 4.26) at 96 hours. Significant (Dunnett's multiple-range test, one-way analysis of variance) vegetative growth inhibition was observed at applied concentrations exceeding 10 ppb (190 nM) after 288 hours' (12 days) exposure, indicating possible chronic toxicity of the products of reactions between hypochlorite and organic constituents in seawater. Organisms exposed to 10 ppm chlorine were completely destroyed by the treatment. Only spore husks remained at the end of 12 days' exposure.

Zn(II) significantly inhibited germ-tube length at 500 ppb (8 uM) and at concentrations exceeding 2000 ppb (31 uM) (Table 4.19; Figure 4.27A). Digital image-analysis failed to detect inhibition at the germination stage (Figure 4.27B). When the just-germinated gametophytes were followed for another 72 hours and measured with digital image-analysis, significant growth inhibition was observed in all test concentrations exceeding 50 ppb (800 nM) (Figure 4.28A). Gametophytes initially exposed to Zn(II) at age four days were inhibited by concentration ranges of 200-500 ppb and 2000-5000 ppb in two different cultures (Table 4.19 and Figure 4.28B).

Table 4.18: Summary of 96-hour compound toxicity to to vegetative growth of Macrocystis gametophytes. Concentration significantly inhibiting vegetative growth. (Student's t-test, one-tailed, $p < 0.05$). Ranked in order of increasing molar toxicity.

COMPOUND		CONCENTRATION nM	CONCENTRATION ppb
Borate (as H_3BO_3)		>3,200,000	>240,000
Lithium (as Li^+)		>2,500,000	>17,000
Chlorine (as OCl^-)	*	20,000 - 200,000	10^3 - 10^4
Zinc [as Zn(II)]	*	3,100 - 7,800	200 - 500
Hydrazine (as $N_2H_5^+$)	*	64 - 128	2 - 4
Tributyltin chloride	*	36 - 360	12 - 120
4,4'-dichlorobiphenyl[1]		9 - 23	2 - 5
2,4,5,2',4',5'-hexachlorobiphenyl		3 - 8	2 - 5

Asterisk (*) means analyzed via digital image analysis.

OCl^- data not corrected for approx. 2 ppm seawater chlorine demand.

[1]Source for data for 4,4'-dichloro and 2,4,5,2',4',5'-hexachloro biphenyl is James et al.,1987. Biphenyl data are for total added to seawater, not true solution concentration.

Zinc data are reported as total added Zn(II), because speciation was not easily determined in undefined medium.

Figure 4.25: Range-finding test for toxicity of tributyltin chloride. M. pyrifera Series V. September 1987.

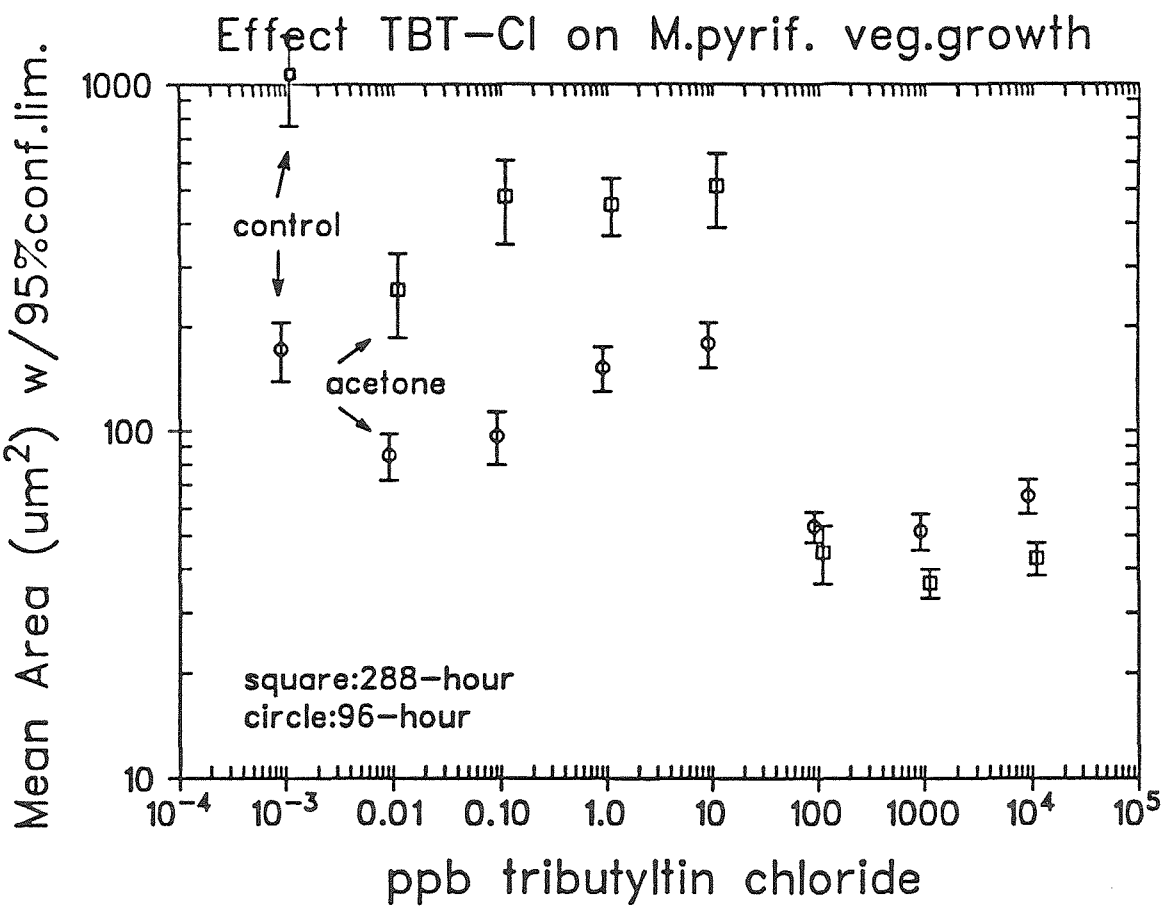

Figure 4.26: Range-finding test for toxicity of sodium hypochlorite. M. pyrifera Series V. September 1987.

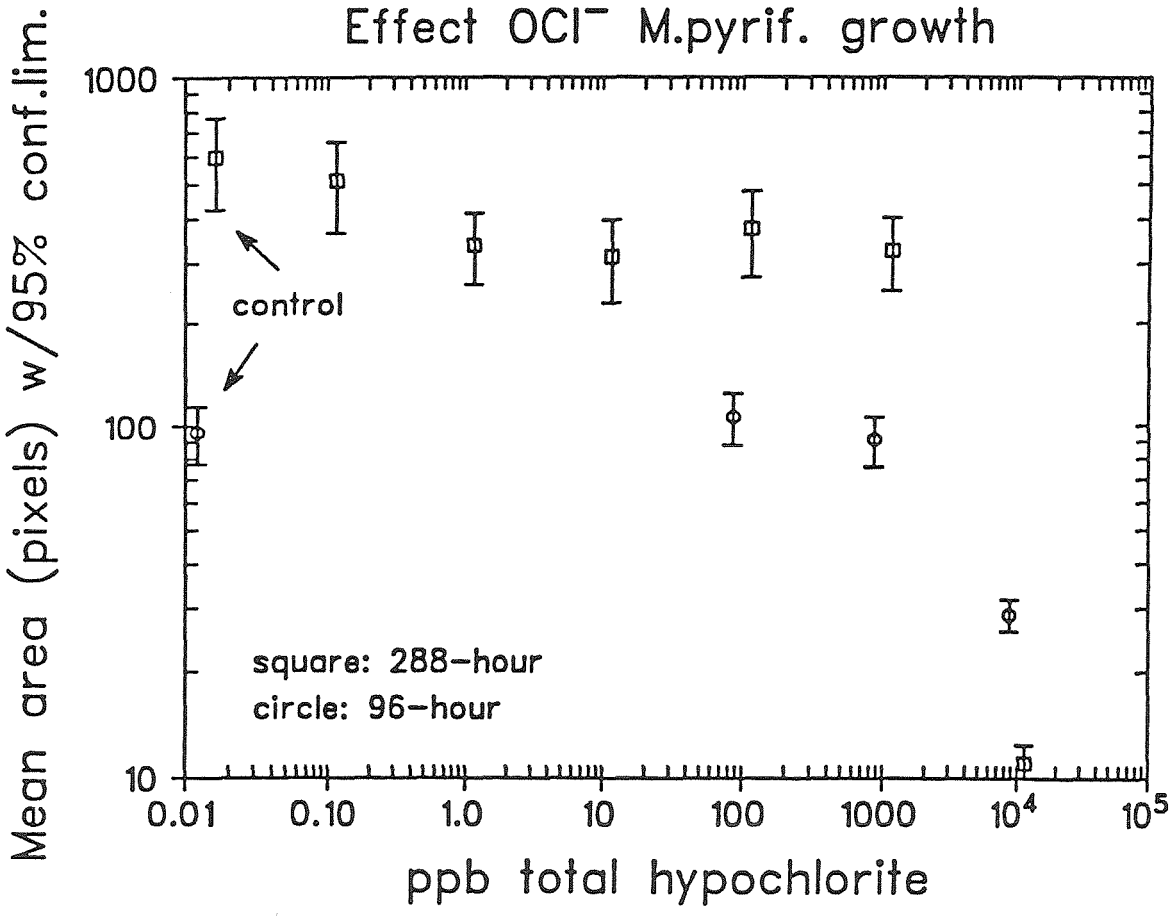

Figure 4.27: Effect of total added Zn(II) on germ-tube length of settled M. pyrifera zoospores. Top: Eyepiece micrometer. Bottom: Digital image analysis. May 1988.

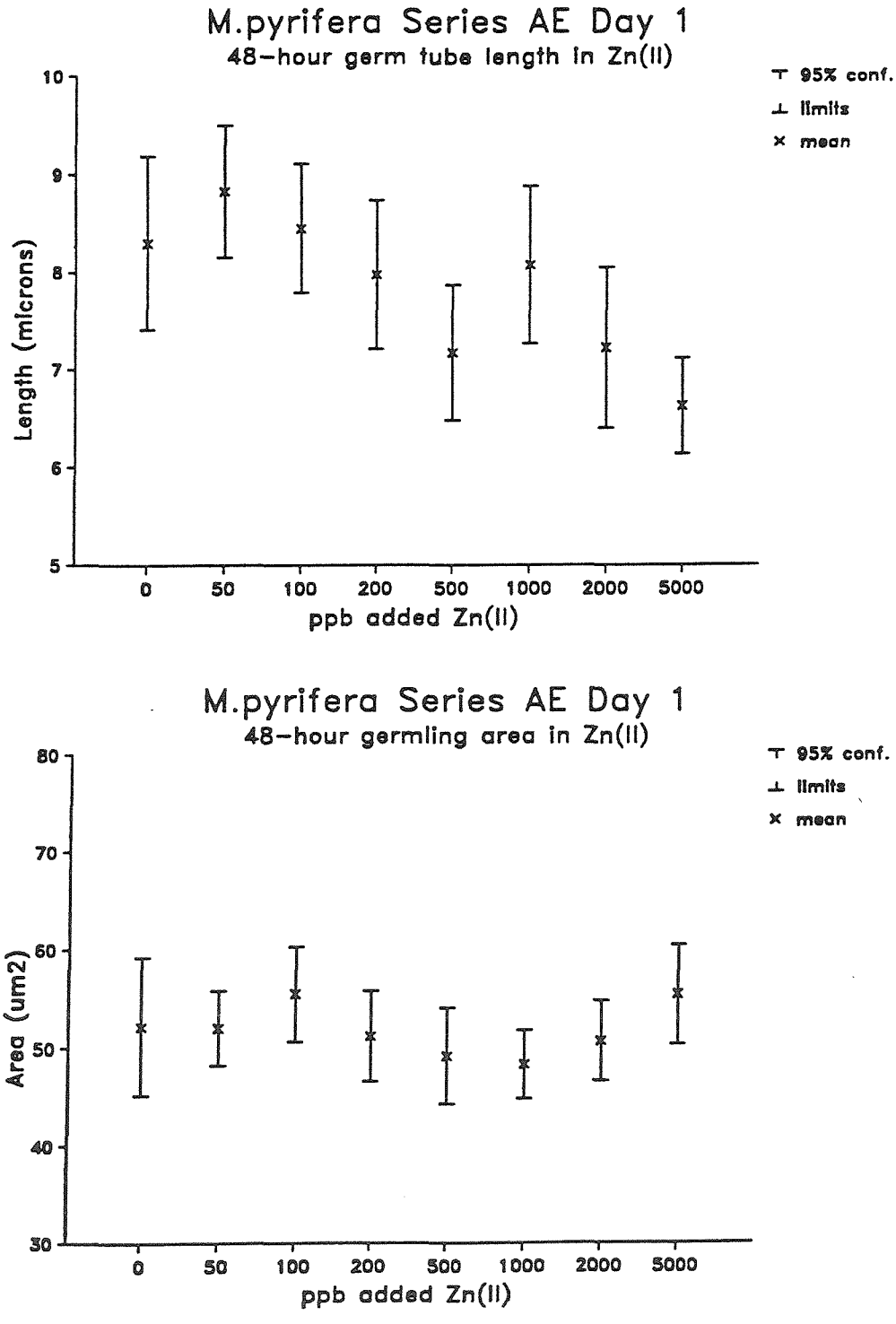

Figure 4.28: Effect of total added Zn(II) on vegetative growth of M.pyrifera gametophytes. Measured by digital image analysis; May 1988. Top: Exposed during germination on Day -1. Bottom: Exposed during rapid growth; Day 4.

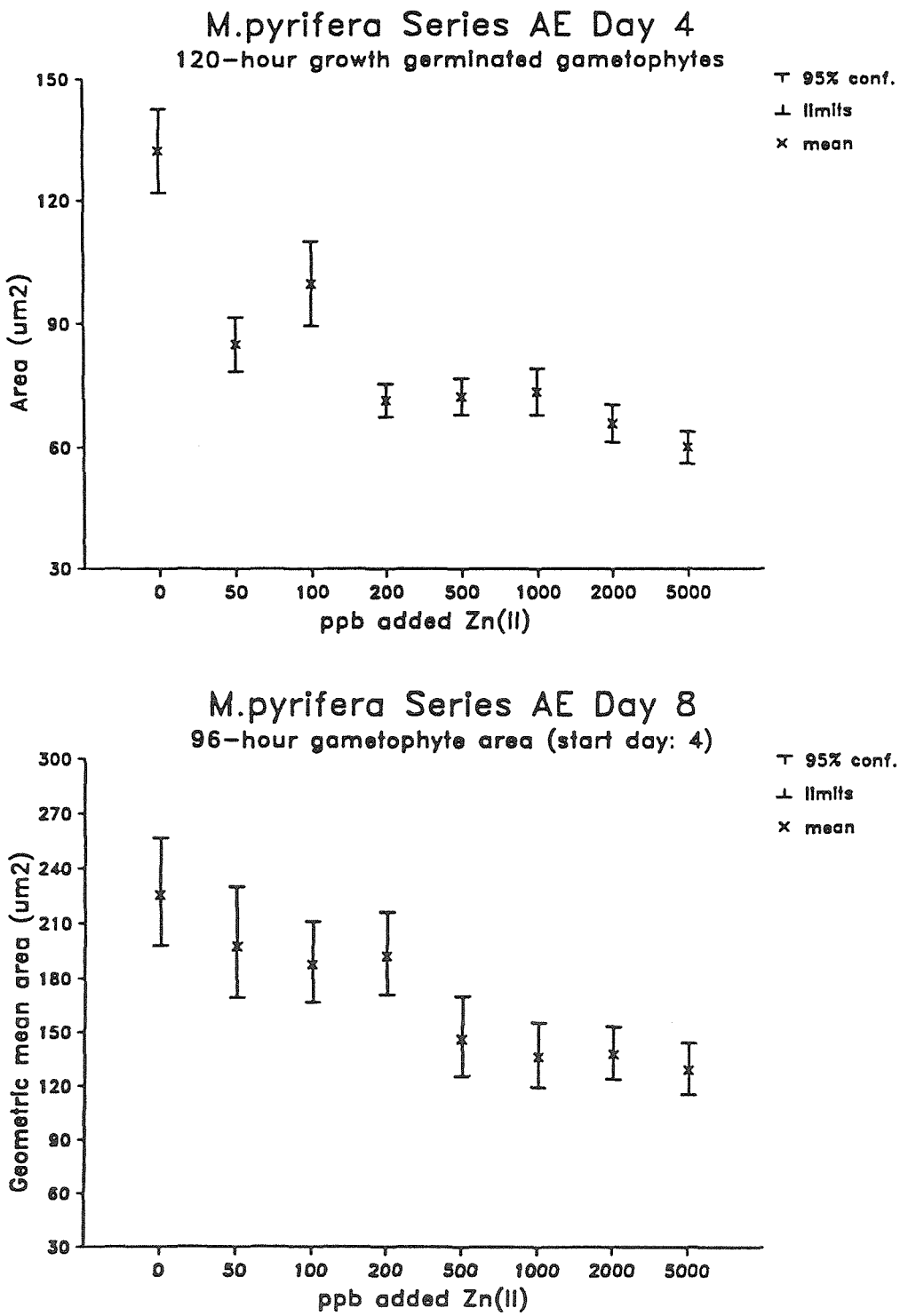

Table 4.19 Comparison of Zn(II) toxicity to M.pyrifera spore germination and gametophytic growth. Life stage legend: s means germinating spore; g means gametophytic growth.

Test Date/method	Start day	Life stage	Duration of test	Inhibiting concentration range	Fraction control size	Size of controls mean/95% conf.limits
5/88 microm	-1	s	48 hour	1000-2000 ppb*	0.90	39/ 3 um2
5/88 digit	-1	s	48 hour	> 5000 ppb$	1.10$	52/ 7
5/88 digit	-1	g	120 hour	0- 50 ppb	0.65	130/10
5/88 digit	4	g	96 hour	200- 500 ppb	0.50	240/30
5/88 digit	4 N_2H_4	g	96 hour	2- 5 ppb	0.50	325/45
3/88 digit	-1	s	48 hour	> 1000 ppb$	1.30$	46/ 3
3/88 digit	4	g	96 hour	2000-5000 ppb	0.56	314/50
3/88 digit	4 N_2H_4	g	96 hour	3- 5 ppb	0.62	314/50

*erratic result: 500 ppb significantly less than control; 1000 ppb not significantly less (See text).
$inconclusive: signif. inhibition not observed at any value in test range. Highest tested concentration and corresponding size are listed.

Discussion

Germination (as measured by germ tube elongation) was a less sensitive indicator of toxicity than measurements of vegetative growth made with the same culture. This was also observed by Hunt et al., (1987), who estimated no-effect levels of 7,500, > 10,000 and < 560 ppb nominal Zn(II) in three tests for inhibition of Macrocystis spore germination and inhibition of gametophyte elongation at respective concentrations of 1000, 560 and 560 ppb in the same cultures. Significant inhibition of germ-tube length at 500 and 2000 but not 1000 ppb, using measurements taken with the eyepiece micrometer, may have been an artifact of high internal variability of measurements. Analysis of variance showed that within-group error accounted for 83 percent of the variance in the sampled measurements.

Digitizer detection was masked by the large contribution of empty spore cases to area measurements of individual organisms. Spore cases may contribute more than half the measured area when a culture is still at the germination stage.

Macrocystis gametophytes were more sensitive to continuous Zn(II) exposures when exposed just after germination than at a later stage, This pattern was also observed with episodic hydrazine exposures (Section 4.III). Zn(II) was previously observed to inhibit significantly growth of Laminaria saccharina embryonic sporophytes at 100 ug/litre (about 98 ppb) nominal concentration (Thompson and Burrows, 1984). Hunt et al., (1987), observed significant inhibition of elongation of Macrocystis gametophytes at nominal Zn(II) concentrations exceeding 560 ppb.

Molar concentrations of total Zn(II) required for significant inhibition of Macrocystis gametophyte vegetative growth were 5 to 50 times higher than hydrazine concentrations (64-160 nM). Continuous exposure toxicity results were more variable with Zn(II) than with hydrazine. Gametophytes from identical source materials tested in hydrazine simultaneously with the Zn(II) exposures were consistently inhibited at 2-5 ppb hydrazine when 96-hour inhibitions in Zn(II) varied by an order of magnitude (Table 4.19). Several phenomena could explain this discrepancy:

a) Resistance to Zn(II) could have varied whereas resistance to hydrazine did not.

b) Seawater chemistry varied. Free Zn^{+2} activity has been shown to determine the degree of influence of Zn(II) on phytoplankton growth

rates (Jackson and Morgan, 1978), and Macrocystis gametophytes (Kuwabara, 1980). Kuwabara also showed that Macrocystis gametophyte growth was a function of zinc/copper and zinc/iron interactions. Distribution of Zn(II) among various species depends on pH (Stumm and Morgan, 1981), concentration of dissolved and colloidal organic (Mantoura et al., 1978), and concentration of inorganic particles (Grimme, 1968, cited in Kuwabara, 1980). Hydrazine speciation is simpler; distribution between N2H4 and N2H5+ is principally determined by pH in marine waters. Complexation with metals in seawater is minimal (cf. Chapter 5).

Spot-checked pH of offshore seawaters collected for culturing varied from 8.0 to 8.1 during the three-year study period. Total organic carbon was not determined. Zn(II) speciation could have varied in the different batches of offshore seawater used in the two experiments. Resolution of the discrepancy would require repeated culturing in a defined medium such as Aquil.

Results indicated that State of California protocols, which do not use defined media, may lead to variable indications of Zn(II) toxicity to Macrocystis gametophytes. Zn(II) speciation will vary according to composition of test media made up from local seawaters. Variable contents of dissolved and colloidal organic material in coastal waters could affect Zn(II) concentrations and the experimental outcome. Confidence limits on concentrations of total added Zn(II) necessary to inhibit growth or germination should be developed through repeated experimentation if receiving water

standards are to be based on outcomes of a Macrocystis gametophyte toxicity assay.

Four-day hypochlorite toxicity to Macrocystis gametophytes occurred in a concentration range similar to that observed by Clendenning and North (5-10 ppm, 1959) for 50 percent inhibition of photosynthesis by laminae from adult Macrocystis plants. Phytoplankton have been inhibited in 24-hour exposures at concentrations in the 0.08-0.2 ppm range (cf. authors cited in Mattice and Zittel, 1976). After 12 days' exposure, Macrocystis gametophytic growth was inhibited at concentrations exceeding 10 ppb added hypochlorite, indicating that products of chlorine reaction with seawater (chlorine-produced oxidants) may have exerted some chronic toxicity. Typical free available chlorine residuals discharged by the Diablo Canyon Power Plant during 164 days in 1986 were 36 $\pm$ 26 ppb (700 $\pm$ 510 nM) with five one-day spikes exceeding 100 ppb (Pacific Gas and Electric Company, 1987). Vanderhorst (1982) observed significant depression of species richness in experimental microcosms exposed to continuous concentrations of 10 and 50 ppb chlorine-produced oxidants compared to a set of control and intermittently chlorinated microcosms. Results indicated that continuous low-level chlorination at observed levels could inhibit Macrocystis vegetative growth.

TBT inhibited growth at molar concentrations lower than those reported for hydrazine (Table 4.18). Results should be regarded as

preliminary estimates. TBT's partially sorb to suspended particles[17], lowering the aqueous concentration. Toxicity of TBT leached from painted panels to the mysid shrimp Acanthomysis sculpta was 0.42 ug/litre for a 96-hour juvenile LC50 and 0.14 ug/litre for inhibition of reproduction (Davidson, et al. 1986). Significant reductions in shell length of juvenile mussels (Mytilus edulis) were observed in seven days at TBT-oxide concentrations exceeding 0.4 ug/litre (Stroemgren and Bongard, 1987). TBT concentrations in San Diego Bay were found in 1986 to vary from 0.027-0.235 ug/litre in yacht harbors and marinas to less than 0.005 ug/litre (the analytical detection limit) in both well-flushed areas and the southern portion of the Bay (Seligman, et al., 1986). Initial toxicity values for Macrocystis gametophytes indicate that they were less sensitive indicators than mysid shrimp and that the highest concentrations observed in local marine surface waters probably would not inhibit vegetative growth.

---

[17]Valkirs et al., 1986 reported that 17 percent or less of carbon 14-labelled tributyltin was taken up by suspended particles in seawater and estimated a suspended sediment-water partition coefficient of 3000.

REFERENCES

Alder, H.E. and E.B. Roessler 1972. Introduction to Probability and Statistics, W.H.Freeman and Company: San Francisco, 373pp.

Antia, N.J. and J.Y. Cheng 1975. Culture studies on the effects from borate pollution on the growth of marine phytoplankters. Journal of the Fisheries Research Board of Canada. 32(12): 2487-2494.

Bevington, P.R. 1969. Data Reduction and Error Analysis for the Physical Sciences, McGraw-Hill: New York pp.56-65.

Blanck, H., G. Wallin and S.A. Wangberg 1984. Species-dependent variation in algal sensitivity to chemical compounds. Ecotoxicology and Environmental Safety. 8:339-351.

Bray, R. 1988. Random-t, Software for performing complete and sampled randomization tests of significance between means of two groups of data, California State University: Long Beach, CA. Magnetic media.

Bruland, K.W. 1983. Trace Elements in Seawater, Chapter 45 in Riley, J.P. and R. Chester, (eds.), Chemical Oceanography; Volume 8, Academic Press: London pp.157-220.

California Water Quality Control Board, Central Coast Region 1985. Amended Order No. 85-101, NPDES No. CA0003751, Waste Discharge Requirements for Pacific Gas and Electric Company: Diablo Canyon Nuclear Power Plant, Units 1 and 2, San Luis Obispo County.

Clendenning, K.A. 1959. "Laboratory Investigations", in W.J. North, ed. Annual Progress Report; 1 July 1958 - 30 June 1959; The Effects of Waste Discharges on Kelp. University of California Institute of Marine Resources. Publication 59-11:9-13.

Davidson, B.M., A.O.Valkirs, and P.F.Seligman 1986. Acute and chronic effects of tributyltin on the mysid Acanthomysis sculpta (Crustacea, Mysidaceae), in Oceans '86 Conference Record: Science-Engineering-Adventure, Volume 4: Organotin Symposium, IEEE Publishing Service: New York, pp.1219-1225.

Deysher, L. and T.A. Dean 1986. Interactive effects of light and temperature on sporophyte production in the giant kelp, Macrocystis pyrifera. Marine Biology. 93:17-20.

Dykstra, D.H., R.Robertson, J.L.Elliott, H.Elwany, K.Zabloudil 1988. Oceanographic Processes and Water Quality, in Report on 1987 Data: Marine Environmental Analysis and Interpretation, Report 88-RD-35, Southern California Edison Company: Rosemead, Ca. p.2.1-2.36.

Fisher, J.W., C.B. Harrah, and R. Berry 1980. Hydrazine: Acute toxicity to bluegills and sublethal effects on dorsal light response and Aggression. Transactions American Fisheries Society. 109:304-309.

Glasstone, S. and A. Sesonske, 1981. "Radiation Protection and Environmental Effects", Chapter 9 in Nuclear Reactor Engineering Third Edition, Van Nostrand Reinhold Co: New York pp.592-596.

Grovhoug, J.G., P.F. Seligman, G. Vafa, R.L. Fransham 1986. Baseline measurements of butyltin in U.S. harbors and estuaries. in Oceans '86 Conference Record: Science-Engineering-Adventure, Volume 4: Organotin Symposium, IEEE Publishing Service: New York,pp.1283-1288.

Harrah, C.B., 1978. Biological Effects of Aqueous Hydrazine Solutions, in Proceedings: Conference on Environmental Chemistry of Hydrazine Fuels, U.S. Air Force. Civil and Environmental Engineering Development Office: CEEDO-TR-78-14, pp. 167-176.

Hunt, J., B. Anderson and M. Martin 1987. Interim Summary Report on the Results of Reference Toxicant Testing; February 1, 1987 Granite Canyon Laboratory. California Department of Fish and Game. Prepared for State Water Resources Control Board. 34pp.

Jackson, G.A. and J.J. Morgan 1978. Trace-metal chelator interactions and phytoplankton growth in seawater media: Theoretical analysis and comparison with reported observations. Limnology and Oceanography. 23:268-282.

James, D., S. Manley, M.Carter, and W. North 1987. Effects of PCBs and Hydrazine on LIfe Processes in Microscopic Stages of Selected Brown Seaweeds, in C.J. Bird and M.A. Ragan, eds. Proceedings of the XIIth International Seaweed Symposium; Sao Paulo, Brazil, July 1986. Hydrobiologia. 151-152:411-415.

Kuwabara, J.S. 1980. Micronutrient Requirements for Macrocystis pyrifera (L.) C.A. Agardh (Giant Kelp) Gametophytes determined by means of a chemically defined medium, "Aquil". Ph.D. Thesis, California Institute of Technology, Pasadena, CA. 164pp.

Lee, J.A. and B.H. Brinkhuis 1986. Reproductive phenology of Laminaria saccharina (L.) LaMour (Phaeophyta) at the southern limit of its distribution in the northwestern Atlantic Ocean. Journal of Phycology. 22:276-285.

Lee, J.A. and B.H. Brinkhuis 1988. Seasonal light and temperature interaction effects on development of Laminaria saccharina (Phaeophyta) gametophytes and juvenile sporophytes. Journal of Phycology. 24:181-191.

Mantoura, R.F.C., A. Dickson and J.P. Riley 1978. The Complexation of Metals with Humic Materials in Natural Waters Estuarine, Coastal and Marine Science, 6:387-408.

Martin, M., D. Schlafmann, J. Hunt, B. Anderson, L. Espinoza 1986a. Selection of an Inorganic Reference Toxicant (Interim Report, Marine Bioassay Project, California Department Fish and Game: Sacramento, CA. 4 June 1986) 23pp.

Martin, M., J. Hunt, B. Anderson, L. Espinoza, F. Palmer 1986b. Acute Toxicity Tests and Protocols: Mysid Shrimp, Red Abalone, and Giant Kelp (Second Report, Marine Bioassay Project, California Department of Fish and Game: Sacramento, CA. 1 May 1986) 65pp.

Mattice, J.S. and H.E. Zittel 1976. Site-specific evaluation of power plant chlorination. Journal of Water Pollution Control Federation. 48(10):2284-2308.

Nacci, D., E. Jackim, and R. Walsh 1986. Comparative evaluation of three rapid marine toxicity tests: Sea urchin early embryo growth test, sea urchin sperm cell toxicity test and Microtox (r). Environmental Toxicology and Chemistry. 5:521-525.

North, W.J., 1985. Intertidal and Subtidal Survey Observations, August 1984. Chapter 2 in South Diablo Cove Algal Observations, Diablo Canyon Power Plant, Pacific Gas and Electric Company: San Ramon, CA. Report 411-85.199.

North, W.J. E.K. Anderson, F.A. Chapman, and D.E. James, 1989. Characteristics of the power plant and its operations. Chapter 3 in Biological Investigations at Diablo Canyon, Pacific Gas and Electric Company: San Ramon, CA. 185pp.

Pacific Gas and Electric Company 1985. Appendix, Operational Data, in South Diablo Cove Algal Observations, Diablo Canyon Power Plant. Pacific Gas & Electric Company, San Ramon, CA. Report 411-85.199.

Pacific Gas and Electric Company 1987. NPDES Environmental Monitoring Report, calendar year 1986. submitted to Central Coast Regional Water Quality Control Board, January 31, 1987. Pacific Gas & Electric Company: San Ramon, CA.

Reed, D. 1988. Kelp gametophyte competition and its effect on sporophyte recruitment. Abstracts of Phycological Society of America Meeting, Monterey California, 24-29 July, 1988. published in Journal of Phycology; Supplement to June 1988. 24:9.

Scanlan, C.M. and M.Wilkinson, 1986. The use of seaweeds in biocide toxicity testing. Part 1. The sensitivity of different stages in the life-history of Fucus, and of other algae, to certain biocides. Marine Environmental Research. 21:11-29.

Segel, I. 1968. Biochemical Calculations, Appendix III: Enzyme Kinetics. J.Wiley and Sons, Inc: New York, pp.381-389.

Seligman, P.F., J.G. Grovhoug, and K.E. Richter 1986. Measurement of butyltins in San Diego Bay, CA: A monitoring strategy, in Oceans '86 Conference Record: Science-Engineering-Adventure, Volume 4: Organotin Symposium, IEEE Publishing Service: New York, pp.1289-1296.

Slonim, A.R. 1986. Acute toxicity of some hydrazine compounds to salamander larvae, Ambystroma spp. Bulletin of Environmental Contamination Toxicology. 37(5):739-46.

Sokal, R.R. and F.J. Rohlf 1981. Biometry; 2nd edition, W.H. Freeman and Company: New York, 859pp.

Southern California Edison Company 1986. Maximum water flow for Unit 2, San Onofre Nuclear Generating Station, Southern California Edison Company and San Diego Gas and Electric Company, Camp Pendleton, San Diego County, California; 4pp.

Stroemgren, T. and T.Bongard. 1987. The effect of tributyltin oxide on growth of Mytilus edulis. Marine Pollution Bulletin. 18(1):30-31.

Stull, J., R. Baird, and T. Heesen 1988. Relationship between declining discharges of municipal wastewater contaminants and marine sediment core profiles, in D.A. Wolfe and T.P. O'Connor, eds. Oceanic Processes in Marine Pollution. Volume 5. Urban Wastes in Coastal Marine Environments. Robert E. Krieger Publishers: Malabar, Florida, pp.1240-1245.

Stumm, W., and J.J. Morgan 1981. Aquatic Chemistry. J.Wiley and Sons: New York, 896pp.

TERA Corporation 1985. Diablo Canyon subtidal algal observations of the Thermal Effects Monitoring Program; Chapter 1 in South Diablo Cove Algal Observations, Diablo Canyon Power Plant, Pacific Gas and Electric Company: San Ramon, Calif. Report 411-85.199.

Thompson, R.S. and E.M. Burrows 1984. The toxicity of copper, zinc and mercury to the brown macroalga Laminaria saccharina", in G.Persoone, E.Jaspers, C.Claus, eds. Ecological Testing for the Marine Environment, Volume 2, State University of Ghent: Ghent, Belgium. pp. 259-270.

Valkirs, A.O., P.R. Seligman, R.F. Lee 1986. Butyltin partitioning in marine waters and sediments. in Oceans '86 Conference Record: Science-Engineering-Adventure, Volume 4: Organotin Symposium. IEEE Publishing Service: New York. pp.1165-1170.

Vanderhorst, J.R. 1982. Effects of Chlorine on Marine Benthos, Report EA-2696, Research Project 1224-4, prepared by Battelle Northwest Laboratories for Electric Power Research Institute, Palo Alto, California, 108pp.

Walsh, G.E., C.H. Deans, and L.L. McLaughlin 1987. Comparison of the EC_{50}'s of algal toxicity tests calculated by four methods, Environmental Toxicology and Chemistry. 6:767-770.

White, G.C. 1970. Handbook of Chlorination. Van Nostrand Reinhold: New York, 744pp.

CHAPTER 4: APPENDIX

Macrocystis pyrifera gametophyte continuous exposure growth inhibition in hydrazine. Plotted data used to determine significance ranges ($p < 0.05$) and GC_{50} estimates in Table 4.14, p.135.

Data points plotted at 0.30 ppb hydrazine are actually control (0 ppb hydrazine) values positioned at 0.30 ppb for visual convenience.

Figure 4.A.1: Macrocystis pyrifera; Series X and Y growth inhibition in hydrazine. Mean gametophyte area ± 95 percent confidence limits after 120 hours continuous exposure in indicated concentrations.

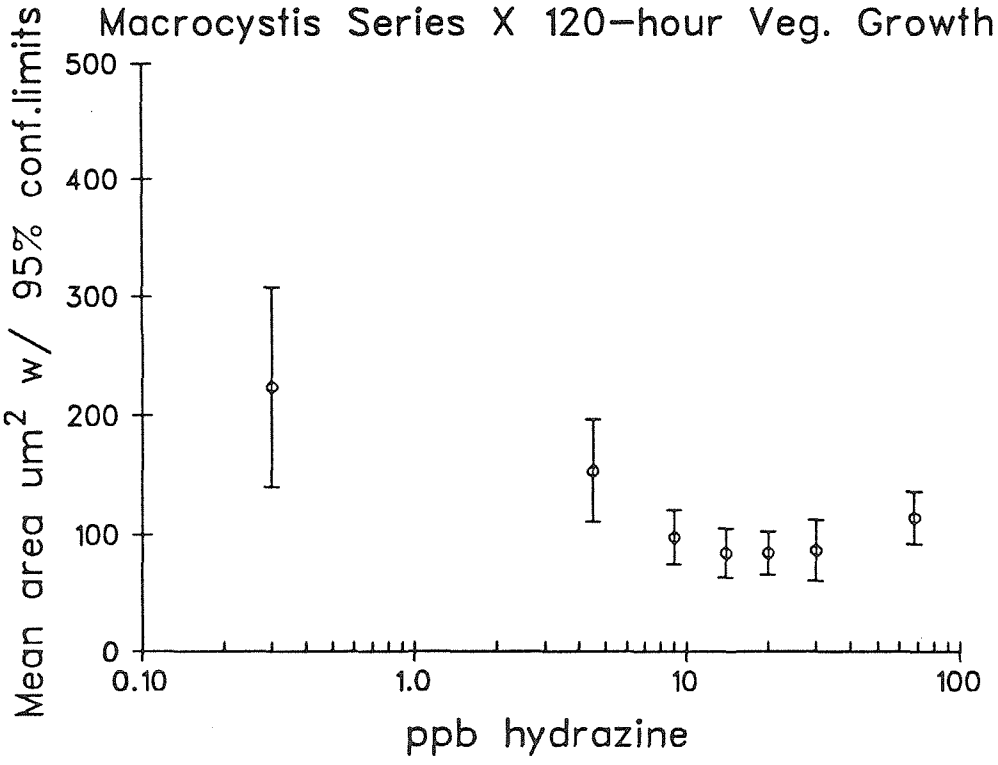

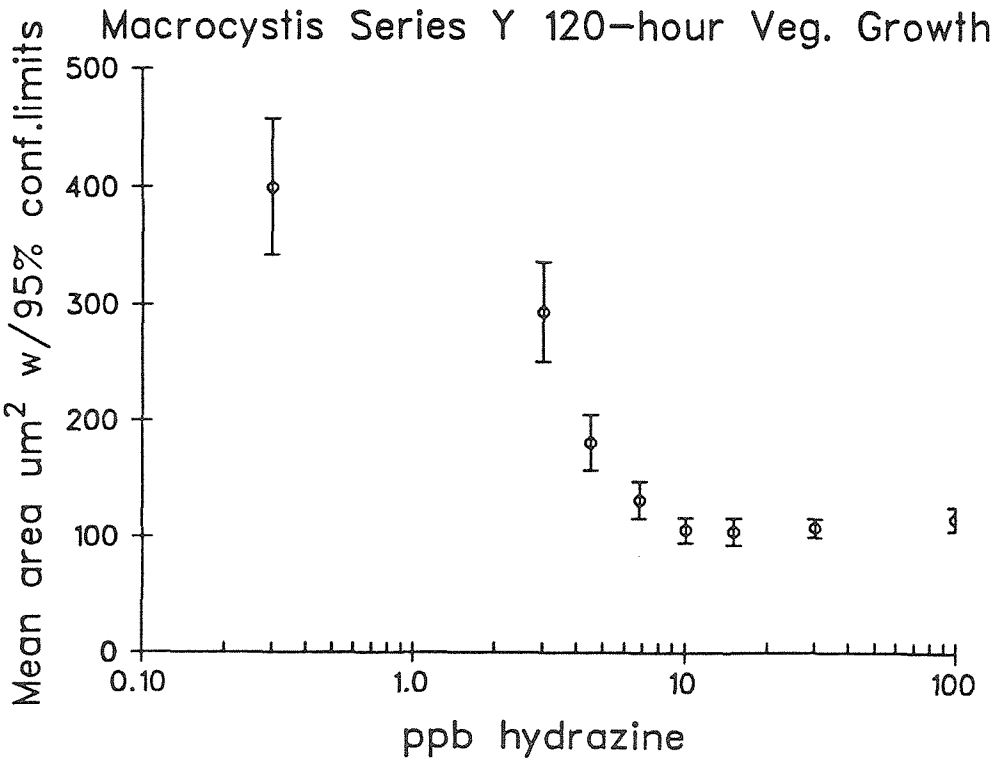

Figure 4.A.2: Macrocystis pyrifera; Series Z and AA growth inhibition in hydrazine. Mean gametophyte area ± 95 percent confidence limits after 120 hours and 100 hours continuous exposure in indicated concentrations, respectively.

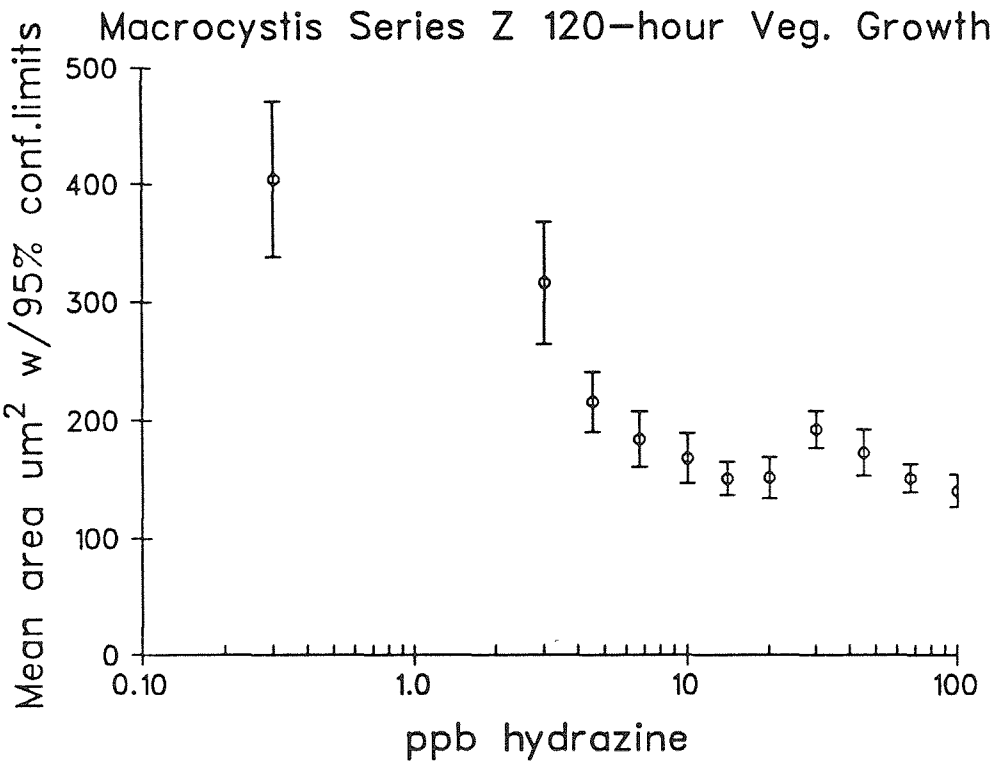

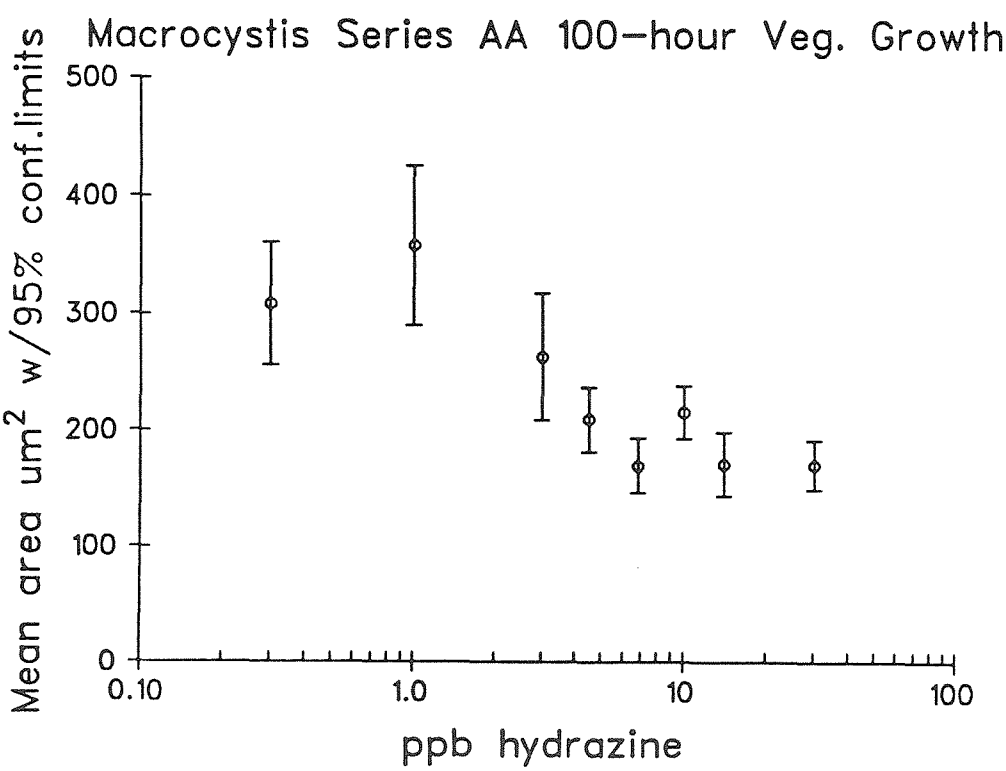

Figure 4.A.3: Macrocystis pyrifera; Series AB and AC growth inhibition in hydrazine. Mean gametophyte area ± 95 percent confidence limits after 96 and 100 hours continuous exposure in indicated concentrations, respectively.

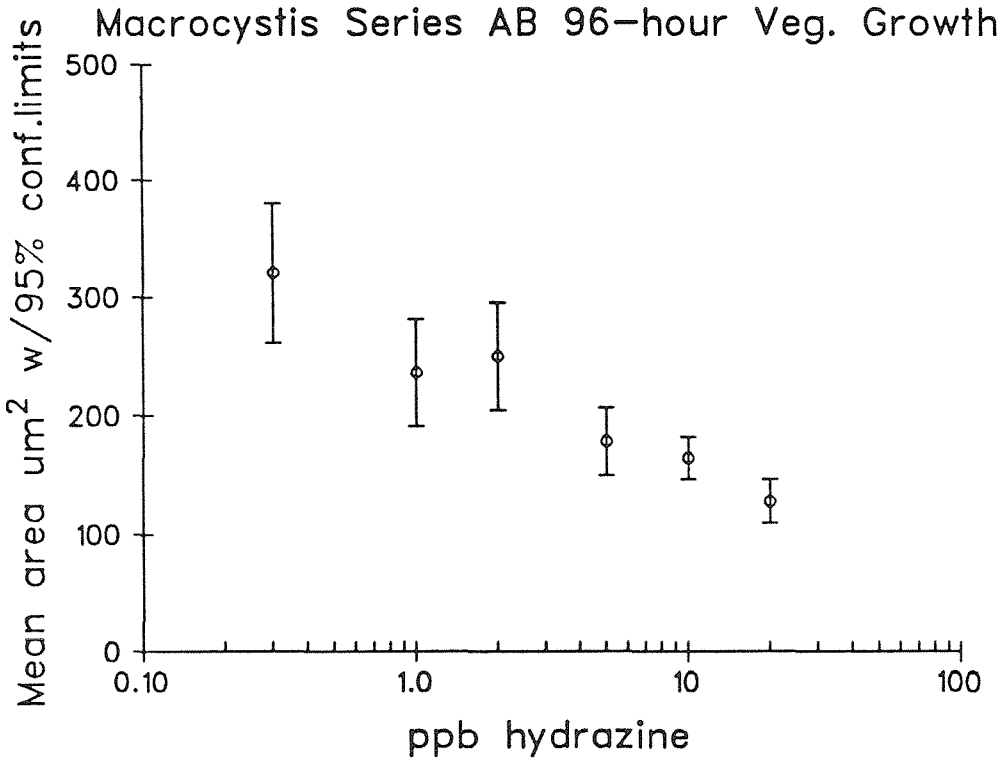

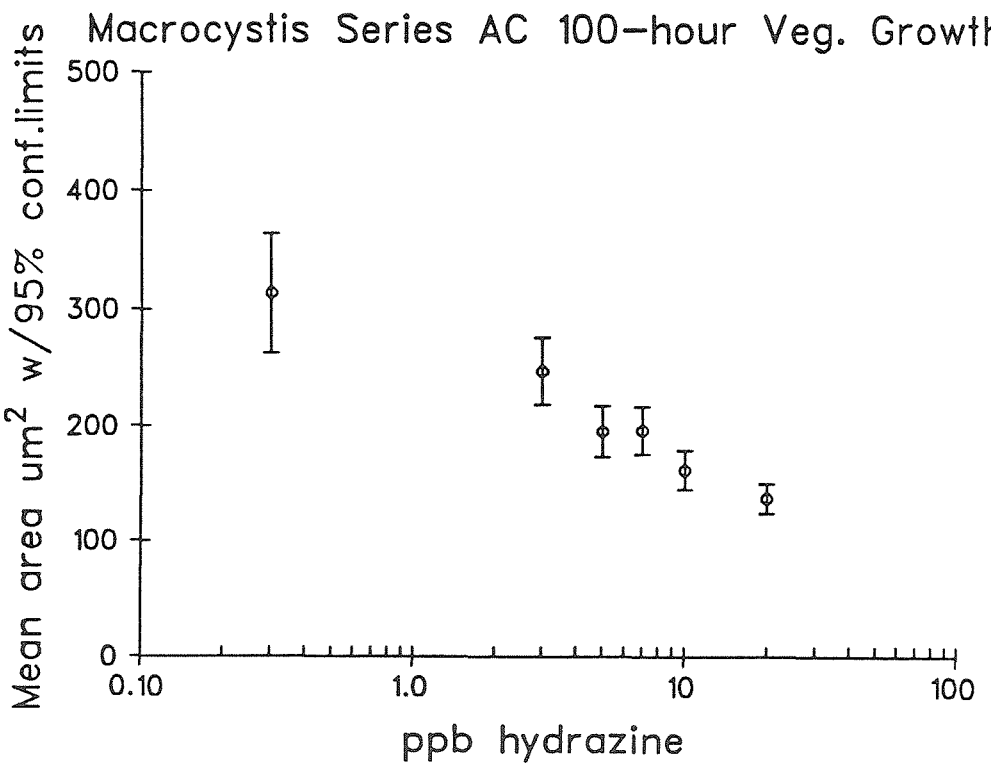

Figure 4.A.4: Macrocystis pyrifera; Series AD and AE growth inhibition in hydrazine. Mean gametophyte area ± 95 percent confidence limits after 96 hours continuous exposure in indicated concentrations.

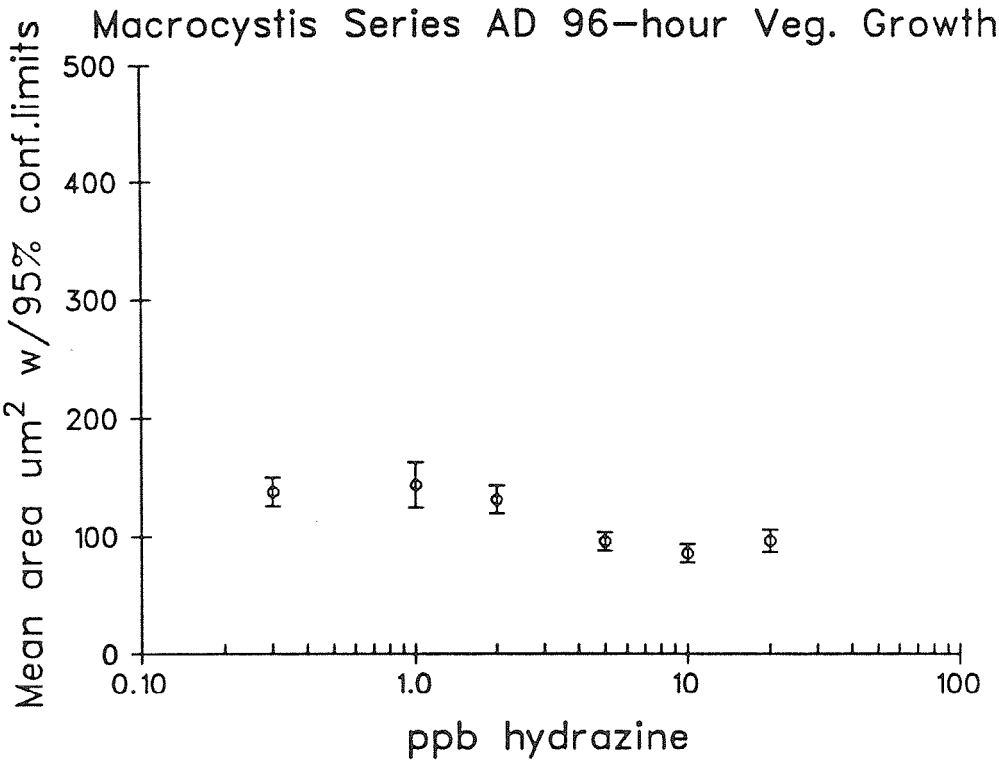

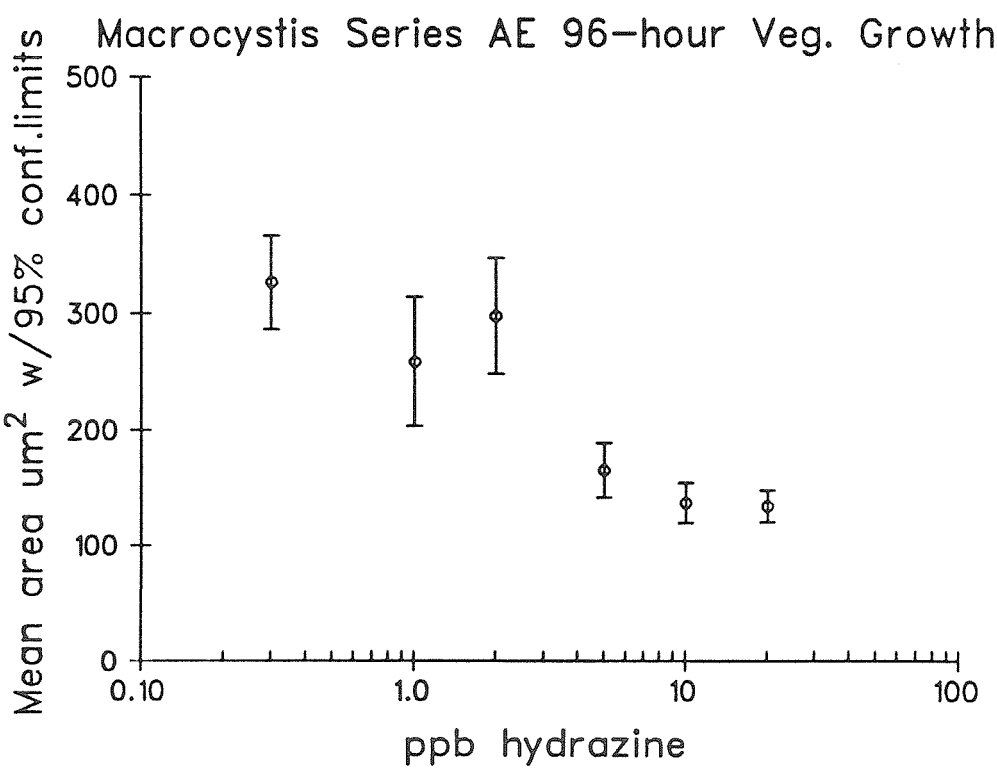

Figure 4.A.5: Macrocystis pyrifera; Series AF and AG growth inhibition in hydrazine. Mean gametophyte area ± 95 percent confidence limits after 120 hours continuous exposure in indicated concentrations.

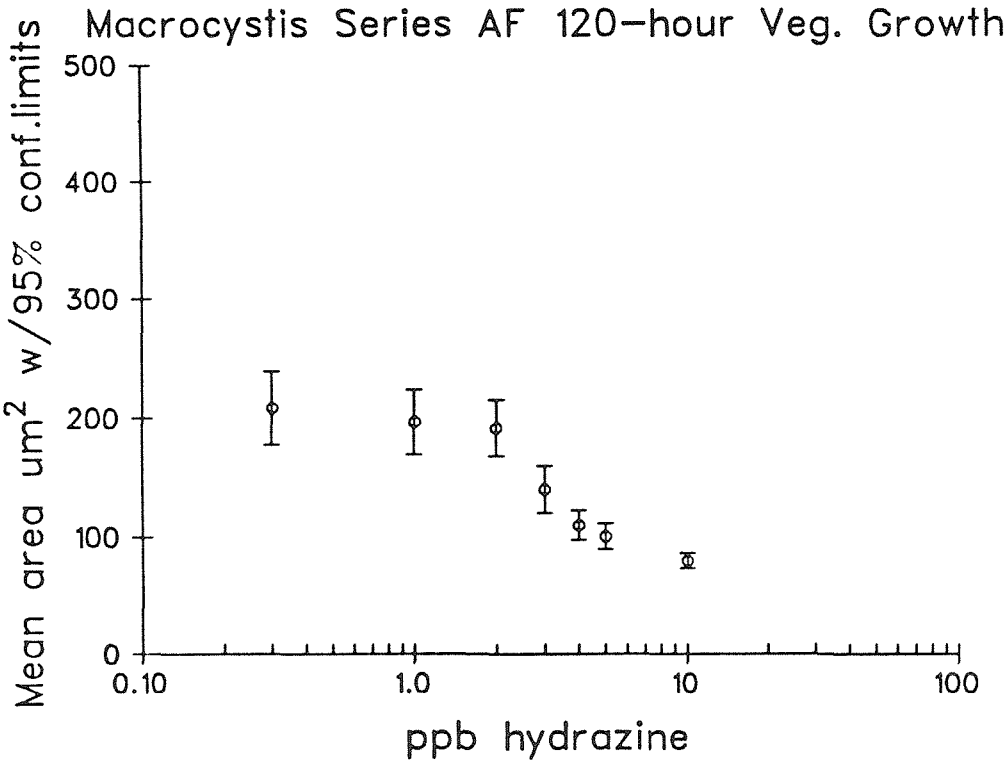

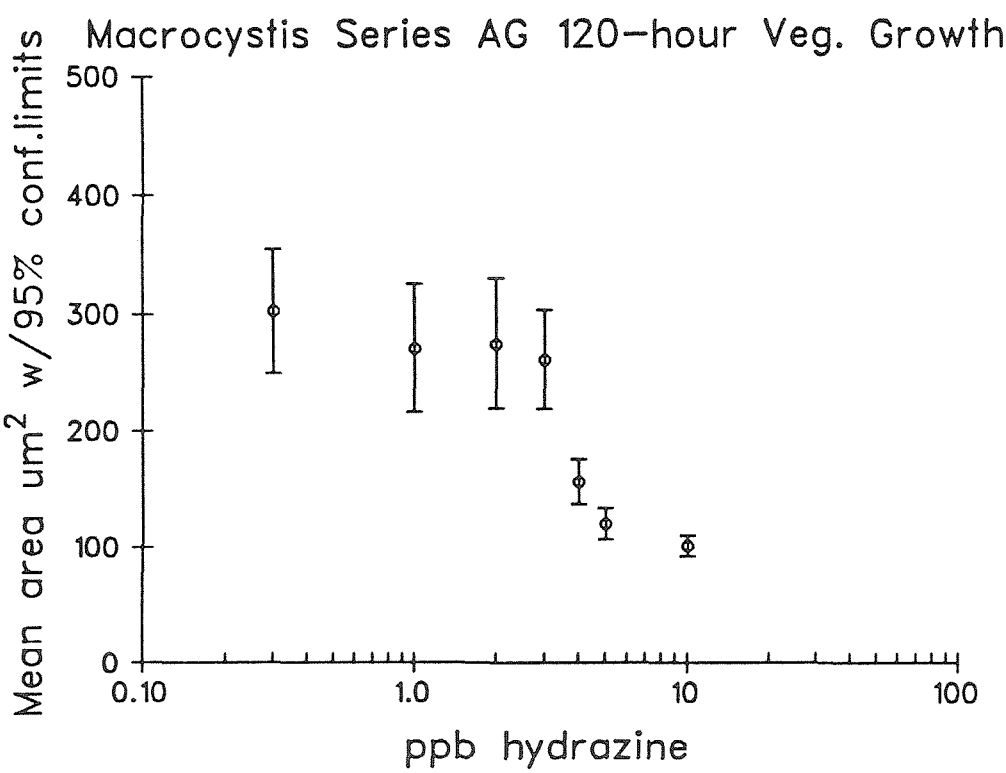

CHAPTER 5: HYDRAZINE EMISSIONS AND SEAWATER CHEMISTRY

I. INTRODUCTION AND BACKGROUND

The high toxicity exhibited by hydrazine in preliminary screening assays prompted questions about its chemistry and emissions.

1) Is the compound emitted in sufficient quantities to cause harm?

2) Does hydrazine last long enough in seawater to reach target organisms?

Hydrazine, N_2H_4 (molecular weight 32.05) has been widely used for industrial purposes since the late 19th century (Schmidt, 1984). It is a common reducing agent in industrial chemical reactions and is used in methyl-substituted form in combination with fuming nitric acid as a hypergolic rocket propellant (Kirk-Othmer, 1978). The compound is used extensively for corrosion control in high-pressure steam circuits of marine propulsion and steam-electric power-generation systems (Institute of Marine Engineers, 1978; Babcock and Wilcox, 1978).

The pure compound is a liquid at atmospheric pressures and temperatures with physical properties similar to water (Schmidt, 1984):

Boiling point: 114°C, Density at 20°C: 1.007,

Melting point: 2°C.

Hydrazine is flammable in air. It is often sold blended with water as hydrazine-hydrate for safer handling (AtoChem, Inc. 1986) and is also available in solid form as salts of inorganic acids, $N_2H_4 \cdot 2HCl$ and $N_2H_4 \cdot H_2SO_4$. Hydrazine has been used in algaecides, insecticides and fungicides (Kirk-Othmer, 1978; Audrieth and Ogg, 1951) and as a

probe of photosynthetic mechanisms in plants (Heath, 1971). It is highly toxic, with vapor limits of 0.03 ppm (0.04 mg/m^3) for a 2-hour exposure (NIOSH 1978; cited in Sittig, 1985) and is a known carcinogen (Hathaway, 1984).

II. USE OF HYDRAZINE IN ELECTRIC GENERATING STATIONS

Hydrazine was first used to deoxygenate boiler waters of steam-electric powerplants during the early 1950's (Baker and Marcy, 1956). It is currently the preferred method for the high-pressure (> 1300 psi) systems used in modern fossil-fueled and nuclear powerplants (Schmidt, 1984, Babcock and Wilcox, 1978). The alternative method is deoxygenation with sodium sulfite, Na_2SO_3. Sodium sulfite is still used in lower-pressure systems, but in high-pressure systems it increases nonvolatile solids content of steam to levels that cause scale deposits, thereby reducing heat-transfer efficiency.
Reaction of hydrazine with molecular oxygen follows the overall stoichiometry:

$$N_2H_4 + O_2 \text{ <--> } N_2 + 2H_2O. \qquad (5.1)$$

The compound is used as 35 percent solution in water with 0.2-0.8 percent proprietary organometallic catalyst containing Co^{+2}.
Catalyzed hydrazine, called Scav-Ox (Olin Chemical Corp) or Amerizine (Drew Chemical Company), reacts rapidly with molecular oxygen at temperatures exceeding 90° Celsius. The compound is metered with automated monitoring equipment into condenser make-up water after mechanical de-aeration (Figure 5.1). A stoichiometric excess ranging from 20 to 400 ppb is usually maintained in the steam circuit

Figure 5.1: Hydrazine Injection and Discharge in Pressurized Light-Water Reactor Circuits. (Repeat of Figure 4.2)

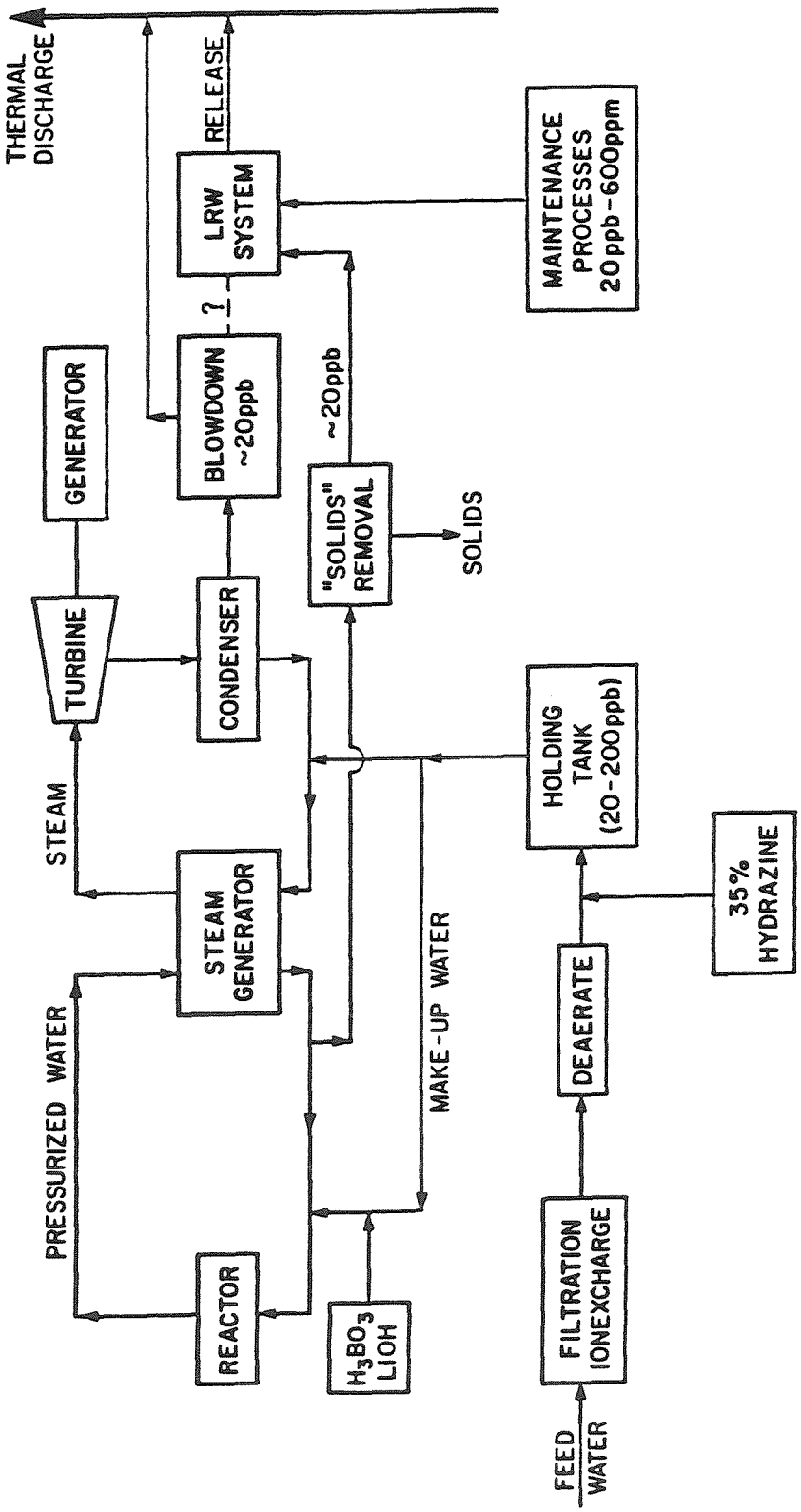

Simplified Schematic Of Hydrazine Injection And Discharge In Pressurized Light-Water Reactor Circuits.

(Schmidt, 1984, Babcock and Wilcox, 1978). Excess hydrazine disproportionates at boiler temperatures and pressures to ammonia and nitrogen.

Trace amounts of hydrazine are released into the cooling water discharge when condensed steam is "blown-down" at the condenser hotwell (Figure 5.1). Blow-down is partial removal of condensate with replacement by fresh, demineralized make-up water to maintain dissolved solids concentrations at constant low levels. Dissolved solids concentrations rise during boiler operation as material erodes from boiler, turbine and heat-exchanger surfaces at typical 500-1000°C temperatures and 1600-2800 psi pressures common in modern steam circuits. Representative operating limits for nonvolatile dissolved solids in these conditions are 0.05-0.20 ppm. Foaming of condensate and formation of scale on boiler and condenser surfaces could occur if total dissolved solids (TDS) concentrations were allowed to increase beyond these values, inhibiting heat transfer rates and reducing power generation efficiency (Babcock and Wilcox, 1978).

Frequency and duration of hydrazine discharges during blow-down depends on schedules followed by power-plant operators. Some installations blow-down large volumes several times a day. Others may remove condensate and add new make up water continuously (Skrotzki and Vopat, 1960). Schmidt (1984) described a fossil-fueled power plant on Lake Charles, Louisiana, that consumed 74 pounds of hydrazine a day while continuously making-up 560,000 pounds of water per hour with a 300 parts per billion (ppb) hydrazine residual,

translating to release of 1.344 million gallons per day (MGD) of blow-down effluent with a somewhat lower residual. Units 2 and 3 of the San Onofre Nuclear Generating Station (SONGS) continuously blow-down 0.72 MGD of secondary condensate into a daily cooling water discharge volume of 2792 MGD (Southern California Edison Company, 1986). Units 1 and 2 of the Diablo Canyon Power Plant (DCPP) continuously release 0.65 MGD condensate directly into the main cooling water discharge with a daily volume of 2540 MGD (California Water Quality Control Board, Central Coast Region, 1985). Assuming complete mixing, dilutions of this type of discharge are about 1 part condensate to 4000 parts cooling water (1:4000).

Hydrazine is also used in maintenance processes inside power-plants (Babcock and Wilcox, 1978; California Water Quality Control Board, 1985, Schmidt, 1984). Cleaning operations to remove scale and corrosion use solutions composed of dilute acid, surfactants, and up to 1000 parts per million (ppm) total hydrazine (Babcock and Wilcox, 1978). Boiler surfaces exposed to air may corrode during cleaning. Wetting the surfaces with a hydrazine solution inhibits corrosion and promotes conversion of any extant red iron oxide (hematite, Fe_2O_3, which has poor heat transfer properties), into black iron oxide (magnetite), Fe_3O_4, which has good heat transfer characteristics (Babcock and Wilcox, 1978, Institute of Marine Engineers, 1978).

Hydrazine is employed during short-term storage (layup) of an entire boiler. Wet-layup of a boiler is the preferred method for shutdown periods of a few months or less. A boiler is filled under a blanket of nitrogen gas with a passivating solution composed of

demineralized water, ammonia for pH control and 100-500 ppm hydrazine (Babcock and Wilcox, 1978) to minimize corrosion and scale formation during storage.

Hydrazinated cleaning and passivating solutions are released to waste-holding tanks, analyzed, treated and released into the cooling-water discharge. Characteristic discharge volumes are 10,000-50,000 gallons. Release schedules depend on maintenance procedures inside the plant. In nuclear powerplants, reactors are refueled every 1.5 to 2 years. A power-plant operating two or more generating units on staggered maintenance schedules may release storage and cleaning solutions containing high hydrazine concentrations at least once a year.

III. POWER-PLANT EMISSIONS

A. DATA COLLECTION AND REPORTING METHODOLOGY

Hydrazine emission data for 1984-87 were obtained from State-required Q2 forms filed monthly by nuclear power-plant operators with California Regional Water Quality Control Boards[1,2]. Data were obtained for Units 1,2 and 3 of the San Onofre Nuclear Generating Station (SONGS; operated by Southern California Edison Company, located near San Clemente in southern California) and for Units 1 and 2 of the Diablo Canyon Power Plant (DCPP; Pacific Gas and

---

[1]California currently requires only nuclear power plants to report hydrazine emissions. Discussions of boiler operations in Schmidt (1984), and Babcock and Wilcox (1978) indicate that hydrazine is used in similar ways in modern high-efficiency fossil-fueled generating stations.

[2]The forms are filed to comply with National Pollutant Discharge Elimination System (NPDES) requirements.

Electric Company) near San Luis Obispo in central California. Hydrazine usage should be similar in fossil stations fitted with high-pressure steam equipment (Institute of Marine Engineers, 1978; Babcock and Wilcox, 1978, Schmidt, 1984), but hydrazine emissions from these stations are not currently reported.

Frequency distributions of power-plant hydrazine emissions are not the result of independent, random, natural processes but are combined artifacts of NPDES permit-mandated sampling frequencies and discharge schedules which reflect specific, unique operational events inside each power station. DCPP and SONGS were subject to different reporting requirements. DCPP was required to report all hydrazine releases from the LRW system between January 1982 and October 1986. After October 1986, this reporting requirement was changed to one sample a month. SONGS has been required to report one value per month for each operating Unit from January 1984 through December 1987. DCPP data were sampled for peak monthly values to permit comparison of DCPP and SONGS peak emissions frequencies. SONGS data were reported already diluted by the main discharge. DCPP data were reported as concentrations in waste-holding tanks before release to the main discharge and were adjusted by assuming complete mixing and calculating dilution as the ratio of reported flow rate from the waste-holding tanks (25 gallons per minute) to the flow rate in the cooling water discharge at the time of release.

The lack of daily discharge data combined with known daily blow-down schedules for SONGS and DCPP suggests that releases of hydrazine residuals resulting from routine blow-down of deoxygenated steam

generator condensate are not reported to regulatory agencies. At estimated within-plant dilution factors of 1:4000, the 20-60 ppb (640-1920 nanomolar) residual concentrations in blow-down would be diluted to 5-15 parts per trillion (0.160-0.480 nM) in the cooling-water discharge before release to the environment. Low concentrations of hydrazine in blow-down do not contribute significantly to final concentration values in the discharge, but may be a significant portion of the annual total mass emitted from the plant.

The pattern of actual hydrazine emissions at the two studied power-plants is probably a constant low "background" (part per trillion, subnanomolar) value (originating from condenser blow-down) punctuated with spikes caused by episodic releases from waste-holding tanks during maintenance activities (California Regional Water Quality Control Board, Central Coast Region, 1985).

B. DIABLO CANYON POWER-PLANT EMISSIONS

The common outfall for DCPP Units 1 and 2 discharges water across the beach into Diablo Cove (Figure 4.1). The plume of discharged water takes the form of a laterally spreading buoyant near-surface jet. Estimated average dilution factors at the Cove entrances were 3:1 to 5:1 (Tu, 1986), but plume dilution varies with location in the Cove and fluctuates with weather and sea conditions.

Most DCPP emissions were low, but several large releases (Table 5.1, Figure 5.2) skewed distributions to the right and caused unrealistically large standard deviations when the untransformed data were used to compute arithmetic means and variances. Zeroes in Table 5.1 indicated either values below the limit of detection or

Table 5.1: DCPP Monthly Hydrazine Emissions; 1982-1984: 001D is the designation of the discharge line from the Liquid Radioactive Waste Treatment System (see text). 001 is the designation of the main thermal discharge. Concentrations in 001 calculated assuming 25 gpm flow from 001D and complete mixing.

YEAR	MONTH	Hydrazine Concentrations diluted 001D peaks in 001	PEAK 001D	Monthly avg 001D	001 flow (MGD) on day of peak 001D discharge
1982	Jan	.00 ppb	.00 ppm	.00 ppm	15.86
	Feb	.00	.00	.00	15.87
	Mar	.00	.00	.00	15.71
	Apr	.00	.00	.00	15.45
	May	.00	.00	.00	59.92
	Jun	.00	.00	.00	30.44
	Jul	.00	.00	.00	12.46
	Aug	.00	.00	.00	13.54
	Sep	.00	.00	.00	15.07
	Oct	.08	.01	.01	4.32
	Nov	1.67	.20	.02	4.32
	Dec	.05	.01	.01	7.92
1983	Jan	1.27	.56	.11	15.84
	Feb	.34	.15	.04	15.89
	Mar	.01	.00	.00	15.85
	Apr	.00	.00	.00	15.87
	May	.10	.04	.02	15.87
	Jun	.00	.00	.00	15.23
	Jul	.00	.00	.00	20.70
	Aug	10.91	9.60	2.00	31.69
	Sep	2.27	1.00	.00	15.84
	Oct	.00	.00	.00	15.84
	Nov	.02	.02	.00	31.68
	Dec	.00	.00	.00	31.69
1984	Jan	2.27	1.00	.00	15.84
	Feb	.11	2.00	1.00	626.44
	Mar	.59	10.00	1.00	610.60
	Apr	164.83	132.00	14.00	28.83
	May	118.79	580.00	18.00	175.77
	Jun	4.60	80.00	19.00	626.40
	Jul	6.15	107.00	14.00	626.58
	Aug	1.55	27.00	3.60	626.00
	Sep	2.12	35.00	13.00	595.00
	Oct	.72	12.40	2.43	620.00
	Nov	20.36	345.00	53.50	610.00
	Dec	.54 ppb	19.20 ppm	1.23 ppm	1270.00

Table 5.1 (cont): DCPP Monthly Hydrazine Emissions; 1985-1987. 001D is the designation of the discharge line from the Liquid Radioactive Waste Treatment System (see text). 001 is the designation of the main thermal discharge. Concentrations in 001 calculated assuming 25 gpm flow from 001D and complete mixing.

YEAR	MONTH	Hydrazine Concentrations diluted 001D peaks in 001	PEAK 001D	Monthly avg 001D	001 flow (MGD) on day of peak 001D discharge
1985	Jan	61.20 ppb	34.00 ppm	5.80 ppm	20.00 MGD
	Feb	.61	12.00	1.51	703.00
	Mar	9.52	320.00	20.30	1210.00
	Apr	22.21	29.00	3.10	47.00
	May	.30	10.00	.88	1207.00
	Jun	1.43	48.00	3.37	1210.00
	Jul	.02	.70	.10	1250.00
	Aug	1.29	65.00	7.20	1810.00
	Sep	3.60	110.00	7.50	1100.00
	Oct	.58	40.10	2.64	2510.00
	Nov	.02	.55	.06	1310.00
	Dec	.04	2.56	.04	2460.00
1986	Jan	2.34	78.50	7.55	1210.00
	Feb	.13	6.50	1.14	1830.00
	Mar	.07	5.02	0.42	2460.00
	Apr	.02	1.50	0.12	2450.00
	May	.00	.07	0.03	2454.00
	Jun	.56	38.00	2.09	2454.00
	Jul	.05	2.40	0.17	1830.00
	Aug	.00	.09	0.03	2454.00
	Sep	.25	4.25	0.92	623.00
	Oct	.43	15.00	1.06	1247.00
	Nov	.69	24.00	24.00*	1247.00
	Dec	.00	.01	.01*	1417.00
1987	Jan	.01	.50	.50*	2359.00
	Feb	.00	.02	.02*	2400.00
	Mar	.00	.01	.01*	2455.00
	Apr	.00	.01	.01*	1358.00
	May	.01	.42	.42*	1118.00
	Jun	.04	1.60	1.60*	1583.00
	Jul	.00	.11	.11*	2254.00
	Aug	.00	.01	.01*	2442.00
	Sep	.00	.03	.03*	2471.00
	Oct	.00	.05	.05*	2436.00
	Nov	.00	.18	.18*	2336.00
	Dec	.00 ppb	.05 ppm	.05*ppm	2342.00 MGD

NOTE: * Only one grab sample reported per month. Earlier figures are from daily monitoring.

Figure 5.2: Monthly peak emissions from Diablo Canyon Nuclear Power Plant. Calculated assuming 25 gpm flow of LRW holding tank into thermal discharge with complete mixing in discharge structure and no dilution by receiving waters

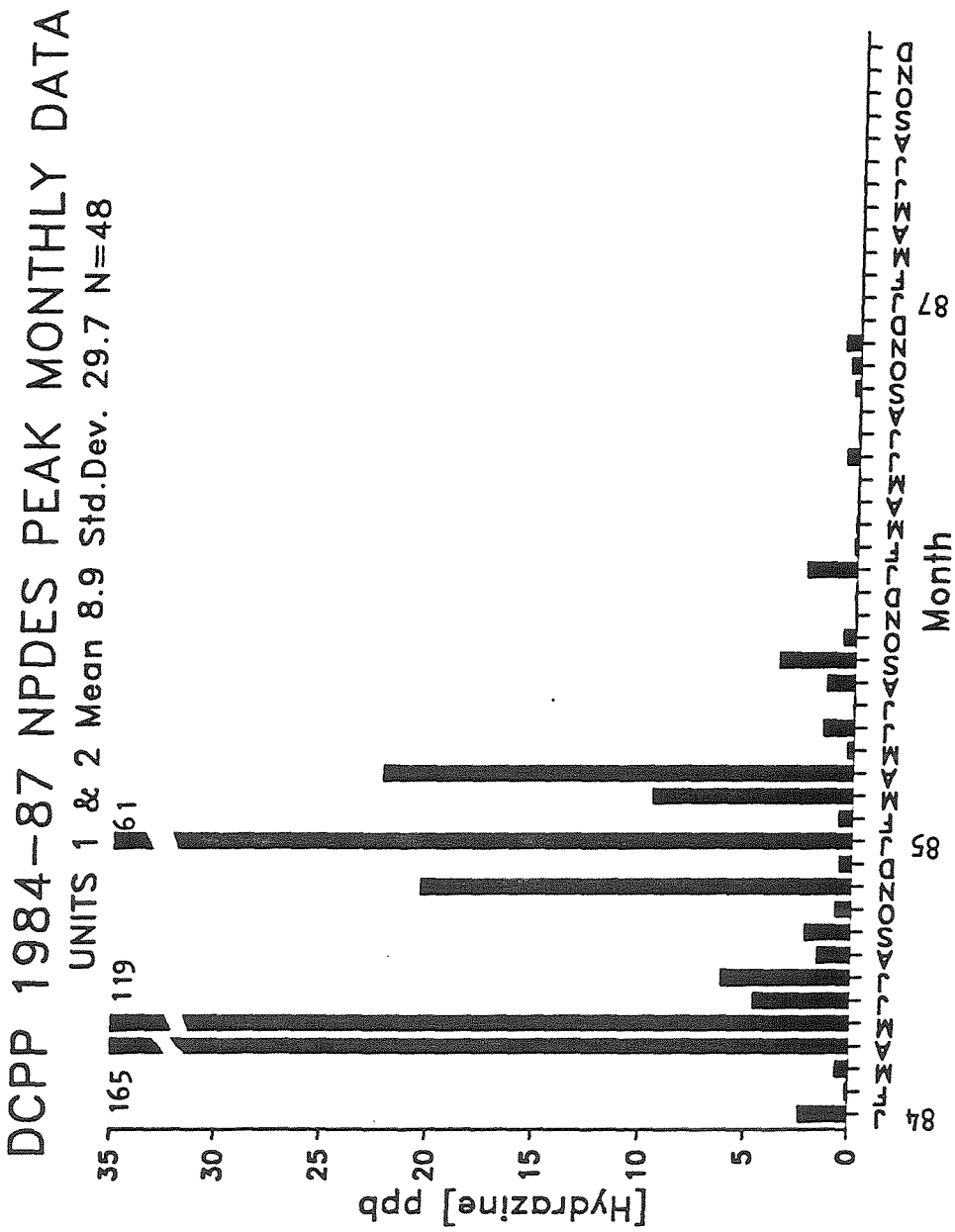

Figure 5.3A: Frequency distribution of peak undiluted monthly emissions from Diablo Canyon Power Plant.

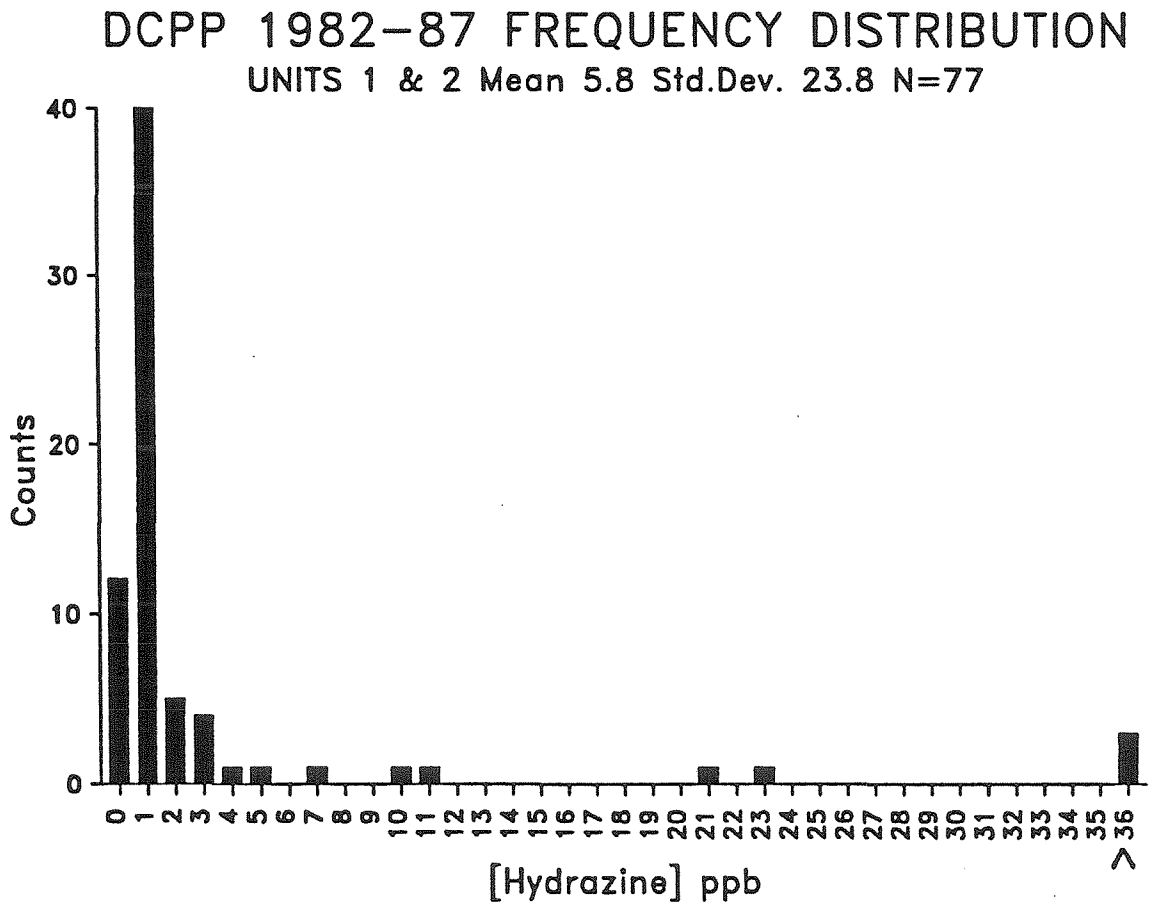

missing data. Mean concentration for all peak discharges between 1982 and December 1987 was 5.8 ± 23.8 ppb. The calculated mean for January 1984 to December 1987 data (computed to permit direct comparison to data for SONGS) was 8.9 ± 27.0 ppb. The median value determined from the frequency distribution (Figure 5.3A) was 1 ppb. The cumulative frequency distribution (Figure 5.3B) for these data showed that the 90th percentile value was 6 ppb (10 percent of the discharges exeeded 6 ppb). The 95th percentile value was 21 ppb.

DCPP records showed eight peak hydrazine emissions exceeding the 5 ppb upper bound for significant inhibition of Macrocystis pyrifera gametophyte vegetative growth (Table 5.2). The April and May, 1984

Table 5.2: Hydrazine emissions exceeding 5 ppb at Diablo Canyon estimated at point-of-discharge from holding tank concentrations and ratio of tank flow rate to main discharge flow rate.

YEAR	Concentration and month of occurrence of each event			
1983	11 ppb, August			
1984	165 ppb, April	119 ppb, May	6 ppb, July	20 ppb, Nov.
1985	61 ppb, Jan	9 ppb, March	22 ppb, April	

and January 1985 spikes occurred during known low-flow periods and may have arisen from dump of either cleaning or passivating solutions into the cooling water discharge during maintenance, refueling or restart of Unit 1[3].

[3]Unit 1 of DCPP went critical on April 29, 1984, commenced low-power testing October 18, 1984 and began commercial power generation in May 1985.

Figure 5.3B: Cumulative distribution of data in Figure 5.3A. Line is fourth-order polynomial fit to data.

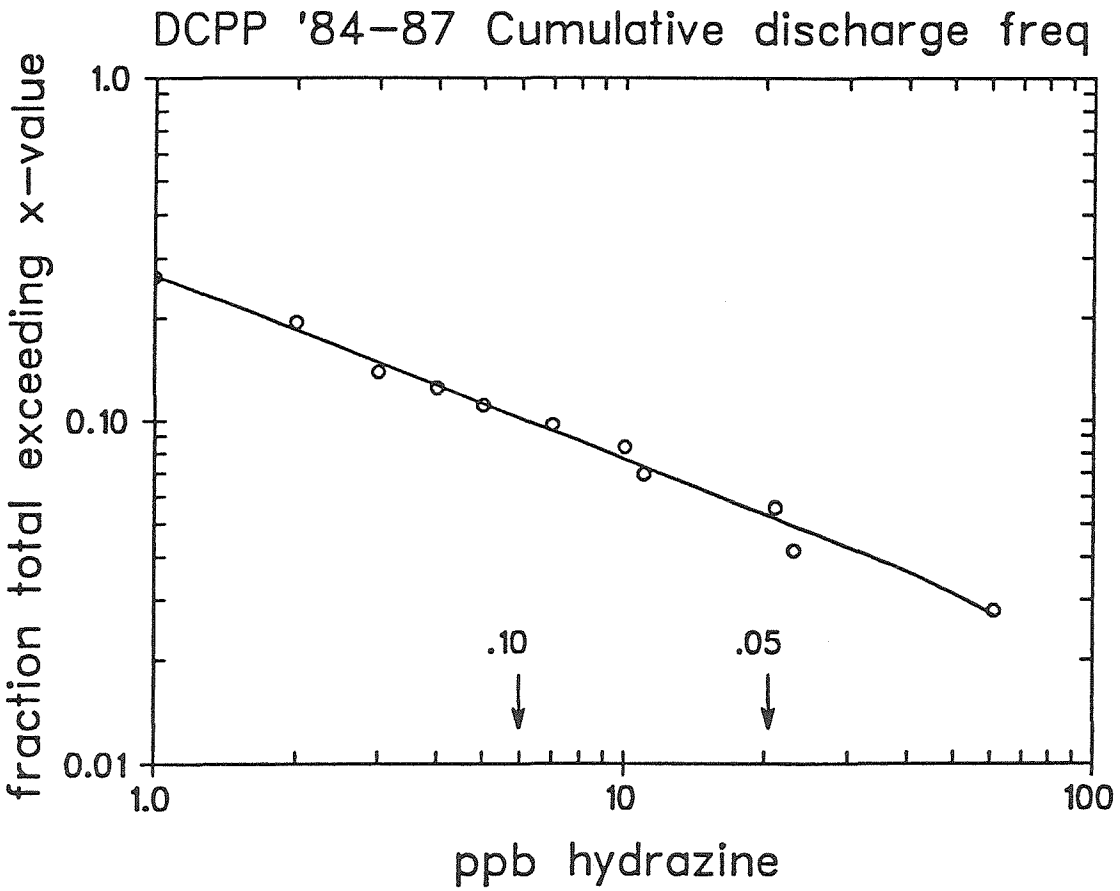

Figure 5.4: Example of annual emissions pattern. Data assume complete mixing within discharge and no dilution by receiving waters.

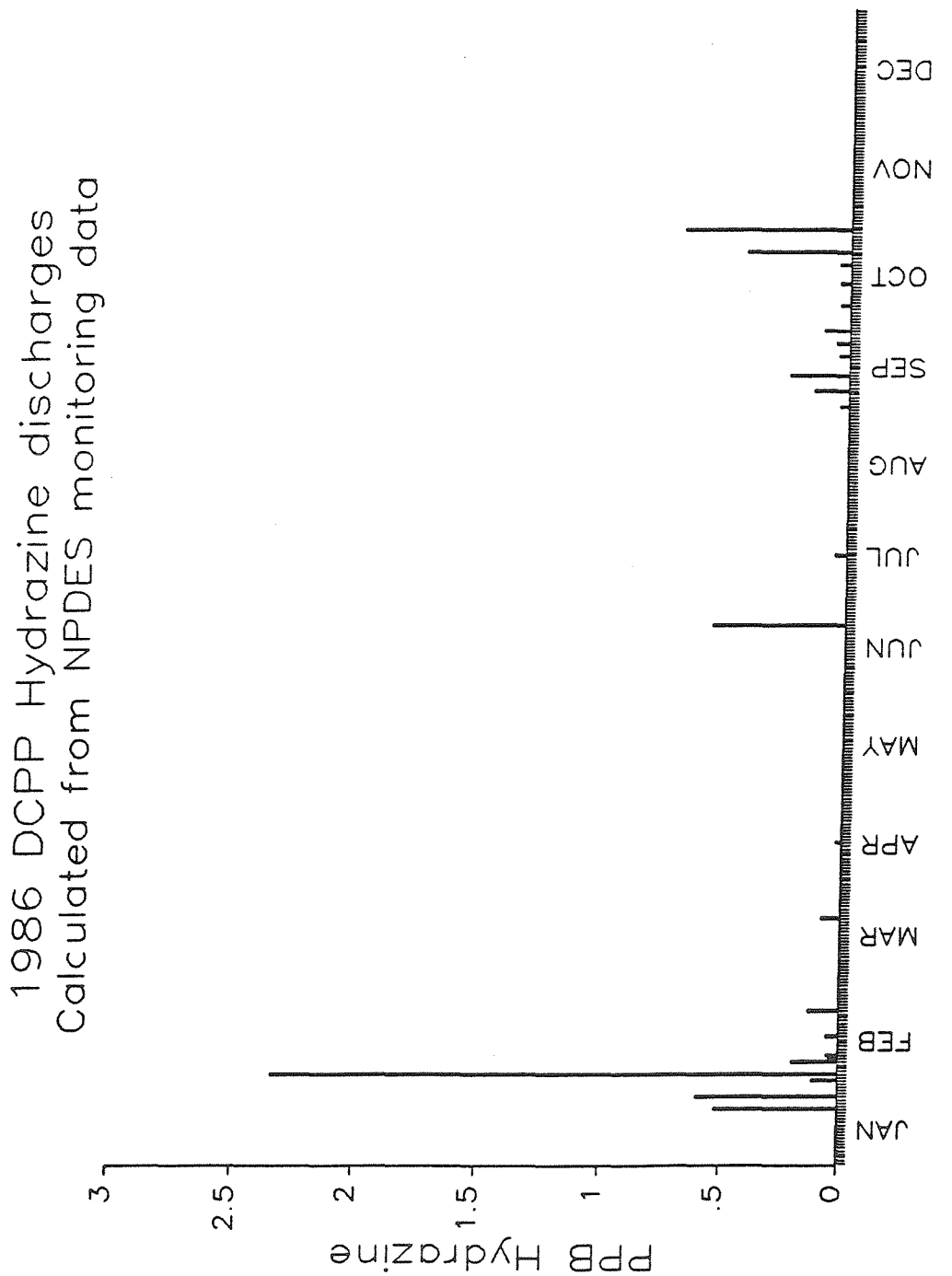

Table 5.3: Major Calendar Year 1986 Hydrazine Releases from Diablo Canyon Power Plant. Discharges less than 0.02 ppb not tabulated.

1986 Day #	Mains Flow MGD	Holding Tank (LRW system) Flow gpm	N_2H_4 ppm	Mains Flow gpm	Dilution Factor: Mains flow / LRW flow	Estimated Mixed $[N_2H_4]$ in Outfall ppb
18	1210	25	17.50	840,300	33,610	0.52
22	1210	25	20.00	840,300	33,610	0.60
27	1210	25	3.60	840,300	33,610	0.11
29	1210	25	78.50	840,300	33,610	2.34 MAX
33	1130	25	6.00	784,700	31,390	0.19
34	1210	25	1.29	840,300	33,610	0.04
35	1210	25	1.60	840,300	33,610	0.05
41	1830	25	2.54	1271,000	50,830	0.05
49	1830	25	6.50	1271,000	50,830	0.13
78	2460	25	5.02	1708,000	68,330	0.07
102	2450	25	1.50	1701,000	68,060	0.02
171	2454	25	38.00	1704,000	68,170	0.56
193	1830	25	2.40	1271,000	50,830	0.05
240	1247	25	1.15	866,000	34,640	0.03
245	1247	25	5.00	866,000	34,640	0.14
250	623	25	4.25	432,600	17,310	0.25
256	1247	25	1.35	866,000	34,640	0.04
260	1247	25	1.84	866,000	34,640	0.05
264	1247	25	3.60	866,000	34,640	0.10
272	1247	25	1.33	866,000	34,640	0.04
279	1247	25	1.36	866,000	34,640	0.04
285	1247	25	1.47	866,000	34,640	0.04
289	1247	25	15.00	866,000	34,640	0.43
296	1247	25	24.00	866,000	34,640	0.69

Data for the entire calendar year 1986 show that hydrazine releases occurred in clusters (Figure 5.4, Table 5.3). None of the releases exceeded 2.3 ppb (if the assumed 25 gallon-per-minute flow rate is correct). Most of the releases were less than 0.2 ppb.

C. SAN ONOFRE NUCLEAR GENERATING STATION EMISSIONS

The outfalls for SONGS Units 2 and 3 discharge 105 m^3/second (2792 MGD) effluent via 63-port diffusers into 32-38 feet (Unit 3) and 40-50 feet water (Unit 2) with a design delta T of 2.2°C at shoreline, on the bottom or 1000 feet beyond the discharge structure (Fischer et al., 1979, Grove, 1987). Unit 1 discharges 22 m^3/second (460 MGD) from a single pipe as a surface buoyant plume into 25-foot depths.

Summary statistics computed for NPDES-mandated monthly hydrazine grab samples over the January 1984 to December 1987 period for each San Onofre Nuclear Generating Station Unit showed means of 4.8, 4.0 and 5.6 ppb for Units 1,2 and 3, respectively (Figure 5.5 and Table 5.4). Large reported standard deviations were again caused by skewed data. Blanks in the table had three origins:

1) Several entries in the NPDES reports indicated "data not available," cause unspecified.

2) Generating units were periodically shut down for maintenance.

3) Readings for some samples (shown as <1 in Table 5.4 and omitted from Figure 5.5) were below the analytical detection limit.

Values below the analytical detection limit were excluded when summary statistics for each Unit were calculated.

Table 5.4: Peak Monthly Hydrazine Emissions from San Onofre Nuclear Generating Station, 1984-87. Blanks indicate no data available. Reported as concentration (ppb) in thermal outfall

YEAR	MONTH	Unit 1	Unit 2	Unit 3
1984	Jan	2	2	7
	Feb	< 1	< 1	11
	Mar	< 1	< 1	1
	Apr	5	3	4
	May	10		
	Jun		2	1
	Jul			
	Aug		20	10
	Sep		< 1	4
	Oct	< 1		
	Nov	< 1		< 1
	Dec	8		
1985	Jan	4		3
	Feb	4	5	6
	Mar	2	1	2
	Apr	5	4	12
	May	1	1	2
	Jun	< 1	1	1
	Jul	< 1	< 1	< 1
	Aug	4	5	5
	Sep	3	7	6
	Oct	2	3	
	Nov	< 1	< 1	
	Dec	4	4	5
1986	Jan	< 1	< 1	< 1
	Feb	< 1	< 1	4
	Mar	6	3	5
	Apr	8		2
	May	3		6
	Jun	5	5	4
	Jul	< 1	< 1	< 1
	Aug	< 1	< 1	< 1
	Sep	< 1	< 1	< 1
	Oct	2	5	35
	Nov	3	4	4
	Dec	1	< 1	< 1
1987	Jan	6	6	
	Feb	4	3	
	Mar	1	1	2
	Apr	30	< 1	< 1
	May	< 1	< 1	< 1
	Jun	7	< 1	< 1
	Jul	1	5	3
	Aug	5	3	< 1
	Sep	< 1		< 1
	Oct	1		5
	Nov	3	1	1
	Dec	4	3	7

Notes:
< 1 means below detection limit

Summary statistics

Unit#	Mean	Std.dev.	N
1	4.8	5.2	30
2	4.0	3.7	24
3	5.6	6.3	28

Grand Mean	Grand Std.dev.	N
4.9	5.3	82

Figure 5.5: Peak monthly undiluted emissions from San Onofre Nuclear Generating Station Units 1,2 and 3.

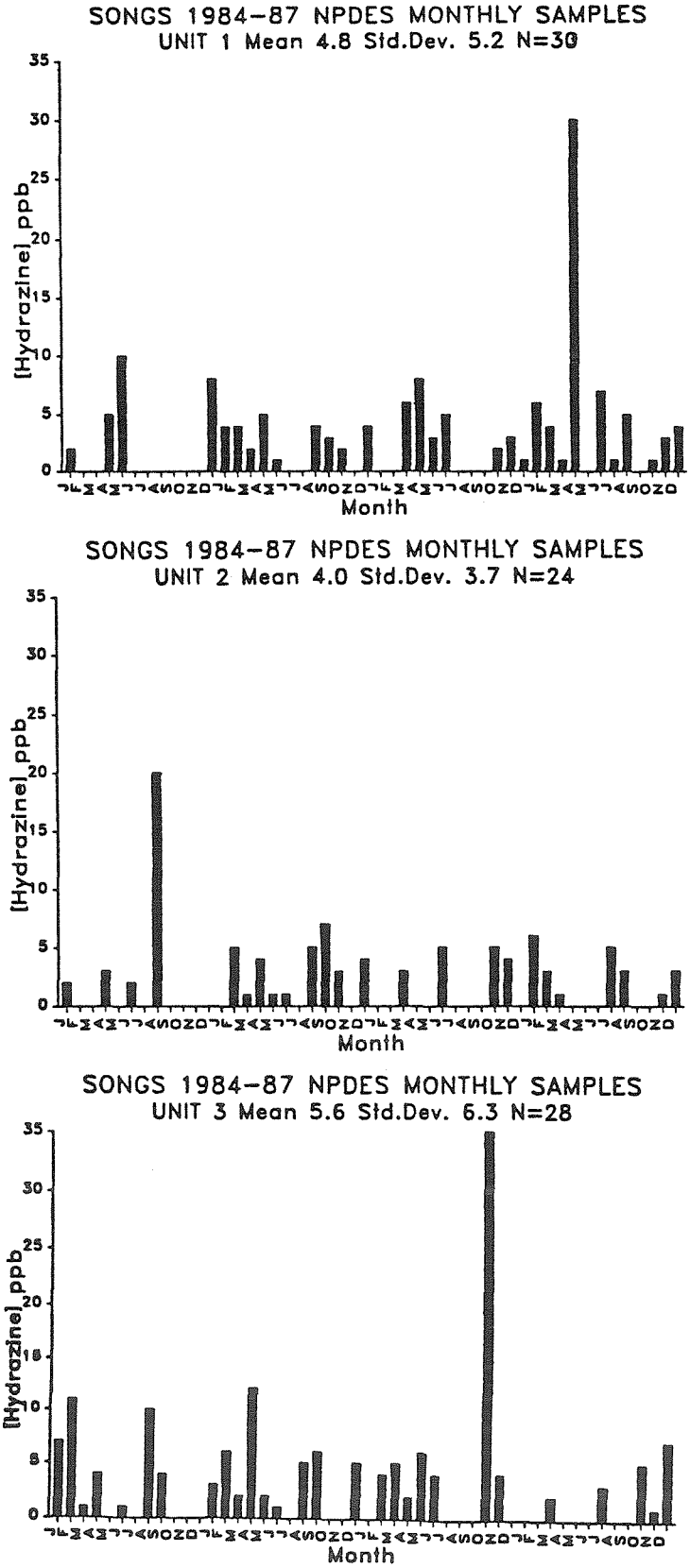

Assuming that NPDES values accurately reflect hydrazine concentrations in the cooling water discharge, each SONGS Unit showed several before-dilution emissions exceeding the 5 ppb upper bound reported in Chapter 4 for significant inhibition of Macrocystis pyrifera gametophyte vegetative growth (Table 5.5).

Table 5.5: Hydrazine emissions exceeding 5 ppb at San Onofre reported by Southern Calif. Edison as value at point of discharge. Value in cooling discharge estimated from measurement in waste-stream discharge line.

SONGS #	Concentration and date of occurrence of event						
UNIT 1	10 ppb, 5/84	8 ppb, 12/84	6 ppb, 3/86	8 ppb, 4/86	6 ppb, 12/86	30 ppb 4/87	
UNIT 2	20 ppb, 8/84	7 ppb, 9/84	6 ppb 12/86				
UNIT 3	7 ppb, 1/84	11 ppb, 2/84	10 ppb, 8/84	6 ppb, 2/85	12 ppb, 4/85	6 ppb, 9/85	6 ppb, 5/86
UNIT 3 (cont)	35 ppb, 10/86	7 ppb 12/86					

When data for all three Units were pooled into a combined frequency distribution (Figure 5.6), the mean released concentration (excluding values below the detection limit) was 4.9 $\pm$ 5.3 ppb. The median value, including values below the detection limit (Figure 5.6) was less than 1 ppb, below the lower bound for significant vegetative growth inhibition of Macrocystis gametophytes in continuous assays (Chapter 4). The 90th percentile concentration was 8 ppb. The 95th percentile value was 12 ppb.

Discharge patterns from DCPP and SONGS may reflect varying operating conditions and changes in maintenance practices inside the generating stations. Comparison of SONGS Units 2 and 3 with DCPP

Figure 5.6A: Frequency distribution for peak monthly data shown in Figure 5.5.

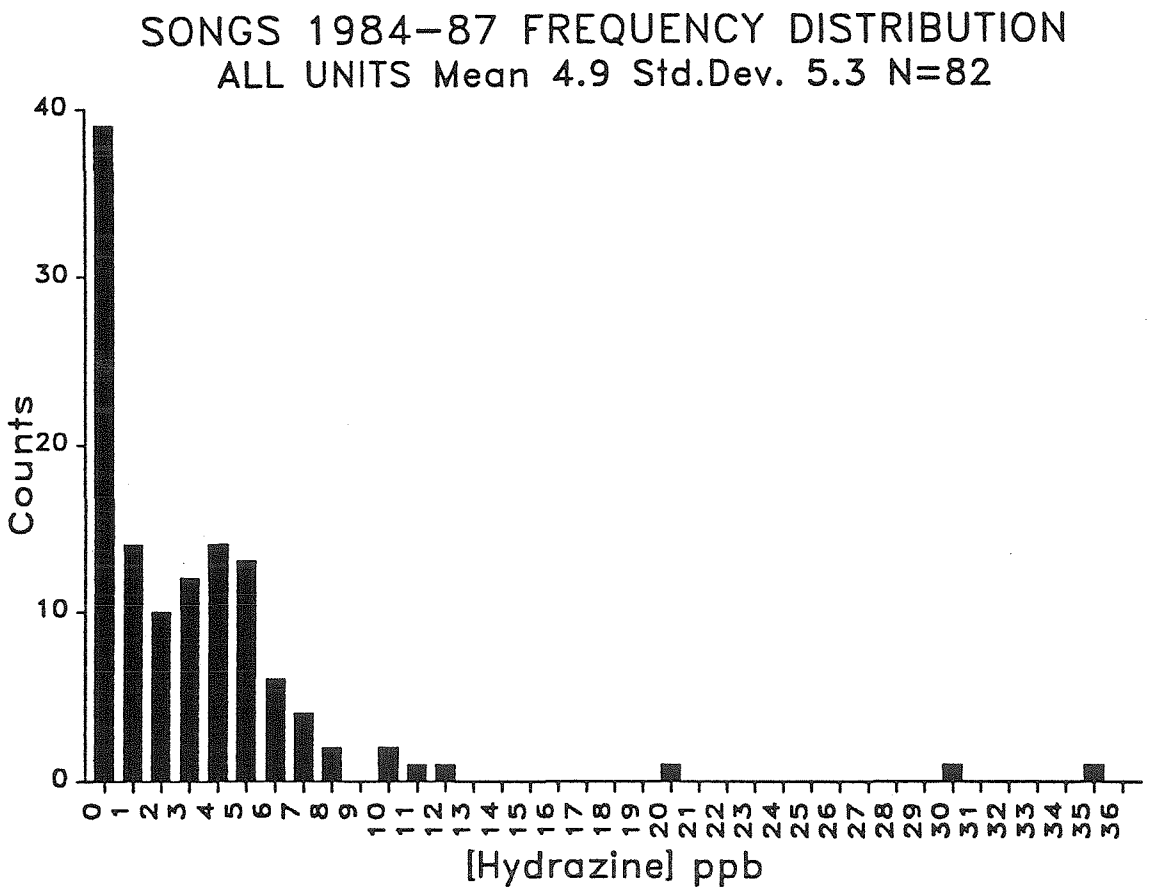

Figure 5.6B: Cumulative distribution of data in Figure 5.6A. Line is sixth-order polynomial fit to data.

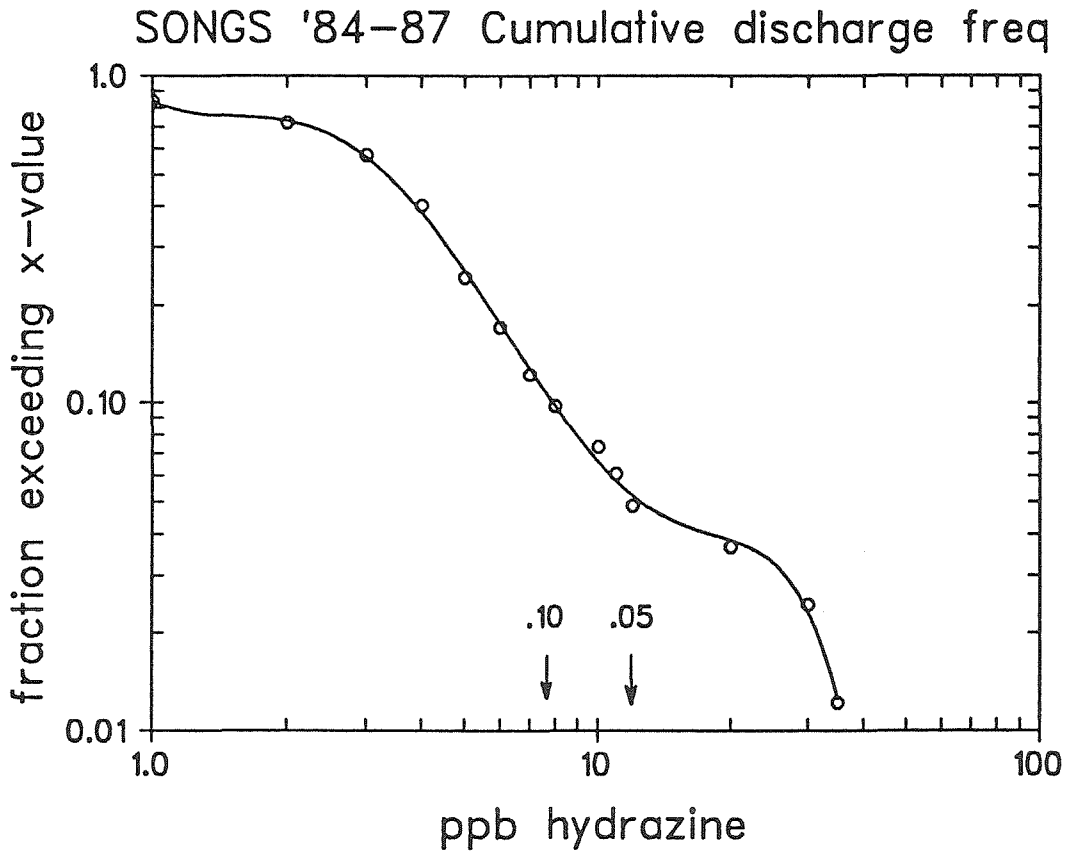

Units 1 and 2 shows that during the 1984-87 calendar year period, SONGS had 12 events exceeding 5 ppb hydrazine. DCPP had 8 events, but released 4 of the 5 highest tabulated values. DCPP emissions appear to be declining with time. Emissions decreased in each of the calendar years 1985, 1986 and 1987. This could be due to an end in activities associated with powerplant start-up but may also be an artifact of the change in reporting methodology.

IV. HYDRAZINE CHEMISTRY IN SEAWATER

A. HYDRAZINE SPECIATION IN SEAWATER

(1) Effect of pH and temperature

The role of fluctuations in seawater temperature and pH in determining hydrazine speciation was investigated using simple equilibrium relationships.

Mass balance:

$$[N_2H_4]_T = [N_2H_4] + [N_2H_5^+], \tag{5.2}$$

which rearranges to:

$$[N_2H_5^+]/[N_2H_4]_T = [N_2H_5^+]/([N_2H_4] + [N_2H_5^+]), \tag{5.3}$$

and is redefined as:

$$\text{fraction } [N_2H_5^+] = 1/([N_2H_4]/[N_2H_5^+] + 1). \tag{5.4}$$

The equilibrium relationship for the reaction:

$$N_2H_4 + H^+ = N_2H_5^+, \tag{5.5A}$$

is represented by:

$$\frac{\{N_2H_4\}\cdot\{H^+\}}{\{N_2H_5^+\}} = K \tag{5.5B}$$

where K is the numerical equilibrium constant for the reaction and

the quantities in braces, { }, are the activities of aqueous-phase reactants and products.

Equation (5.5B) rearranges to:

$$[N_2H_4]/[N_2H_5^+] = Kg_1/\{H+\}g_0, \qquad (5.6)$$

where $\{N_2H_4\} = g_0[N_2H_4]$ and $\{N_2H_5^+\} = g_1[N_2H_5^+]$, with g_0 and g_1 being the activity coefficients in seawater for species of charge 0 and 1, respectively. Incorporating pH as the observed variable, with $pH = -\log_{10}\{H^+\}$:

$$[N_2H_4]/[N_2H_5^+] = Kg_1/g_0 \cdot 10^{(-pH)} \qquad (5.7)$$

and substituting into equation (5.4),

$$\text{fraction } N_2H_5^+ = \frac{1}{(K \cdot g_1 \,/\, g_0 \cdot 10^{(-pH)} + 1)}. \qquad (5.8)$$

Conditions were selected that were similar to California coastal seawater. An equilibrium constant of $10^{-8.18}$, reported for ionic strength 1.0 and 25°C (Smith and Martell, 1976), was chosen as most representative value for K in seawater. Complexation of hydrazine to trace metals was ignored as a first approximation. Unprotonated hydrazine, N_2H_4, was assigned an activity coefficient typical for neutral species in seawater, $g_0 = 1.17$ (Stumm and Morgan, 1981). Protonated hydrazine, $N_2H_5^+$, was assigned activity coefficient $g_1 = 0.695$, using the Davies equation (Stumm and Morgan, 1981). The effect of temperature on K was computed using the van t'Hoff equation (Stumm and Morgan, 1981) and enthalpy change data from Smith and Martell (1976). Activity coefficients were not adjusted for temperature. Protonated hydrazine was prevalent at the ordinary range of temperatures and pH's found in Diablo Cove (Table 5.6; Figure 5.7).

Fraction $N_2H_5^+$ varied from .68 to .91 over the pH and temperature range most often observed in Diablo Cove. Fraction N_2H_4 varied from 0.32 to 0.09 over the same range.

TABLE 5.6: FRACTION $N_2H_5^+$ IN SEAWATER VS pH AND TEMPERATURE
BOLDFACE VALUES TYPICAL FOR CENTRAL AND SOUTHERN CALIF. SEAWATER

TEMPERATURE °C		5	**10**	**15**	**20**	25	30
pH	7.6	0.955	0.939	0.920	0.896	0.866	0.832
	7.8	0.930	**0.907**	**0.878**	**0.844**	0.804	0.757
	8.0	0.894	**0.860**	**0.820**	**0.774**	0.721	0.663
	8.2	0.841	**0.795**	**0.742**	**0.683**	0.620	0.554
	8.4	0.770	0.710	0.645	0.576	0.507	0.440

(2) Transition metal complexation in presence of organic ligands

Equilibrium chemical speciation of hydrazine in seawater was calculated with the computer program SURFEQL (Morel and Morgan, 1972). Stability constants for association of hydrazine with divalent metal ions were obtained from Sillen and Martell (1964, 1968) and Smith and Martell (1976). Metal ion concentrations typical of seawater were obtained from Barcelona et al., (1982); Brewer (1975), and Stumm and Morgan (1981). A small amount, 10^{-5} M, of organic humic material was assumed to exist to simulate coastal seawater. Stability constants for association of metals with marine humic acid were obtained from Mantoura and Riley (1978). Calculations were run for a range of hydrazine concentrations, 10^{-6}, 10^{-5}, 10^{-4}, 10^{-3} M (0.032, 0.32, 3.2 and 32 ppm) at 0.67 ionic strength. Neutral species activity coefficients were set at unity in the model. Oxidation-reduction reactions and surface chemistry were ignored.

SURFEQL calculations predicted the three major species to be N_2H_4 (34 percent), $N_2H_5^+$ (63 percent), and $Mg(N_2H_4)^{+2}$ (3 percent) at

Figure 5.7: Dependence of Hydrazine speciation on pH and temperature. g0 and g1 are activity coefficients for neutral and singly-charged chemical species in seawater.

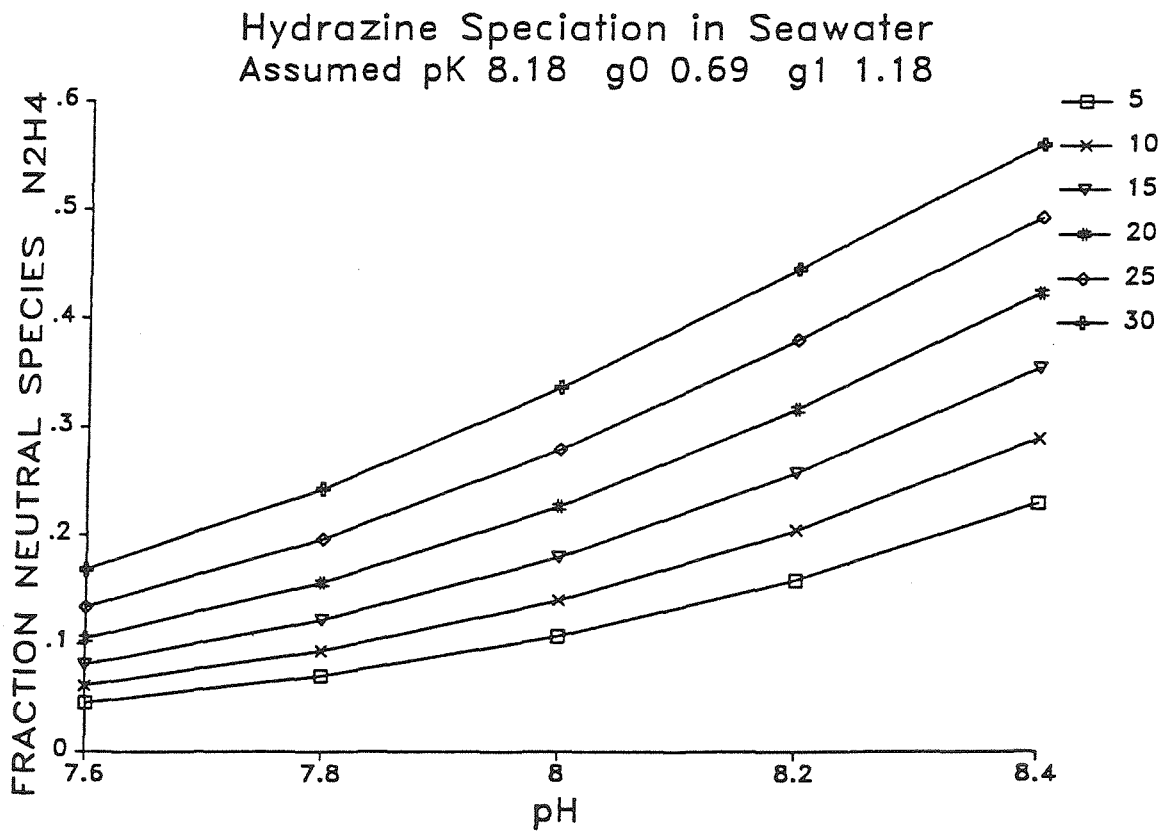

pH 8.00 and 25°C. Ninety percent of the humic material was associated with Mg^{+2} and Ca^{+2}. Humic material sequestered most of the copper at low hydrazine concentrations. Essential trace metals such as Cu^{+2}, Mn^{+2}, Zn^{+2} were not significantly complexed with hydrazine at concentrations below 3.2 ppm (10^{-4} M) (Figure 5.8; Table 5.7). Copper was the only trace metal with substantial fractions associated with hydrazine at hydrazine concentrations exceeding 10^{-4} M.

TABLE 5.7: SPECIATION OF 8 nM COPPER(II) IN SEAWATER WITH N_2H_4

Hydrazine Concentration	Percentage bound to each ligand at 25°C, pH 8			
	Organic	Carbonate	Hydrazine	Minor species
0.032 ppm	81	14	0	5
0.32	81	14	1	4
3.2	66	12	18	4
32	4	0	95	1

Hydrazine speciation was not significantly influenced by complexation with divalent metal ions in seawater. Transition metal ion availability to organisms was not affected until hydrazine concentrations well above toxic thresholds for gametophytes were reached.

B. AUTOXIDATION IN SEAWATER

(1) Introduction

Use of hydrazine in fuel cells and rocket propellants led to studies of its environmental chemistry by the U.S. Air Force in the 1970's (cf. Lurker, 1976; Zirolli et al., 1980, cited in Schmidt, 1984). Zirolli et al., (1980) observed 30 percent decay of unsymmetrical dimethyl hydrazine in 10 days in seawater; 40 percent in pond water. McNaughton et al., (1978) observed disappearance rates

Figure 5.8: Association of several divalent cations with hydrazine. Calculated using SURFEQL (see text).

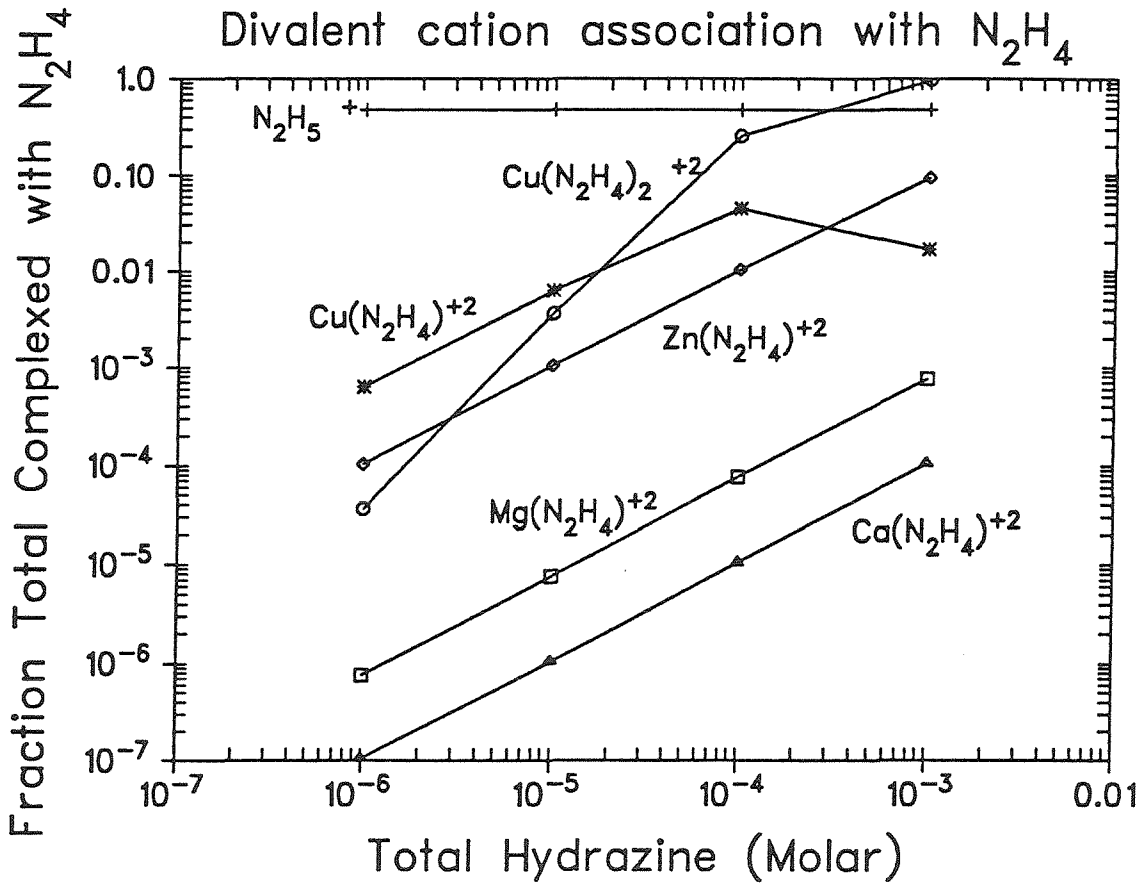

of 2 percent, 20 percent and 40 percent in 120 hours in 10^{-4} molar hydrazine solutions in distilled water, pond water and seawater, respectively. They found autoxidation rates increased linearly with additions of copper between 10^{-7} and 10^{-5} molar and were unaffected by changes in dissolved oxygen concentration between 0.5 and 40 mg/liter. Rates exhibited strong temperature dependence with a slope break at 10°C in the Arrhenius plot of log (1/k) vs. 1/T.

Ellis et al., (1960) observed catalysis of hydrazine autoxidation in distilled water by added copper and hypothesized existence of a multistep reaction mechanism. Gaunt and Wetton (1966) proposed a three-step reaction mechanism for autoxidation in alkaline solutions. McNaughton et al., (1978) concluded that catalysis by added copper in distilled water and the activation energy slope break indicated a multi-step reaction series for autoxidation of hydrazine in natural waters similar to that proposed earlier by Gaunt and Wetton (1966) but with a different final oxidation step (5.11c below). The proposed reaction sequence is:

$$N_2H_4 + Cu^{+2} \rightarrow N_2H_3^\circ + Cu^+ + H^+ \quad \text{(slow)} \qquad (5.9)$$

$$Cu^+ + O_2 + H^+ \rightarrow Cu^{+2} + HO_2^\circ \quad \text{(fast)} \qquad (5.10)$$

$$2N_2H_3^\circ \dashrightarrow N_4H_6 \rightarrow N_2 + 2NH_3 \quad \text{(Gaunt \& Wetton, dimerization)} \qquad (5.11a)$$

$$N_2H_3^\circ \xrightarrow{-(e)} N_2H_2^\circ \xrightarrow{-2(e)} N_2 \quad \text{(Gaunt \& Wetton, oxidation)} \qquad (5.11b)$$

$$HO_2^\circ + N_2H_3^\circ \rightarrow N_2 + 2H_2O \quad \text{(MacNaughton, fast)} \qquad (5.11c)$$

$$N_2H_4 + O_2 \leftrightarrow N_2 + 2H_2O \quad \text{OVERALL.} \qquad (5.12)$$

MacNaughton et al., (1978) did not specify which step was rate-limiting in each temperature region. They observed a linear increase in rate with increasing free Cu^{+2} concentration but did not verify

the third step of their proposed mechanism by measurement of HO_2°. concentration. Lurker (1976), cited in Schmidt (1984) and MacNaughton et al. (1978), also observed copper-catalyzed disappearance of hydrazine at environmentally relevant concentrations and a slope break in the Arrhenius plot at low (5-10°C) temperatures.

The rate-limiting step in the mechanism proposed by McNaughton et al., (1978) and Gaunt and Wetton (1966), suggests the rate law:

$$d[N_2H_4]_T/dt = -k\ [N_2H_4]\ [Cu^{+2}]. \qquad (5.13)$$

Assuming constant pH and rapid equilibrium, using (5.2) and (5.4):

$$[N_2H_4] = [N_2H_4]_T\ /\ (1 + g_0 10^{(-pH)}/g_1K). \qquad (5.14)$$

When integrated, assuming rapid regeneration of Cu^{+2}:

$$\ln [N_2H_4]_T = \ln [N_2H_4]_{oT} - kobsvd \cdot t, \qquad (5.15)$$

where $kobsvd = k\ [Cu^{+2}]\ /\ (1 + g_0 10^{(-pH)}/g_1K)$,

which leads to pseudo-first-order autoxidation kinetics with time. Ellis et al., (1960) and Gaunt and Wetton (1966) observed deviation from first-order kinetics at long reaction times. Ellis et al., (1960) found that empirical polynomials of the form $ac + bc^2$ (c = concentration) best described their decay data. Dalgaard (1982) concluded that the reaction was half-order in hydrazine and first-order in oxygen. MacNaughton et al., (1978) did not develop a rate law to describe their observations.

Schmidt (1984), reviewing extant literature on metal-catalyzed hydrazine oxidation in aqueous solutions, found that mechanisms were not fully elucidated and cited Higginson et al.'s (1953) hypothesis that the ability of transition metal ions to absorb hydrazine into their coordination sphere determined the reaction path.

Schmidt (1984) also cited references to reactions of hydrazine with nitrate, hydrogen peroxide, hydroxyl radical, Fe(III), and Mn(III) in natural waters.

Combined literature reports suggested that several chemical species found in seawater, Cu(II), HO_2°, and $^{\circ}OH$, could influence hydrazine autoxidation rates. Rates could vary with changing concentration of the reactants. While it was beyond the scope of this thesis to elucidate hydrazine reaction mechanisms in seawater, it was necessary to confirm or refute previous literature reports of slow autoxidation rates in natural waters in light of assertions by staff members at California electric power utilities that hydrazine, once released from a power station, reacted rapidly with oxygen in seawater.

(2) Materials and Methods

Hydrazine concentrations were determined using the method of Pesez and Petit (1947) and Watt and Chrisp (1952) as modified by the American Society for Testing Materials in method D-1385-78 (ASTM, 1982). The method employs reaction of hydrazine with p-dimethylamino-benzaldehyde (p-DABA) in a blend of dilute acid and methanol to form a colored adduct whose concentration can be determined spectrophotometrically, Watt and Chrisp (1952). Kinetics are rapid; the reaction is completed within 5 minutes at room temperature. The resulting yellow-colored (458 nanometer absorbance) complex is stable for several hours in room lighting at ambient temperatures.

Glassware and rubber stoppers were cleaned by soaking for 24 hours in 4N HNO_3 to remove surface adsorbed impurities that might catalyze

the reaction rate. All reagents were made up with 15-18 megohm double-distilled water. Hydrazine master solutions were made up by addition of reagent-grade hydrazine sulfate to double distilled water.

Hydrazine was added to seawater sampled from several sources (Catalina Channel, Newport Harbor and Diablo Canyon) at concentrations of 1×10^{-4} molar (1×10^{-3} M in Catalina water). Flasks were sealed with air head spaces. Aliquots were withdrawn from the flasks at regular intervals for measurements and mixed with a standard volume of acidified indicator solution. Unknown hydrazine concentrations in the aliquots were determined against colorimetric hydrazine standards of known concentration. Absorption at 458 nm was measured with a Bausch and Lomb Spectronic 88 spectrophotometer. The theoretical analytical detection limit with freshly made indicator solution was 20 ppb for a 1 cm path length cell. The practical detection limit was 40 ppb when machine drift was included. Use of a 10 centimeter path-length cell decreased the detection limit by a factor of 5, limited by positioning errors for the large cells. Choice of cell depended on hydrazine concentration in experimental solutions.

Seawater copper contents were directly determined using a Beckman Spectra-Span SV8 atomic absorption spectrophotometer. Seawater readings were compared to 10, 15, 30 and 45 ppb Cu standards made up in 5X distilled water.

Decay rates and half-lives were compared for cases of zero-order, half-order and first-order kinetics. Data were transformed

and fit by linear least-squares regressions to expressions for each reaction order:

For zero-order kinetics,

$$d\,[N_2H_4] / dt = -k, \tag{5.16}$$

which, when integrated with $[N_2H_4]=[N_2H_4]_o$ at t=0 gives

$$[N_2H_4] = -k \cdot t + [N_2H_4]_o. \tag{5.17}$$

For half-order kinetics:

$$d\,[N_2H_4] / dt = -k \cdot [N_2H_4] \tag{5.18}$$

which, with identical boundary conditions, integrates to

$$[N_2H_4] = - k \cdot t + [N_2H_4]_o. \tag{5.19}$$

Half-order kinetics were suggested by a data transformation technique attributed to Powell by Moore and Pearson (1981) which is used to find approximate reaction orders in kinetic data.

(3) Results

Hydrazine autoxidation rates varied by an order of magnitude with sampling location of the seawater (Figure 5.9, Table 5.8). Observed rates were generally slower than those obtained by MacNaughton et al., (1978).

Rates expressed as fractional decay of starting concentration in Catalina Channel seawater (collected approximately 5 km from shore) were one order of magnitude slower than those reported by MacNaughton et al., (1978). A 10^{-3} M solution gave 35 percent degradation in 984 hours and 70 percent degradation in 2500 hours (at 19°C, pH 8.1, DO 7.4 mg/liter).

Figure 5.9: Autoxidation of hydrazine in different seawaters. Rates shown are for zero-order fits to fraction remaining vs. time. Lines are not fits but connect points of individual experiments.

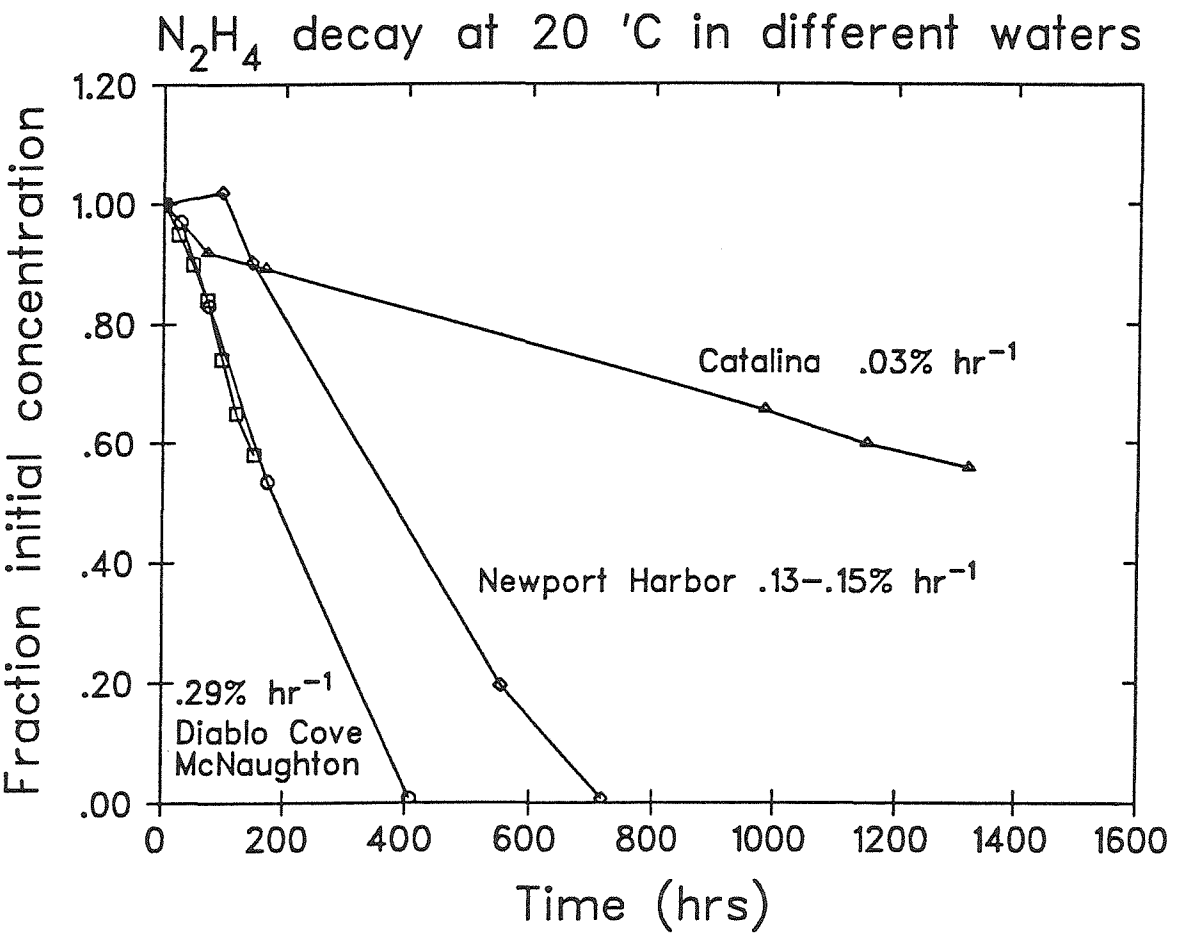

Table 5.8: Observed Hydrazine Autoxidation Rates in Seawater

Date	Experimental Media	Initial Concentration (Molar)	Temperature	zero order fit Decay Rate percent/hour	zero order Predicted Half Life (Hours)
1/86	NEWPORT HARBOR #1	10^{-4}	18-19°C	0.15 ± 0.01	325
1/86	CATALINA CHANNEL	10^{-3}	18-19°C	0.03 ± 0.001	1770
4/86	N.H. #2 AERATED	10^{-4}	21°C	0.12 ± 0.01	545
	N.H. #2 UNAERATED	"	21°C	0.13 ± 0.01	378
	N.H. #2 FILTERED	"	21°C	0.12 ± 0.01	430
1/87	DIABLO COVE #1	10^{-4}	20°C	0.25 ± 0.01	200
1978	FLORIDA SEAWATER (MacNaughton et al., 1978)	10^{-4}	20°C	0.29 ± 0.02	171

Newport Harbor seawater containing 10^{-4} M hydrazine exhibited autoxidation rates of 0.12-0.15 percent/hour in two different experiments (Table 5.8). Neither continuous aeration nor 0.22 um filtration significantly affected decay rates.

Several least-squares fits to the data adequately described time course of the autoxidation reaction (Table 5.8A) but showed different types of deviation. Fits to Newport Harbor seawater data using zero-order kinetics gave accurate estimates of half-life but over-predicted decay for the last 50 percent of the reaction (Figure 5.10). Estimation of rates using first-order kinetics from Equation (5.15) gave better agreement with data for the last half of the reaction but tended to predict too much decay for the first half of reaction duration (Figure 5.11).

Table 5.8A: Summary of Kinetic Parameters for Hydrazine autoxidation

Reaction order	Newport Harbor Seawater: Zero	Half	First
rate constant	-0.001324	-1.55×10^{-5}	-0.00332
uncertainty	0.00009	$.06 \times 10^{-5}$	0.00022
r^2	0.987	0.980	0.983
predicted half-life	378 hrs	373 hrs	208 hrs
Reaction order	**Offshore Seawater: Zero**	**Half**	**First**
rate constant	-2.81×10^{-4}	-1.20×10^{-5}	-4.82×10^{-4}
uncertainty	0.15×10^{-4}	0.016×10^{-5}	0.25×10^{-4}
r^2	0.987	0.997	0.987
predicted half-life	1800 hrs	1530 hrs	1440 hrs

When decay-rate data for both offshore seawater and Newport Harbor water were plotted as $[N_2H_4]/[N_2H_4]_o$ vs. log (time) (using the method of Powell as described in Moore and Pearson, 1981), the fitted curve shapes best approximated the plot for ideal half-order kinetics in the family of curves developed for fraction remaining vs. log (time) for reactions of various orders (Figure 5.12). The resulting half-order kinetics predicted half-lives similar to zero-order fits and did not overpredict decay at long reaction times (Figures 5.10 and 5.11).

Measured copper contents were about the same in all seawater samples used for hydrazine autoxidation experiments (Table 5.9). Copper data may indicate a calibration error or seawater matrix interferences, because computed molar concentrations were one to two orders of magnitude higher than expected for seawater. Young (1979), cited in Barcelona et al., (1982), found enrichment up to 40 nM over oceanic background in Newport Harbor seawater.

Figure 5.10: Comparison of half-order and first-order fits to hydrazine autoxidation in Newport Harbor Seawater.

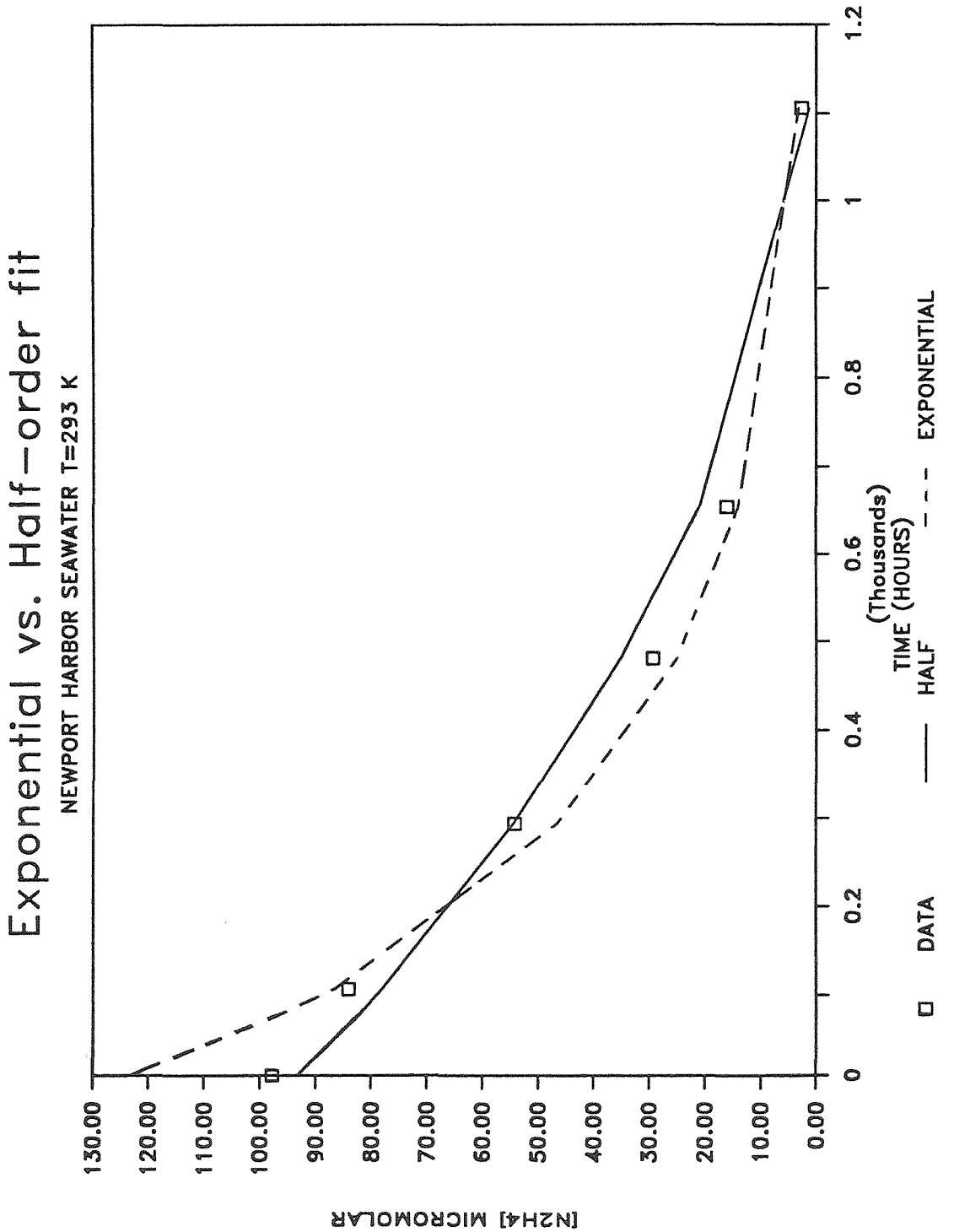

Figure 5.11: Comparison of half-order and zero-order fits to hydrazine decay data for Newport Harbor seawater.

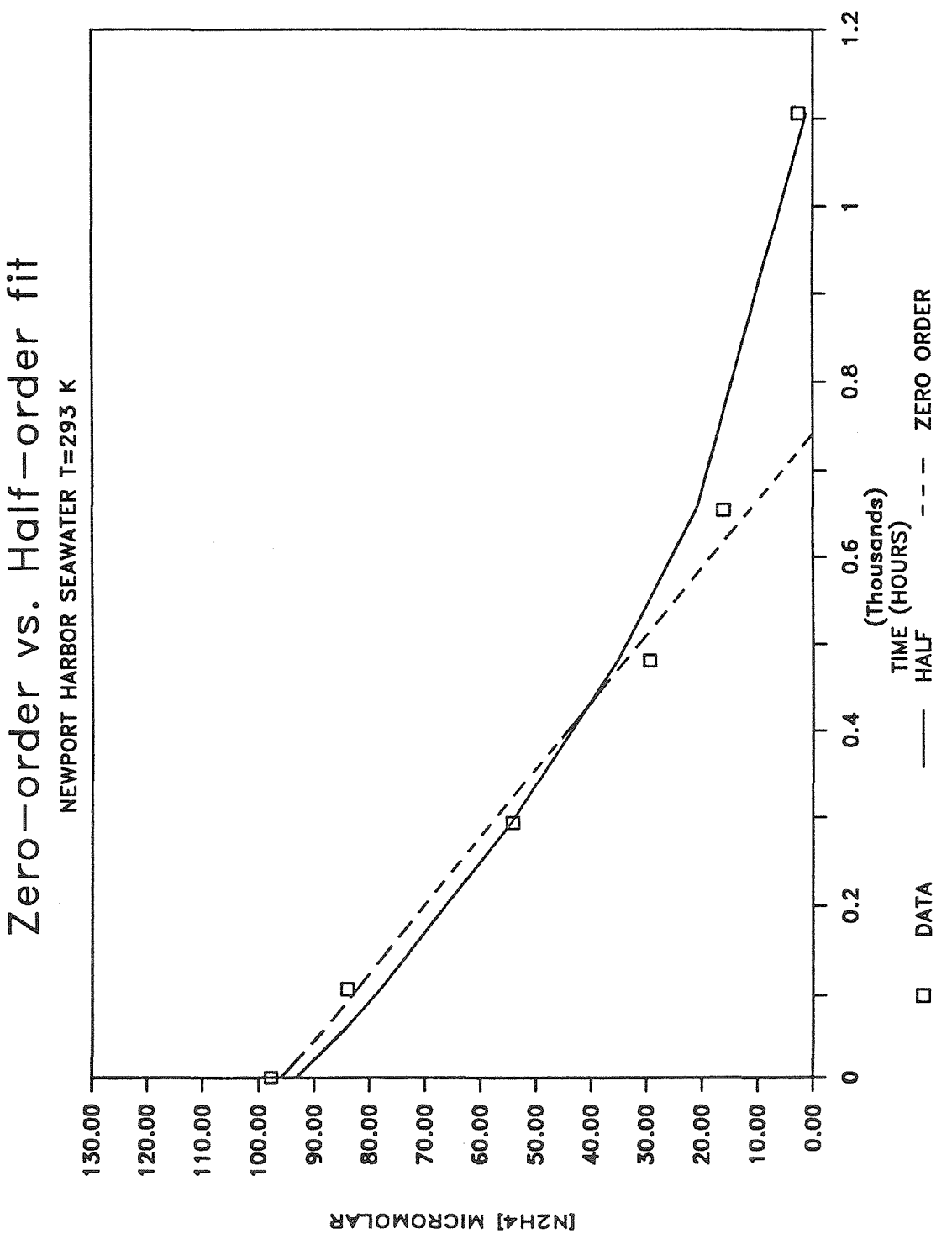

Figure 5.12A Comparison of experimental data for offshore seawater to time course of reactions for several types of ideal kinetics. Experimental data shifted to left by 3.41, moving several points offscale.
$\log_{10}\text{tau} = \log_{10}\text{time} - \log_{10}(kc_o^{n-1})$.

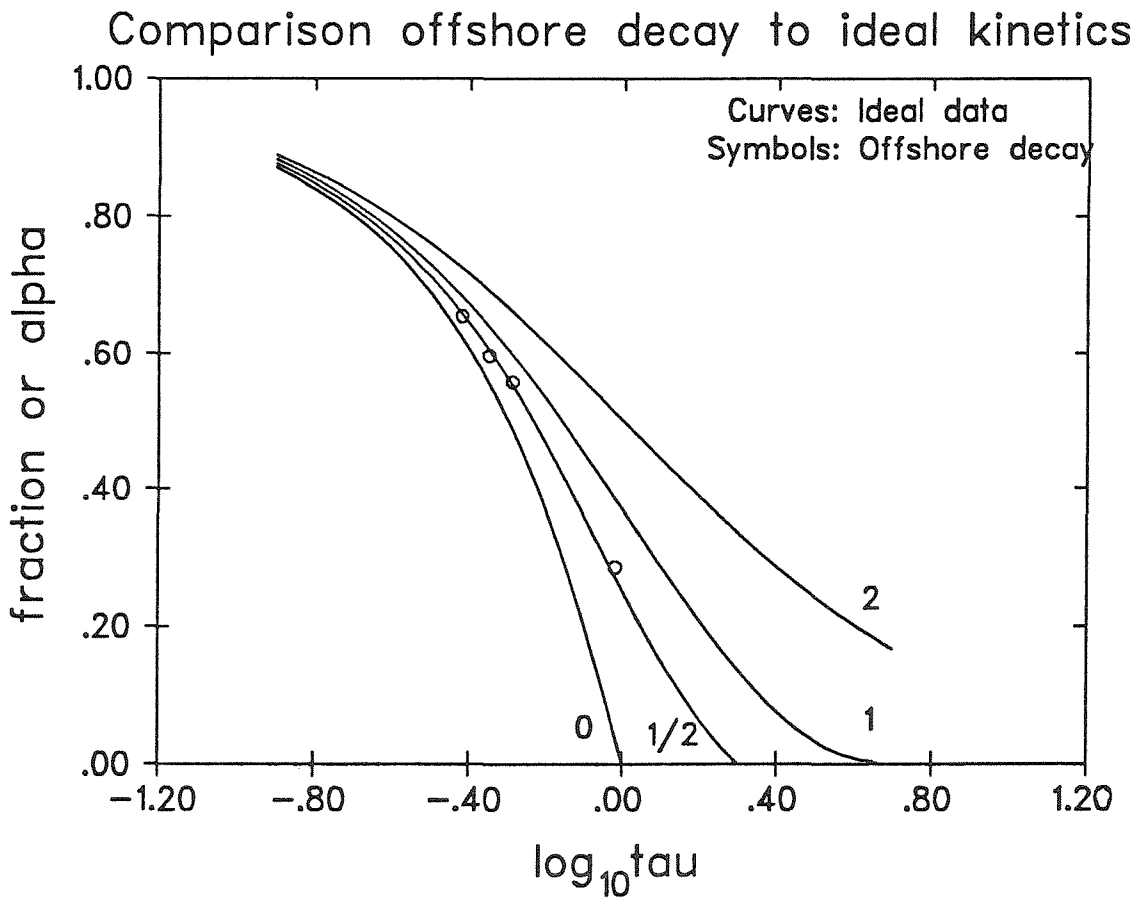

Figure 5.12B: Fit of three kinetic models to hydrazine autoxidation offshore seawater.

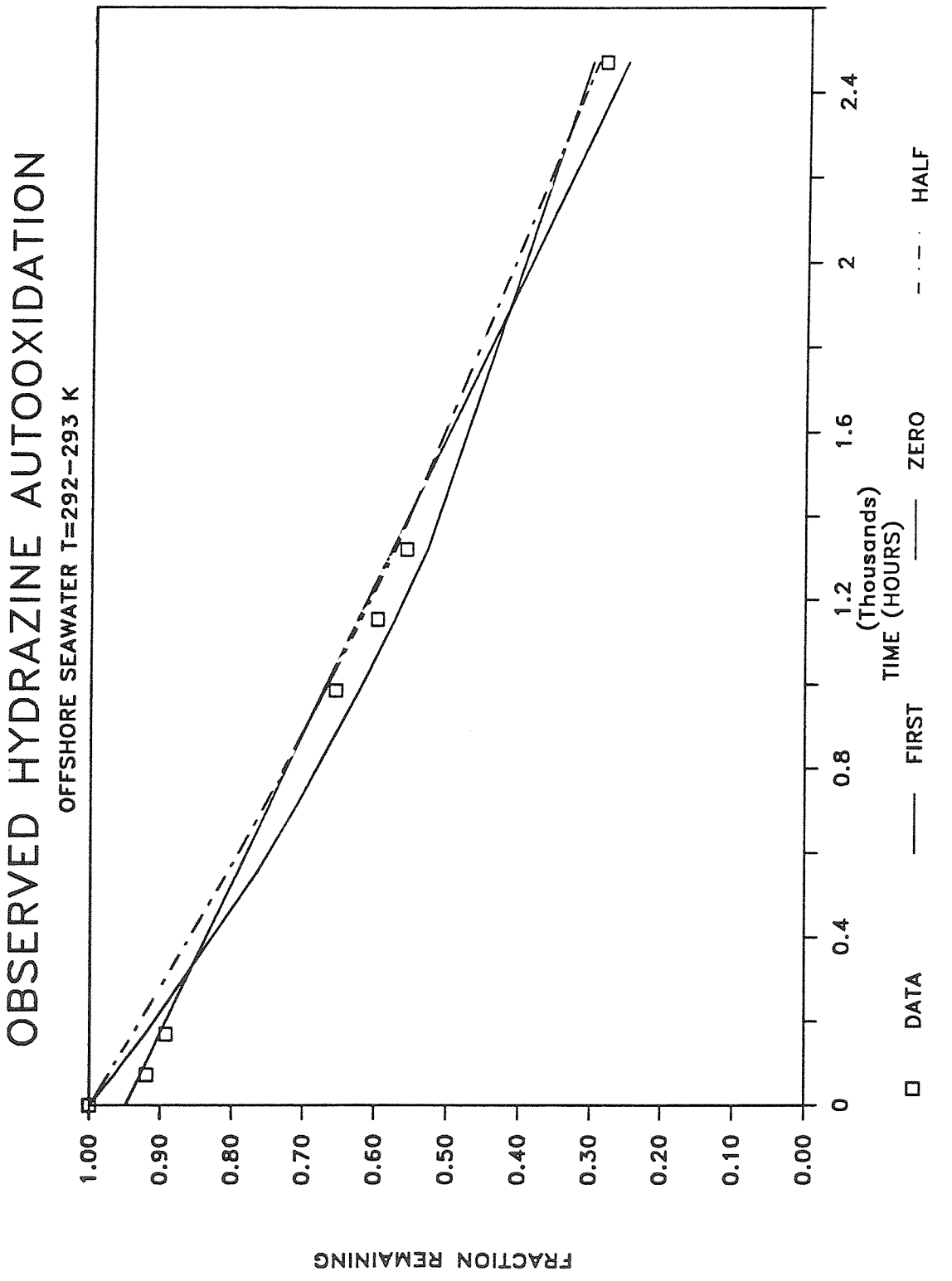

Table 5.9: Total copper contents in studied seawaters

Sampling Date	Source	Measured content ppb	nM	# determinations
1/86	Catalina Channel	32 ± 2	516 ± 32	2
4/86	Newport Harbor	34 ± 2	548 ± 32	2
	Newport Harbor filtered	35	564	1
1/87	Diablo Cove	35 ± 4	564 ± 64	3

TABLE 5.10 Effect of temperature on initial decay rate and predicted half-life of 10^{-4}M hydrazine in Diablo Cove seawater.
n = number of paired points used in calculating regressions
r = regression coefficient for fit to data.

Temperature	Initial decay rate (linear fit)	Predicted Half-life (exponential fit)
0°C	-0.02 %/hour r = -.732 n = 5	2800 hours r = -.748 n = 5
10°C	-0.02 %/hour r = -.980 n = 5	3000 hours r = -.982 n = 5
20°C	-0.25 %/hour r = -.998 n = 5	57 hours r = -.958 n = 5
35°C	-0.57 %/hour r = -.961 n = 4	20 hours r = -.973 n = 4

Barcelona et al., (1982) observed values ranging from 3.4 to 15.6 nM in southern California coastal seawaters. Values on the order of 500 nM have not been observed. Contamination was not the cause of the high readings, since identically prepared blanks read below the detection limit. Interferences that were due to matrix effects in the

Figure 5.13: Effect of temperature on autoxidation rate. Lines through 20°C and 35°C points are zero-order fits to data. Lines through 0°C and 9°C only connect points for each temperature.

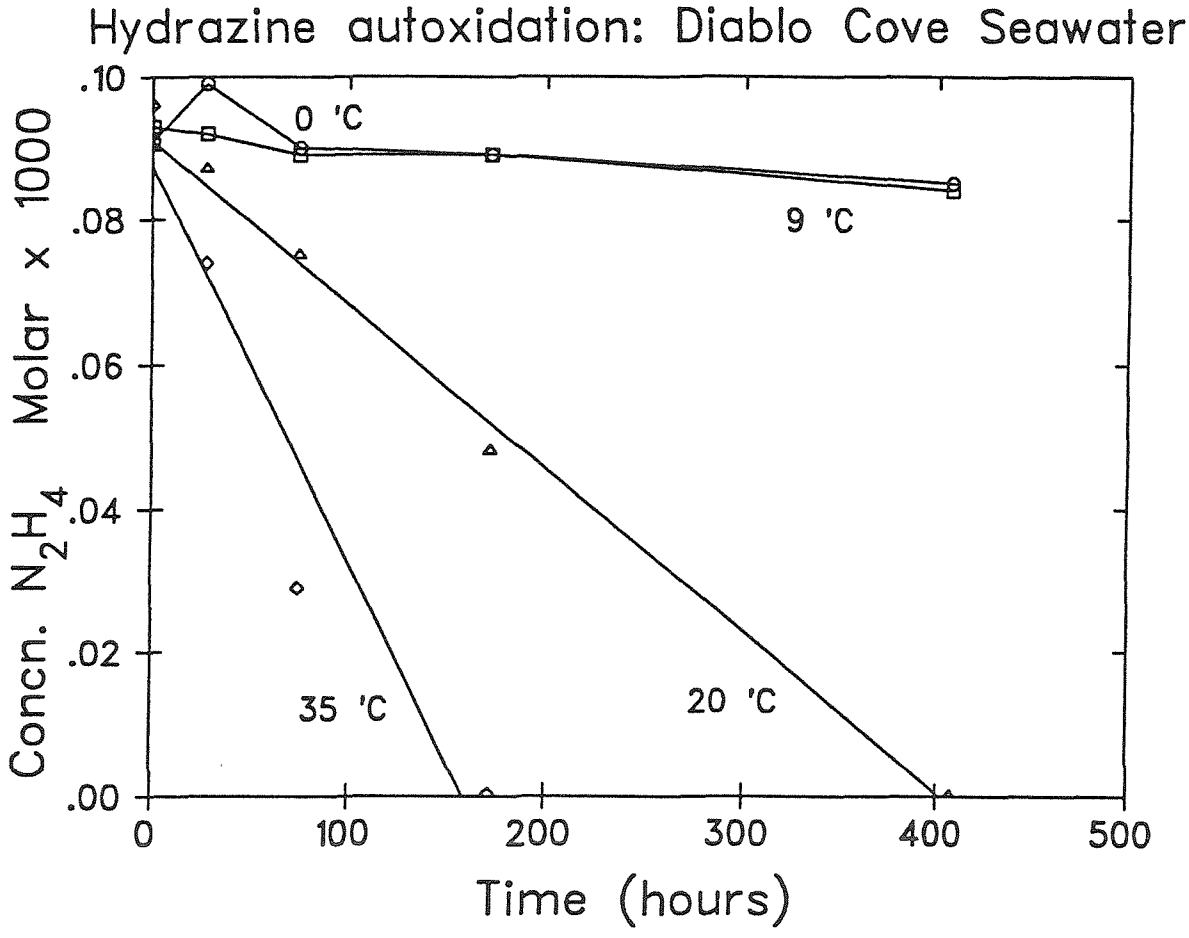

directly determined samples may have masked any variability in copper content. Decay of 1 x 10^{-4} molar solutions in Diablo Cove seawater was followed for 408 hours at several temperatures. Disappearance rate rose with increasing temperature (Table 5.10; Figure 5.13). Decay at room temperature was as fast as observed by McNaughton et al., (1978) and faster than previously observed (Table 5.8) in southern California seawaters.

Log_e-transformed pseudo-first-order rate constants determined from the data using Equation (5.15) were plotted against 1/Temperature to estimate[4] activation energy for hydrazine autoxidation in seawater using the relations (Stumm & Morgan, 1981):

$$d\frac{\ln k}{dT} = \frac{Ea}{RT^2} \qquad (5.20)$$

$$\ln k = -\frac{Ea}{RT} + \text{Constant} \qquad (5.21)$$

A slope break was observed between 10°C and 20°C (Figure 5.14), confirming findings of Lurker (1976) and MacNaughton, et al., (1978).

---

[4]This procedure is valid for the following assumptions:

1) Changes in activity coefficients, distributions of N_2H_4 and Cu^{+2}, and enthalpy change are small over the tested temperature range.

2) The expression for the rate-limiting step: $d[N_2H_4]/dt = -k[N_2H_4][Cu^{+2}]$, can be approximated as $d[N_2H_4]/dt = -k_{obs}[N_2H_4]$ where $k_{obs} = k[Cu^{+2}]$, leading to,

3) $\ln k_{obs} = \ln k + \ln [Cu^{+2}]$ becomes $\ln k = \ln k_{obs} - \ln[Cu^{+2}]$.

4) Then, assuming small changes in $[Cu^{+2}]$,

$-Ea/R = (\ln k_2 - \ln k_1)/(1/T_2 - 1/T_1)$.

A plot of lnk against 1/T should have a slope of -Ea/R.

Activation energies estimated from the slopes in the 20-35°C and 9°C to 20°C regions were 53 kilojoules/mole and 272 kJ/mole respectively. MacNaughton et al.'s (1978) values (obtained from plotting data in their Figure #13 and running a least-squares fit) for reaction with 10^{-6} M Cu^{+2} were 63 $\pm$ 10 kJ/mole for the region 15-30°C and 265 kJ/mole for the region 5-10°C.

A sample of 0.22 um-filtered Diablo Cove seawater exhibited one-tenth the decay rate at 20°C of the unfiltered sample (Table 5.11). The enhanced degradation could be due to either biological (bacteria, plankton) or nonbiological (colloidal materials, humic and fulvic acids with associated metal ions) processes.

TABLE 5.11: Effect of 0.22um filtration on hydrazine degradation rate in Diablo Cove seawater after 408 hours' reaction.

Temperature	Filtered	Unfiltered
9°C	0.00	-0.02 percent/hour
20°C	-0.02 percent/hour	-0.25 percent/hour

(4) Discussion

Chemical complexity of seawater complicates any attempt to propose an exact mechanism which explains the observed data. Similarity of MacNaughton et al.'s (1978) computed activation energies for copper-spiked distilled water to our seawater results indicates that copper-catalyzed autoxidation could be taking place in seawater.

Figure 5.14: Arrhenius plot for Diablo Cove data using calculated pseudo-first order rate constants. Squares are second-order rate constants from McNaughton et al., 1978.

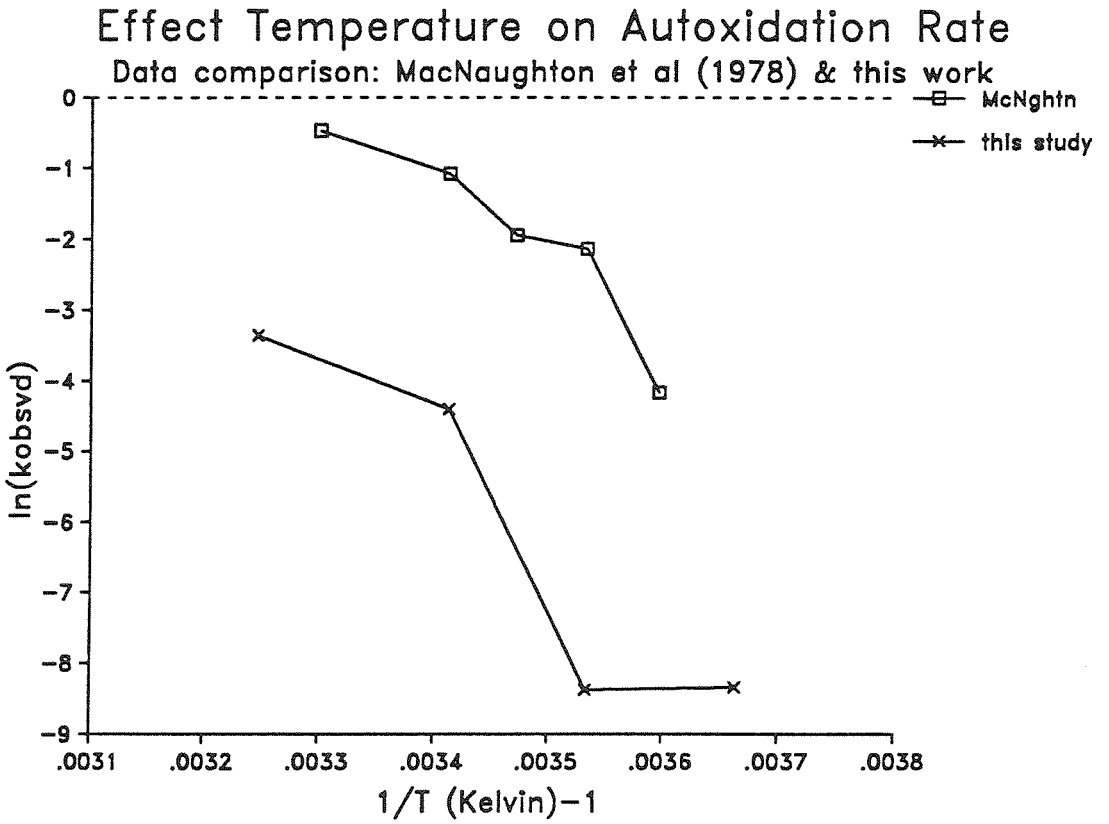

MacNaughton et al., (1978) and Gaunt and Wetton (1966) showed dependence of autoxidation rate on Cu(II) concentration in low ionic strength aqueous solutions, presumably because Cu^{+2} activity varied linearly with Cu(II) content. Autoxidation rates have also been shown to vary with hardness in fresh waters (Slonim and Gisclard, 1976) because high calcium concentrations sequester hydrazine as $Ca(N2H4)^{+2}$, and Cu^{+2} associates with carbonate and OH^- in soluble aqueous complexes.

If the low variability in measured Cu(II) seawater concentrations was real, then either Cu^{+2} activity was higher in coastal seawater, or other oxidants accelerated observed N_2H_4 autoxidation rates. Gschwend (personal communication) suggested that higher peroxide radical concentrations in coastal seawater could have increased autoxidation rates, citing work by Zafirou (1976) which showed that photochemical reactions with nitrate and nitrite in seawater produced elevated concentrations of hydroxyl (OH°) and peroxy (OOH°) radicals. Reaction between dilute peroxide and hydrazine was found to be slow and catalyzed by copper (Gordon, 1949; and Wright, 1972, cited in Schmidt, 1984). The reaction mechanism has not been completely elucidated. However, reaction with peroxide would represent an additional autoxidation path in coastal seawater. Observed rates could increase if two parallel paths of roughly equal magnitude were operating. Verification would require analysis in simple model systems.

MacNaughton et al.'s (1978) conclusion that hydrazine must be modelled as a conservative pollutant after release to natural waters

was verified by autoxidation rates observed in this study. Decay in concentration will occur principally due to dilution and dispersion, since these processes have characteristic times that are shorter than the characteristic reaction times for autoxidation.

V. CONCLUSIONS

1) Both California coastal nuclear powerplants occasionally emitted end-of-the-pipe hydrazine concentrations exceeding levels known to inhibit Macrocystis gametophyte vegetative growth in laboratory experiments. Allowing for dilution of the discharges, comparison of the frequency distribution for discharged hydrazine concentrations to the frequency distribution for continuous toxicity assays indicates that hydrazine toxicity events will not occur at San Onofre. The across-the-beach discharge location and lower dilutions inherent in the Diablo Canyon discharge lead to possible overlaps of discharge frequency distribution and toxicity response frequency distribution.

2) Hydrazine speciation was moderated only by pH and temperature in seawater. Hydrazine may affect trace metal speciation at hydrazine concentrations exceeding 10^{-4} molar.

3) Hydrazine autoxidation in seawater was slow, decaying at rates of 0.03-0.29 percent per hour. Least-squares fits of zero, half and first order kinetic models satisfactorily described time course of the reaction in seawater. Half-order kinetics best described initial and long-term rates. Measured copper content did not vary in the tested seawaters and thus cannot be invoked to explain the variation in autoxidation rate. Autoxidation rates showed strong temperature

sensitivity. Rates at 0-10°C were 10-20 percent of the rates at 20°C. 4) Half-life of hydrazine was on the order of 200-3000 hours, much longer than characteristic regional flushing times in coastal waters. The compound may therefore be modelled as a conservative pollutant, confirming the conclusions of MacNaughton et al., (1978).

CHAPTER 5: APPENDIX

Prediction of toxicity event risk from powerplant emission data and *Macrocystis pyrifera* gametophyte sensitivity to episodic hydrazine exposure.

The historical risk of hydrazine discharges was estimated by comparing frequency distribution data from repeated toxicity testing of *Macrocystis* gametophytes to frequency distributions for estimated hydrazine concentrations emitted from power stations. The method of comparing the two frequency distributions was used because, except for data for Diablo Canyon during the March-May 1984 period, specific information about the duration of hydrazine emissions events was lacking. The procedure assumed that power-plant hydrazine emission durations were of seven to 16 hours' length, dilutions of power station thermal plumes were well-defined and confined to a fairly narrow range of dilution factors, and organisms did not become more or less tolerant of low-level hydrazine exposures as during their life cycle. Hydrazine emission frequency data from two California coastal nuclear power stations were used, but the technique could also be applied to fossil plants.

Cumulative frequency data for reported hydrazine emission events in the discharges of the Diablo Canyon Power Plant and the San Onofre Nuclear Generating Station (Figures 5.3B and 5.6B, respectively) were graphed for several dilution factors appropriate to each power-plant. Dilutions ranging from 3:1 to 5:1 were assumed to occur for the across the beach discharge at Diablo Canyon (Tu, 1986). Dilutions of (10 $\pm$ 2):1 were assumed to occur at San Onofre (R.C.Y. Koh, pers. comm). No-dilution (1:1) values were plotted for each power station,

and a curve shifted by a 12:1 dilution factor was graphed for the Diablo Canyon Power Plant to create a dilution envelope identical to that plotted for San Onofre.

A frequency distribution of the hydrazine concentration required for 50 percent inhibition of Macrocystis gametophyte growth in 96-120 hours of exposure was generated from the last column of data in Table 4.14, p. 135. This distribution was then scaled to higher concentrations using the constant-dose hypothesis from Chapter 6, Section III, pp. 252-271, to compensate for the shorter 7 to 16 hour time period characteristic of hydrazine discharge durations known to occur at Diablo Canyon. The adjusted Macrocystis growth inhibition distributions were then graphed with the power-plant emissions frequency data and the plots examined for overlap on the concentration scale. Frequency estimates were generated by reading off the fraction of diluted power-plant emissions which overlapped the lowest Macrocystis toxicity concentration threshold.

No overlap occurred between Macrocystis toxicity distributions and diluted frequency distributions for San Onofre Nuclear Generating Station (Figure 5.15A), indicating that power-plant hydrazine emissions posed very low risk to reproducing kelp populations.

Overlap occurred between 1 to 3 percent of Diablo Canyon hydrazine emissions and the Macrocystis toxicity distributions (Figure 5.15B), signifying that some historical risk to kelp gametophytes could have occurred in the vicinity of this outfall. Dilutions in Diablo Cove are known to exhibit high spatial and temporal variability (cf., Chapman et al., 1987, cited in Chapter 6).

Figure 5.15: Comparison of historical hydrazine discharge risk to vegetative growth of Macrocystis pyrifera gametophytes.
Right-side curve pair: Estimated frequency distributions for 96-hour 50 percent growth inhibition of M. pyrifera after 7 and 16 hour hydrazine doses.
Left-side points and curves: Frequency distributions for emitted hydrazine concentrations, scaled by various dilution factors. Curves are fifth-order polynomial fits to data and bracket dilution factors observed during normal operations from field monitoring studies for both power-plants. The 12:1 value for DCPP was drawn to give similar overall dilution "envelopes" in each plot.
Top plot: San Onofre Nuclear Generating Station; diffuser discharge.
Bottom plot: Diablo Canyon Power Plant; across-the-beach discharge.

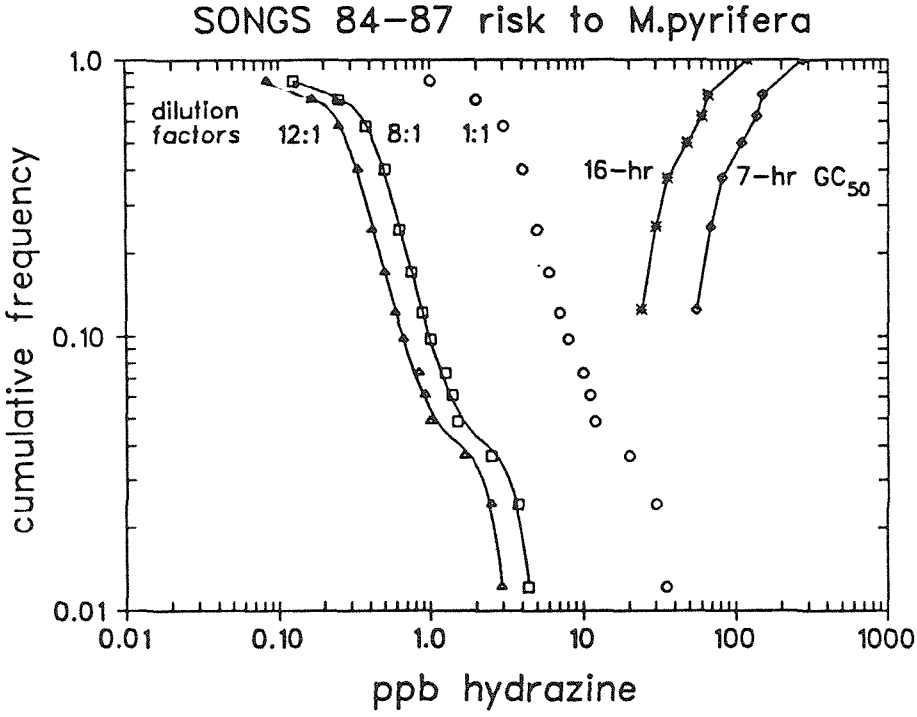

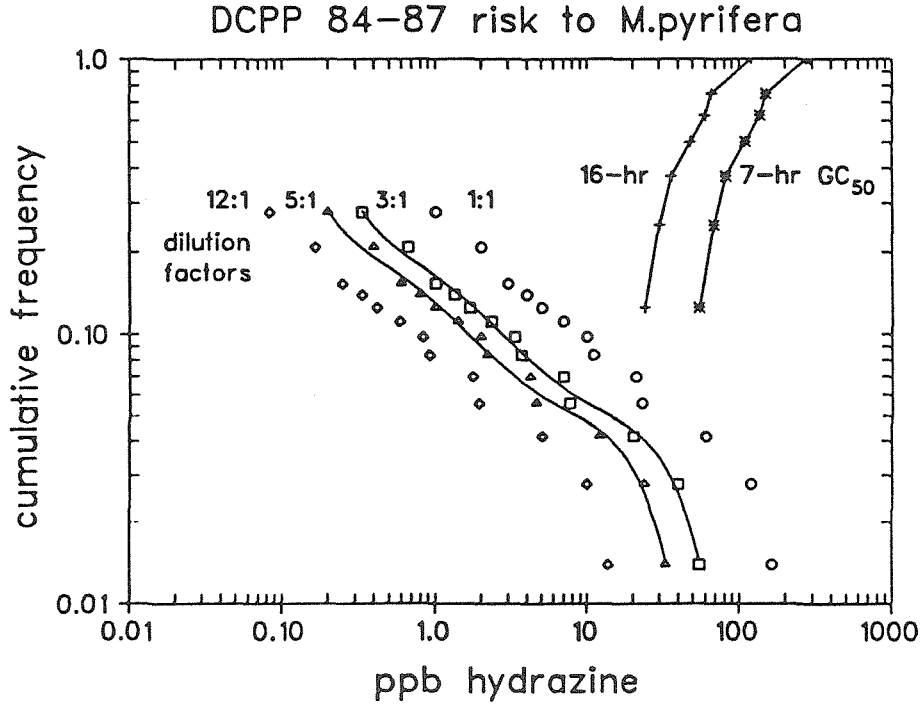

Two phenomena combined to cause higher risk at DCPP than at SONGS. 1) Although 90th percentile levels for undiluted hydrazine discharge concentrations from DCPP and SONGS were 6 ppb and 8 ppb, respectively (Figures 5.3B and 5.6B), DCPP exhibited several events of much higher concentration than any that occurred at SONGS. This caused the undiluted DCPP cumulative frequency distribution curve to extend into higher concentration ranges (or, have a lower slope) than the SONGS curve for events occurring in the 0.01 to 0.10 frequency range (Figure 5.15). Seven percent of the undiluted DCPP emission frequencies overlapped with Macrocystis gametophyte 16 hour toxicity estimates, but only four percent of the undiluted SONGS concentrations overlapped the toxicity data.

2) Estimated dilution factors from the DCPP across-the-beach discharge were lower than those estimated for the for the multi-port diffuser system installed at SONGS. In consequence, the shallow "tail" of the DCPP data was not displaced as far to the left as the steep "tail" of the SONGS data. The net result was that some overlap of toxicity and concentration frequency data remained for DCPP after its concentration frequency data were shifted by appropriate dilution factors.

Estimates of 3:1 to 5:1 dilution averaged over a seven to 16 hour period would only be valid in specific regions of Diablo Cove for particular combinations of wind and sea state. Risk estimates at any specific site in the Cove might be reduced if probabilities of contact between organism and an intermittently hydrazinated plume of varying dilution were to be accurately estimated.

REFERENCES

American Society for Testing Materials, Committee on Water, Section D-19, 1982. Standard Test Method for Hydrazine in Water, Annual Book of ASTM Standards, Part 31, ASTM: Philadelphia, Pa. Section D-1385-78.

Audrieth, L.F. and B.A. Ogg, 1951. The Chemistry of Hydrazine, J. Wiley and Sons: New York. Chapter 6.

Babcock and Wilcox, Inc. 1978. Steam, Its Generation and Use, Babcock and Wilcox, Inc.: New York, Chapter 31.

Baker, M.D. and V.M. Marcy 1956. Hydrazine as an oxygen scavenger. A progress report on tests at Springdale Station. Transactions of the ASME. 78:299-304.

Barcelona, M, J., L.C. Cummings, S.H. Lieberman, H.S. Fastenau, and W.J. North 1982. Marine farming the coastal zone: chemical and hydrographic considerations, California Cooperative Oceanic Fisheries Investigations Reports. 23:180-187.

Brewer, P.G. 1975. Minor Elements in Seawater, in, J.P.Riley and G.Skirrow, eds, Chemical Oceanography Volume I, 2nd. edition, Academic Press: London, pp.415-496.

California Regional Water Quality Control Board, Central Coast Region, 1985. Amended Order No. 85-101, NPDES No. CA0003751, Waste Discharge Requirements for Diablo Canyon Nuclear Power Plant, Units 1 and 2, San Luis Obispo County.

Dalgaard, S.B. 1982, Review of hydrazine/oxygen kinetics, Materials Performance. 21(4):32-38.

Ellis, S.R.M., G.V. Jeffreys, and P. Hill 1960. Oxidation of hydrazine in aqueous solution. Journal of Applied Chemistry. 10:347-351.

Fischer, H.B., E.J. List, R.C. Y. Koh, J. Imberger, N.H. Brooks 1979. Mixing in Inland and Coastal Waters. Academic Press: Orlando, Florida, 483pp.

Gaunt, H. and E.A.M. Wetton 1966. The reaction between hydrazine and oxygen in water, Journal of Applied Chemistry. 16:171-176.

Grove, R. S. 1987. Study introduction and generating station description, Report on 1987 Data, Marine Environmental Analysis and Interpretation; San Onofre Nuclear Generating Station, Southern California Edison Company, 88-RD-35, Rosemead, CA. pp.1:1-1:15.

Heath, R.L. 1971. Hydrazine as an electron donor to the water-oxidation site in photosynthesis, Biochimica et Biophysica Acta. 245:160-164.

Higginson, W.C.E., D. Sutton and P. Wright 1953. The oxidation of hydrazine in aqueous solution. I. Nature of 1- and 2-electron transfer reactions, Journal of the American Chemical Society. 77:1380-1386.

Institute of Marine Engineers 1978. Chemicals in Ships, Marine Management (Holdings), Ltd.: London, pp. 200-217.

Kirk-Othmer Encyclopedia of Chemical Technology 1978. Hydrazine and Its Derivatives. J.Wiley and Sons: New York. 12:734-741.

Lurker, P.A. 1976. Catalytic deoxygenation of aqueous solutions by by hydrazine, Aerospace Medical Research Laboratory. AMRL-TR-76-23, 25pp.

McNaughton, M.G., G.A. Urda, and S.E. Bowden 1978. Oxidation of hydrazine in aqueous solutions, CEEDO-TR-78-11; National Technical Information Service Index, 78(24):118, 37pp.

Mantoura, R.F.C., A. Dickson and J.P.Riley 1978. The complexation of metals with humic materials in natural waters, Estuarine, Coastal and Marine Science. 6:387-408.

Morel, F. M. M. and J.J. Morgan 1972. A numerical method for computing equilibria in aqueous chemical systems, Environmental Science and Technology. 6:58-67.

Moore, J.W. & R.G. Pearson 1981. Kinetics and Mechanism, 3rd edition, J. Wiley & Sons: New York, 455pp.

National Institutes for Occupational Safety and Health (NIOSH) 1978. Criteria for a Recommended Standard: Occupational Exposure to Hydrazines, NIOSH Document No. 78-172, Washington, D.C.

Pacific Gas and Electric Company, Nuclear Plant Operations Division 1987. Annual Summary Report on Discharge Monitoring at Diablo Canyon Power Plant During 1986, submitted to California Central Regional Water Quality Control Board, January 30, 1987. 98 pp.

Pesez, M. and A. Petit 1947. Bulletin societe chimique de France. **1947**: 122-123.

Schmidt, E.W. 1984. Hydrazine and Its Derivatives: Preparation, Properties, Applications, J. Wiley and Sons, New York pp.329-348.

Sillen, L.G. and A.E. Martell 1964. Stability Constants, Special Publication #17, The Chemical Society, London.

Sillen, L.G. and A.E. Martell 1968. Stability Constants: Supplement #1 Special Publication #25, The Chemical Society, London.

Sittig, M. 1985. Handbook of Toxic and Hazardous Chemicals and Carcinogens; 2nd edition, Noyes Publications, Park Ridge, NJ., 950pp.

Skrotzki, B.G. and W.A. Vopat 1960. Power Station Engineering and Economy, McGraw-Hill Book Company: New York, pp.360-362.

Slonim, A.R. and J.B. Gisclard 1976. Hydrazine Degradation in Aquatic Systems, Bulletin of Environmental Contamination Toxicology. 16:301-309.

Smith, R.M. and A.E. Martell 1976. Critical Stability Constants; Volume #4: Inorganic Complexes, Plenum Press: New York.

Stumm, W. and J.J. Morgan 1981. Aquatic Chemistry, 2nd. edition. Wiley Interscience: New York, 780pp.

Watt, C.W. and J.D. Chrisp 1952. A spectrophotometric method for the determination of hydrazine, Analytical Chemistry. 24:2006-2008.

Young, D.R., 1979. A comparative study of trace metal contamination in southern California and New York bights, in Proceedings, Ecological Effects of Environmental Stress in the New York Bight and Estuary, Symposium, June 10-15, 1979, New York.

Zafirou, O.C. 1976. Nitrite photolysis in seawater by sunlight, Marine Chemistry. 8(1):9-32.

Zirolli, J.A., 1980. Environmental Chemistry of Hydrazine Fuels, in JANNAF Safety and Environmental Protection Specialist Session, CPIA Publication 1313, April, 1980, pp.1-10.

CHAPTER 6

PREDICTING INHIBITION UNDER VARYING ENVIRONMENTAL CONDITIONS

I. INTRODUCTION

Ninety-six hour assays were useful standardized tests for comparing compounds of different toxicities or for comparing toxicity of one compound among several organisms, but they have several limitations:

1) Tests could not predict inhibition caused by exposures for intervals shorter than 96 hours. Power-plant discharge records showed that hydrazine was usually released in seven-to-fifteen hour pulses of varying concentration (Table 4.1, Figure 4.9).

2) Bioassays are usually run at constant temperature to minimize variability in results, but gametophytes exist in a fluctuating thermal environment. Temperatures in central California waters varied seasonally from 10° to 17°C (James et al., 1988). Bottom temperatures in shallow waters in the vicinity of a surface buoyant plume may vary as tidal action alternately raises and lowers the plume with respect to the bottom.

3) The gametophytic life cycle has several distinct phases (Levyns, 1933; Luning and Neushul, 1978). Effects on vegetative growth of an early hydrazine exposure (i.e., during germination) might differ from effects of a late exposure (i.e., during generation of reproductive structures).

Assays simulating episodic hydrazine discharges into varying conditions were required to develop adequate predictions of toxicity

effects. Kuwabara (1980, 1981, 1982) and Anderson (1982) previously used multivariate experimental designs to determine optimum micronutrient requirements for Macrocystis pyrifera gametophytes and blade-stage sporophytes. Similar methods were applied to predictions of growth inhibition in experiments, where

a) Temperature, age and hydrazine concentration were varied for a fixed exposure time.

b) Hydrazine concentration and duration were varied at fixed age and temperature.

c) Temperature and hydrazine concentration were cycled to simulate tidal raising and lowering of a low-dilution plume.

II. MATERIALS AND METHODS

Macrocystis pyrifera gametophytes were cultured using methods described in Chapter 2. Cultures were maintained in macronutrient-enhanced off-shore seawater, changed daily, until the designated day for exposure to toxicant. Short-duration hydrazine exposures (24 hours or less) were applied as a square wave (Figure 6.1). Control seawater was poured off and toxicant concentration poured into the culture dish. Toxicant solution was replaced with unadulterated macronutrient offshore seawater at the end of the designated exposure duration. Clean seawater was then changed daily until the end of the experiment. Toxicant solutions were replaced daily with fresh solutions of similar concentration when exposures exceeded 24 hours. Cultures at the 96-hour endpoint were placed in a 2°-4°C dark

Figure 6.1: Time sequence of events in transient-exposure vegetative growth toxicity assays using Macrocystis pyrifera gametophytes.

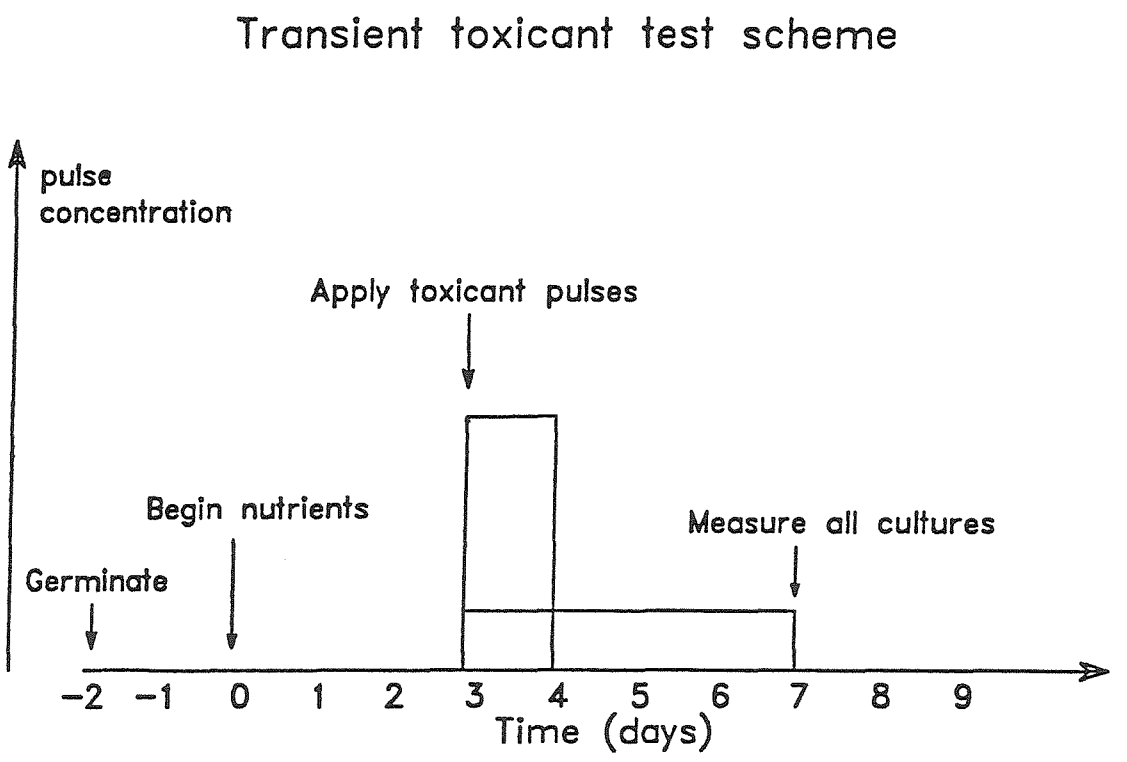

refrigerator to stop growth and then measured with digital image analysis techniques as described in Chapter 3.

Data for all combinations of independent variables in each experiment were combined into large (500-1200 point) ASCII files for analysis of variance and multiple regression tests on an IBM-PC/XT microcomputer (STSC, 1987). All tests of significance were performed using individual data points. Large within-group error caused by large variation in individual gametophyte areas, varying sample sizes and unbalanced experimental designs occasionally gave computational errors which limited the number of statistical tests that could be performed on the data. Linear, least-squares minimization regressions were derived when analyses of variance in the entire data sets showed significant effects of the independent variables, but only means were plotted to illustrate trends more clearly. The resulting equations were algebraically manipulated to construct contour maps predicting inhibitions at intermediate combinations of independent variables.

III. MULTIVARIATE EXPERIMENTS

A. M.PYRIFERA SERIES AB: INTERMITTENT HYDRAZINE EXPOSURES

(1) Data Reduction Methodology

Relationships between concentration and time in the destruction of organisms were first developed by Chick (1908), who found that destruction of anthrax spores by several disinfectants followed the relation:

$$\frac{dN}{dt} = -kN \qquad (6.1)$$

When integrated:
$N = N_o$ at $t = 0$

$$\ln \frac{N}{N_o} = -kt, \qquad (6.2)$$

where k is the destruction rate per unit time specific for each disinfectant, N is population density, and t is elapsed time.

Watson (1908) modified the k in Chick's law to include chemical concentration and a lethality factor:

$$\ln \frac{N}{N_o} = - E C^n t, \qquad (6.3)$$

where E is the lethality factor, C is constant disinfectant concentration and n is the experimentally determined reaction order.

Although destruction of some bacteria and viruses in water-treatment and wastewater-treatment systems followed kinetics described by the Chick-Watson theory (Berg, 1964; Floyd et al., 1978), disinfection processes may deviate from the constant kill rate described in Equation (3). Kill rates may increase (multicellular organisms) or decrease (some viruses) as a function of contact time (J.M. Montgomery, 1985). Gard (1957, cited in Selleck et al., 1978) proposed a mathematical form for declining kill rate as a function of time in the destruction of viruses:

$$\frac{dN}{dt} = \frac{- kN}{1 + a (Ct)}, \qquad (6.4)$$

where N, C and t are defined as above,

k = first order rate of deactivation at time = 0

a = rate coefficient.

When integrated, the equation becomes:

$$\frac{N}{N_o} = [1 + a(Ct)]^{-k/a}. \quad (6.5)$$

Selleck, et al., (1970; cited in Metcalf and Eddy, 1979) applied similar methodology to the destruction of Escherichia coli in a chlorine contactor and found that the data fit the relation:

$$\frac{N}{N_o} = (1 + 0.23\ Ct)^{-3}. \quad (6.6)$$

where C was expressed in units of parts per million (ppm) and t in was contact time in minutes. Collins and Selleck (1972, cited in J.M. Montgomery, 1985) and Selleck et al., (1978) revised this model to include a toxicity threshold below which no inhibition occurred:

$$\frac{N}{N_o} = 1 \quad \text{for} \quad Ct < D \quad (6.7)$$

$$\frac{N}{N_o} = \left[\frac{Ct}{D}\right]^{-n}, \quad (6.8)$$

where D is a threshold dose[1] below which no effect was observed.

Chick-Watson and Gard-Selleck models have been applied to larger organisms in several ecotoxicological studies. Lammering and Burbank (1961) and Brown et al., (1969) showed that Chick-Watson relationships could be applied respectively to destruction of bluegill sunfish by phenols, and rainbow trout by ammonia, phenol and zinc. Chen and Selleck (1969) showed that a threshold model similar to Equations (6.7) and (6.8) explained data obtained in toxicity

[1]Dose is defined here as the product of concentration and time.

studies of the common guppy. Jensen and Hann (1976) combined Chick-Watson relations with dispersion models to predict toxicity effects of hazardous material spills in rivers and estuaries.

Although not mechanistic, empirical Chick-Watson and Gard-Selleck models have adequately described mortality for a number of organisms and toxicants. Use of this methodology to develop predictive relationships between inhibition of gametophyte vegetative growth and concentration and duration of episodic hydrazine releases might assist regulation of power-plant emissions. Vegetative growth inhibition was chosen as the output variable in gametophyte studies because mortality (the criterion used in animal and bacterial studies) was difficult to detect. A fixed-time endpoint was used when assessing impacts of episodic toxicant exposures on Macrocystis gametophyte growth. Renewed vegetative growth after some short, mild treatments sometimes partially obscured results, but a fixed endpoint measurement was relevant since the goal was detection of inhibition compared to controls. Gametophytic areas were measured at the end of 96 hours' exposure regardless of toxicant pulse duration. Fixed-time endpoints were similarly used in studies of intermittent chlorination toxicity to fish (EPRI, 1982), where mortality was measured at a fixed endpoint regardless of duration of the chlorine exposure.

(2) Results

Two-way analysis of variance on the complete data set showed that although scatter was large, each independent variable explained a significant portion of the experimental variance in the raw data.

Twenty-five percent of the variance was explained when concentration and time were multiplied together and log-transformed to form a single variable (Table 6.1). The combined variable explained more of the variance in the data set than was accounted for by either independent variable when considered separately. Logarithmic transformations of the data redistributed measurements evenly across the ranges of the independent variables, minimizing "steering" of the computed regression by extreme values. A declining trend in size vs. dose was observed when $\log_e$-transformed size data were plotted against the $\log_e$-transformed combined independent variable (Figure 6.2).

Mean sizes, measured 96 hours after the start of all pulses (Table 6.2) generally declined with increasing concentration at any exposure time and with increasing exposure time at any concentration. Means were rendered dimensionless by dividing by the mean area of the control culture (Table 6.3). Inhibition generally increased linearly with increasing concentration at each duration (Figure 6.3). Data were transformed to logarithms and plotted against $\log_{10}(1 + \text{concentration} \times \text{time})$ (Gard, 1957, Selleck et al., 1970). Results clustered in a pattern suggesting a linear relationship between log hydrazine dose (concentration * time) and degree of vegetative growth inhibition[2] (Figure 6.4A).

---

[2]Degree of inhibition is the ratio of mean treated organism size to mean control organism size.

Table 6.1: Analysis of Variance for Series AB area on pulse duration (hours) and concentration (ppb)

Source of variation	Sum Squares	d.f.	Mean square	F-ratio	Sig. level
MAIN EFFECTS	51.011895	15	3.4007930	16.619	.0000
MABTOT.hours	32.913383	10	3.2913383	16.084	.0000
MABTOT.ppb	31.435271	5	6.2870541	30.723	.0000
RESIDUAL	159.20676	778	.2046359		
TOTAL (CORR.)	210.21865	793	0 missing values were excluded.		

One-Way Analysis of Variance using combined variables

Data: LOG MABTOT.area Level codes: LOG (1 + MABTOT.ppb * MABTOT.hours)

Source of variation	Sum Squares	d.f.	Mean square	F-ratio	Sig. level
Between groups	57.42066	21	2.7343173	13.815	.0000
Within groups	152.79799	772	.1979249		
Total (corrected	210.21865	793	0 missing value(s) were excluded.		

Tests for Homogeneity of Variances

Cochran's C test: 0.0983115 P = 9.44115E-4
Bartlett's test: 1.08271 P = 1.02012E-5
Hartley's test: 4.39945

All three tests show that we must reject null hypothesis that data come from population w/ normal distribution.

REGRESSION ANALYSIS USING COMBINED VARIABLES IN THE FORM OF A DOSE:
Dose = Concentration * Exposure Time
Regression Analysis - Linear model: Y = a+bX

Dependent variable: Log (Area): Independent variable: Log(1 + ppb*hours)

Parameter	Estimate	Standard Error	T Value	Prob. Level
Intercept	6.31974	0.0922447	68.5106	.00000
Slope	-0.173535	0.0124707	-13.9154	.00000

Analysis of Variance in regression

Source	Sum Squares	Df	Mean Square	F-Ratio	Prob. Level
Model	41.29960	1	41.29960	193.6388	.00000
Error	168.91905	792	.21328		
Total (Corr.)	210.21865	793			

Correlation Coefficient = -0.443238 R-squared = 19.65 percent
Stnd. Error of Est. = 0.461824

Figure 6.2: Relationship between combined concentration-time variable and level means for M.pyrifera Series AB n=793.

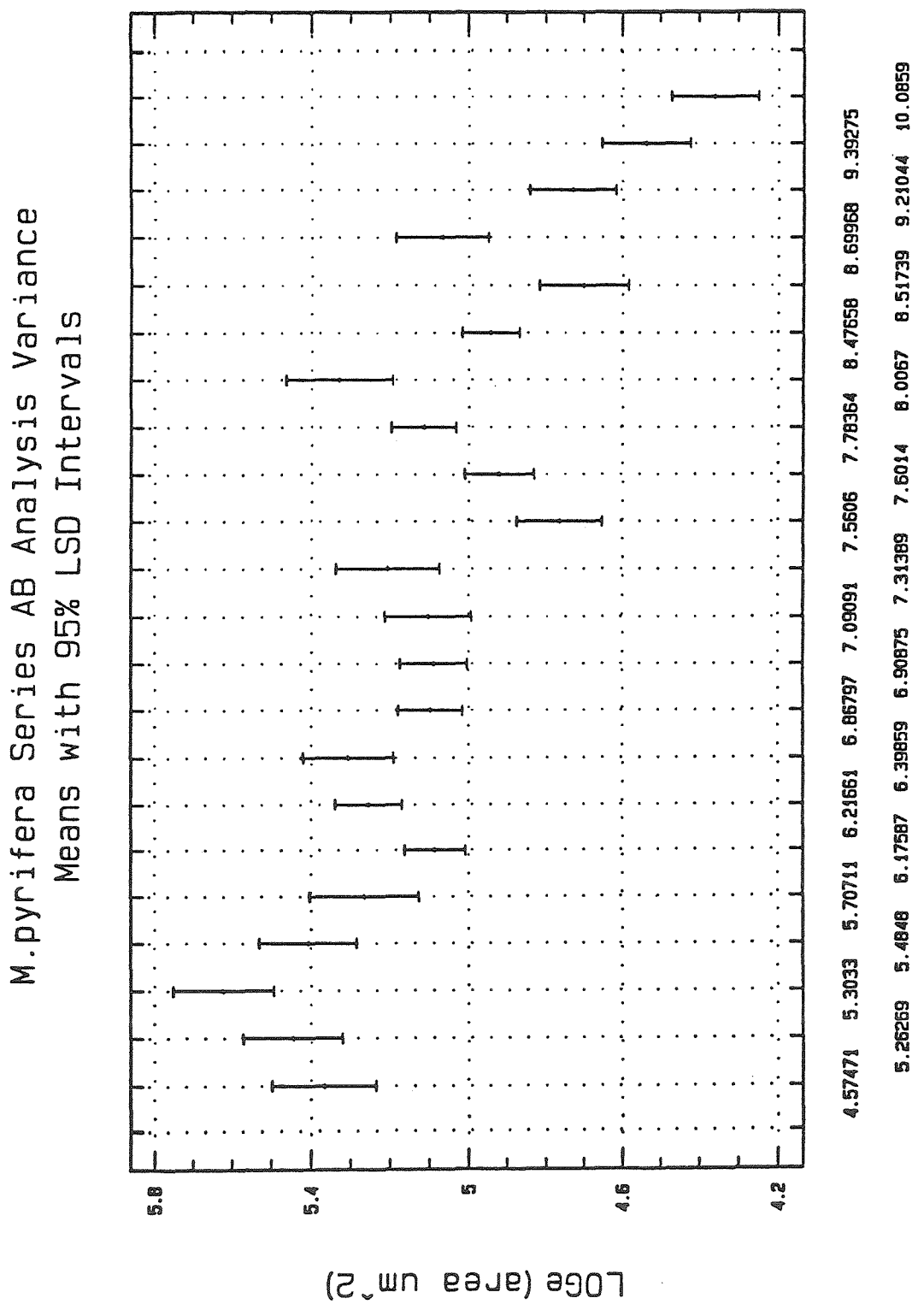

TABLE 6.2: Vegetative-Growth Inhibition of M.pyrifera Series AB gametophytes. Mean area w/95% confidence interval (um^2)

Control: 320/60 um^2

TIME hr	1	3	10	24	48	96
CONC ppb						
1						236/47
2						250/46
5					240/39	*179/29
10					*177/29	*165/18
20					*187/32	*128/19
50			*191/32	*178/25	*178/21	
100		*208/41	*161/27	*172/21	*135/13	
200	297/52	233/39	*162/24	*168/25		
500	227/41	*203/36	*118/16	*102/16		
1000	*205/40	228/45	*121/16	* 84/12		
2000	*154/34	*172/27				
5000	* 34/15$					

NOTES: * Significant (Student's t, $p < 0.05$) inhibition vs. control
$ Complete mortality and erosion of tissue. Size at time of death (84 um^2) was used in the regression equation.

TABLE 6.3: Ratio of test data to control; M.pyrifera Series AB
Control: 1.00

TIME hr	1	3	10	24	48	96
CONC ppb						
1						0.74
2						0.78
5					0.75	0.56
10					0.55	0.52
20					0.58	0.40
50			0.60	0.56	0.56	
100		0.65	0.50	0.54	0.42	
200	0.93	0.73	0.51	0.53		
500	0.71	0.63	0.37	0.32		
1000	0.64	0.71	0.38	0.26		
2000	0.48	0.54				
5000	0.10$					

Notes:$ Complete mortality and erosion of tissue. Used size at time of death (0.25 of control) in statistical fits.

Figure 6.3: Macrocystis pyrifera Series AB mean inhibitions (error bars removed) vs. $\log_{10}$hydrazine concentration.

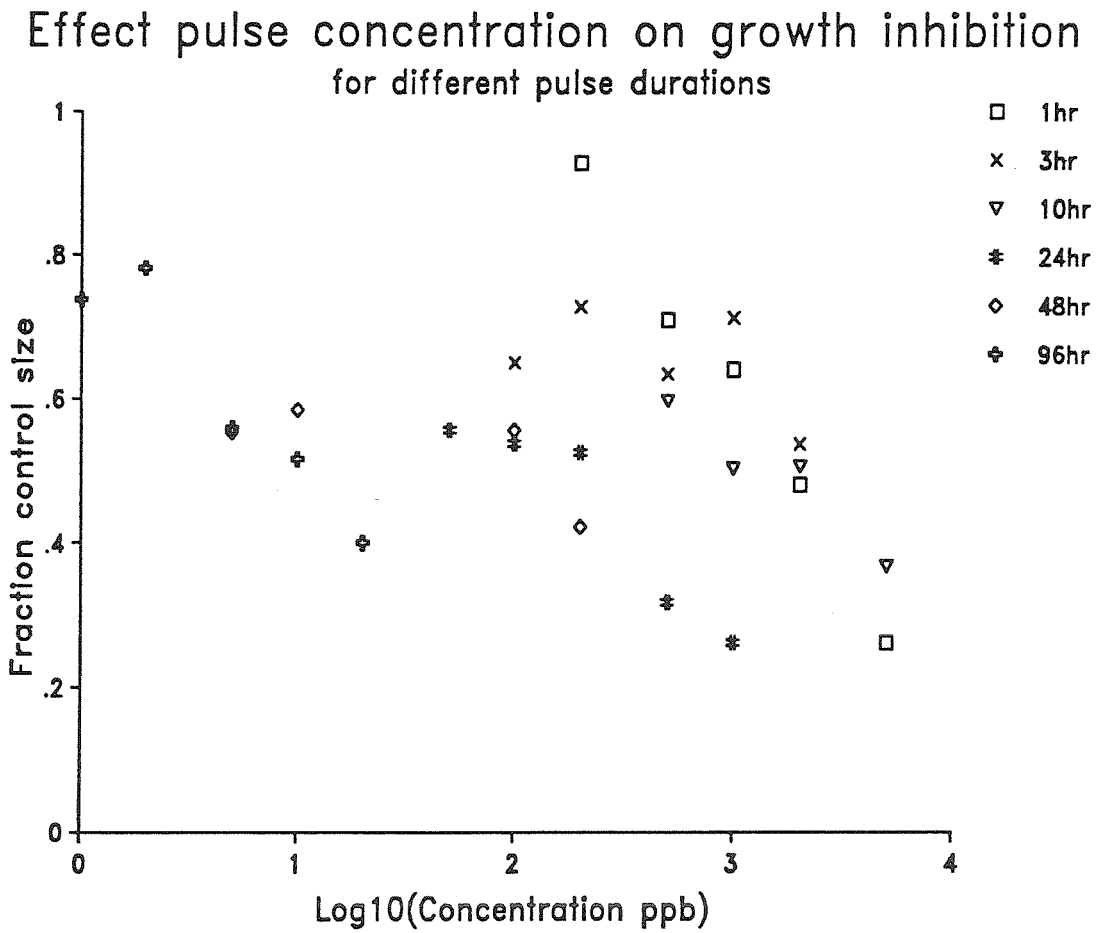

Figure 6.4A: M. pyrifera Series AB; Mean inhibition against combined hydrazine concentration-exposure time variable.
Units: Concentration expressed as parts per billion total hydrazine. Time expressed as hours of exposure to hydrazine

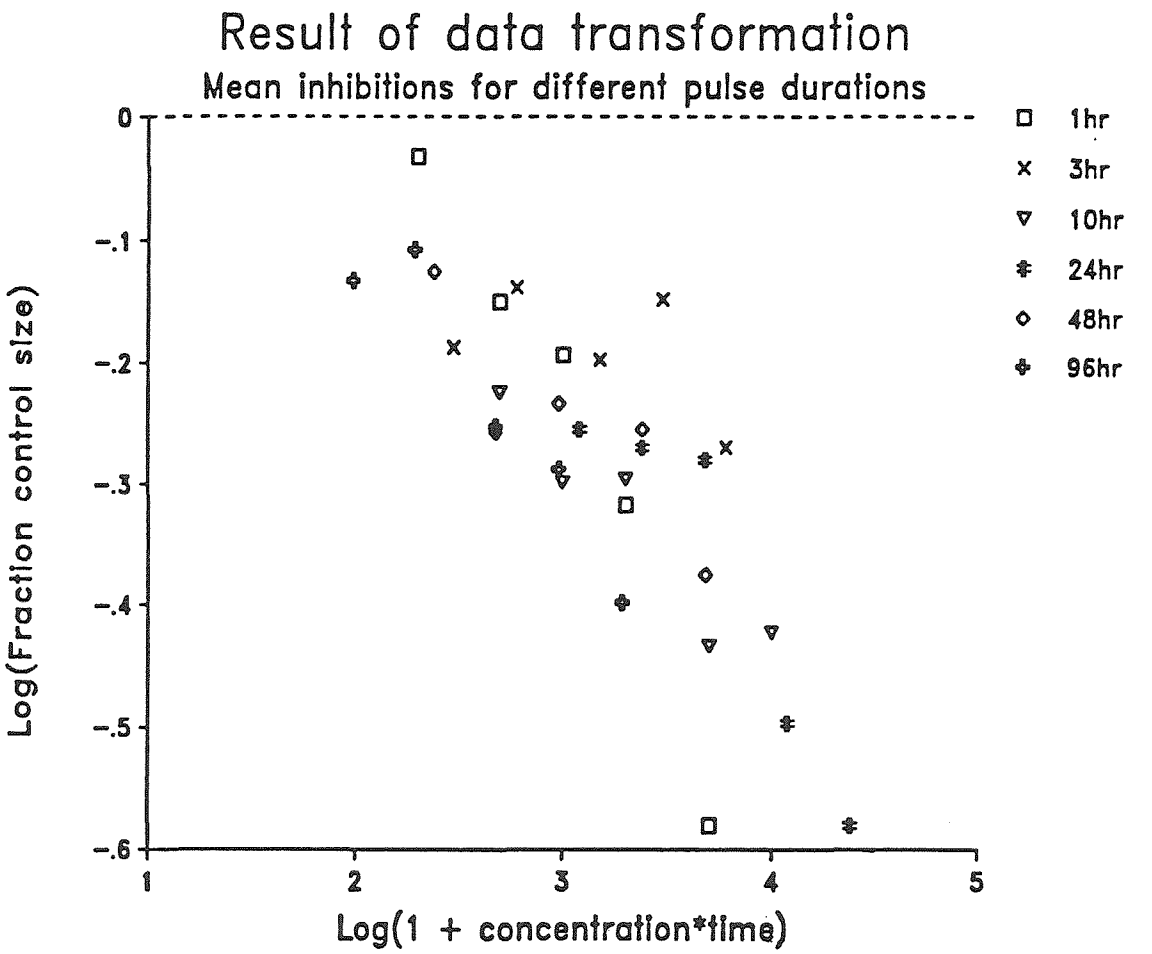

The best-fit equation from linear least-squares minimization was:

$\log_{10}$(fraction control size) = 0.314 - 0.187 $\log_{10}(1 + c \cdot t)$. (6.9)

uncertainty in coefficients: 0.078 0.017,

(valid for range $100 < ct < 24{,}000$), n = 30,

which explained 66 percent of the variance, a highly significant ($p < 0.001$) result (Figure 6.4B). Comparison of experimental mean inhibitions at each tested concentration to the predicted inhibitions reveals that four of the five three-hour means and three of the five one and twenty-four hour means occur above the regression, indicating that predicted inhibitions are likely to be conservative compared to actual experimental results.

A linear least-squares regression of $\log_e$ (size) on $\log_e$ (1 + concentration x time) for the complete data set produced a similar result after removal of 11 outliers:

$$\log_e (\text{Area}) = 6.388 - 0.180 \cdot \log_e (1 + c \cdot t), \quad (6.10)$$

uncertainty: 0.084 0.011 n = 782.

Twenty-five percent of the variance was explained by the regression[3], smaller than for the fit to the means because the within-group "noise" was not removed, but still a very significant ($p < 0.001$) result for a large data set. A scatter plot of actual and predicted inhibitions against $\log_e(1+ct)$ (Figure 6.5) showed symmetrical distribution of observations around predictions for the log-

---

[3]20% of the variance was explained before removal of the 10 outliers, still a significant result. Effect of outlier removal on coefficients was negligible.

Figure 6.4B: M. pyrifera Series AB least-squares fit to data means. Units: Concentration expressed as parts per billion total hydrazine. Time expressed as hours of exposure to hydrazine

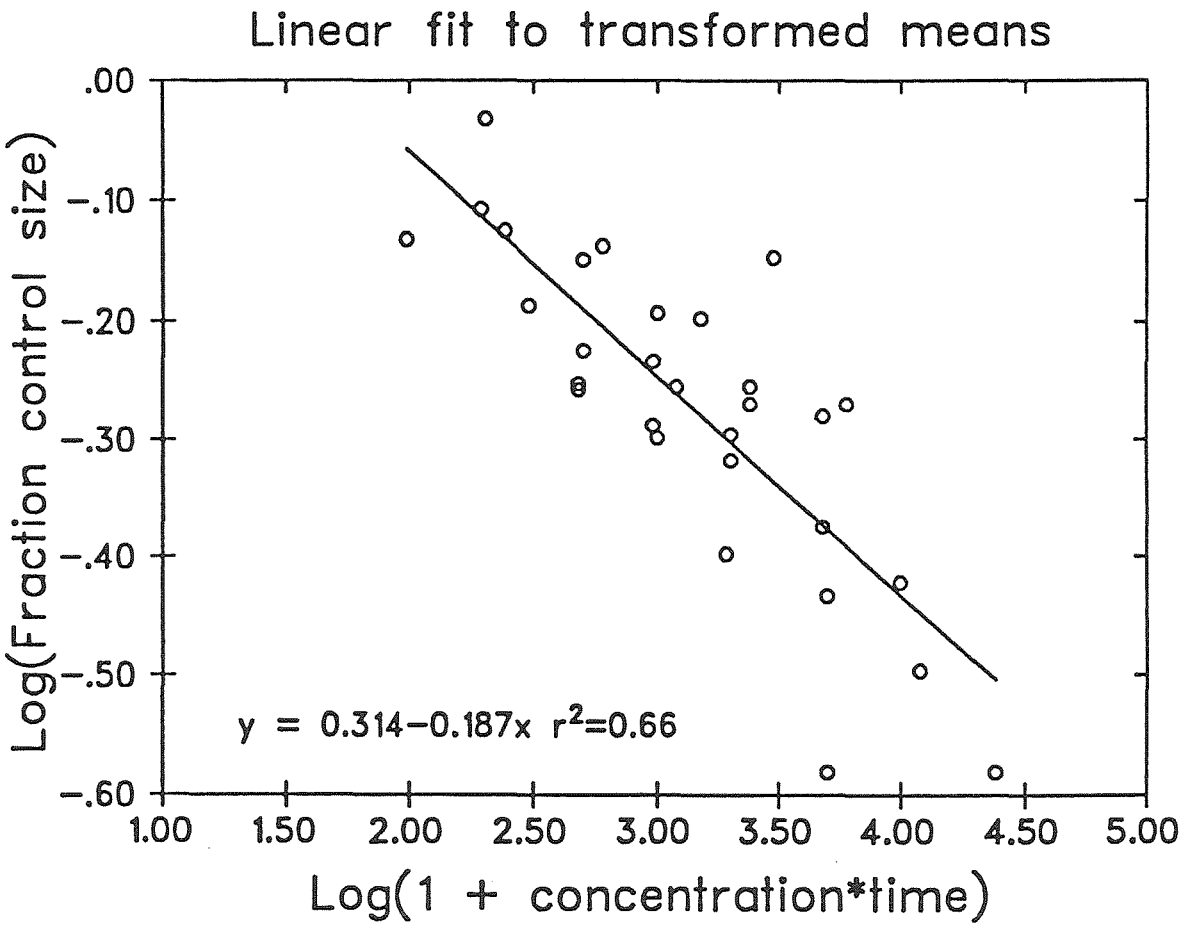

Figure 6.5: M. pyrifera Series AB; Least-squares fit to entire data set (n=793). X's indicate 11 outliers removed from analysis.

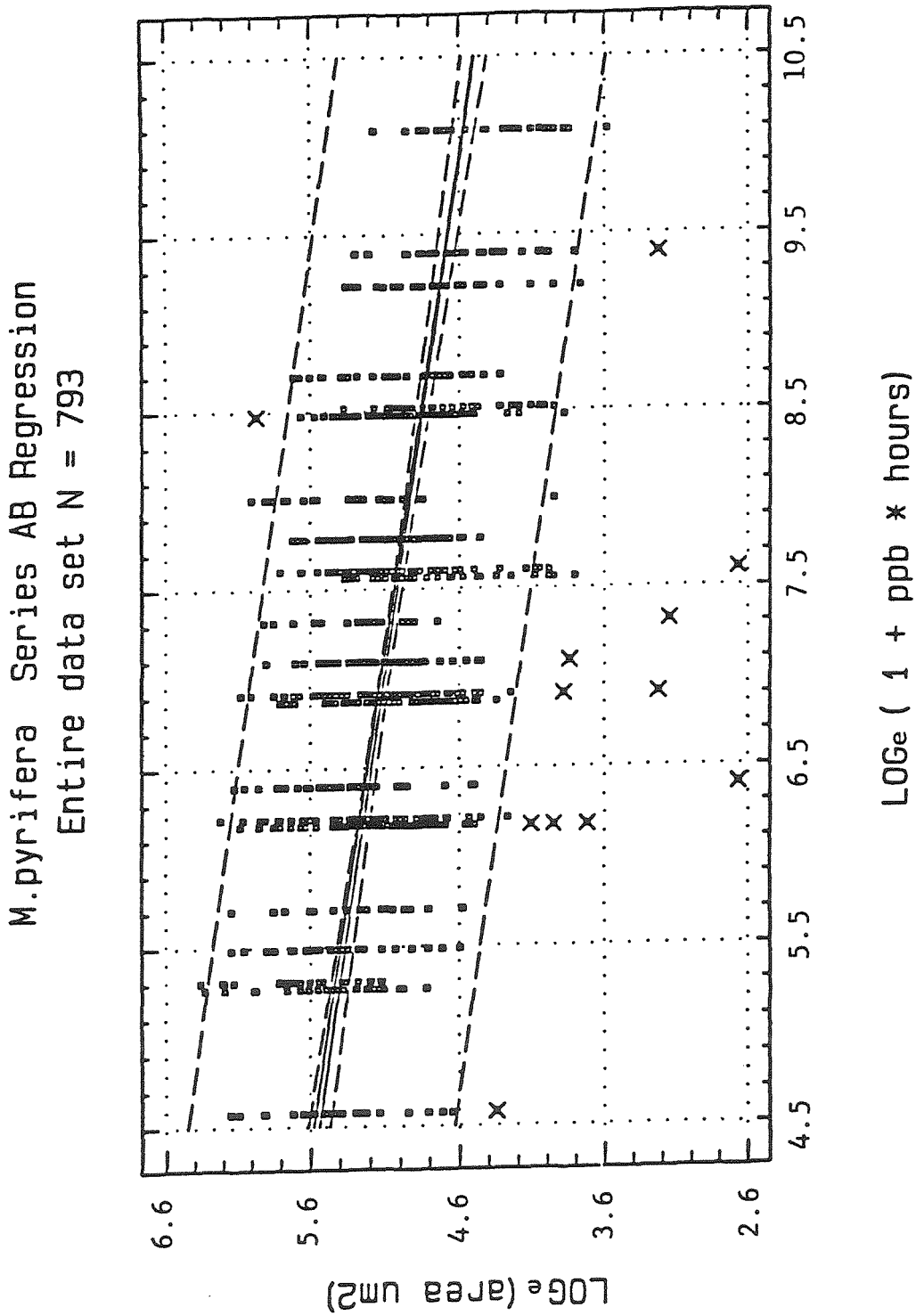

Figure 6.6: Contours of constant inhibition derived from regression on M. pyrifera Series AB data set plotted as hydrazine concentration vs. time of exposure. Symbols used to identify different curves. Uncertainty in each contour is ± 0.15 (i.e., the 0.50 contour is 0.50 ± 0.15).

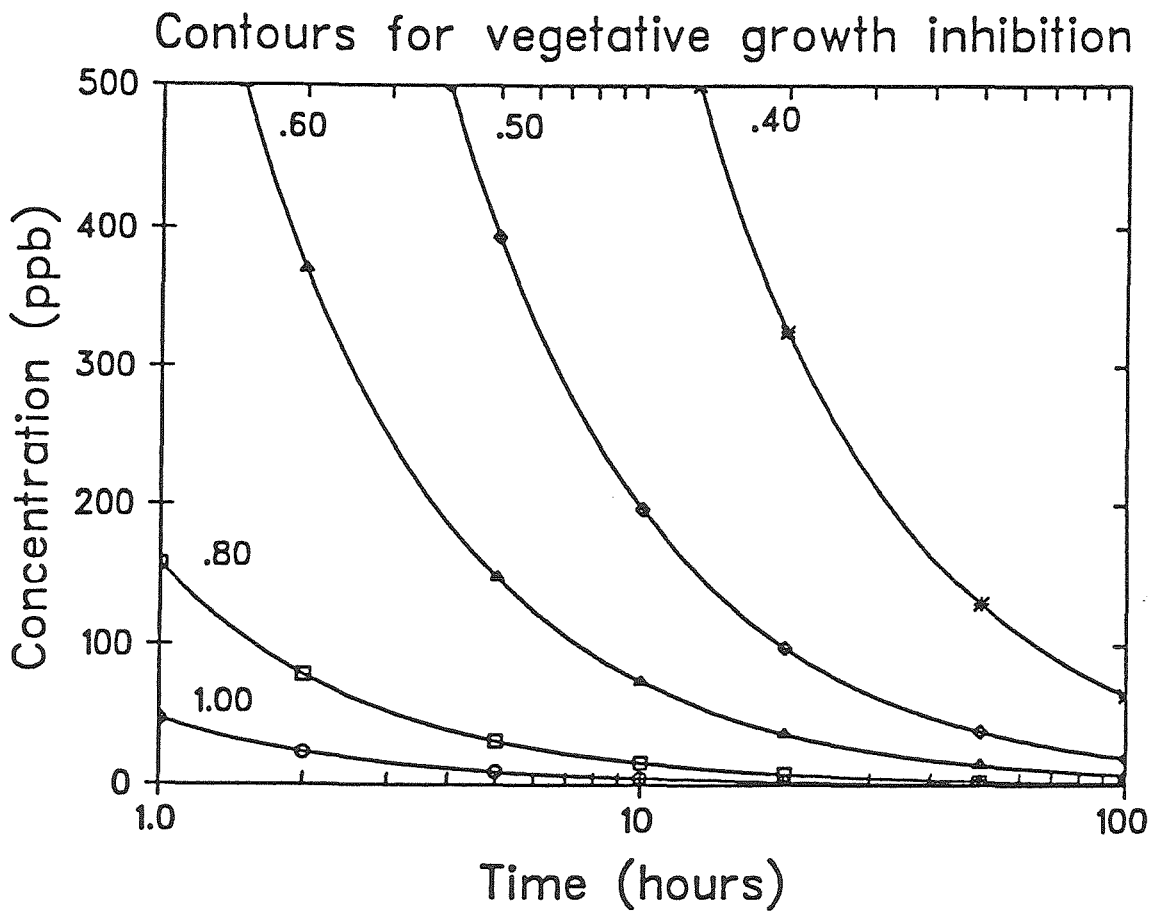

transformed data set. Slope was nearly identical to slope in the equation developed from the means.

When Equation (6.9) was rearranged to the following form:

$$ct = 10^{1.68}(\text{fraction control size})^{-5.35} - 1 \qquad (6.11)$$

and constant values of (fraction control size) were chosen, contours were generated that predict inhibition for combinations of pulse concentration and duration (Figure 6.6).

(3) Application to Electric Power Plant Emissions

Contour plots derived from Equation 6.11 were used to estimate the extent of growth inhibition for "events" of combined concentration and duration that might be released from an outfall. Estimates were made for the discharge "at the end of the pipe," before any dilution had occurred. Concentration-duration scatter plots for hydrazine emissions from the Diablo Canyon Power Plant (DCPP) during the April-May 1984 "incident," and calendar year 1986 normal operations (Figure 6.7) were combined with Macrocystis gametophyte inhibition contours derived from Equation (11) on one set of coordinate axes (Figure 6.8).

Three 1984 hydrazine releases could have caused vegetative growth inhibition. Virtually all 1986 emissions were below the abscissa on the toxicity contour plot, so none were toxic. A contour map was drawn to amplify the minimal vegetative growth inhibition region using criteria of 90, 95, and 99 percent of control growth (Figure 6.9) to show the utility of the technique in minimizing risk of inhibition. The contours are drawn for combinations of concentration and time occurring at the organism which produce the

Figure 6.7: Relationship of toxicity data range to undiluted power-plant emissions data for 1986 and April-May 1984.

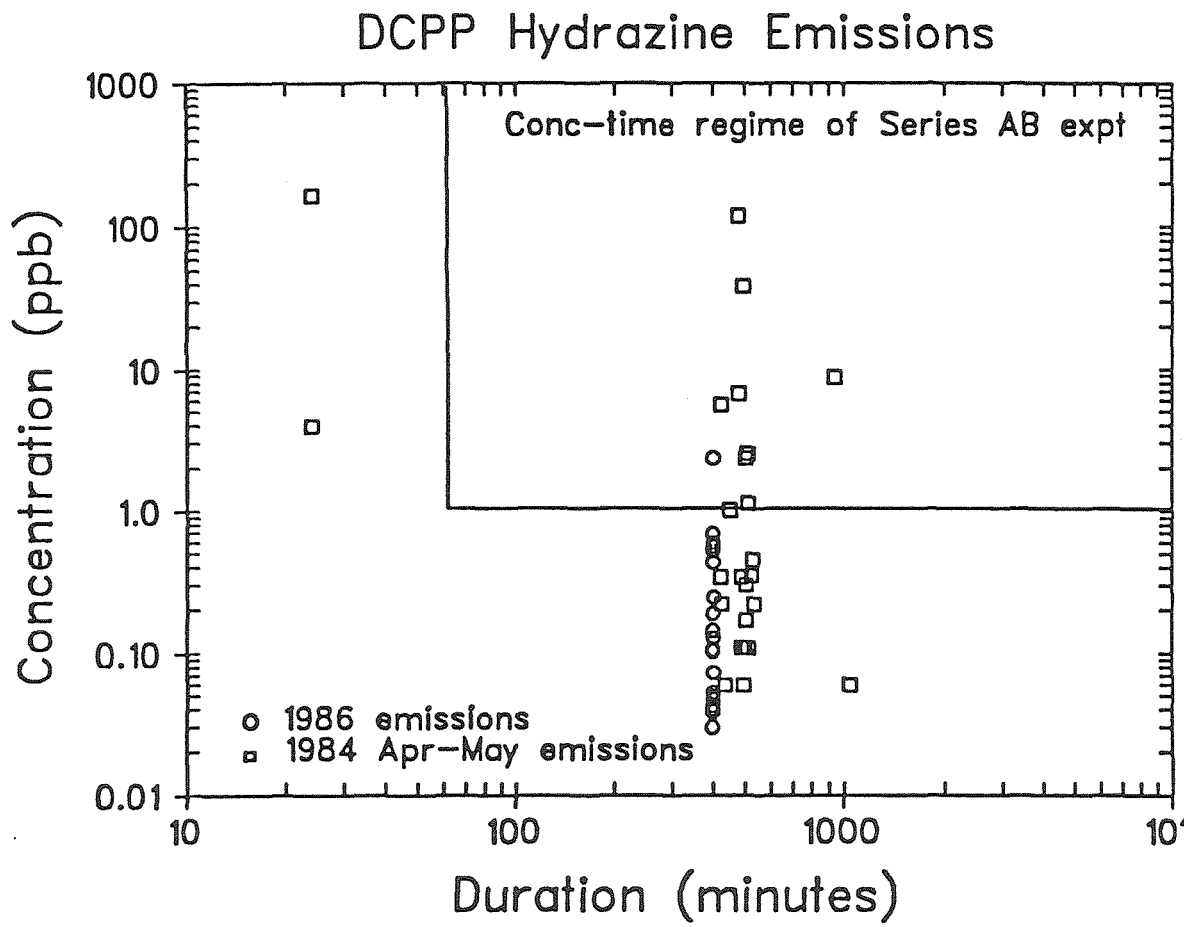

Figure 6.8: Superposition of estimated power-plant hydrazine concentrations (points) on contours for expected M. pyrifera Series AB 96-hour growth inhibition (lines). Points are shown for Diablo Canyon Power Plant for April-May 1984 (both undiluted and diluted 4:1) and for calendar year 1986, undiluted.

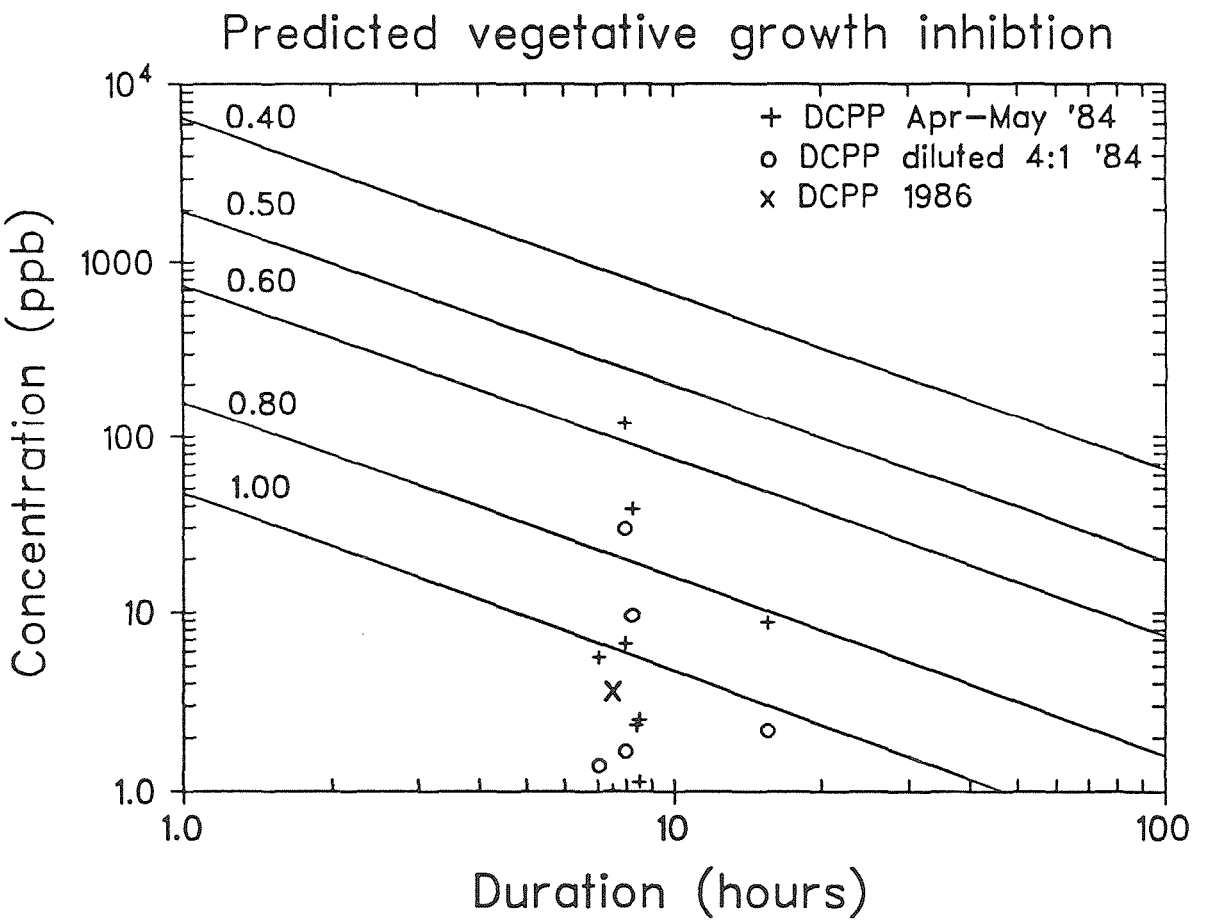

Figure 6.9: Contours near 100% of control growth demonstrating applicability for power-plant emissions regulation.

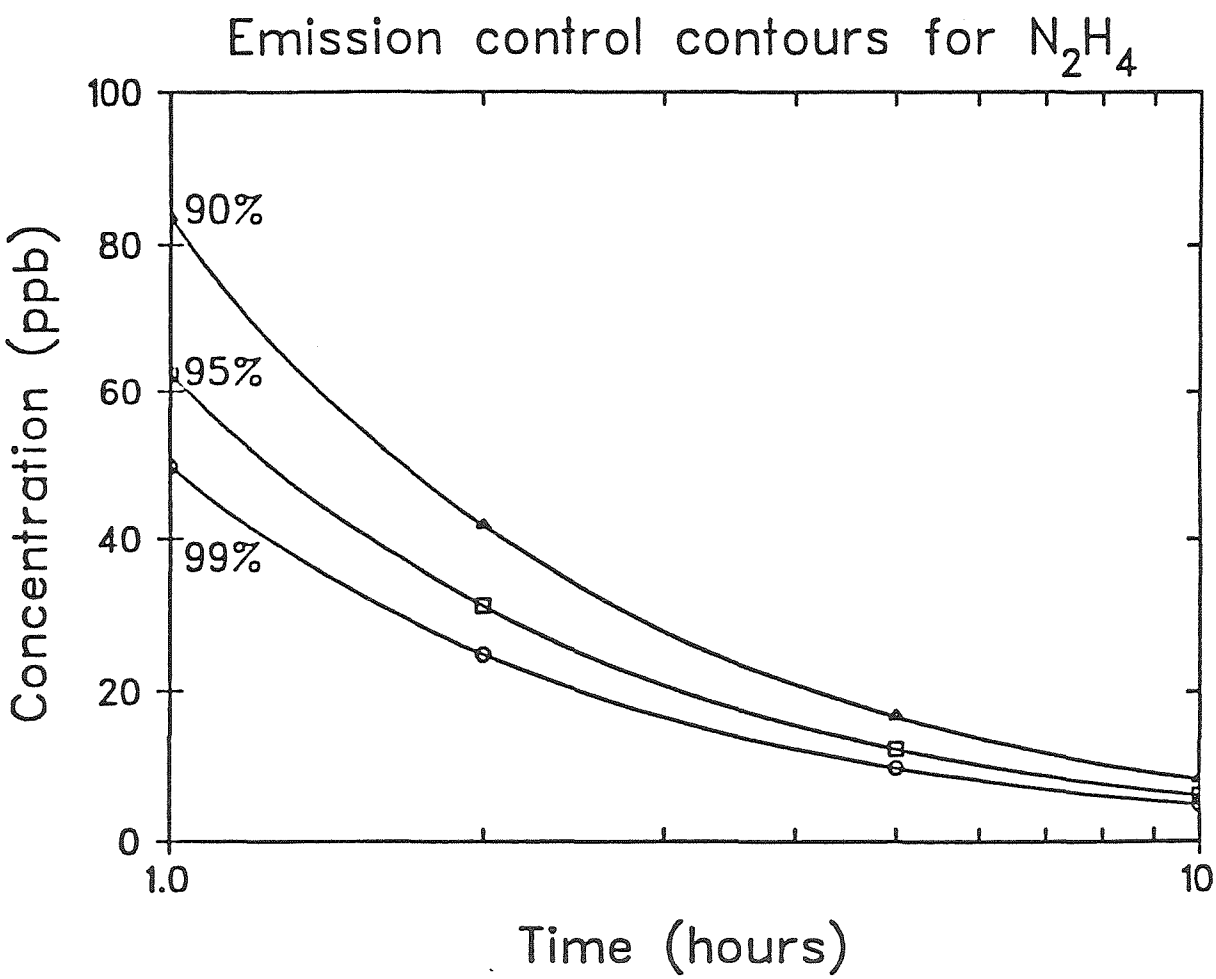

predicted inhibitions shown by the contours. This procedure builds in a factor of safety for toxicity estimates, as a power-plant operator could apply conservatively estimated dilution factors[4] for a specific outfall and calculate allowable hydrazine concentrations which could be emitted for specific durations at the end of the pipe which would not be toxic to Macrocystis gametophytes at the receptor sites. This result should be used with some caution, because uncertainty in any individual contour value is about ± 15 percent.

This method could be extended to other life stages and other species to predict their sensitivity to transient discharges of hydrazine or other compounds from marine industrial outfalls. Selleck et al., (1970, 1978) originally developed the technique to optimize destruction of bacteria in chlorine contactors. The technique could be applied to optimization of chlorine or heat treatments in power-plants so that control of fouling heat exchangers and other equipment is achieved with minimization of environmental impact.

(4) Test of Constant Dose Hypothesis

Series AB results suggested that degree of vegetative growth inhibition depended on a constant dose, the product of hydrazine concentration and exposure time. A repeat experiment was designed to verify this conclusion. Series AF gametophytes were exposed to a progression of six increasing exposure times and decreasing concentrations all of which had the same concentration x time

---

[4]Dilution factor is defined as the ratio of the total volume of a sample to the effluent volume in the sample. For example, a dilution factor of 4:1 means that in 1000 liters of well-mixed sample there is 250 liters of effluent.

product. Organism sizes were measured with digital image analysis equipment 96 hours after application of the pulses. Results were compared to predictions from the constant dose hypothesis.

Series AF gametophytes were half the size of Series AB gametophytes at the time of measurement (Table 6.3A). The degree of

Table 6.3A: Mean sizes and fraction inhibitions of *M. pyrifera* Series AF gametophytes after constant doses of pulsed hydrazine. Reported as Mean ± 95% confidence limits 96 hours after exposure. Asterisk (*) indicates significance ($p < 0.05$) compared to mean.

Time		Series AF		Series AB	
hours	Concentr. ppb	Size um^2	Fraction control	Size um^2	Fraction control
0	0	159 ± 23	1.00 ± 0.20	320 ± 60	1.00 ± 0.19
1	2000			154 ± 34*	0.48 ± 0.29*
2	1000	98 ± 8*	0.62 ± 0.18*		
5	400	83 ± 10*	0.52 ± 0.20*		
10	200	109 ± 14	0.68 ± 0.23	162 ± 24*	0.51 ± 0.24*
20	100	121 ± 14	0.76 ± 0.20		
50	40	88 ± 9*	0.55 ± 0.19*		
96	20	85 ± 9*	0.53 ± 0.19*	128 ± 19*	0.40 ± 0.24*
Predicted inhibition for ct = 2000 from eqn.(6.9): 0.50 +0.17/-0.14					

inhibition was less than observed for Series AB when identical treatments were compared. The 5, 50 and 96-hour Series AF exposures gave results that agreed closely with Series AB predictions. Readings at 10 and 20 hours were larger than expected. The data suggest that partial recovery may occur after doses of intermediate duration. Series AF results indicate that estimates of inhibition using the constant dose hypothesis may be conservative. Repeated experiments using the Series AB experimental plan might generate an inhibition regression with more general applicability.

B. M.PYRIFERA SERIES AD: EFFECTS OF AGE AND TEMPERATURE ON PREDICTED 96-HOUR INHIBITION OF GAMETOPHYTES BY HYDRAZINE

(1) Methods

Macrocystis pyrifera gametophytes were subjected to 96-hour 5 ppb doses of hydrazine at temperatures of 10°, 12°, 14°, 16° and 18°C and 96-hour 5 ppb and 10 ppb 10°C doses at ages of 1, 3, 5, 7 and 9 days to simulate field exposure at any time of year and at any time in their two-week life cycle. Five ppb hydrazine was chosen because it was the upper threshold concentration for prior 96-hour continuous assays (Chapter 4). Data were analyzed by two-way ANOVA and multiple linear regression techniques.

(2) Results

Five ppb hydrazine significantly inhibited growth at all tested combinations of age and temperature (Figures 6.10A and 6.11A). No significant difference in degree of inhibition at 5 ppb could be observed at any temperature (Figure 6.11B). Organisms aged five days and older generally showed larger inhibitions than organisms exposed earlier (Figure 6.10B).

Temperature had a significant effect on observed 96-hour control growth. Control organisms cultured at 12°, 14°, 16° and 18°C were significantly larger than the 10°C control cultures (Figure 6.10A). Although gametophytes grew at reduced rates in hydrazine, organisms cultured at 14°, 16° and 18°C in 5 ppb of this toxicant were significantly larger than the 10°C control organisms at the end of the 96-hour test (Figure 6.10A).

Figure 6.10: Age-dependence of M. pyrifera Series AD 96-hour continuous growth inhibition. Top: Dimensional data. Bottom: Ratio of control to treated inhibition.

(A)

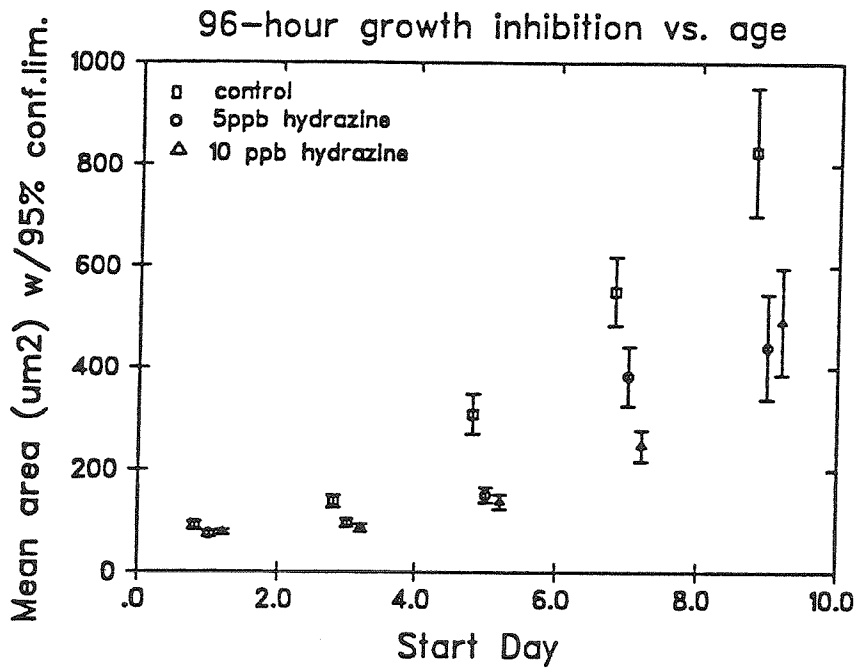

(B)

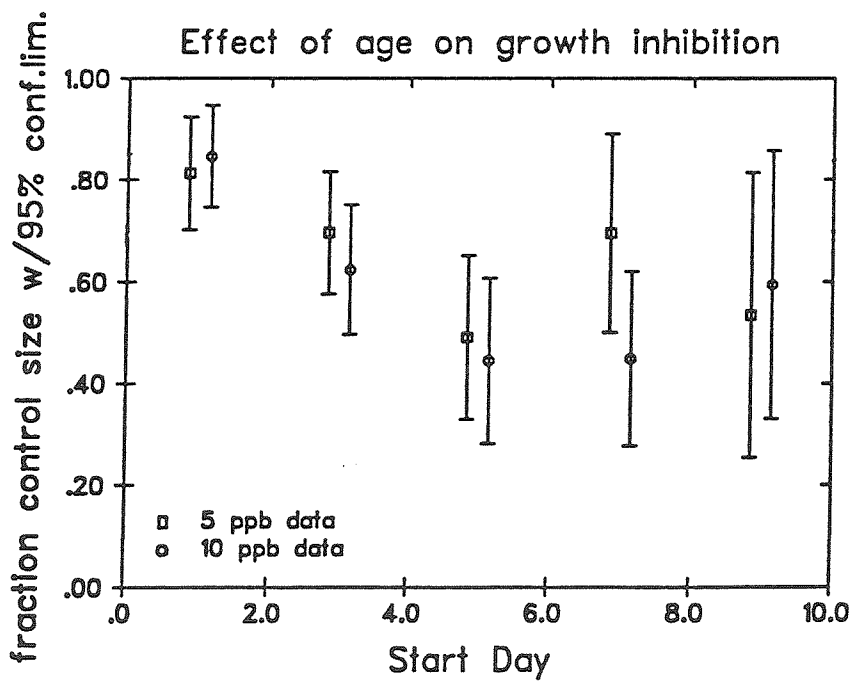

Figure 6.11: Temperature-dependence of M. pyrifera Series AD 96-hour continuous growth inhibition. Top: Dimensional data. Bottom: Ratio of control to treated inhibition.

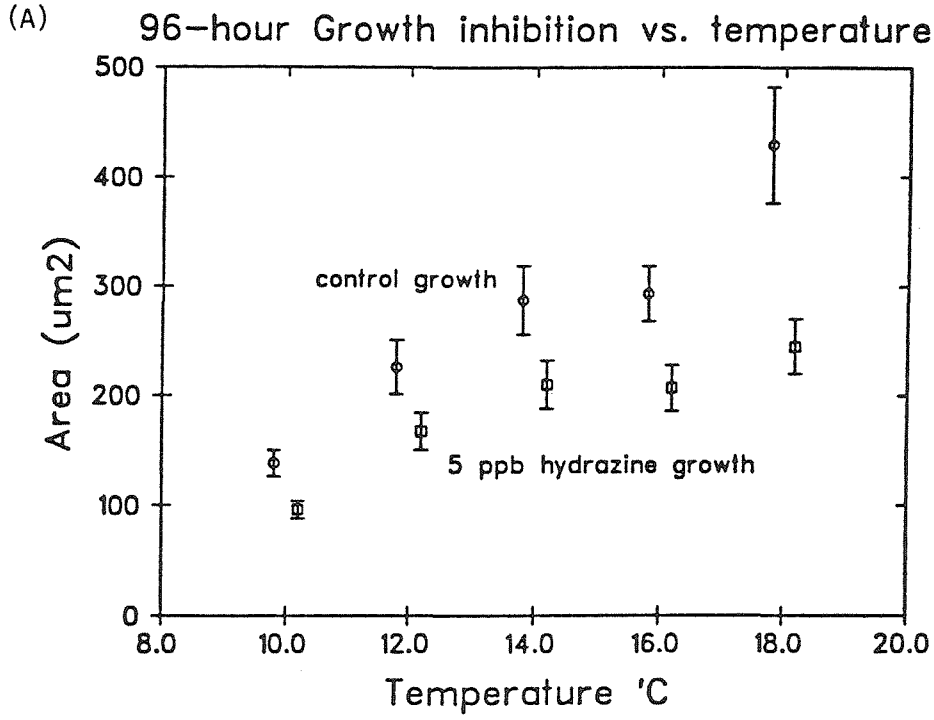

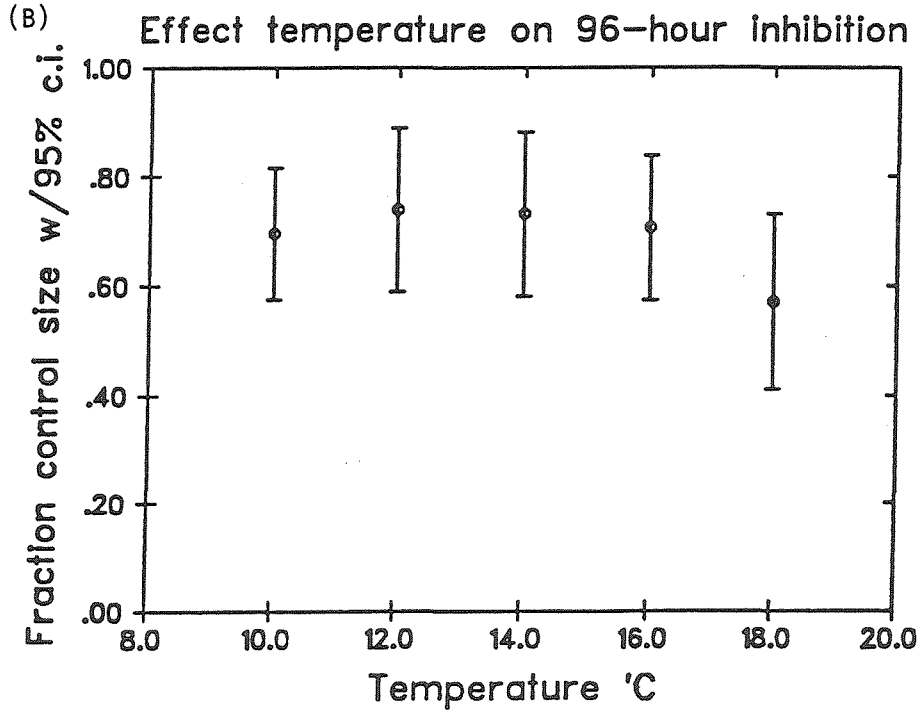

Three-way ANOVA (Table 6.4) indicated significant effects without interaction of each independent variable (start day, hydrazine and temperature), so a multiple linear regression was performed on the entire 1138 point data set using age, temperature and hydrazine as independent variables:

$$\text{Log}_e(\text{Area um2}) = 3.24 + 0.24\text{day} - 0.043\text{hydr} + 0.11\text{temp} \qquad (6.12)$$

Coefficient errors: 0.42 0.006 0.003 0.005

Equation (6.12) explained 66 percent of the variance in the complete data set, a highly significant ($p < 0.001$) result for this sample size. Opposite signs for the hydrazine and temperature coefficients showed that the two factors exert opposite effects on size of cultured organisms. Relative error in any predicted size was $\pm$ 20 percent. A few large organisms in each sample tended to skew size distributions towards the right (the top of each column of symbols in Figure 6.12A). Logarithmic transformations gave uniform distribution of observed variables around each prediction (Figure 6.12B).

A response surface (Figure 6.13) and contour map (Figure 6.14) of predicted size vs. temperature and hydrazine concentration was generated for five day-old gametophytes to illustrate the utility of Equation (6.12).

Results should be treated with caution because the experimental design was unbalanced. Not all possible combinations of age, temperature and hydrazine concentration were tested (Table 6.A.1). Validity of the regression depends on non-interaction of the independent variables in regions not tested in this experiment.

Table 6.4: Analysis of Variance for Series AD
Dependent variable: Log_e (gametophyte area in pixels)

Source of variation	Sum Squares	d.f.	Mean square	F-ratio	Sig. level
MAIN EFFECTS	400.34303	17	23.549590	151.530	.0000
Start day	294.29611	8	36.787014	236.707	.0000
Hydrazine concentr	42.13728	5	8.427456	54.227	.0000
Temperature °C	55.89104	4	13.972759	89.908	.0000
RESIDUAL	174.06115	1120	.1554117		
TOTAL (CORR.)	574.40419	1137			

Analysis of Covariance for Loge (area); Series AD

Source of variation	Sum Squares	d.f.	Mean square	F-ratio	Sig.level
COVARIATES	237.94348	1	237.94348	1000.000	.0000
Start Day	237.94348	1	237.94348	1000.000	.0000
MAIN EFFECTS	155.34777	9	17.260863	107.692	.0000
Hydrazine concentr	58.13415	5	11.626830	72.541	.0000
Temperature	72.37128	4	18.092820	112.883	.0000
2-FACTOR INTERACTIONS	1.1192343	5	.2238469	1.397	.2228
Hydrazine by temperature	1.1192343	5	.2238469	1.397	.2228
RESIDUAL	179.99370	1123	.1602793		
TOTAL (CORR.)	574.40419	1137			

0 missing values have been excluded.

COVARIATES	coefficient	
MADALL.start	.2476738	(average logarithmic growth rate)

Figure 6.12: Comparison of data distributions about predictions.
Top: Original data. Bottom: Log_e transformed data.

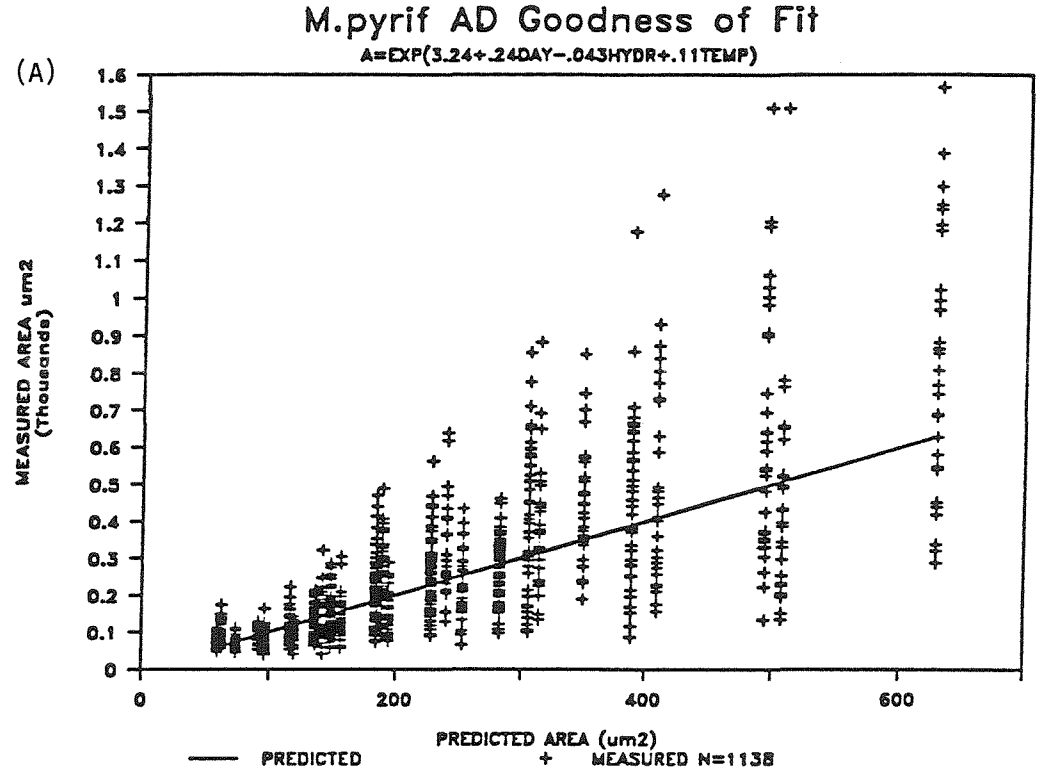

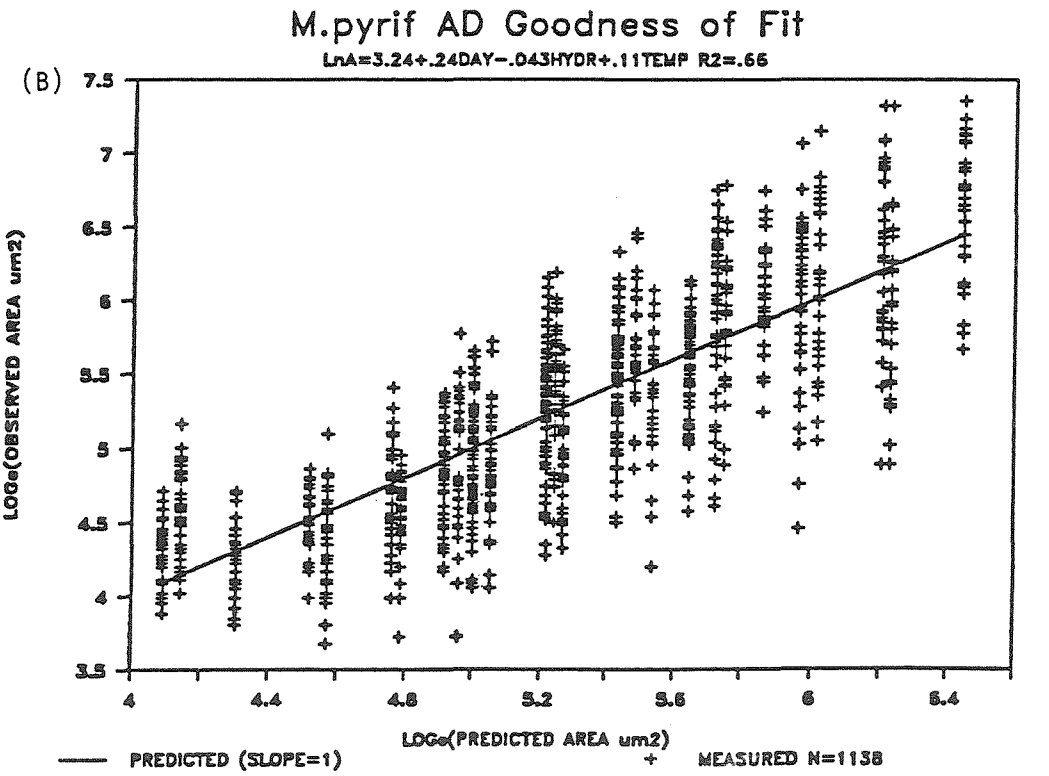

Figure 6.13: Predicted response surface from regression developed for M. pyrifera Series AD.

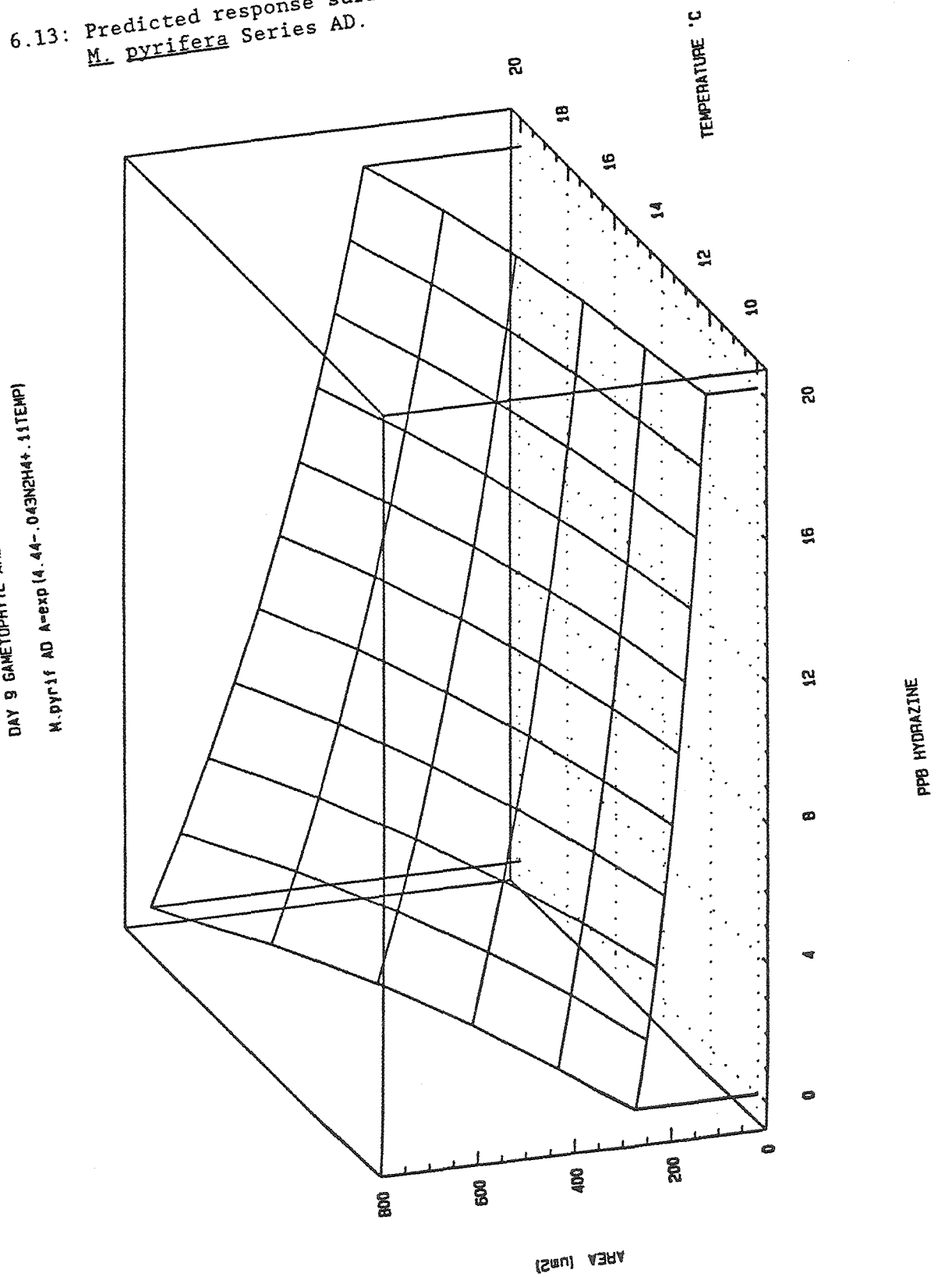

Figure 6.14: Contour map for prediction of Macrocystis pyrifera 96-hour gametophyte vegetative growth as function of hydrazine concentration and temperature. Contour values are mean expected gametophyte sizes as areas in square microns.

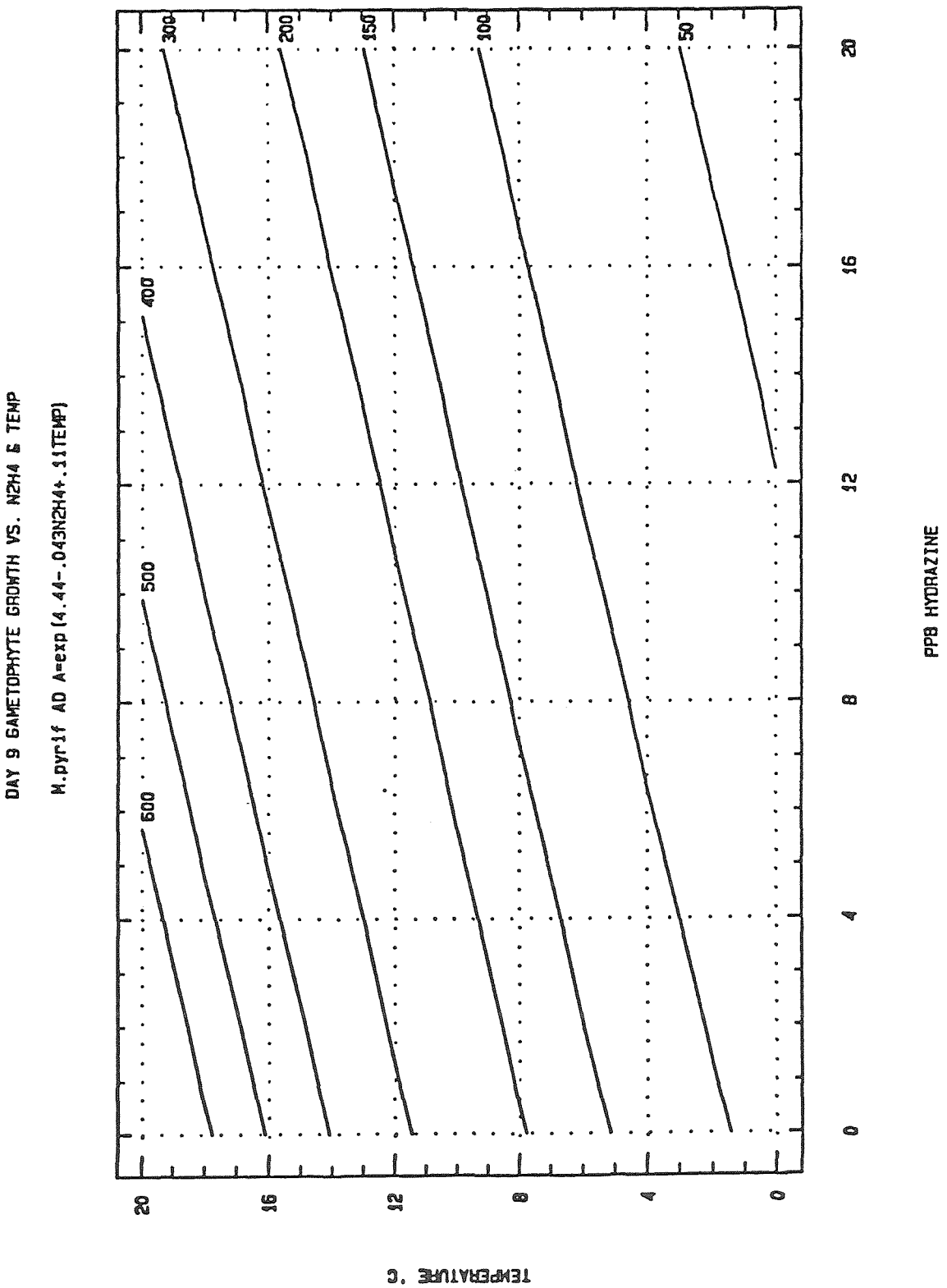

IV. MODELING CYCLIC EXPOSURE TO HYDRAZINE

INTRODUCTION

Several experiments were conducted which attempted to model worst-case hydrazine releases into Diablo Cove. Hydrazine and thermal exposure were combined in two experiments because the surface-buoyant plume remains partially distinct from receiving waters as it exits Diablo Cove. Hydrazine exposure might thus be expected to occur when gametophytes are exposed to warmer waters in the plume. Area of bottom contacted by the plume is known to vary with tidal height. Experiments simulated exposure to a single worst-case event and to 6 and 18 hour daily cyclic chemical exposures.

A. M.PYRIFERA SERIES AG: SINGLE WORST-CASE EVENT

(1) Methods

Two-day old Macrocystis pyrifera gametophytes collected from the vicinity of Diablo Cove were exposed to single 10°C and 20°C 10-hour 100, 200 and 300 ppb hydrazine pulses. Cultures were returned to 10°C clean seawater with daily static renewal and measured at the 96-hour endpoint.

(2) Results

Significant ($p < 0.05$, two-tailed Student's t-test) inhibition of vegetative growth occurred in all pulses (Figure 6.15). Analysis of variance (Table 6.A.2) showed significant interaction of temperature and concentration in determining size. Cultures exposed to 20°C, 200 and 300 ppb pulses were significantly smaller than cultures exposed to 10°C pulses. Cultures exposed 20°C, 0 or 100 ppb hydrazine were somewhat larger than those exposed at 10°C.

Figure 6.15: Interaction of concentration and temperature in vegetative growth inhibition of M. pyrifera Series AG gametophytes. Areas in Log_e(pixels).

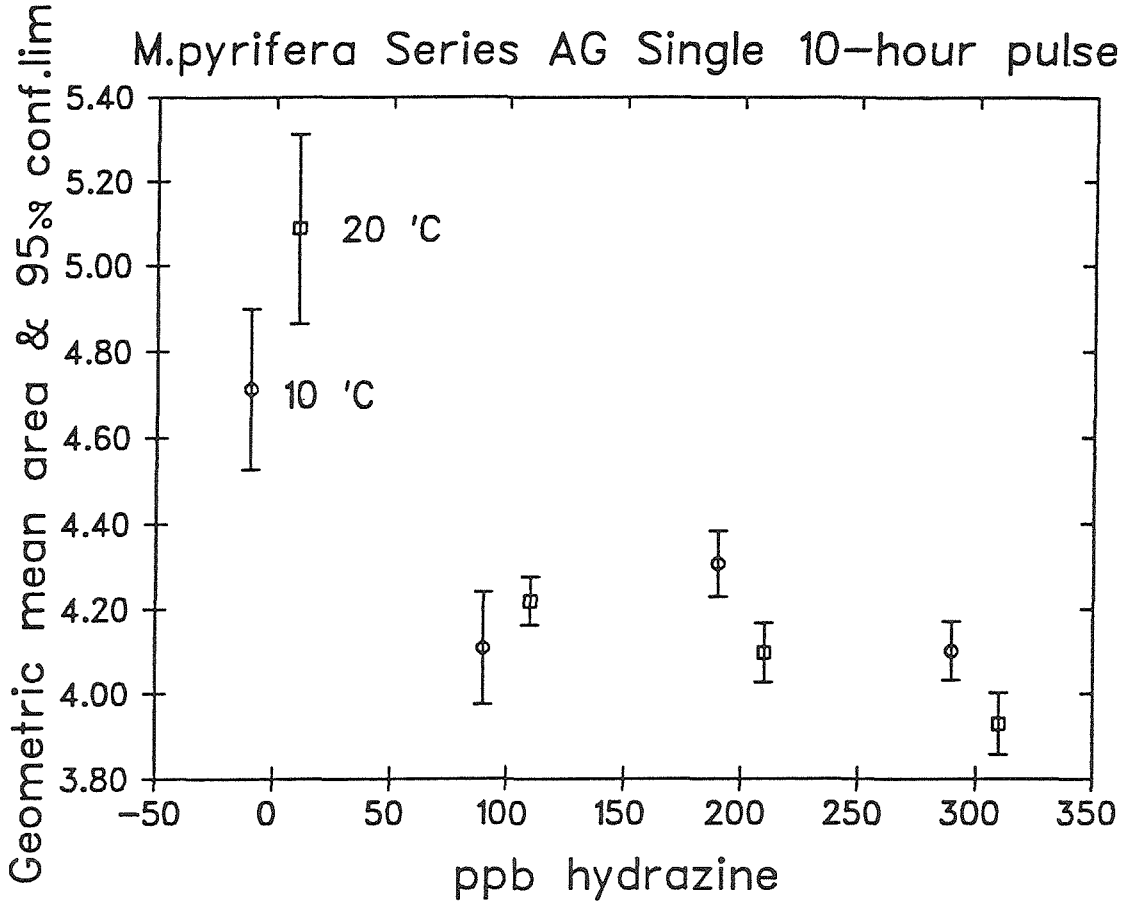

Cultures grown in clean seawater in a range of temperatures for 96 hours showed increases in size to 17.5°C then a slight drop at 20°C (Figure 6.16).

(3) Discussion

Short-term temperature exposure alone did not inhibit growth. Interaction of temperature and hydrazine concentration in this pulsed assay indicates that hydrazine toxicity might have been slightly elevated in "warm" conditions typical of powerplant effluent immediately after discharge into Diablo Cove.

Interaction between temperature and hydrazine obtained in this experiment runs contrary to findings in the Series AD continuous assays. The difference may be partially due to lower thermal tolerance of the Diablo Canyon vicinity gametophytes used for this experiment, although growth alone was stimulated at 20°C. Higher thermal optima for fertility and growth in southern California Macrocystis gametophytes has been previously observed (Luning and Neushul, 1978). Series AD organisms were sampled from Laguna Beach and may have had higher thermal tolerance. Resolution of the discrepancy could be obtained by performing continuous and pulsed hydrazine assays side by side in the same culture.

B. M.PYRIFERA SERIES M: CYCLED CHEMICAL EXPOSURE

(1) Methods

Cultures of Macrocystis pyrifera gametophytes were subjected to daily six-hour pulses of 0, 5, 25 and 250 ppb hydrazine, simulating exposure in a buoyant plume occurring only at low tide. Toxicant pulsing continued through gametogenesis and recruitment of embryonic

Figure 6.16: 96-hour growth of M. pyrifera gametophytes continuously exposed to different temperatures.

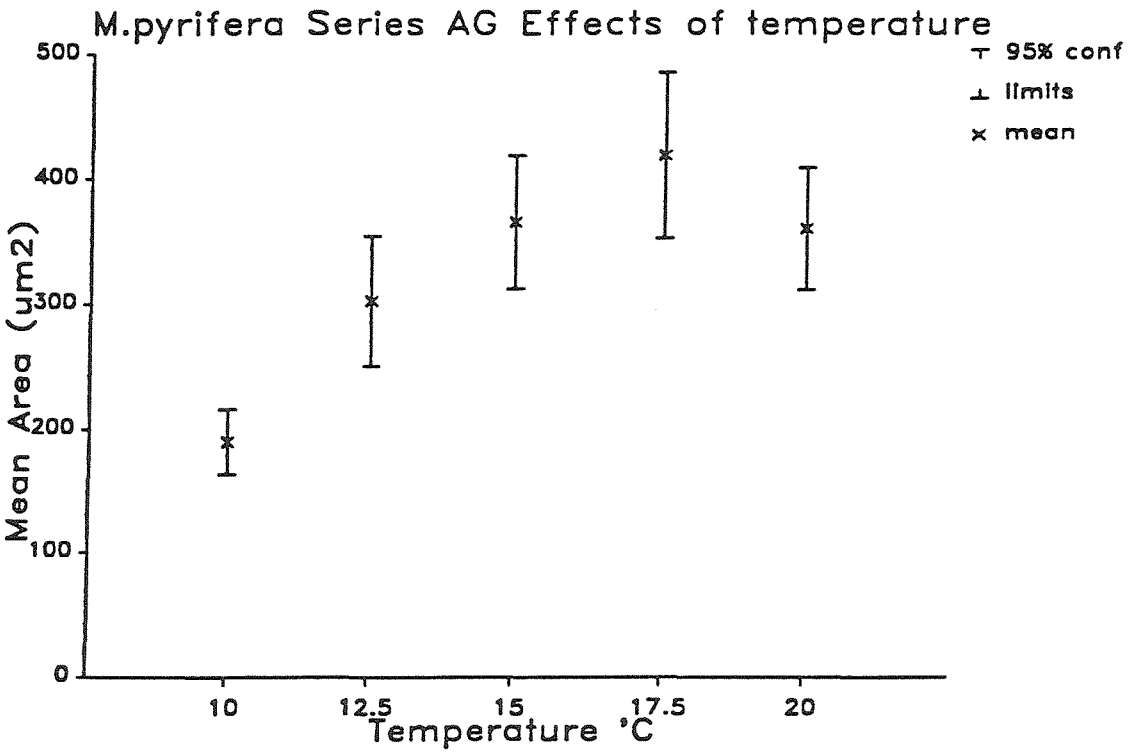

Table 6.5: One-way analysis of variance of effect of hydrazine concentration in 6-hour daily pulses on Series M gametophyte growth
Test of log-transformed area data against concentration (ppb)

Source of variation	Sum Squares	d.f.	Mean square	F-ratio	Sig.level
Between groups	1.553366	2	.7766830	5.603	.0046
Within groups	18.157989	131	.1386106		
Total (corrected)	19.711355	133			

Each group is a concentration. There were four concentrations: 0, 5, 25 and 250 ppb, but only three were evaluated on the day (Day 10) that gametophytic sizes in pulsed cultures were measured.

Table of means $\log_e$-transformed areas vs. concentration

ppb	Count	Loge(area) [average]	Stnd. Error (internal)	Stnd. Error (pooled s)	95 Percent Confidence intervals for mean	
0	41	5.5284038	.0469964	.0581442	5.4133551	5.6434525
25	47	5.4715399	.0643768	.0543062	5.3640854	5.5789945
250	46	5.2765004	.0518994	.0548933	5.1678842	5.3851167
Total	134	5.4219847	.0321622	.0321622	5.3583460	5.4856234

sporophytes. Areas of gametophytes and embryonic sporophytes were measured with the image analysis system. Embryonic sporophytes were manually counted and classified according to size and health into multicelled (>8), few-celled (2-8), single-celled and morbid categories. The distribution of organisms among categories in the treated cultures was statistically compared to controls via the Chi-square test (Alder and Roessler, 1972). Data from Chi-square tests are summarized in Table 6.A.3.

(2) Results

One-way analysis of variance of gametophyte size vs. hydrazine concentration showed that only the 250 ppb exposure significantly inhibited gametophyte vegetative growth (cf. Table 6.5; Means table). Significant (Student's t, $p < 0.05$) growth inhibition was observed four days after initiation of cyclic exposures (Figure 6.17).

Chi-square tests on the distribution of sporophytes among size classes generally showed inhibition at 250 ppb hydrazine (Table 6.6A) and reduction of mortality relative to controls at 5 ppb.

Table 6.6A: Results of Chi-square tests on distribution of embryonic sporophytes among health and size classes. M. pyrifera Series M in pulsed hydrazine exposures. Significance criterion $p < 0.05$

Day #	significant increase fraction dead	significant decrease fraction dead	significant decrease fraction large	significant increase fraction large
19	250 ppb		250 ppb	
22	250 ppb	5 ppb	> 5 ppb	
23	250 ppb	5, 25 ppb	250 ppb	25 ppb
25	250 ppb	5 ppb	250 ppb	
Relative to controls	inhibition	stimulation	inhibition	stimulation

Figure 6.17: M. pyrifera Series M gametophyte growth inhibition in daily 6-hour hydrazine exposures. Means with 95% confidence limits.

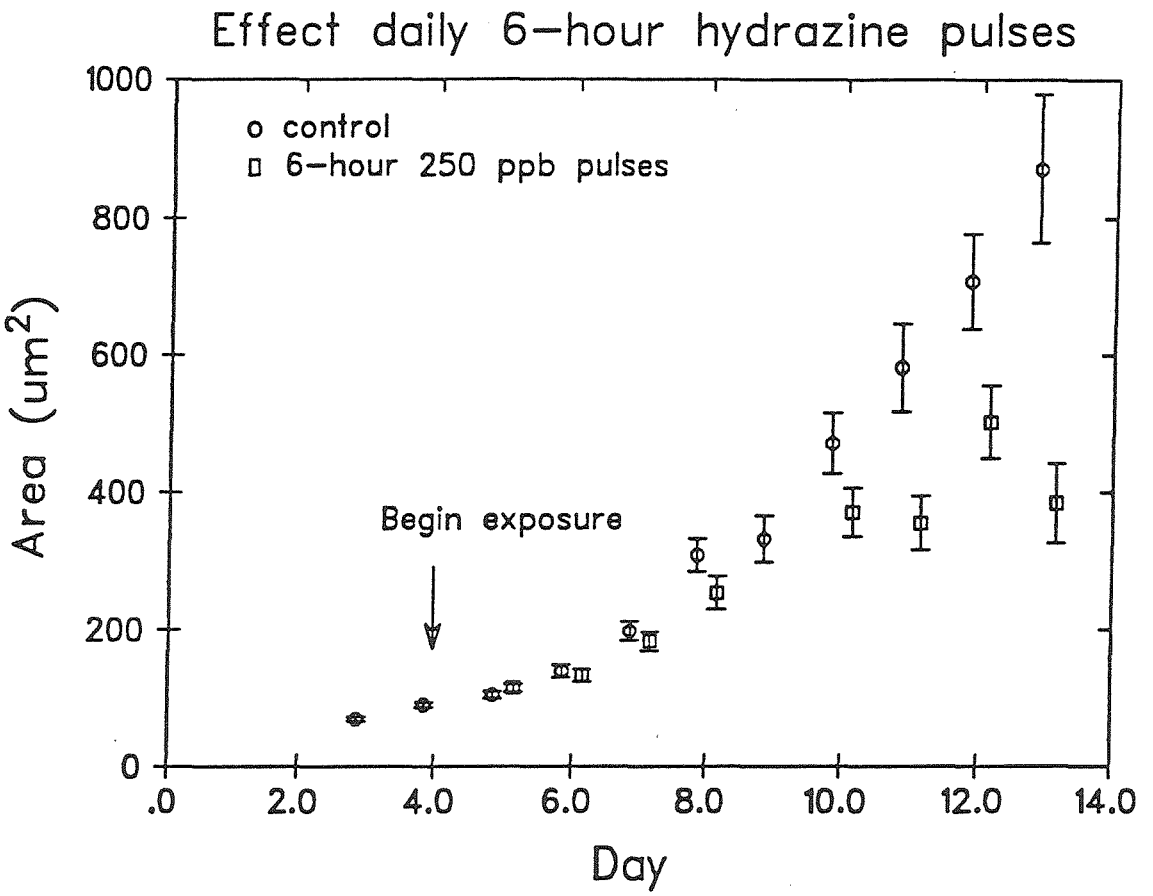

Reproductive failure occurred in the 250 ppb pulsed cultures. Embryonic sporophytes recruited but very few survived to the multicelled stage (Table 6.A.3).

Sporophytes recruited from the pulsed cultures and measured by the digitizer on Day 26 were significantly (Student's t: $p < 0.05$) smaller at 5 ppb and 25 ppb hydrazine than the controls (Table 6.6B).

Table 6.6B: Mean Size of Embryonic Sporophytes in Pulsed Culture Measured on Day 26.

TREATMENT ppb/hour	MEAN AREA $um^2 \pm$ 95 percent conf.interval	N	SIGNIFICANT? $p < 0.05$
Control (0 / 0)	145,500 ± 34,000	15	
5 / 6	68,000 ± 13,000	26	Yes
25 / 6	82,000 ± 21,000	19	Yes
250 / 6	None to measure in > 20 scans	0	Yes

Sporophyte size inhibition occurred at lower concentrations than for inhibition of gametophytic growth when actual sizes were measured. Smaller size in treated cultures could have been caused by either delayed recruitment or reduced growth rate. Available size class distribution data (Table 6.A.3) do not indicate delay in recruitment (which would be shown by an increase in the relative proportions of small or few-celled organisms), so it is possible that smaller sizes of juvenile sporophytes in 5 and 25 ppb hydrazine were due to reduced growth rates of recruited organisms. Sporophytes should be enumerated and classified during the crucial period (Days 12 to 15) of initial sporophytic recruitment to verify this conclusion.

C. M.PYRIFERA SERIES O COMBINED THERMAL AND CHEMICAL CYCLING

(1) Methods

Macrocystis pyrifera gametophyte cultures were exposed during each 24-hour period to 6 hours of cool (10°C) hydrazine-free seawater and 18 hours of warm (18°C) seawater containing hydrazine concentrations of 0, 1, 5, 25 and 125 ppb, simulating exposure to a warm, hydrazine containing plume at all times except for each day's highest tide. Illumination was 13 hours of light at 158 uE/m2-sec (hemispherical irradiance) and 11 hours of darkness.

Table 6.7: Effect of hydrazine and thermal pulses on sporophyte recruitment (averages from 10 random scans at 160X)

TREATMENT	COUNTS DAY 16	COUNTS DAY 19	COUNTS DAY 27 (4 days of recovery)
CONTROL 10°C	No data	7.0	22.3
CONTROL 18°C	1.5	3.7	8.6*
1 PPB 18°C	1.2	1.5*	7.8*
5 PPB 18°C	0.4#	2.4*	9.4*
25 PPB 18°C	0.0#	0.0*	0.0*
125 PPB 18°C	0.0#	0.0*	0.0*

Significance determined by Wilcoxon rank-sum test ($p < 0.05$).
\# Day 16: Compared to 18 C control.
* Day 19 and 23: Significant compared to 10 C control.

(2) Results

Significant inhibition of gametophyte vegetative growth occurred at 25 and 125 ppb (Figure 6.18). Wilcoxon rank-sum tests (Alder and Roessler, 1972) showed that significant inhibition of early sporophyte recruitment occurred at 1, 5, 25 and 125 ppb compared to controls (Table 6.7). Sporophyte recruitment recovered at 1 and 5 ppb compared to the 18°C control when cultures were restored to hydrazine-free solutions with cool temperatures and 24 hours

Figure 6.18: M. pyrifera Series O gametophyte growth in 18-hour daily exposures.

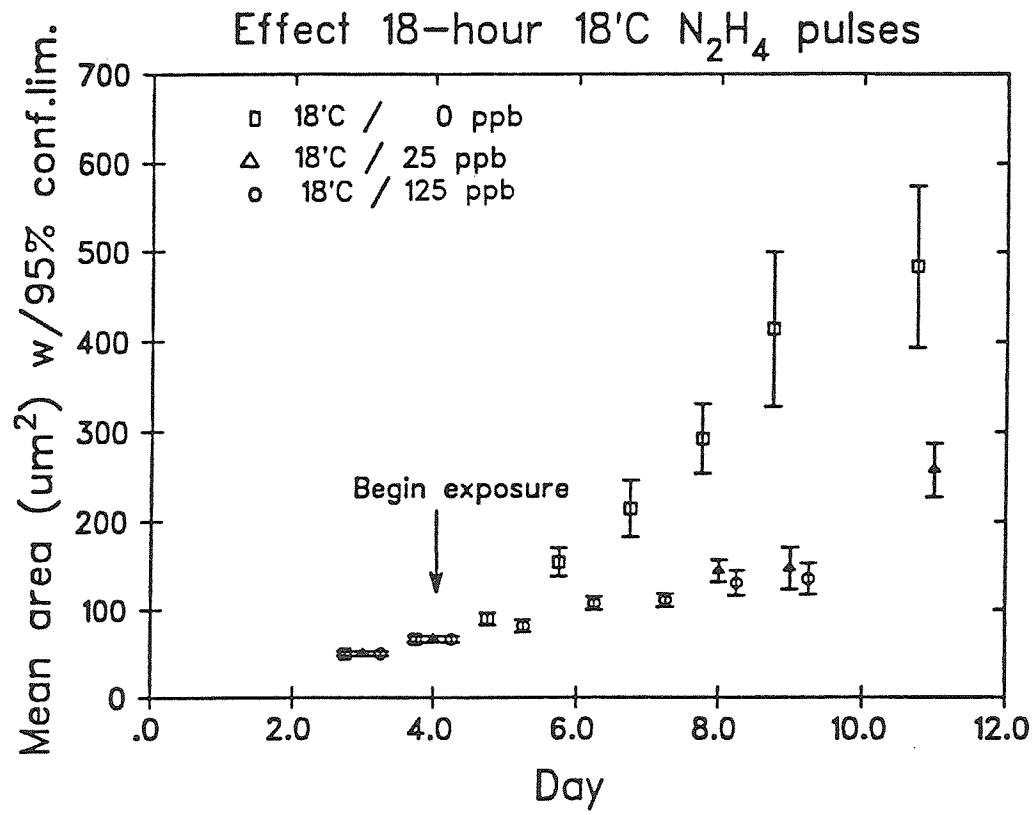

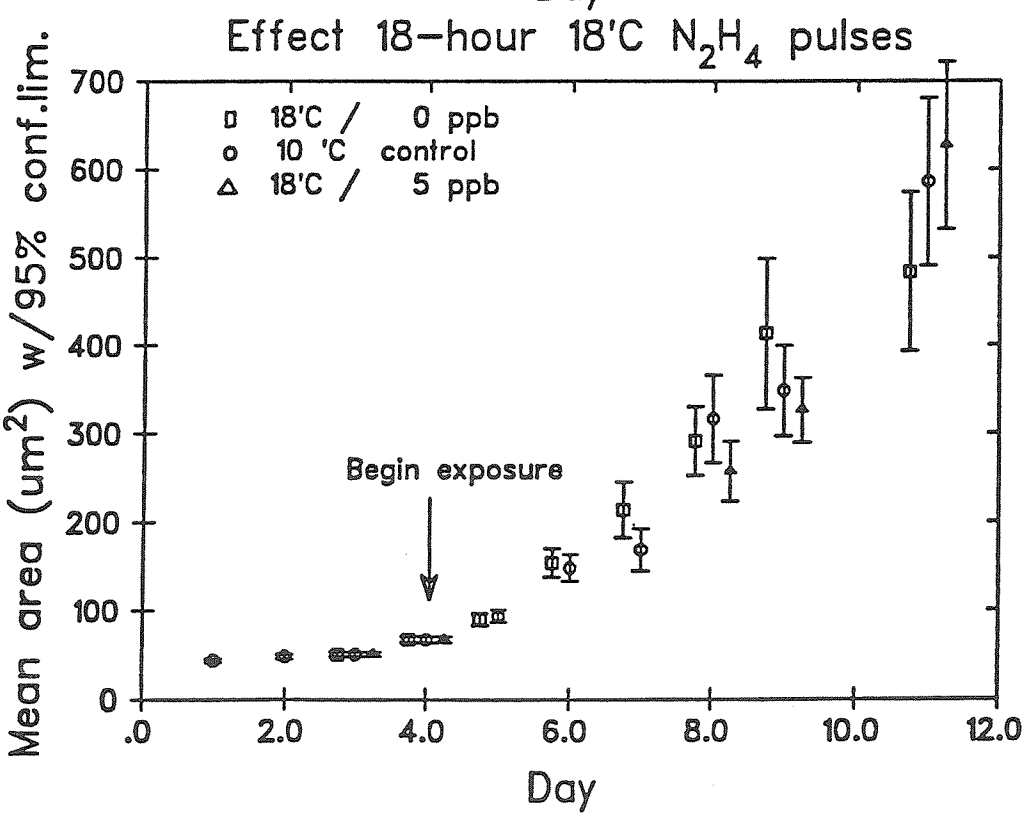

continuous light, so exposure at these concentrations could be reversible. Recruitment densities were below 10°C control values.

(3) Discussion of Series M and Series O Results

Regimes of cyclic pollutant stress adversely affected growth and reproduction of Macrocystis gametophytes. The harsher Series O exposure protocol (18 hours hydrazine/ 6 hours clean) inhibited gametophytic growth at lower concentrations (25 ppb vs. 250 ppb) than the Series M regime (6 hours hydrazine/ 18 hours clean). Sporophyte recruitment was inhibited in both cultures at hydrazine concentrations exceeding 5 ppb. The results indicated that daily exposure of shallow subtidal areas to a warm plume containing toxic compounds might inhibit reproduction when compared to areas receiving occasional exposures. Adverse impacts would require an episode involving simultaneous occurrence of exposure to the buoyant discharge and release by the power-plant of a toxic compound into the plume.

Concentration ranges for inhibition of Macrocystis reproduction in the Series M and O experiments were similar to concentration ranges necessary for 96-hour vegetative growth inhibition (Chapter 4), indicating that the continuous 96-hour exposure protocol might be able to predict consequences of certain types of episodic exposures.

The actual physical setting for exposure to DCPP effluent in Diablo Cove is more complex than that modeled by simple episodic experiments. Wave-driven mixing generates a very turbulent mobile interface between underlying waters and the overlying plume, resulting in highly variable bottom temperatures in much of the Cove

(Figure 6.19; Chapman et al., 1987). Exposure durations and dilutions of the plume constantly fluctuate for benthic organisms in much of Diablo Cove. Simple square-wave exposures indicate possible regimes of sensitivity for field exposures but will not be able to predict actual consequences of every exposure at a specific location.

V. CONCLUSIONS

1) Inhibition of Macrocystis gametophyte vegetative growth could be predicted for combinations of hydrazine exposure time and concentration using least-squares regression techniques. Application of regression equation-derived contours to data for undiluted power-plant emissions indicated that several low-flow discharge events could have inhibited vegetative growth. Size variations among experiments indicated that size ratios may be more reliable estimators of inhibition, but this advantage is partially offset by a near doubling of the relative uncertainty in the ratio that is caused by propagation of sample variances into the calculated result.

2) Macrocystis gametophyte size could be predicted as a function of continuous hydrazine concentration, age at start of exposure and temperature. This finding may enable comparison of toxicity assays run at different ages and ambient temperatures through adjustment of data using experimentally-developed regression equations.

3) Repeated, cyclic exposures to hydrazine, simulating exposure of shallow, subtidal organisms to a contaminated, tidally driven, buoyant plume, inhibited reproduction at 5 ppb, a concentration similar to the 2-4.5 ppb range observed for significant inhibition of vegetative growth during continuous exposures.

Figure 6.19: Example temperature record from station near DCPP discharge.

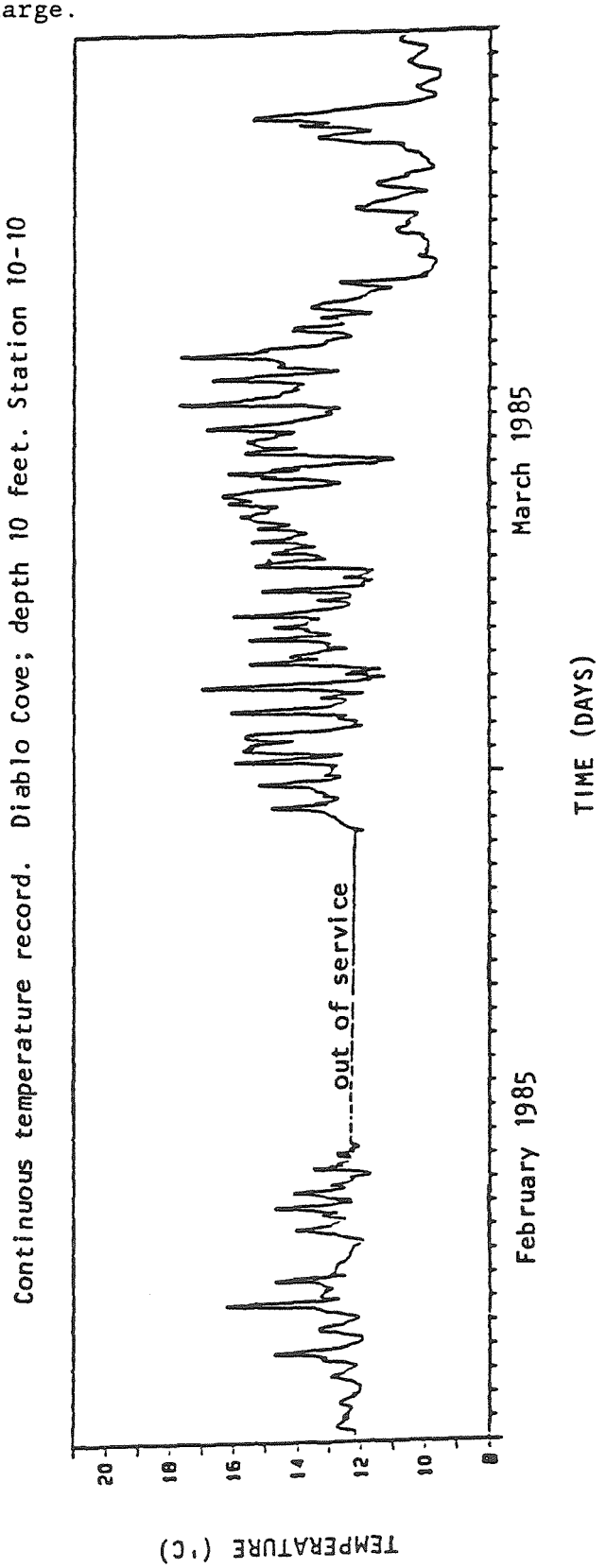

CHAPTER 6: APPENDIX

Additional statistical tables for Macrocystis pyrifera growth and recruitment inhibition experiments:

Table 6.A.1 Series AD means table for all combinations of concentration and temperature. Effect of hydrazine on gametophyte vegetative growth.

Table 6.A.2 Series AG Two-way analysis of variance for interaction of concentration and temperature. Effect of hydrazine on vegetative growth.

Table 6.A.3 Series M Total counts of embryonic sporophytes in each size class. Effect of hydrazine pulses on sporophyte recruitment.

Table 6.A.1: Macrocystis pyrifera Series AD gametophyte sizes. Table of means for Log_e Area with time trend removed. Zeroes in table indicate combinations not tested in this experiment

Level		Count	Average	Stnd. Error (internal)	Stnd. Error (pooled s)	95 % conf. limits for mean	
0ppb N_2H_4		495	5.5337542	.0321559	.0179944	5.4984401	5.5690683
1		37	4.8894269	.0697578	.0658170	4.7602604	5.0185934
2		49	4.8289189	.0475847	.0571927	4.7166776	4.9411602
5		328	5.1672003	.0335392	.0221056	5.1238179	5.2105827
10		191	4.9664380	.0511504	.0289682	4.9095875	5.0232885
20		38	4.5255064	.0480966	.0649452	4.3980508	4.6529621
10 °C		835	5.1750066	.0267538	.0138546	5.1478167	5.2021965
12		75	5.1856581	.0487162	.0462283	5.0949346	5.2763817
14		80	5.4485125	.0432216	.0447604	5.3606698	5.5363553
16		78	5.4588230	.0422167	.0453306	5.3698612	5.5477848
18		70	5.7201532	.0523605	.0478509	5.6262453	5.8140610
ppb	/ Temp						
0	10	346	5.4891217	.0431965	.0215229	5.4468828	5.5313607
0	12	35	5.3290291	.0749571	.0676713	5.1962233	5.4618348
0	14	41	5.5964566	.0579916	.0625240	5.4737526	5.7191607
0	16	39	5.6385146	.0493772	.0641072	5.5127036	5.7643256
0	18	34	6.0029240	.0601850	.0686593	5.8681794	6.1376686
1	10	37	4.8894269	.0697578	.0658170	4.7602604	5.0185934
1	12	0	.0000000	.0000000	.0000000	.0000000	.0000000
1	14	0	.0000000	.0000000	.0000000	.0000000	.0000000
1	16	0	.0000000	.0000000	.0000000	.0000000	.0000000
1	18	0	.0000000	.0000000	.0000000	.0000000	.0000000
2	10	49	4.8289189	.0475847	.0571927	4.7166776	4.9411602
2	12	0	.0000000	.0000000	.0000000	.0000000	.0000000
2	14	0	.0000000	.0000000	.0000000	.0000000	.0000000
2	16	0	.0000000	.0000000	.0000000	.0000000	.0000000
2	18	0	.0000000	.0000000	.0000000	.0000000	.0000000
5	10	174	5.0793658	.0566930	.0303504	5.0198029	5.1389288
5	12	40	5.0602086	.0573820	.0633007	4.9359802	5.1844370
5	14	39	5.2929816	.0547985	.0641072	5.1671706	5.4187925
5	16	39	5.2791314	.0555452	.0641072	5.1533204	5.4049424
5	18	36	5.4530918	.0555753	.0667248	5.3221436	5.5840400
10	10	191	4.9664380	.0511504	.0289682	4.9095875	5.0232885
10	12	0	.0000000	.0000000	.0000000	.0000000	.0000000
10	14	0	.0000000	.0000000	.0000000	.0000000	.0000000
10	16	0	.0000000	.0000000	.0000000	.0000000	.0000000
10	18	0	.0000000	.0000000	.0000000	.0000000	.0000000
20	10	38	4.5255064	.0480966	.0649452	4.3980508	4.6529621
20	12	0	.0000000	.0000000	.0000000	.0000000	.0000000
20	14	0	.0000000	.0000000	.0000000	.0000000	.0000000
20	16	0	.0000000	.0000000	.0000000	.0000000	.0000000
20	18	0	.0000000	.0000000	.0000000	.0000000	.0000000
Total		1138	5.2479216	.0118677	.0118677	5.2246310	5.2712121

Table 6.A.2: Analysis of Variance for Log_e(Area): M.pyrifera Series AG

Source of variation	Sum of Squares	d.f.	Mean square	F-ratio	Sig. level
MAIN EFFECTS	29.928672	4	7.4821680	63.041	.0000
N2H4 concentration	29.321443	3	9.7738142	82.349	.0000
Temperature	.039005	1	.0390052	.329	.5730
2-FACTOR INTERACTIONS					
concentration/temp.	4.090810	3	1.3636032	11.489	.0000
RESIDUAL	39.523034	333	.1186878		
TOTAL (CORR.)	73.542516	340	3 missing values were excluded		

Table of means for Log_e(Area)

Level	Count	Average	Std.Error (internal)	Std.Error (pooled s)	95 Percent Confidence for mean	
ppb N2H4						
0	62	4.8577872	.0745087	.0437529	4.7717012	4.9438732
100	78	4.1647395	.0358128	.0390082	4.0879890	4.2414900
200	95	4.1976370	.0281708	.0353461	4.1280919	4.2671821
300	106	4.0089371	.0265863	.0334619	3.9430993	4.0747750
temp C						
10	171	4.2935571	.0343141	.0263454	4.2417212	4.3453929
20	170	4.2091593	.0367049	.0264228	4.1571712	4.2611474
ppb temp						
0 10	38	4.7124839	.0933822	.0558871	4.6025234	4.8224444
0 20	24	5.0878508	.1098643	.0703230	4.9494868	5.2262147
100 10	38	4.1078914	.0664225	.0558871	3.9979310	4.2178519
100 20	40	4.2187451	.0284242	.0544720	4.1115689	4.3259213
200 10	46	4.3055818	.0388088	.0507954	4.2056394	4.4055241
200 20	49	4.0963011	.0352947	.0492158	3.9994665	4.1931356
300 10	49	4.1013721	.0348215	.0492158	4.0045375	4.1982067
300 20	57	3.9294755	.0364315	.0456316	3.8396931	4.0192579
Total	341	4.2514819	.0186563	.0186563	4.2147747	4.2881891

Multiple range analysis for Loge(Area) by hydrazine concentration

Level	Count	Average	Homogeneous Groups (by 95% conf. levels)
300	106	4.0089371	*
100	78	4.1647395	*
200	95	4.1976370	*
0	62	4.8577872	*

Multiple range analysis for Loge(Area) by temperature

Level	Count	Average	Homogeneous Groups (by 95% LSD intervals)
20	170	4.2091593	*
10	171	4.2935571	*

Table 6.A.3: Macrocystis pyrifera Series M sporophyte recruitment. Total counts in each size class from 20 random scans at 100X. Classification criteria are:
Multi-celled: > 8 cells; Few-celled: 2-8 cells; Single: 1 cell;
Moribund: Loss of pigmentation and/or orderly cellular orientation.

Size category:	Multi	Few	Single	Moribund	Total
Measurement day & Treatment					
Day 19					
Control	14	18	25	5	62
5 ppb	6	0	23	2	31
25 ppb	14	15	18	2	49
250 ppb	2	4	11	27	44
Day 22					
Control	32	10	13	16	71
5 ppb	7	12	41	6	66
25 ppb	19	13	24	21	77
250 ppb	0	9	19	22	50
Day 23					
Control	27	15	38	15	95
5 ppb	24	15	35	2	76
25 ppb	48	17	27	6	98
250 ppb	6	22	47	71	146
Day 25					
Control	64	27	71	31	193
5 ppb	42	20	77	3	142
25 ppb	61	35	98	43	237
250 ppb	0	6	48	142	196

REFERENCES

Alder, H.E. and E.B. Roessler 1972. Introduction to Probability and Statistics, W.H. Freeman and Company: San Francisco, 373pp.

Anderson, L.M. 1982. Iron Reduction and Micronutrient Nutrition of Juvenile Macrocystis pyrifera (L.) C.A. Agardh (Giant Kelp) Determined by a Chemically Defined Medium, Aquil. Ph.D. Thesis, California Institute of Technology, Pasadena, CA. 146pp.

Berg, G. 1964. The Virus Hazard in Water Supplies, Journal of the New England Water Works Association. 78:79.

Brown, V.M., D.H.M. Jordan, and B.A. Tiller 1969. Acute toxicity to rainbow trout of fluctuating concentrations and mixtures of ammonia, phenol and zinc, Journal of Fisheries Biology. 1(1):69.

Chapman, F. A., W.J. North, and E.K. Anderson 1987. W.J. North Marine Ecological Transects: 1985 and 1986, Chapter 1, in Environmental Investigations at Diablo Canyon, 1986; Volume 1: Marine Ecological Studies, Pacific Gas and Electric Company, San Ramon, CA. December 1987.

Chen, C.W. and R.E. Selleck 1969. A kinetic model for fish toxicity threshold, Journal of the Water Pollution Control Federation. 41:R294-R308.

Chick, H. 1908. An Investigation of the Laws of Disinfection, Journal of Hygiene. 8:92-157.

Collins, H. and R.E. Selleck 1972. Process Kinetics of Wastewater Chlorination, SERL Report No 72-5, University of California at Berkeley.

Electric Power Research Institute 1982. The Effects of Chlorine on Freshwater Fish Under Various Time and Chemical Conditions, Report EA-2481/ Research Project #1435-1, Electric Power Research Institute, Palo Alto, CA. 68pp.

Floyd, R., D.G. Sharp and J.D. Johnson 1978. Inactivation of Single Poliovirus Particulates in Water by Hypobromite Ion, Molecular Bromine, Dibromamine and Tribromamine, Environmental Science and Technology. 12:1031-1036.

Gard, S. 1957. Chemical Inactivation of Viruses. in CIBA Foundation Symposium on the Nature of Viruses, Little, Brown and Company: Boston. p.123.

James, D., J. Steinbeck, E. Anderson, and W.J. North 1988. Use of Long-Term Mean Background Temperatures to Analyze Changes and Trends in Waters Off Diablo Canyon (San Luis Obispo County, California), in 1986 Annual Report: Environmental Monitoring, Diablo Canyon Power Plant, Pacific Gas and Electric Company, San Ramon, Calif. 25pp.

James M. Montgomery, Consulting Engineers, 1985. Water Treatment Principles and Design, J. Wiley and Sons: New York, 696pp.

Jensen, P.A. and R.W. Hann, 1976. The Interrelationship of Material Toxicity, Stream Properties and Quantity of Spilled Material in Assessing the Risk of Hazardous Material Spills. Texas A and M University. Report TAMU-SG-75-212. 261pp.

Kuwabara, J.S. 1980. Micronutrient Requirements for Macrocystis pyrifera (L.) C.A. Agardh (giant kelp) Gametophytes Determined by Means of a Chemically Defined Medium, Aquil, Ph.D. Thesis, California Institute of Technology, Pasadena, CA. 185pp.

Kuwabara, J.S. 1981. Gametophytic Growth by Macrocystis pyrifera (Phaeophyta) in response to various iron and zinc concentrations, Journal of Phycology. 17:417-419.

Kuwabara, J.S. 1982. Micronutrients and kelp cultures: evidence for cobalt and manganese deficiencies in southern California deep seawater, Science. v.216:1219-1221.

Lammering, M.W. and N.C. Burbank 1961. The toxicity of phenol, o-chlorophenol and o-nitrophenol to bluegill sunfish, Proceedings of the 15th Industrial Waste Conference. Purdue University, Extension Series. 106:541.

Levyns, M.R. 1933. Sexual Reproduction in Macrocystis pyrifera, Ag. Annals of Botany. 27(186):349-353.

Luning, K and M.Neushul 1978. Light and temperature demands for growth and reproduction of Laminarian gametophytes in southern and central California, Marine Biology. 45:297-309.

Metcalf and Eddy, Inc. 1979. Wastewater Engineering: Treatment, Disposal, Reuse, McGraw-Hill Book Company: New York, p.299.

Selleck, R.E., H.R. Collins and G.C. White 1970. Kinetics of Wastewater Chlorination in Continuous Flow Processes. Presented at International Association of Water Pollution Research Conference, San Francisco, CA. July 29, 1970.

Selleck, R.E., B.M. Saunier, and H.F. Collins 1978. Kinetics of Bacterial Deactivation with Chlorine, Journal of Division of Environmental Engineering, Proceedings American Society of Civil Engineers. **104**(EE6):1197-1212.

Watson, H.E. 1908. A Note on the Variation of the Rate of Disinfection with Change in Concentration of the Disinfectant. Journal of Hygiene. **8**:536.

CHAPTER 7: SUMMARY AND CONCLUSIONS

I. SUMMARY OF RESULTS IN SEPARATE CHAPTERS

(3.1) Errors in determining sizes of individual objects resulted from a combination of random positioning in the digitizing grid and random fluctuations of light intensity. The relative error (expressed as a coefficient of variation[1]) arising from repeated digitization of single objects ranged from 1.5 to 3.0 percent of object size. Theoretical calculations showed that propagation of small (less than 10 percent) constant relative errors increased computed sample variances by twice the value of the relative error. Propagation of individual object error into a computed variance for size distributions of Macrocystis gametophytes resulted in negligible increase of the variance and did not obscure determinations of significance. Application of digital image analysis techniques to gametophyte measurement reduced relative error in area determinations when compared to eyepiece micrometer methods.

(4.1) Four compounds emitted from nuclear power plant cooling discharges were screened for toxicity to Macrocystis gametophytes at concentrations similar to those discharged. Boric acid (H_3BO_3) and lithium ion (Li^{+1}) were not toxic at environmentally relevant levels. Hydrazine significantly inhibited growth in 96-hour assays at 3-5 ppb (96-160 nM). No synergism or antagonism of hydrazine with borate or lithium occurred.

---

[1]Coefficient of variation is defined as the ratio of the computed standard deviation of a set of measurements to the calculated mean for the same set of measurements.

Chlorine (as OCl^-) inhibited vegetative growth in 96 hours at concentrations between 1-10 ppm and caused 100 percent destruction at 10 ppm. A longer, 12-day test showed significant growth inhibition at 10-1000 ppb total added hypochlorite, indicating possible toxicity of chlorine-produced oxidants.

(4.2) Inhibition of other phases of the Macrocystis life-cycle was investigated:

a) Spore motility was inhibited at 250 ppb after 18 minutes' exposure.

b) Spore germination was significantly inhibited by 250 ppb/1 day hydrazine, but a consistent trend of increasing inhibition with increasing concentration and duration was not observed. Spore germination rates were found to vary between collection sites.

c) Sperm production was significantly inhibited at 250 ppb after a 1 day exposure, but not at 25 ppb/1 day or 250 ppb/1 hour.

d) Sporophyte recruitment was variably affected by hydrazine exposures. Inhibition of Macrocystis pyrifera sporophyte recruitment was observed in single-exposure episodes with concentration/duration dosages exceeding 125 ppb/1 day. Some stimulation of recruitment was observed after application of milder single pulses to eight-day old gametophyte cultures. In contrast, daily exposure to 6-hour or 18-hour hydrazine pulses inhibited reproduction at 5 ppb hydrazine.

(4.3) Consistent vegetative growth assay results were obtained over nine calendar months in ten continuous 96-hour assays measured by digital image-analysis. Macrocystis pyrifera gametophytes from

two different sites were repeatedly inhibited at 3-5 ppb (96-160 nM) total hydrazine. Growth rate inhibition appeared to follow sigmoidal kinetics. Macrocystis gametophyte area growth rates measured with the digitizer varied from 14-32 percent per day with a mean of 24 percent per day and 95 percent confidence limits of 3 percent per day. Growth was most rapid at about 18°C for both southern and central California gametophytes. Growth of central California gametophytes was retarded at 20°C. Vegetative growth by gametophytes from both localities at 10°C was sufficiently rapid to enable tests of significance in toxicity studies.

(4.4) Variations in vegetative growth sensitivity to hydrazine were observed among eight brown algal species in standard pulsed assays. Surface canopy formers such as Macrocystis, Nereocystis and Pelagophycus showed larger sensitivities compared to short-statured kelps. Laminaria farlowii and Pterygophora californica were the least sensitive. Eisenia arborea, Laminaria dentigera, Laminaria ephemera and Egregia mensziesii showed intermediate resistances. Gametophytes of other fast-growing canopy formers, Nereocystis luetkeana and Pelagophycus porra, were inhibited in 96-hour continuous assays at 3 ppb (96 nM) and 1 ppb (32 nM), respectively.

(4.5) Hydrazine was, on a molar basis, 30X more toxic than Zn(II), the State of California Standard Inorganic Reference Toxicant. Inconsistent results with Zn(II) supplementations were obtained in cultures grown in different batches of southern California offshore seawater that gave consistent results for hydrazine. Changes in distribution of Zn(II) species between the batches could have caused

differences in measured toxicity to Macrocystis gametophytes. A screening test for toxicity of tributyl-tin chloride, a component of marine anti-fouling paint, showed that molar toxicity to Macrocystis gametophytes was in the range 36-360 nM.

(5.1) Hydrazine exhibited simple chemistry in seawater. Calculations showed that 60 to 90 percent of the compound existed as $N_2H_5^+$ at ambient pH's (7.8-8.2) and temperatures (10-15°C) expected for central California waters. Transition metal speciation was not changed by hydrazine concentrations below 50 uM. SURFEQL model runs demonstrated that Cu(II) was the metal most likely to complex with hydrazine. Significant alteration of Cu(II) speciation began to occur at 100 uM total hydrazine.

Measured autoxidation rates for hydrazine in seawater were slow, varying over the range 0.03-0.29 percent per hour at 22 °C, confirming work of (MacNaughton et al., 1978). Measured half-life in coastal seawater was 370-500 hours. Half-life in oceanic seawater was 1700 hours. Decline in concentration was best-fit by assuming half-order kinetics with respect to hydrazine concentration. Autoxidation occurred more rapidly in coastal than in offshore seawater. Measured Cu(II) contents and pH were identical in offshore and coastal seawater, indicating that oxidation rates may have been controlled by either organic-influenced Cu(II) speciation or by other oxidants, such as peroxy radicals.

(5.2) Hydrazine emissions from coastally sited California nuclear power plants comprised occasional episodes of 1-30 ppb concentration and 7 to 15 hours' duration (probably caused by maintenance

activities) superimposed on a low concentration (10 ng/litre (parts per trillion)) background, originating from continuous blow-down of steam generator condensate. Arithmetic mean concentrations of episodic releases (calculated at the end of the pipe before mixing with receiving waters) were 6 ± 24 ppb for DCPP and typically 5 ± 5 ppb for each SONGS Unit. The large standard deviations were caused by occasional high concentration discharges which skew data distributions to the right.

5.3) Frequency distributions for emitted concentrations varied between two different nuclear power stations. Before dilution, 88 percent of the 1984-87 monthly peak emissions from Diablo Canyon Power Plant (DCPP) and 77 percent of the 1984-87 peak monthly emissions from San Onofre Nuclear Generating Station Units 1,2 and 3 (SONGS) were below concentration thresholds that inhibited Macrocystis gametophyte vegetative growth in the laboratory. Two percent of DCPP and 0 percent of SONGS peak monthly emissions were estimated to be inhibitory when scaled by overall dilution factors of 4:1 and 8:1-12:1, respectively, and combined with the estimated frequency distribution for 50 percent inhibition of vegetative growth of Macrocystis gametophytes in 7-hour to 16-hour discharge "events."

(6.1) Results from multivariate experiments showed that the extent of Macrocystis vegetative growth inhibition could be predicted for:

a) emitted hydrazine "pulses" covering a wide range of concentration and duration, and

b) continuous hydrazine exposures at different gametophytic ages and environmental temperatures.

Analyses of variance and linear least-squares regression techniques explained significant proportions of variance in the experimental results. Regression equations were developed, which predicted:

a) degree of vegetative growth inhibition as a function of discharged hydrazine concentration and duration of discharge, and

b) gametophytic size as a function of continuous hydrazine concentration,age at start of exposure and environmental temperature.

(6.2) Comparison of predictions from factorial-design bioassays to power-plant emission data indicated that before dilution, the combined concentration and duration of three specific 1984 Diablo Canyon Power Plant hydrazine emissions (Figure 6.8) might have been sufficient to inhibit gametophytes of local algal populations.

II. MAIN CONCLUSIONS OF THESIS

1) Reliable vegetative growth assay results were obtained with digital image-analysis measurements of gametophytes in experiments modeling continuous exposure to hydrazine. The concentration range necessary for detecting significant inhibition of vegetative growth did not vary with season or latitudinal location of adult spore sources. However, concentrations required to estimate 50 percent growth inhibition varied by a factor of five.

2) Vegetative growth can be predicted from polynomial relationships derived from linear least-squares fits to gametophyte

size data within certain ranges of pulse concentration and duration. This development permitted:

a) analysis of historical discharge data to determine if past powerplant releases could have inhibited growth or reproduction of brown algal microscopic phases, and

b) establishment of guidelines for hydrazine emissions, which indicate allowable combinations of concentration and duration of episodic marine hydrazine discharges that minimize risk of adverse impacts on brown algal gametophytes (Figures 6.8 & 6.9).

3) Gametophytic vegetative growth assays detected inhibition 72-96 hours after exposure to a toxicant. Significant growth inhibition occurred consistently at 3-5 ppb (96-160 nM; Table 4.) total added hydrazine, well below the 20 ppb spectrophotometric detection limit in seawater.

4) Observed differences in sensitivity among gametophytes of different species of the Laminariales indicate that changes in the composition of brown algal communities caused solely by hydrazine emissions could occur in the vicinity of the Diablo Canyon Power Plant outfall. Resistant species could increase in abundance and sensitive species become scarce. However, hydrazine-caused changes might be masked by thermal and turbulence effects from the discharge.

5) Hydrazine autoxidation kinetics were slow relative to characteristic times for mixing and dilution in marine waters. Hydrazine concentrations emitted into marine nearshore environments

will decline primarily through physical dilution with surrounding waters.

6) Continuous hydrazine concentrations should be kept below a safe-threshold value of 1 part per billion[2] at the point of discharge to prevent damage to algal communities. Analysis of residual scatter after data transformation (Figure 6.4A) shows that, for equal hydrazine "dosages" (concentration x time) applied to Macrocystis gametophytes, high concentration, short time events generally produced less inhibition of vegetative growth than did low concentration, long time events. However, planktonic organisms entrained into and transported with the discharge plume would be more likely to be inhibited by short-duration, high concentration events. The latter phenomenon leads to a recommendation that hydrazine releases, if they occur, should be restricted to long duration, low concentration (less than 1 ppb as measured at point of discharge) events. Dilution of the discharge plume between point of discharge and target organisms would thus provide an additional factor of safety. Hydrazine concentrations could be lowered by reducing the introduction rate of hydrazine-containing wastewaters into the main cooling water flow or by chemical destruction of hydrazine prior to discharge.

---

[2]This safe limit was determined for the most sensitive tested alga, Pelagophycus porra. The safe threshold for Macrocystis pyrifera gametophytes was 2 ppb.

REFERENCE

MacNaughton, M.G., G.A. Urda, and S.E. Bowden 1978. Oxidation of Hydrazine in Aqueous Solutions. CEEDO-TR-78-11; National Technical Information Service Index 78(24):118; 37pp.